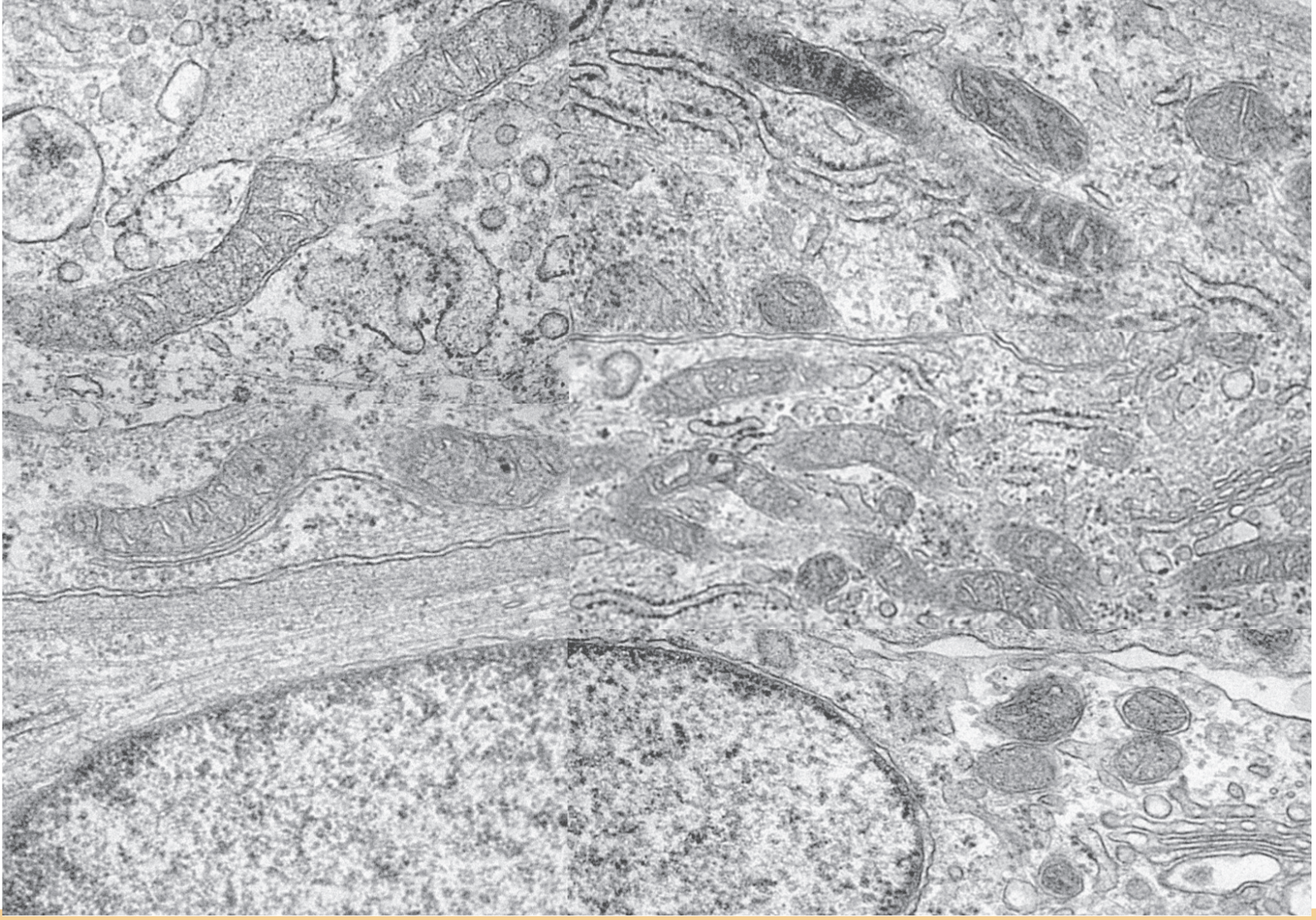

Mafalda Rita Avó Bacalhau

Establishing the Pathogenicity of Novel Mitochondrial DNA Sequence Variations: a Cell and Molecular Biology Approach

Tese de doutoramento do Programa de Doutoramento em Ciências da Saúde, ramo de Ciências Biomédicas, orientada pela Professora Doutora Maria Manuela Monteiro Grazina e co-orientada pelo Professor Doutor Henrique Manuel Paixão dos Santos Girão e pela Professora Doutora Lee-Jun C. Wong e apresentada à Faculdade de Medicina da Universidade de Coimbra

Julho 2017

· U C ·

Universidade de Coimbra

· U C ·

UNIVERSIDADE DE COIMBRA

Faculty of Medicine

Establishing the pathogenicity of novel mitochondrial DNA sequence variations: a cell and molecular biology approach

Mafalda Rita Avó Bacalhau

Tese de doutoramento do programa em Ciências da Saúde, ramo de Ciências Biomédicas, realizada sob a orientação científica da Professora Doutora Maria Manuela Monteiro Grazina; e co-orientação do Professor Doutor Henrique Manuel Paixão dos Santos Girão e da Professora Doutora Lee-Jun C. Wong, apresentada à Faculdade de Medicina da Universidade de Coimbra.

Julho, 2017

Financial Support

This work was financed by FCT - Portuguese Foundation for Science and Technology through the strategic plan UID/NEU/04539/2013, the projects PTDC/DTP-EPI/0929/2012 and Pest-C/SAU/LA0001/2013-2014, and the PhD grant FCT-SFRH/BD/86622/2012, by a SPDM 2014 grant and co-supported by Feder funds through the Operational Competitiveness Program – COMPETE2020 (Strategic projects: POCI-01-0145-FEDER-007440, HealthyAging2020 CENTRO-01-0145-FEDER-000012-N2323 and New Strategies to Manage Brain Diseases 2013 to 2015| CENTRO-07-ST24-FEDER-002002/6/8 Programa Operacional Regional do Centro - Projecto Mais Centro).

“Mystery creates wonder and wonder is the basis of man’s desire to understand”. – Neil Armstrong

ACKNOWLEDGEMENTS

A realização desta tese não teria sido possível sem a colaboração, apoio e incentivo de várias pessoas. Gostaria de expressar um profundo agradecimento a todas as pessoas que ao longo destes anos contribuíram de uma ou de outra forma para que esta etapa na minha vida académica se concretizasse.

Em primeiro lugar, quero agradecer à Professora Doutora Manuela Grazina por me ter desafiado a realizar este projeto e ter acreditado nas minhas capacidades para a sua concretização. Obrigada por me ter dado a oportunidade de amadurecer, tanto a nível profissional como pessoal, e por não ter duvidado que eu conseguiria atingir os objetivos propostos, mesmo nos dias em que tudo parecia estar contra o sucesso da concretização desta etapa. As suas palavras foram uma motivação para continuar em frente.

I would like to thank the scientific co-supervision of the Professor Henrique Girão and Professor Lee-Jun Wong, and also the essential collaboration of the Professor Cristina Rego and Professor Robert Taylor. Thank you all for sharing your ideas and knowledge that has contributed to this thesis.

Aos clínicos que cooperaram para a concretização desta tese, nomeadamente a Professora Doutora Luísa Diogo, Dra. Maria do Carmo Macário, Dr. Pedro Fonseca, Dr. João Durães, Dra. Olinda Rebelo, Dra. Paula Garcia e Dra. Margarida Venâncio, assim como aos doentes e familiares, agradeço a disponibilidade pois sem a sua colaboração não teria sido possível a realização deste estudo.

A todos os colaboradores do LBG que foram imprescindíveis e estiveram ao meu lado nesta etapa, o meu mais sincero obrigado! Marta, agradeço-te teres sido o meu braço direito na realização da parte experimental, por estares sempre disposta a ajudar-me em qualquer momento, por toda a tua dedicação e pelo incentivo que me transmitiste. Carolina, agradeço-te toda a ajuda, preocupação, companheirismo, apoio e, principalmente, a amizade. Maria João, além da contribuição experimental no trabalho e todo o apoio e troca de ideias, agradeço-te o facto de encontrares sempre uma solução para qualquer contratempo. João, Cândida e Mónica, obrigada por toda a ajuda na parte experimental e pela vossa amizade. Carla, Célia, Rita e Fernanda, agradeço-vos os momentos de boa disposição e apoio. Não posso deixar de agradecer aos alunos que passaram pelo laboratório e que me continuaram a apoiar, especialmente à Raquel, à Maria Inês e à Diana pelo incentivo na fase final.

À Doutora Carla Lopes agradeço a ajuda na parte experimental e conhecimentos que me transmitiu.

À Doutora Mónica Zuzarte gostaria de agradecer o empenho na realização da técnica de microscopia de transmissão eletrónica, assim como o apoio e preocupação.

I would like to gratefully acknowledge the team from the Mitochondrial Diagnostic Laboratory of Baylor College of Medicine in Houston and also, the team from the Mitochondrial NSCT Diagnostic Service, Wellcome Trust Centre for Mitochondrial Research, Newcastle University that have been essential to perform the experimental work conducted in their laboratories.

À Doutora Mariana Rocha agradeço a disponibilidade para ajudar e trocar ideias.

Agradeço a todos os meus amigos, nomeadamente à Joana Balça e à Elisa Campos que estiveram sempre disponíveis e presentes, e também às amizades que surgiram no contexto deste trabalho além-fronteiras, obrigada pelo vosso apoio Isabel Cordero, Vanessa Mendes e Andreia Silva.

Aos meus familiares e aos que são como uma família para mim, nomeadamente a Dona Fernanda, o Sr. Sérgio e a Nanda, gostaria de agradecer o apoio incondicional.

Aos meus pais e ao meu irmão gostaria de agradecer a educação, a força, o apoio, a preocupação, a dedicação e a compreensão que me permitiram atingir esta etapa. Mãe, obrigado por seres a minha melhor amiga e conselheira.

Ao Marcos quero agradecer o carinho e compreensão, as palavras de apoio e motivação, o companheirismo e a paciência infinita em todos os momentos.

INDEX

INDEX OF FIGURES

CHAPTER 1

CHAPTER 3

Case report I

Case report II

INDEX OF TABLES

ABBREVIATIONS

A	
aaRs	Aminoacyl-tRNA synthetases
Acetyl-CoA	Acetyl coenzyme A
ACMG	American College of Medical Genetics and Genomics
ADP	Adenosine diphosphate
ATP	Adenosine triphosphate
B	
BCA	Bicinchoninic acid
BER	Base excision repair
BN-PAGE	Blue native polyacrylamide gel electrophoresis
C	
CAMKKβ	Calcium/calmodulin-dependent protein kinase kinase 2
CAT	Catalase
CCCP	Carbonyl cyanide m-chlorophenylhydrazone
CHUC	Centro Hospitalar da Universidade de Coimbra
CNC-UC	Center for neuroscience and cell biology – University of Coimbra
CoQ	Coenzyme Q
COX	Cytochrome c oxidase
CPEO	Chronic progressive external ophthalmoplegia
CS	Citrate synthase
CYB	Cytochrome b
Cyt c	Cytochrome c
CYC1	Cytochrome c1
CI	Complex I
CII	Complex II
CIII	Complex III
CIV	Complex IV
CV	Complex V
D	
DCM	Dilated cardiomyopathy
DMEM	Dulbecco's modified eagle medium
DDM	n-Dodecyl-D-maltoside
DNM1L	Dynamin 1 like protein
DNP	2,4-dinitrofenol

DSBs	Double-strand breaks
E	
ECAR	Extracellular acidification rate
ECL	Enhanced chemiluminescence
EDTA	Ethylenediaminetetraacetic acid
EOM	Extraocular muscle
ER	Endoplasmic reticulum
F	
FAD	Flavin adenine dinucleotide
$FADH_2$	Flavin adenine dinucleotide reduced
FCCP	carbonyl cyanide-p-trifluoromethoxyphenylhydrazone
G	
GPx	Glutathione peroxidase
GR	Glutathione reductase
GSH	Glutathione
H	
HCM	Hypertrophic cardiomyopathy
HEPES	Hydroxyethyl piperazineethanesulfonic acid
HR	Homologous recombination
HRP	Horseradish
HSP	H-strand promotor
I	
IMM	Inner mitochondrial membrane
IMS	Intermembrane space
K	
KSS	Kearns-Sayre syndrome
L	
LBG	Laboratory of biochemical genetics
LE	Left eye
LHON	Leber's hereditary optic neuropathy
LRPPRC	Leucine-rich pentatricopeptide repeat (PPR)-containing
LS	Leigh syndrome
LSD	Lysosomal storage disorder
LSP	L-strand promoter

LVNC	Left ventricular non compaction
M	
MAMs	Mitochondria-associated membranes
MCU	Mitochondrial calcium uniporter
MDVs	Mitochondrial derived vesicles
MELAS	Mitochondrial encephalopathy, lactic acidosis with stroke-like episodes
MERRF	Myoclonic epilepsy with ragged-red fibres
MFF	Mitochondrial fission factor
MFN	Mitofusin
MMR	Mismatch repair
MNGIE	Mitochondrial neuro-gastrointestinal involvement and encephalopathy
MRC	Mitochondrial respiratory chain
MRP	Mitochondrial ribosomal proteins
MRGs	Mitochondrial RNA granules
mtDNA	Mitochondrial DNA
mtEFG1	Mitochondrial elongation factor G1
mtEFTu	Mitochondrial elongation factor
MTERF	Mitochondrial transcription termination factor
mt-mRNA	Mitochondrial messenger RNA
MTPAP	Mitochondrial poly(A) polymerase
mt-rRNA	Mitochondrial ribosomal RNA
mtRRF1	mitochondrial recycling factor 1
mtRRF2	mitochondrial recycling factor 2
mtSSB	Mitochondrial single-stranded DNA binding protein
mt-tRNA	Mitochondrial transfer RNA
N	
NAD+	Nicotinamide adenine dinucleotide
NADH	Nicotinamide adenine dinucleotide reduced
NARP	Neuropathy, ataxia and retinitis pigmentosa
nDNA	Nuclear DNA
NDUFS4	NADH dehydrogenase [ubiquinone] iron-sulphur protein 4
NDUFV1	NADH dehydrogenase [ubiquinone] flavoprotein 1
NER	Nucleotide excision repair
NHEJ	Nonhomologous end joining

NGS	Next generation sequencing
O	
OCR	Oxygen consumption rate
OMM	Outer mitochondrial membrane
OSCP	Oligomycin sensitivity-conferring protein
OXPHOS	Oxidative phosphorylation
P	
PBS	Phosphate buffer saline
PCR	Polymerase chain reaction
PINK1	PTEN-induced putative kinase 1
PGC1α	Peroxisome proliferator-activated receptor γ coactivator 1- alpha
POLG	DNA polymerase γ
POLRMT	Mitochondrial RNA polymerase
PUS1	Pseudouridylate synthase 1
PVDF	Polyvinylidene difluoride
R	
RE	Right eye
RER	Ribonucleotide excision repair
RISP	Rieske iron-sulphur protein
ROS	Reactive oxygen species
RRF	Ragged-red fibres
S	
SCD	Sudden cardiac death
SEM	Standard error of the mean
SLIRP	Stem loop-interacting RNA-binding protein
SOD	Superoxide dismutase
SSBR	Single strand break repair
SSBs	Single-strand breaks
ssDNA	Single-stranded DNA
T	
TBS-T	Tris buffer saline with Tween®20
TCA	Tricarboxylic acid
TEM	Transmission electron microscopy
TFAM	Mitochondrial transcription factor A

TFB2M	Mitochondrial transcription factor B2
TIM	Translocase of the inner membrane
TOM	Translocase of the outer membrane
TRMU	TRNA 5-Methylaminomethyl-2-Thiouridylate Methyltransferase
U	
UPRmt	Mitochondrial unfolded protein response
UPS	Ubiquitin-proteasome system
UQCRB	Cytochrome b-c1 complex subunit 7
UQCRC1	Cytochrome b-c1 complex subunit 1
UQCRC2	Cytochrome b-c1 complex subunit 2
UQCRQ	Cytochrome b-c1 complex subunit 8
UQCRH	Cytochrome b-c1 complex subunit 6
UQCR10	Cytochrome b-c1 complex subunit 9
W	
WES	Whole-exome sequencing
WGS	Whole-genome sequencing

ABSTRACT

Mitochondrial disorders are among the most frequent metabolic disorders and a major burden for society. There are more than 60 confirmed mitochondrial DNA (mtDNA) point mutations associated with several diseases. Since the mtDNA is highly polymorphic with peculiar properties, the pathogenicity of a novel sequence variation needs to be determined using a series of criteria, including functional studies, for establishing genotype/phenotype correlations.

The present study comprises four unclassified mtDNA variants with potential pathogenic effect, identified in four unrelated Portuguese patients suspected of mitochondrial disease, at Laboratory of Biochemical Genetics, Center for neuroscience and cell biology – University of Coimbra.

Patient 1 (P1) presented severe bilateral optic neuropathy. Patient 2 (P2) manifested severe intellectual disability, cerebellar atrophy, severe ataxia, coarse face, relative macrocephaly, congenital hypotonia, absent speech, and other features such as clinodactyly. Patient 3 (P3) presented chronic progressive external ophthalmoplegia. Finally, patient 4 (P4) was suspected of cardiomyopathy after sudden death. A mtDNA variant has been identified in each patient, affecting genes encoding subunits of oxidative phosphorylation (OXPHOS) enzymatic complexes or variants in mt-tRNA genes. The alterations identified were m.8418T>C, p.Leu18Pro (*MT-ATP8*), m.14771C>A, p.Pro9Thr (*MT-CYB*), m.7486G>A, mt-tRNA$^{Ser(UCN)}$ (*MT-TS1*) m.14706A>G, mt - tRNA^{Glu} (*MT-TE*), in patients 1, 2, 3 and 4, respectively.

Accordingly, a series of biomolecular studies, using a functional genomics' approach was conducted for evaluating the pathogenicity of the unclassified mtDNA variants, for establishing the genetic diagnosis of the patients and clarify the pathogenic mechanism.

The methods used included Sanger sequencing, pyrosequencing, next generation sequencing, long-range PCR, real-time PCR, histochemistry, histology, cell culture, western-blot, blue native polyacrylamide gel electrophoresis, spectrophotometry, fluorimetry, Seahorse Bioscience® technology and transmission electron microscopy.

The samples investigated included cultured fibroblasts (derived from skin biopsy) of the four patients described above plus three controls, and blood (family studies of P2 and P4, and controls), muscle (P3 and P4) and liver (P4) samples when available.

The functional evaluation in the skin fibroblasts of P1 showed a decrease in A6L protein level of complex V (encoded by *MT-ATP8* gene), a reduction of the fully assembled complex V, mitochondrial dysfunction (namely alterations in OXPHOS enzymatic activity and oxygen consumption, glycolysis, intracellular ATP levels, mitochondrial membrane potential and reactive oxygen species production) and evidences of endoplasmic reticulum stress.

In the cells of P2, a decrease in the cytochrome b levels and activity of complex III was observed. Moreover, in addition to mitochondrial dysfunction detected, the presence of multilamellar bodies were identified in skin fibroblasts, suggesting autophagy impairment.

Skin fibroblasts of P3 presented a reduction in the assembly of the four complexes with subunits encoded by mtDNA, mitochondrial dysfunction, changes in mitochondrial membrane potential and in the production of reactive oxygen species. Also, multilamellar bodies were observed in fibroblasts. Additionally, morphological and histochemical evidences for mitochondrial disease were detected in patient's muscle.

In P4, deficiency of OXPHOS enzymatic activity was only observed in muscle and liver biopsy, suggesting tissue specificity. The reduction in assembly of the four complexes with subunits encoded by mtDNA was the more significant finding detected in patient's fibroblasts, in addition to abnormal increase of mitochondria's size.

Furthermore, deeper molecular genetic investigation revealed a second mtDNA alteration in P3, described in association with the pathology, known as "common deletion". Also, a mutation in *SNX14* gene (P2) and a mutation in *MYBPC3* gene (P4) were detected, in parallel studies performed by other collaborators.

The present work allowed: (i) to confirm the high pathogenic potential of the four unclassified mtDNA variants; (ii) to report the variants showing functional evidences for its pathogenicity; (iii) to include these sequence variations in the genetic investigation of the patients presenting similar phenotypes; (iv) to contribute for significant developments in the field of mitochondrial diseases pathogenicity.

In conclusion, the evidences taken together suggest that: (i) the mtDNA variants analysed are probably involved in the observed mitochondrial dysfunction; (ii) mitochondrial impairment may influence cellular mechanisms, namely endoplasmic

reticulum stress and macroautophagy; (iii) mitochondrial diseases are heterogeneous and complex diseases that may have a double genetic origin, besides the known depletion or deletion-associated syndromes.

Keywords: mitochondrial DNA; mutation; pathogenicity; mitochondrial dysfunction; mitochondrial diseases; functional genomics.

RESUMO

As doenças mitocondriais são das doenças metabólicas mais frequentes e representam um grande encargo económico na sociedade. Atualmente, existem mais de 60 mutações no DNA mitocondrial (mtDNA) associadas a patologias. Uma vez que o mtDNA é altamente polimórfico e apresenta características peculiares, a patogenicidade de uma nova alteração detetada, apoia-se numa série de critérios para estabelecer a correlação genótipo-fenótipo.

O presente trabalho inclui o estudo de quatro variações de sequência no mtDNA, não classificadas, com potencial efeito deletério, identificadas em quatro doentes portugueses com suspeita de doença mitocondrial e sem parentesco, estudados no Laboratório de Bioquímica Genética, Centro de Neurociências e Biologia Celular e Molecular – Universidade de Coimbra.

O doente 1 (P1) apresentou neuropatia ótica bilateral grave. O doente 2 (P2) manifestou deficiência mental grave, atrofia cerebelar, ataxia grave, fácies grosseira, macrocefalia relativa, hipotonia congénita, afasia, e outras características tal como clinodactilia. O doente 3 (P3) apresentou oftalmoplegia externa progressiva crónica. O doente 4 (P4) sofreu morte súbita infantil, com a suspeita posterior de cardiomiopatia.

Foi identificada uma variante no mtDNA em cada doente em genes que codificam subunidades dos complexos enzimáticos da fosforilação oxidativa ou RNAs de transferência. As variantes identificadas foram m.8418T>C, p.Leu18Pro (*MT-ATP8*), m.14771C>A, p.Pro9Thr (*MT-CYB*), m.7486G>A, mt-tRNA$^{Ser(UCN)}$ (*MT-TS1*), m.14706A>G, mt-tRNA^{Glu} (*MT-TE*), nos doentes 1, 2, 3 e 4, respetivamente.

Foram realizados estudos biomoleculares, usando uma abordagem de genómica funcional para avaliar a patogenicidade das variantes no mtDNA de forma a estabelecer o diagnóstico genético dos quatro doentes e clarificar o mecanismo de patogenicidade.

Os métodos usados incluíram sequenciação de Sanger, pirosequenciação, sequenciação de nova geração, PCR longo e PCR em tempo real, histologia, histoquímica, cultura de células, espectrofotometria, fluorimetria, *Western-blot*, eletroforese nativa em gel de acrilamida, tecnologia *Seahorse Bioscience*® e microscopia de transmissão eletrónica.

As amostras investigadas foram obtidas a partir da cultura primária de fibroblastos (derivada de biópsia de pele) dos quatro doentes descritos acima e de três controlos,

além de sangue (estudo familiar dos P2 e P4, e controlos), músculo (P3 e P4) e fígado (P4).

A avaliação funcional nas células do P1 mostrou um decréscimo nos níveis da proteína A6L (codificada pelo gene *MT-ATP8*) do complexo V, uma redução do *assembly* do complexo V, disfunção mitocondrial (nomeadamente alterações na atividade enzimática da cadeia respiratória mitocondrial, consumo de oxigénio, glicólise, níveis de ATP intracelulares, potencial de membrana mitocondrial e produção de espécies reativas de oxigénio), com evidencias de stresse no reticulo endoplasmático.

Nas células do P2 foi detetada disfunção mitocondrial, com diminuição dos níveis da proteína citocromo b e da atividade do complexo III. Observou-se também a presença de corpos multilamelares, sugerindo um comprometimento da autofagia.

Os fibroblastos do P3 apresentaram redução no *assembly* dos quatro complexos com subunidades codificadas pelo mtDNA, disfunção mitocondrial, alterações no potencial de membrana mitocondrial e na produção de espécies reativas de oxigénio, bem como a presença de corpos multilamelares. Foram ainda detetadas evidências histoquímicas e morfológicas, sugestivas de doença mitocondrial, no músculo.

No P4, a deficiência na atividade enzimática da fosforilação oxidativa foi detetada apenas na biópsia de fígado e músculo, o que sugere a existência de especificidade tecidular. A redução no *assembly* dos quatro complexos com subunidades codificadas pelo mtDNA foi o resultado mais significativo, além do aumento anormal do tamanho das mitocôndrias.

Para além disso, a investigação genética revelou uma segunda alteração (conhecida como “deleção comum”) no mtDNA (P3), descrita em associação com a patologia. Foi ainda detetada uma mutação no gene *SNX14* e outra no gene *MYBPC3* nos P3 e P4, respetivamente, em estudos paralelos realizados por colaboradores.

O trabalho permitiu: (i) confirmar o potencial patogénico das quatro variantes no mtDNA; (ii) reportar variantes com evidências funcionais de patogenicidade; (iii) incluir estas variantes na investigação genética de doentes que apresentem fenótipo semelhante; (iv) contribuir para desenvolvimentos significativos na patogenicidade em doenças mitocondriais.

Em conclusão, as evidências sugerem que: (i) as variantes analisadas estão provavelmente envolvidas na disfunção mitocondrial; (ii) défice mitocondrial pode influenciar mecanismos celulares, nomeadamente stresse no reticulo endoplasmático e a macroautofagia; (iii) as doenças mitocondriais são heterogéneas e complexas, com possível dupla origem genética, além das associadas a síndromes de depleção/deleção, já conhecidas.

Palavras-chave: DNA mitocondrial; mutação; patogenicidade; disfunção mitocondrial; doenças mitocondriais; genómica funcional.

Chapter 1 – General introduction

Mitochondria are ubiquitous organelles in most eukaryotic cells, having a size of ~1µm. On average, there are ten to thousand mitochondria per cell, depending on the energetic demands. Accordingly, in cells that are metabolically more active, and therefore, have higher energy requirements, the amount of mitochondria is higher[1].

Each eukaryotic cell has a variable number of mitochondria which exhibit a spherical or rod-shape in a large reticular network, forming tubular or punctate structures, as they can fuse and divide[2,3], with variable morphology shape in different tissues.

Analysis by transmission electron microscopy (TEM) revealed a double-membrane structure, the outer (OMM) and the inner mitochondrial membrane (IMM). The OMM individualizes mitochondria from the cytosol. The IMM is creased into a series of internal folds named cristae, and define two internal compartments: the intermembrane space (IMS), between the outer and the inner membranes; and the matrix, bounded by IMM.

Each of the mentioned components has specific features according to their role in mitochondrial function. The OMM is permeable to small molecules and ions, due to the presence of integral proteins, such as aqueous channels (porins). Large molecules (>10kDa) are translocated by a complex of membrane proteins that form the translocase of the outer membrane (TOM), as they are mitochondrial targeted proteins[4].

The IMM has also a complex to import proteins from the IMS to the matrix, the translocase of the inner membrane (TIM)[4]. In addition, transport shuttles are responsible for the flux of adenosine triphosphate (ATP), adenosine diphosphate (ADP), pyruvate, Ca^{2+}, H^{+}, citrate, among others, since the IMM is almost impermeable to ions and polar molecules, due to its lipid bilayer composed by high proportion of the IMM-specific phospholipid cardiolipin. This selective permeability allows the generation of gradients that are essential to the mitochondrial function maintenance. The fact that the IMM is creased, forming cristae, increases the total surface area, in order to increase the efficiency of the energy production in the process of oxidative phosphorylation (OXPHOS), at the mitochondrial respiratory chain (MRC) “units”, inserted in this membrane.

The matrix contains several molecules of mitochondrial DNA (mtDNA), ribosomes, and many enzymes that catalyse essential reactions to cell homeostasis, since key metabolic processes, such as Krebs cycle, β-oxidation of fatty acids and urea cycle, take place in this mitochondrial compartment.

Mitochondria harbour the major enzymatic systems used to complete the oxidation of carbohydrates, fats and proteins in order to produce energy in the form of ATP. Each of the three substrates can be converted to acetyl coenzyme A (acetyl-CoA) that is integrated in the tricarboxylic acid (TCA) cycle, also known as citric acid cycle or Krebs cycle, taking place in the mitochondrial matrix. Carbohydrates enter into mitochondria as pyruvate and are converted to acetyl-CoA by the pyruvate dehydrogenase. Fatty acids are converted to acetyl-CoA inside the mitochondria, through β-oxidation. On the other hand, several enzymes are responsible for the conversion of specific amino acids into pyruvate, acetyl-CoA or into TCA intermediates.

The TCA cycle is composed by seven subsequent enzymatic steps, where the electrons removed during the process are transferred to the substrate nicotinamide adenine dinucleotide (NADH) and flavin adenine dinucleotide ($FADH_2$), which in turn, carry this free energy to the MRC. The MRC consists of five multisubunit protein complexes, embedded in the IMM, where the OXPHOS process occurs, culminating in the synthesis of ATP[5].

Mitochondria are in continuous communication with the cytosol in order to coordinate the balance between energy demands of the cell and energy production by OXPHOS. Therefore, some other functions are mediated by mitochondria (Figure 1.1), namely the reactive oxygen species (ROS) production and detoxification, regulation of calcium homeostasis, biosynthesis of *haem* and iron-sulphur clusters, metabolism of lipids, cholesterol, steroids, nucleotides, immune response and apoptosis[2,6–9].

The regular metabolism of oxygen generates ROS mainly at the MRC, as a by-product, which are essential in several processes of cell signalling to control cell proliferation and differentiation, and contribute to adaptive stress pathways, including hypoxia[7,10].

Calcium is fundamental for many processes that are associated with increased demand of energy (e.g. secretion, contraction, motility, electrical excitability), which require increased energy provision. During these processes, cytosolic Ca^{2+}

concentration $[Ca^{2+}]_c$ increases, promoting mitochondrial Ca^{2+} uptake, as Ca^{2+} moves down its electrochemical potential gradient into the matrix, through the selective channel in the IMM – mitochondrial calcium uniporter (MCU). In the matrix, the rise of the Ca^{2+} concentration activates enzymes of TCA cycle in order to stimulate ATP synthesis[11,12], and it also increases the mitochondrial biogenesis by interacting with the calcium/calmodulin-dependent protein kinase kinase 2 (CAMKKβ) to activate the peroxisome proliferator-activated receptor γ coactivator 1- alpha (PGC1α)[13]. Another function of calcium regulation is associated to cellular signalling, namely the activation of apoptotic cascade, leading to cell death.

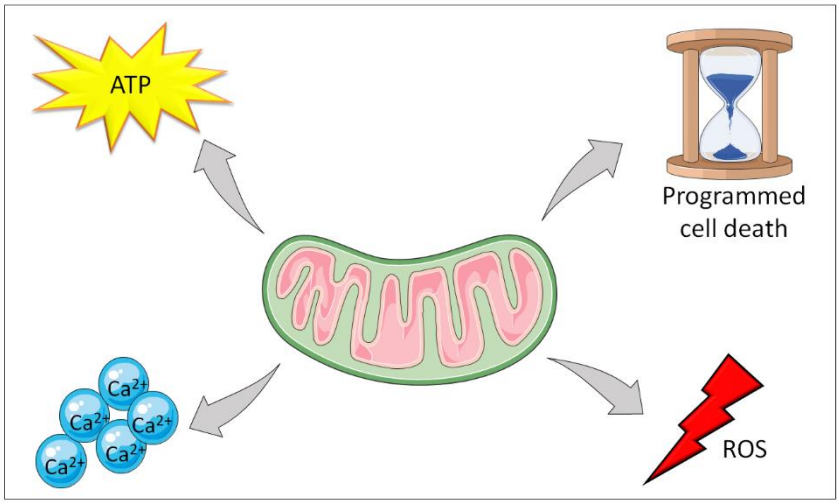

Figure 1.1 - Mitochondrial functions. Mitochondria are the major source of energy in form of ATP, for cells, and they are responsible for the intrinsic pathway of programmed cell death, calcium (Ca^{2+}) signalling and reactive oxygen species (ROS) production and detoxification.

Mitochondria are responsible for the intrinsic pathway of programmed cell death or apoptosis[14]. The B-cell lymphoma 2 (Bcl-2) family proteins are the first regulatory mediators for mitochondrial apoptosis. They can be divided in three major groups: the pro-survival group (e.g. Bcl2, Bcl-xL, Mcl-1); the pro-apoptotic BH123 protein group (Bax and Bak); and the BH3 domain-only proteins (Bad, Bid, Bim, Puma and Noxa), also known as apoptosis initiator group. After a death stimulus, the modification of OMM proteomics, namely the increased expression of BH3 domain-only proteins, lead to the release of Bax/Bak, culminating in OMM permeabilization and cytochrome c (Cyt *c*) release from the IMS to the cytoplasm. In cytosol, this essential component of the MRC

binds to the apoptotic protease activating factor-1 (Apaf-1), inducing the apoptosome formation, a wheel-shaped homo-heptameric Apaf-1 complex. The recruitment of the initiator procaspase-9 allows the activation of apoptosome and trigger the downstream caspases, such as caspase-3 and caspase-7, to complete the apoptotic process[12,15].

Recent evidences have demonstrated that Cyt *c* release and caspases activation are also involved in other biological processes, suggesting that these events are not always a "point of no-return" of mitochondrial programmed cell death. In fact, this mitochondrial pathway may act according to the biological context[16]. However, the mechanisms underlying this process remain unclear.

1.1 Mitochondrial genome

Since the existence of the mtDNA was revealed[17,18], its biology has been extensively studied.

In humans, mtDNA is a small, closed, circular and double-stranded molecule of 16,568-base pairs, which contains 37 genes (Figure 1.2). Of these, 13 are polypeptides that are structural subunits of OXPHOS: seven (ND1-3, ND4L, ND4-6) for complex I (CI) subunits, one (cytochrome b, CYB) for complex III (CIII), three (CO1-3) for complex IV (CIV) subunits, and two (ATP6 and ATP8) for complex V (CV) subunits. The remaining 24 genes code for two ribosomal RNAs (12S rRNA and 16S rRNA) and 22 transfer RNAs (tRNA), required for the mtDNA translation[19,20]. In addition, mtDNA contains the D-Loop region, a ~1,000bp non-coding region, so-called control region because it is responsible for regulation of mtDNA replication and transcription.

The two strands of mtDNA present heterogeneous nucleotide composition, as the 'light' strand (L) is rich in pyrimidines while the 'heavy' strand (H) is rich in purines. Most of genes encoding proteins, the two rRNAs, and 14 of the 22 tRNAs are included in the H-strand while eight tRNAs and the *MT-ND6* gene are located in the L-strand.

The mammalian mtDNA is one of the most compact pieces of genetic information, since it lacks introns, intergenic sequences are either absent or limited to a few bases and, in some cases, genes overlap (*MT-ATP8/6* and *MT-ND4L/4*).

The mtDNA is organized in compact protein-DNA complexes designated as nucleoids that appear to be tethered to the IMM[13,21]. This high degree of compaction is achieved by the mitochondrial transcription factor A (TFAM) that wraps the mtDNA molecules, in order to stabilize the mtDNA[22]. It is hypothesized that the sequestration of mtDNA into nucleoids acts as a protective mechanism, since the mtDNA does not contain protective histones.

Several unique features associated with mtDNA are important to understand and define the mitochondrial genetics.

Human mtDNA is found in multiple copies (up to thousands) per cell, since each mitochondrion contains from two to ten copies. Usually, all mtDNA molecules in a cell or tissue are identical (homoplasmy) but in the case of mitochondrial disease, a mixture of mutant and wild-type mtDNA may exist within the same cell or tissue (heteroplasmy)[23]. The quantity of mutant mtDNA may vary among individuals within the same family, and also from organ to organ or tissue to tissue, within the same individual[24]. A minimum critical number of mutant mtDNA molecules known as "threshold effect" is required to cause mitochondrial dysfunction in a particular organ or tissue, and, consequently, to induce a mitochondrial disease in an individual[25]. It is widely accepted that mutation load must be quite high (> 50%) to induce pathology[2,26].

The mtDNA is maternally inherited[27] and, in the case of heteroplasmic mutations, the inheritance pattern is complicated by a genetic bottleneck effect in the female germline, which means that the transmission of mtDNA molecules from mother to offspring is random and unpredictable, since only a subset of mtDNA molecules from mother will be transmitted[28–30]. Then, if the mother harbour 50% of a mtDNA mutation in her oogonia, the zygote may harbour 80%, through the random inheritance of mtDNA molecules, and the child likely will be affected, or the baby may inherit 40% or even less, and the child will be probably healthy. The bottleneck effect and the maternal inheritance contribute to ensure that mtDNA mutations do not spread through the population[2]. However, this evolutionary "protection" is responsible for the occurrence of a high number of families harbouring extremely rare or private mtDNA mutations, resulting in rare pedigrees. However, even if a pathogenic mtDNA alteration is present in the fetus, there is a possibility of the child to be healthy, since during cell division, mitochondria are randomly included into daughter cells, through a

process called mitotic segregation. So, in the case of heteroplasmy, the distribution of the mutation in daughter cells is approximately the same mutation load as the parental cells, but some daughter cells may have mutated mtDNA molecules in higher or fewer proportions. These genetic principles may explain the nature of different levels of heteroplasmy at the cellular and tissue level.

Mitochondria have independent mtDNA replication, transcription, translation and repair systems, but dependent on nuclear genes (Figure 1.2A). These processes occur with a semi-autonomous regulation, since mitochondrial proteins coded by nuclear DNA (nDNA) are responsible for regulating these processes, including the assembly of the OXPHOS complexes, the involved in maintenance, expression, transcription and translation of mtDNA and the mitochondrial dynamics. Indeed, these proteins and the remaining OXPHOS subunits are synthesized in cytosol, and imported into mitochondria[28,29,31].

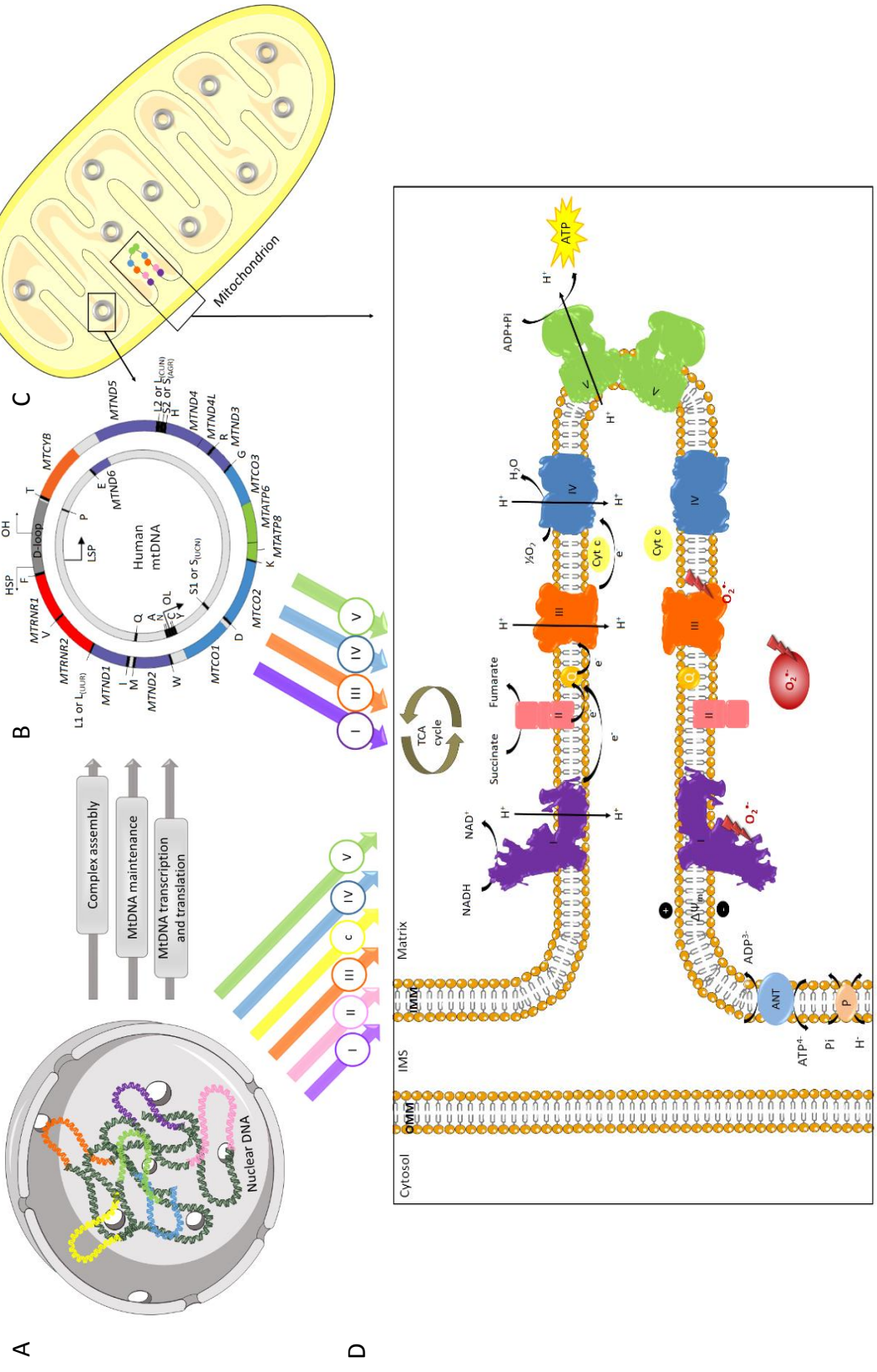

Figure 1.2 - Mitochondrial respiratory chain biogenesis involving mitochondria-nucleus crosstalk. Nuclear DNA **(A)** interacts with mitochondrial DNA molecules **(B)** that are present in several copies inside the mitochondrion **(C)** for encoding all the subunits of mitochondrial respiratory chain **(D)** complexes. The nuclear-encoded proteins include structural subunits, proteins involved in replication, transcription and translation of mtDNA, complex assembly factors, and mitochondrial membrane proteins. The process of oxidative phosphorylation (OXPHOS) uses an electrochemical gradient across the complexes (I-IV) localized in the inner mitochondrial membrane (IMM) to generate adenosine triphophate (ATP) at complex V site. ANT: ADP/ATP translocase Cyt c: cytochrome c; IMS: intermembrane space; OMM: outer mitochondrial membrane; P: phosphatase carrier protein, Q: Coenzyme Q; TCA: tricarboxilic acid.

1.1.1 Replication

It is well established that mtDNA replication is "independent" of the nDNA replication, and the cell cycle. However, all proteins responsible for the mtDNA replication are coded by the nuclear genome, translated in the cytosol and imported for mitochondria, revealing the essential role of nDNA in the mtDNA copy number maintenance.

Replication and transcription of mtDNA are coupled in mitochondria, and share some proteins. For example, the only replicative DNA polymerase known in mammalian mitochondria, DNA polymerase γ (POLG), is involved in both processes. This holoenzyme consists of a large catalytic subunit and two accessory subunits, being also essential in proofreading and DNA binding. The single-stranded DNA binding protein (mtSSB) is involved in DNA stability; mitochondrial DNA helicase (Twinkle) has been shown to unwind DNA during the replication. The TFAM protein is essential in the initiation of replication and transcription. Some other transcription factors and ligases, such as topoisomerases, ligases and RNaseH complete the pool of mitochondrial proteins belonging to the mitochondrial replisome. Mitochondrial RNA polymerase (POLRMT) serves to produce not only transcripts, but also primers needed for mtDNA replication[8].

Briefly, the helicase Twinkle moves on one DNA strand, separating double-stranded DNA into single-stranded DNA (ssDNA). The POLG perform DNA synthesis using the template released by Twinkle while the mtSSB protects the template from nucleolysis.

The mechanism for mtDNA replication remains controversial, since at least three models have been described (recently reviewed in McKinney *et al.* (2013), Holt and Jacobs (2014) and Pohjoismaki *et al*. (2011)[32–34]). The original asynchronous strand-displacement model was considered the accepted model for over 35 years[35]. This model proposed the initiation of the synthesis of the leading strand (heavy strand) within the D-loop region in a site designated as O_H, and as the leading strand synthesis continues, a larger displacement parental H strand is synthesized, preserved in a single-stranded form. Then, H-strand replication exposes the origin of the lagging strand (or light [L] strand,) – O_L, allowing replication of the new lagging strand to

initiate in the opposite direction. Therefore, replication is continuous, asymmetric and asynchronous.

In the second model, referred as the strand-coupled model[36], replication starts at a broad area beyond the D-loop, and proceeds bidirectionally as the conventional double-stranded replication forks through continuous synthesis of leading and discontinuous synthesis of lagging strand. This model relies on the incorporation of Okasaki fragments during lagging strand synthesis, as replication intermediates, and two polymerases working in a single replisome, which existence needs to be demonstrated.

More recently, a third model was proposed[37], based on the observation of RNA incorporation throughout the lagging strand (RITOLS), using two-dimensional agarose gel electrophoresis. This model implicates the strand-coupled replication proceeding unidirectionally from the D-loop region, with the incorporated RNA intermediates being maturated into DNA. Then, displaced H-strand occurs not as a single-stranded DNA, but rather as a DNA/RNA hybrid, until the duplex is made by POLG. Recent studies identified the RNA/DNA hybrids are present in vivo, using *in organelle* DNA synthesis and inter-strand crosslinking experiments[38].

A plausible hypothesis to understand the complexity of the different models for mtDNA replication could be that different models may operate in different tissues and cell types, and represent adaptive processes to ensure appropriate mtDNA maintenance[32].

1.1.2 Transcription

The production of functional RNA molecules required for protein synthesis involves transcription, nucleolytic processing, post-transcriptional modifications, polyadenylation of mitochondrial messenger RNA (mt-mRNA) and aminoacylation of mt-tRNA. However, the details of how these processes occur are still unclear[39,40].

The mammalian mtDNA contains a main promotor, at the D-loop region, for the transcription of each strand designated the H-strand promotor (HSP) and the L-strand promoter (LSP), allowing that the transcription of mtDNA occurs in both mtDNA strands. The transcripts are polycistronic, and produce long transcripts coding mt-

mRNAs, mt-rRNAs and mt-tRNAs[39,41]. The transcription initiation core machinery consists of POLRMT, responsible for RNA synthesis, and at least two transcription factors – TFAM and mitochondrial transcription factor B2 – TFB2M[39]. The TFAM introduces a "U-turn" at LSP of mtDNA, mediating the activation of the transcription; TFB2M is a component of the catalytic site of POLRMT, necessary for transcription initiation[42–44]. The mitochondrial transcription termination factor (MTERF) has also been implicated in transcription initiation[45] and termination to enhance the production of rRNAs, by binding upstream and downstream from transcriptional units, facilitating the transfer of POLRMT from the termination site to the initiation site[46,47].

After the transcription of two long transcripts, one originated from HSP and the other from LSP, the mitochondrial RNA-processing machinery acts in these transcripts in order to release the individual tRNAs, rRNAs, and mRNAs. The processing is initiated on the tRNA sequences through the cleavage at the 5'-end by the RNase P, followed by RNase Z cleavage at the 3'-end, in order to release the mRNAs and rRNAs flanked by tRNAs. However, it is not clear how mRNAs not flanked by tRNAs are processed. The present evidences indicate that the early transcript processing takes place co-transcriptionally in distinct small spots called mitochondrial RNA granules (MRGs)[48–50], followed by a second round of processing outside the MRGs[51].

Maturation steps occur after the release of the mtDNA encoded mRNAs. Then, all mRNAs contain short polyadenylation tails incorporated by MTPAP (mitochondrial poly(A) polymerase), with the exception of MT-ND6. However, the exact role for mitochondrial poly(A) tails is still unknown[39]. Additionally, the regulation of mRNA stabilization is usually mediated by protein complexes. Accordingly, the leucine-rich pentatricopeptide repeat (PPR)-containing (LRPPRC) protein and stem loop-interacting RNA-binding protein (SLIRP) form a stable complex that seems to act synergistically to promote mRNA stability[39,52].

After processing by RNaze Z, the 3' –end of tRNAs is altered by addition of CCA, followed by post-transcriptional modifications, essential for its function, which can be divided into two subgroups: those that are important for the stability and correct folding of the overall structure and those that alter tRNA function by modifying tRNA interaction with other factors and codon-anticodon recognition[39,51]. Several enzymes are involved in mt-tRNA modifications, including the tRNA 5-Methylaminomethyl-2-

Thiouridylate Methyltransferase (TRMU) and the Pseudouridylate Synthase 1 (PUS1). Subsequently, mt-tRNAs are charged with the specific amino acid by aminoacyl-tRNA synthetases (aaRs), before the translation.

The mitoribosome is unique compared to its bacterial and cytoplasmic counterparts[53,54]. The complete mammalian mitoribosome (55S) comprises the large subunit (39S), containing the 16S rRNA and 50 mitochondrial ribosomal proteins (MRP), assembled with the small subunit (28S), containing the 12S rRNA, and more than 29 MRP[55]. Before the assembly of mitoribosome, rRNA is submitted to post-transcriptional modifications in some residues, necessary for correct folding, stability and assembly[39,51].

1.1.3 Translation

Mitochondria contain specific protein synthesis machinery distinct from their cytosolic counterparts, more similar to those from bacteria, allowing the synthesis of polypeptides encoded by mtDNA. The process requires not only tRNA and rRNA encoded by mtDNA, but also hundreds of nuclear encoded proteins, such as ribosomal proteins, aminoacyl-tRNA synthases, tRNA modification enzymes, rRNA base-modification enzymes, and initiation, elongation, termination and recycling factors[56,57].

The mechanisms involved in mitochondrial translation follow the same major steps: initiation, elongation, termination and recycling of the ribosome[56,58]. However, the current understanding of the detailed events underlying the human mitochondrial translation is far from being complete[56].

The mitochondrial translation starts with the formation of the initiation complex, composed by the mitorribosome, the tRNA carrying formylated methionine ($tRNA^{fM}$), mRNA and initiation factors (mtIF2 and mtIF3)[51,57]. When the appropriate start codon is present, the $tRNA^{fM}$ associates with the mitoribosome and mRNA, releasing initiation factors, stimulating the elongation step. Then, mitochondrial elongation factor (mtEFTu) corrects the codon anti-codon pairing, with energy consumption by GTP hydrolysis. Aminoacylated tRNA moves from the A-site (aminoacyl or acceptor site) to the P-site (peptidyl site) of the mitoribosome, in where the peptide bond formation is catalysed, extending the growing polypeptide chain. Next, the elongation factor G1

(mtEFG1) catalyses the elongation step, simultaneously moving the deacylated tRNA from the P to the E-site (Exit site). This elongation repeats itself until the mitochondrial release factor recognizes the stop codon, inducing hydrolysis of the peptidyl-tRNA bond in the A-site, and, consequently, release of the mature protein. Finally, mitochondrial recycling factors (mtRRF1 and mtRRF2) induce the dissociation of the mRNA from mitoribosome, and the disassembly of the two mitoribosome subunits[51,58].

Evidence is accumulating to assert that the mitoribosome is normally bound to the IMM in order to facilitate the co-translationally insertion of peptides[59].

The mitochondrial genetic code has some differences from the nuclear genetic code, such as the codons AUA and AUG that code for methionine, the codon UGA that codes for a tryptophan instead of the usual STOP codon[56] and finally, the existence of only two stop codons (UAA and UAG)[60]. The codons AGA and AGG were also considered STOP codons for thirty years, which is presently the cause of a continued debate between different authors.

After the translation of the mtDNA-encoded proteins, post-translational processes are required for the correct incorporation of mtDNA-encoded and nDNA-encoded proteins at the IMM[56,57]. Therefore, chaperones and proteases are responsible for the quality control system of proteins through the folding and assembly or proteolytic degradation, followed by the insertion and assembly of the subunits in the IMM[57].

1.1.4 mtDNA damage and mechanisms of repair

Sequence variations in mtDNA can arise through spontaneous errors of DNA replication or through the unrepaired chemical damage to mtDNA.

Spontaneous replication errors by POLG are most likely responsible for the accumulation of mtDNA point mutations and deletions in ageing[61]. On the other hand, mtDNA suffers chemical damage from endogenous and exogenous origin, resulting in mutations. A major source of chemical damage to mtDNA is oxidative damage, caused by ROS[61]. In fact, the increased susceptibility of mtDNA to oxidative damage leads to a mutation frequency much higher than that of the nuclear genome[62].

There are several types of mtDNA damage resulting from different origins[63]. Alkylation damage may be caused by exogenous (e.g., chemotherapy drugs) or endogenous (e.g., S-adenosylmethionine) agents. Hydrolytic damage induces the formation of abasic sites and hydrolytic deamination of bases. The synthesis of adducts may be caused by exogenous (e.g., tobacco smoke or UV radiation) and endogenous (e.g., estrogens) substances. Mismatched bases may arise from replication errors or incorporation of nucleotides containing modified bases during the replication process. The DNA strand breaks can be divided into single-strand breaks (SSBs) and double-strand breaks (DSBs), and both types can be induced by direct or indirect (e.g., in the process of the repair of lesions) noxious stimuli[63]. Oxidation damage affects DNA bases and may originate abasic sites and SSBs[64].

It has been claimed for a long time that mitochondria have no efficient repair mechanisms because of the high rate of mutations accumulated in mtDNA. However, recent evidences suggest that specific repair processes are present in these organelles[3,61]. Currently, one main pathway is known to repair mtDNA lesions – Base excision repair (BER). This mechanism recognizes oxidized or damaged bases that are cleaved by a specific glycosylase, remaining an abasic site that is cleaved on the 5' end by the AP endonuclease to generate a nick with a 5'deoxyribose phosphate flap. At this point, the mechanism is different according to the number of damaged bases. Accordingly, during the single-nucleotide BER, mitochondrial POLG cleaves the 5'deoxyribose phosphate moiety and fills the gap. On the other hand, the long-patch-BER requires an activity to remove the displaced 5'-flap structure[61,63,64]. The BER specifically acts on oxidized bases, as well as alkylation and deamination of DNA bases[64].

The nonhomologous end joining (NHEJ) and homologous recombination (HR) activities, which repair double-stranded DNA breaks included in nuclear DNA, have been detected in mammalian mitochondria[64,65]. There is limited evidence of mismatch repair (MMR) activity in mitochondria, and no report of such a mechanism in higher eukaryotes was published. Also, the localization of mitochondrial single strand break repair (SSBR) remains a controversial issue. On the other hand, no evidence was found for a nucleotide excision repair system (NER) or ribonucleotide excision repair system (RER) in mitochondria[61,65].

1.2 Mitochondrial respiratory chain

The MRC (Figure 1.2D), which is vital for human life, catalyses the oxidation of fuel molecules, derived from the intermediate metabolism, and concomitant energy transduction into ATP via five complexes, embedded in the IMM, by the process of OXPHOS[5,20].

The MRC is composed of five multisubunit complexes (CI to CV) and two mobile electron carriers, coenzyme Q (CoQ), or ubiquinone, and Cyt *c*, containing approximately 90 different structural protein subunits. This system produces a transmembrane proton gradient that is dissipated by the CV to synthesize ATP.

All multisubunit complexes of MRC, except complex II (CII), have a double genetic origin and, therefore, they are under dual genetic control of both the mitochondrial and nuclear genomes.

1.2.1 Components, assembly and respirasome

Complex I (NADH: ubiquinone oxidoreductase or NADH dehydrogenase) is a L-shaped enzyme containing an hydrophobic domain embedded in the IMM, which contains all the seven mtDNA-encoded subunits, and an hydrophilic peripheral arm, protruding into the mitochondrial matrix, containing only nDNA-encoded subunits, the NADH binding site and the iron-sulphur clusters. This bigenomic encoded structure can be divided in three functional modules: the P module constitutes the majority of the "membrane" arm, including the seven mtDNA-encoded subunits (MTND1-3, MTND4L, MTND4-6), and it is responsible for proton translocation; the N module contains the dehydrogenase site for the oxidation of NADH to NAD^+; the Q module holds the hydrogenase site for the electron transfer to CoQ[66]. The entire complex consists of 45 subunits and almost 1MDa in mass.

Complex II (Succinate dehydrogenase or succinate: ubiquinone oxidoreductase) catalyses the oxidation and dehydration of succinate to fumarate, being also a component of the TCA cycle. Besides, Complex II is the smallest (~ 130kDa) MRC complex and it is the unique to be entirely coded by the nuclear genome. This enzyme

comprises four polypeptides, two hydrophilic subunits containing FAD as a prosthetic group alongside iron-sulphur clusters, and two hydrophobic subunits, responsible to anchor the complex to the IMM, containing a *haem b* moiety[67,68].

Complex III (Ubiquinol: cytochrome *c* oxidoreductase or cytochrome bc1 complex) forms a dimer structure where each monomer comprises eleven subunits, from which only one is encoded by mtDNA – cytochrome b (MT-CYB), located centrally in the transmembrane region. The remaining subunits are nDNA-encoded, namely the cytochrome c1 (CYC1), the Rieske iron-sulphur protein (RISP), two relatively large "core" proteins and other eight smaller proteins[69]. Each monomer harbour a Rieske - type iron-sulphur cluster in the RISP, two Fe-containing *haem* moieties of MT-CYB and a c-type *haem* where Cyt *c* binds, forming the catalytic redox core of CIII[69]. The exact function of the other subunits remains to be established[70].

Complex IV (cytochrome *c* oxidase, COX) is composed of two copper centres (CuA and CuB), two iron sites (*haem a* and *a3*), as well as zinc and magnesium sites[9], two cytochromes and thirteen different protein subunits, three of which are mtDNA-encoded, MTCO1-3[3,71,72]. The central core is composed by MTCO1 and MTCO2, whilst MTCO3 and the remaining nDNA-encoded subunits constitute the structural scaffold around the central core[73]. The MTCO1-3 subunits allow the electron and proton transfers, and the nuclear-encoded subunits may participate in the modulation of the physiological activity of COX[71].

Complex V (F_1F_0 ATP synthase or ATP synthase) is a multi-subunit complex containing two domains: the hydrophobic F_0 domain is a subcomplex embedded in the IMM, containing subunits that form a rotor-like structure harbouring a proton channel; the F_1 domain is a soluble component that drops into mitochondrial matrix and contains the binding site for ADP and phosphate (Pi), allowing the ATP synthesis through a sequence of conformational changes. These two functional domains are physically connected to each other by two structures: an elongated peripheral stalk that anchors the head of the F_1 domain on the IMM to form the external stator, and a centrally located stalk. The complex V acts as a rotary molecular motor. The rotor (c-ring) is formed by the transmembrane proton channel of the F_0 domain, which transfers the energy created by the differential gradient through the stalk to F_1.

In addition to the complexes, there are two co-factors essential for the OXPHOS process: CoQ and Cyt *c*. The CoQ is a lipid soluble carrier molecule that cycles between a fully oxidized (ubiquinone), semiquinone (ubisemiquinone), and a fully reduced (ubiquinol) state, and it is also involved in nucleotide biosynthesis and antioxidant mechanisms[74]. The Cyt *c* is a low-molecular weight (13kDa) haemoprotein that also plays a role in apoptosis[3,75].

Functional complexes require structural integrity that is maintained by the assembly factors[3].

The most recent model of CI assembly mechanism is based on the independent assembly of the membrane and the peripheral arms, via sequential insertion of subcomplexes that join together to form the characteristic L-shaped structure[76], involving at least eleven assembly factors[77].

The current model for CII assembly is based on the evidence that only two assembly factors and the *haem b* are involved in its assembly and stability[78].

The current model for CIII assembly in humans include an initial subassembly in which MT-CYB join with two other CIII proteins (Cytochrome b-c1 complex subunit 7 – UQCRB and Cytochrome b-c1 complex subunit 8 – UQCRQ) that are later incorporated by a second subassembly, where CYC1 is combined with the two core proteins (Cytochrome b-c1 complex subunit 1 – UQCRC1 and Cytochrome b-c1 complex subunit 2 – UQCRC2), followed by the cytochrome b-c1 complex subunit 6 (UQCRH) and cytochrome b-c1 complex subunit 9 (UQCR10), to form the pre-complex III (pre-$CIII_2$). At this point, the complex is already dimeric, but the precise stage at which the dimerization occurs is currently unclear. Finally, the remaining subunits are incorporated sequentially to the pre-complex of 500kDa, in order to form the enzymatic active CIII[69,73,79]. Currently, six proteins involved in CIII assembly are known in humans[79].

The CIV assembly begins with the insertion of MTCO1 into the IMM, and the insertion of *haem a*, *a3* and CuB into MTCO1. Then, two nuclear-encoded subunits (COX4 and COX5A) are incorporated to allow that MTCO2, associated with the CuA centre, join to form the second assembly intermediate. Afterwards, MTCO3 and smaller subunits are sequentially incorporated, leading to the formation of a holocomplex monomer (~230kDa). Finally, COX dimerizes in an active structure that

contains the cytochrome *c* binding site[69]. Approximately twenty assembly factors are known for complex IV[71,80].

Recent studies suggest that human mitochondrial ATP synthase assembles from two subcomplexes, F_1-c-ring and the b-e-g complex[81]. Therefore, the F_1 domain join, through the stalk, with the pre-formed c-ring of F_0 domain in the IMM, and at the same time, subunits "b", "e" and "g" join together, following the subunit "d", oligomycin sensitivity-conferring protein (OSCP) and F6, in order to complete the stator. The only two mtDNA-encoded proteins (MT-ATP6 and MT-ATP8 or subunit "a" and A6L, respectively) belongs to F_0 and they connect to the stator in the final step of CV monomer (~700 kDa) assembly[81]. The subunit "a" binds to the c-ring to form the integral membrane proton channel, while the A6L subunit is presumed to provide physical link between the proton channel and the stator[82,83]. These last assembled subunits have also a role in forming dimeric and higher oligomeric forms of ATP synthase that seem critical to maintain the shape of mitochondria by promoting the formation of the cristae of IMM[69,84–86]. Currently, only two assembly factors are known, being responsible for joining the α and β subunits of the c-ring.

There have always been two points of view about the organization of the MRC enzymes and co-factors in the IMM. The first model called "solid state" model defended that the components were rigidly held together in a structure ensuring the accessibility and activity[87]. In 1955, Chance and Williams were the first to propose that MRC enzymes exist as a single unit of respiration[88]. On the other hand, Hafeti and colleagues showed that when individual complexes were isolated, they exhibit biochemical activity[89], giving rise to the classic or "fluid state" model. This model defends the existence of two mobile electron carriers, CoQ and Cyt *c*, which are responsible for the "connection" of the enzymatic complexes[90]. Some years later, the isolation of Complex III/IV from bacteria and yeast[91–95] was not explained by the classic model. Finally, the use of blue native polyacrylamide gel electrophoresis (BN-PAGE) to study bovine mitochondria showed Complex I, III and IV in supercomplexes[96]. The most common supercomplexes documented are Complex I/III_n, Complex III_n/IV_n and Complex I/III_n/IV_n. More recently, respiratory active supercomplexes, termed respirasomes, owing to their ability to form functional units of respiration, which may contain both Cyt *c* and CoQ were isolated[97].

Currently, the "plasticity state" model[97] is the most accepted, hypothesizing that differences in the cell types and physiological states give rise to different combinations of respiratory supercomplexes[98]. It has been suggested that the association of complexes may promote stability, preventing destabilization and degradation, as well as improving of the electron transport efficiency, while minimizing ROS formation by decreasing the electron leakage[99–102]. Concerning the assembly of supercomplexes, two different models for supercomplex I/III_2/IV were hypothesized. Because CI stability was found to depend on the assembly of supercomplexes, it was accepted that supercomplexes assembly follows the assembly of individual complexes. However, Moreno-Lastres and co-workers (2012) showed that the association of CIV and CIII subunits with the assembled 830kDa CI is required for the incorporation of the remaining CI subunits, such as NADH dehydrogenase [ubiquinone] iron-sulphur protein 4 (NDUFS4) and NADH dehydrogenase [ubiquinone] flavoprotein 1 (NDUFV1)[100]. Currently, it is not clear if there are exclusive assembly factors that help to assemble supercomplexes after assembly of individual complexes, or if the assembly factors between different MRC enzymes are shared in this step. However, studies showing destabilized supercomplexes, proposed some additional assembly factors[102], such as cardiolipin[103], the mammalian homolog of Rcf-1, Hig2A[104], and the AAC2 in yeast[105]. Other proteins and lipids have been hypothesized to participate in assembly and stability of supercomplexes, but firm evidence is still lacking. Also, the assembly factors required for the last stage of Complex I assembly may be considered supercomplex assembly factors[102].

According to the functional advantages proposed above, namely the stability of complexes and OXPHOS improvement, supercomplexes destabilization may cause decrease in efficiency of the electron transport, subsequently decreasing OXPHOS efficacy and ATP production.

1.2.2 Mitochondrial electrochemical potential and ATP synthesis

The functional individual complexes and supercomplexes of the MRC are responsible for the efficient ATP synthesis, using the electrochemical potential generated by the OXPHOS (Figure 1.2D).

This process begins with the transfer of the electrons from the TCA cycle to the OXPHOS by the co-factors NADH and $FADH_2$[12]. First, NADH brings free energy to the MRC by binding to the largest of the respiratory complexes – CI. These electrons are then passed down the arm via a series of sulphur clusters to the lipid soluble carrier CoQ, linked to the translocations of four protons (H^+) from the matrix across the IMM[12]. At that point, CII catalyses the oxidation of succinate to fumarate, resulting in reduction of the FAD to $FADH_2$ allowing the transfer of the electrons to CoQ through FeS centres. In this step, no protons are pumped to IMS. The reduced CoQ by either CI or CII, is able to freely diffuse through the IMM to transfer electrons to the CIII of the MRC. In turn, CIII passes the electrons to Cyt *c*. Ultimately, electrons are transferred to the iron/copper active site of the CIV, where O_2 (final electron acceptor) is fully reduced to water, allowing the H^+ pumping from the matrix to the IMS.

Subsequently to the H^+ are pumped through CI, CIII and CIV of the MRC, the free energy generated from the redox reactions is converted into a transmembrane proton gradient, which creates a charge differential. Afterwards, the ATP synthase (CV) allows H^+ ions to flow back into the mitochondrial matrix through the proton pore of F0 domain, the rotor turns inside the head of the stator, and conformational changes are induced that promote the combination of ADP and Pi to synthesize ATP.

The OXPHOS is responsible for more than 90% of body's cellular energy[13].

Despite the synthesis of ATP, the mitochondrial transmembrane potential gradient is involved in the transfer of calcium and other ions exchanges, the import of mitochondrial proteins to matrix and ROS homeostasis[31,106].

1.2.3 Inhibitors and uncouplers of MRC

Concerning the several reactions that take place for the correct functioning of MRC using various substrates, there are some substances that influence the mitochondrial electrochemical gradient, namely rotenone, malonate, antimycin A, cyanide and oligomycin B, which inhibit complex I, II, III, IV and V, respectively[107]. Additionally, other chemicals may uncouple proton pumping from ATP synthesis, by introducing protons to the matrix dissipating the proton gradient; common examples are the carbonyl cyanide-p-trifluoromethoxyphenylhydrazone (FCCP), the carbonyl cyanide m-chlorophenylhydrazone (CCCP) and the 2,4-dinitrofenol (DNP)[107].

Furthermore, other environmental contaminants may induce mitochondrial toxicity, including heavy metals, cigarette smoke and pesticides[108].

1.3 Oxidative Stress

Mitochondria are continuously functioning to reduce oxygen. However, 0.4 to 4% of oxygen consumed by mitochondria is incompletely reduced, leading to the production of ROS (Figure 1.2D), namely superoxide anion ($O_2^{\bullet -}$), highly reactive and toxic to cell[13].

Deficiency of complexes I to III gives rise to an increase premature leakage of electrons, allowing their passage directly to oxygen, before reaching the CIV and, consequently, superoxide anion is overproduced[109]. Besides $O_2^{\bullet -}$, ROS are a family of free radicals that includes hydroxyl, peroxyl radicals and other reactive species capable of generating free radicals, such as nitric oxide[13].

In order to avoid severe oxidative damage to mitochondria, several defence mechanisms are used to alleviate the oxidative stress effect induced by the excessive generation of free radicals in the cells. Then, enzymatic defence system includes the beneficial action of various antioxidant enzymes, such as superoxide dismutase (SOD), catalase (CAT), glutathione reductase (GR) and glutathione peroxidase (GPx). Other non-enzymatic defences include the antioxidant compounds, such as Vitamins E and C, glutathione (GSH), various carotenoids and flavonoids[13].

In normal conditions, the production of ROS is restricted via defence systems, in order to protect mitochondria from oxidative damage. However, when an overproduction of ROS occurs or when the antioxidant defences are affected, there is an excessive accumulation of ROS, which causes oxidative damage to DNA, lipids, and proteins in mitochondria[13]. Thus, oxidative stress refers to the imbalance of ROS production versus antioxidant defences capacity, wherein the damaging effects of ROS are more powerful compared to the compensatory effect of antioxidants in the cells.

1.4 Mitochondrial dynamics

Mitochondrial bioenergetics seems to rely on mitochondrial morphology, as modifications in morphology cause variations in bioenergetics state, whilst changes in bioenergetics often affect morphology. Mitochondrial shape is mainly determined by a balance between fusion and fission events, and this equilibrium maintains steady state mitochondrial morphology, mtDNA nucleoid and metabolic mixing, bioenergetics functionality and organelle number[12,110].

Mitochondrial division is essential for organelle biogenesis, inheritance, transport and for the removal of aged or damaged mitochondria through a specialized form of autophagy, termed mitophagy (see mitochondrial quality control section). Alterations in fission event can lead to a heterogeneous population of organelles with uneven mtDNA distribution, inconsistency in the ability to produce ATP, increased production of ROS and vulnerability of cells to undergo apoptosis[12,111].

In mammals, the dynamin 1 like protein (DNM1L) plays a central role in mediating the mitochondrial division[112] by forming helical structures that wrap around mitochondria[113–115]. Therefore, mutations in this protein have been described in a patient presenting abnormal brain development, optic atrophy and early infant mortality[116] and cardiomyopathy[117]. Recently, mitochondrial interactions with endoplasmic reticulum have been associated to the fission mechanism, since these interactions allow DNM1L protein bind to mitochondrial fission factor (MFF) receptors in mitochondria, as well as provide the mechanical force to facilitate the initiation of mitochondrial division[118].

Mitochondrial fusion is essential to maintain a homogeneous organelle population and ensures inter complementation of mtDNA, masking partial defects and transient stresses[12]. Several known proteins are responsible for the fusion of OMM and IMM, despite it is unknown how the fusion machineries are activated[12]. Then, fusion requires two families of dynamin-related proteins, mitofusin 1/2 (MFN1/MFN2), responsible for the fusion of OMM, and Optic atrophy 1 (OPA1), mediating the fusion of IMM. Consequently, mutations in *MFN2* have been described in patient presenting Charcot Marie-Tooth disease 2A[119], whilst *OPA1* mutations have been mainly related to autosomal dominant optic atrophy[120,121].

The importance of fission and fusion homeostasis has been highlighted by a number of disease states, emphasizing the important physiological roles and different requirements of mitochondrial dynamics in different cell types[12,113].

Moreover, mitochondrial dynamics also encompasses motility. Thus, failure to deliver mitochondria to the proper place and in the adequate amount, to various regions of the cell, can cause localized deficiencies in the production of ATP, with deleterious consequences[2]. This process is extremely important in neurons, since mitochondria are essential at the site of neural activity for providing a protection against excitotoxicity[122].

1.5 Mitochondrial quality control

Mitochondrial quality control is the term used to describe the set of events and processes involved in the mitochondria homeostasis maintenance[123].

In normal conditions, chaperones and proteases participate in the folding, assembly and turnover of mitochondrial proteins, which maintain the front line of mitochondrial quality control[124–126]. Loss-of-function alterations, such like mutations in subunits of proteases, lead to several types of neurodegeneration, namely spastic paraplegia[127,128].

In proteotoxic stress conditions, different proteostasis responses have been described. The mitochondrial unfolded protein response (UPR^{mt}) is a transcriptional pathway activated by the accumulation of unfolded or misfolded proteins in the

mitochondrial matrix[129,130] playing a major role in the clearance of accumulated proteins in mitochondria; it involves the activation of proteases, namely the Lon and Clp families. Moreover, the UPR^{mt} regulates a large set of genes that are not only involved in protein folding, but also in changes of ROS defences, metabolism, regulation of iron-sulphur cluster assembly, and modulation of the innate immune response[131,132]. Therefore, mutations in genes of this pathway may give rise to several neurodegenerative and metabolic disorders[124,133]. Damaged proteins from the IMM are cleared by the ATPase Associated with diverse Activities (AAA) proteases[134], whilst proteins residing in OMM, or that become misfolded in the cytosol, on the way to mitochondria, are removed by the cytosol ubiquitin-proteasome system – UPS[135].

In addition, recent evidences suggest that vesicles budding from mitochondrial tubules, termed mitochondrial derived vesicles – MDVs[136], might sequester selected mitochondrial proteins, and then deliver them in lysosomes for degradation. These studies indicate that MDVs are likely a first round of defence for the mitochondria to eject damaged proteins[137].

If misfolded proteins accumulate to a level that exceeds the capacity of the UPR^{mt}, or if the mitochondrial membrane potential is lost, mitophagy appears to alleviate mitochondrial impairment. However, it is not clear how the cell determinates when to repair or to eliminate the organelle[138]. Mitophagy is an autophagy-lysosome system that selectively removes dysfunctional mitochondria[61,135,139,140]. Before this process, a shift in balance of mitochondrial dynamics, namely increased fission and decreased fusion, promotes segregation of damaged mitochondria and facilitates their clearance. Thereafter, the mitochondrial PTEN- induced putative kinase 1 – PINK1 – senses damage and recruits the cytosolic E3 ligase Parkin, which, in turn, ubiquitinates the OMM proteins to activate receptors that will signal the assembly of autophagosome close to the damaged mitochondria. Then, mitochondria are sequestered by autophagosome and autolysosome formation allows the hydrolytic degradation. In humans, loss-of-function mutations in either *PINK1* or *PRKN* genes lead to early onset Parkinson's disease[139].

The existence of cross-regulation between these various mitochondrial quality control pathways has been suggested[124,141]. However, in case of irreversible cellular damage, apoptosis can also ensue[7,124].

1.6 Crosstalk between mitochondria and nucleus

The double genetic origin and the large number of mitochondrial proteins indicate a regulated communication between mitochondria and nucleus[3].

Either in case of depletion of mtDNA or in the accumulation of misfolded proteins within mitochondria, the mitochondrial perturbation triggers a nuclear transcriptional response, including the increased expression of the mitochondrial proteins, namely the majority of OXPHOS subunits, the assembly factors of the OXPHOS complexes, those involved in maintenance, expression, transcription and translation of mtDNA, mitochondrial dynamics and mitochondrial quality control factors[7,129]. The existence of this broad transcriptional response demonstrates that exists communication and coordination between the mitochondria and nucleus, creating a nuclear-to-mitochondria regulation, the so-called "anterograde regulation"[6,7]. In fact, the anterograde signals are activated by upstream sensors that detect changes in metabolic conditions, such as exercise, caloric restriction or cold stress, promoting mitochondrial biogenesis[7]. In addition, anterograde communication can also signal the nuclear stress to the mitochondria, reducing mitochondrial metabolism in order to attenuate the consequences of nuclear DNA damage. For example, telomerase dysfunction results in impaired mitochondrial function and biogenesis[142].

Although there is a considerable interest in nuclear-to-mitochondrial regulation, there is also an important role for mitochondrial-to-nucleus signalling, called "retrograde response"[7]. In this case, mitochondria can generate a response, through which they regulate various cellular activities and protect against mitochondrial dysfunction, by activating the expression of nuclear genes involved in restoration of cellular metabolism and stress defence.

The nature of retrograde signals may be related to oxidative/energetic stress and calcium-dependent responses[7,123]. In mammals, a decrease in ATP synthesis stimulates the mitochondrial energy metabolism, the biogenesis, and the quality control system, namely mitophagy[7,123]. Since mitochondria are essential to regulate the intracellular calcium levels, and mitochondrial calcium uptake relies on mitochondrial membrane potential, disruption of MRC complexes and OXPHOS, triggers the release of calcium into the cytoplasm[143–145]. Elevated levels of cytosolic calcium activate nuclear factors

involved in calcium transport and storage, and glycolytic and gluconeogenic enzymes [146,147]. Finally, increased ROS levels activate detoxification enzymes and antioxidant proteins in mitochondria and cytosol[148–150]. Besides, ROS can also induce mitochondrial biogenesis and the expression of genes involved in OXPHOS process[7,151].

As a result, the mito-nuclear communication constitutes a network that helps the cells to maintain the homeostasis under basal conditions and enables their effective response in stressful situations (see Eisenberg-Bord and Schuldiner, 2016[152] for more details).

1.7 Mitochondrial communication with other organelles

Mitochondrial dynamics is influenced by physical contact between OMM and diverse intracellular membranes, such as autophagosomes, the plasma membrane, endosomes, lysosomes, endoplasmic reticulum (ER) and peroxisomes, termed mitochondria-associated membranes (MAMs). These contacts are unique environments for localization and activity of components that act in shared interorganellar roles, namely the calcium homeostasis and lipid biosynthesis present in the mitochondria-associated endoplasmic reticulum membranes[2,113].

The ER-mitochondria communication has been the most extensively studied, given its role in regulating the transfer of calcium, synthesis of lipids, mitochondrial fission, autophagy, inflammation and apoptosis[153,154].

During the initial phase of mitochondrial fission, ER tubules wrap around and constrict mitochondria, pointing to a crucial role for the ER-mitochondria contact in the initiation of mitochondrial fission[113,118,153,154]. In addition, MFN2 is involved not only in fusion process, but also in ER-connection[154], suggesting a critical role of ER-mitochondria crosstalk in mitochondrial dynamics[153,154].

Considering the key roles played by mitochondrial calcium in the modulation of numerous physiological responses, namely in bioenergetics balance, apoptosis and inflammasome activation, it is logical to suggest that dysregulation of calcium trafficking from ER to mitochondria will have effects on cellular bioenergetics[2,153,154]. Moreover, recent reports show evidences that the ER-mitochondria interface is

involved in autophagosome formation, stimulating the macroautophagy[155,156]. Therefore, mutations in genes coding proteins involved in ER-mitochondria crosstalk are a contributory factor in human diseases, including metabolic disease[157], Alzheimer's disease[158] and cancer[159].

Communication of mitochondria with other organellar structures also occurs via small vesicles that bud off from mitochondria – MDVs[136]. The MDVs comprise protein cargoes, which can be limited to OMM, or can include OMM, IMM and matrix content. The MDVs transport cargo to late endosomes/multivesicular body/lysosomes to be degraded, as referred below. On the other hand, MDVs transport cargo to peroxisomes[160]. However, the purpose of vesicle delivery to the peroxisomes and the cargo content are unclear[136].

Since mitochondria communicate with several organelles, research about the genetics of mitochondrial disorders will continue to reveal unexpected connections between mitochondria and the rest of the cell[161]. Therefore, new reports of mitochondrial disorders, arising from mutations in genes associated with these processes, are expected in the near future.

1.8 Mitochondrial dysfunction and disease

Mitochondrial dysfunction is the term used to refer any alteration in mitochondrial functions, namely the reduction of energy production[162].

Environmental factors, such as toxic substances, can influence the mitochondrial function. For example, the use of tobacco, heavy consumption of alcohol and certain medications (antibiotics and antivirals) are risk factors for loss of mitochondrial function[108,138,161].

In addition, mtDNA mutations, caused by replication of unrepaired DNA modifications, lead to a reduction of OXPHOS efficiency, caused by decreased of catalytic activity of MRC complexes, leading to mitochondrial dysfunction.

On the other hand, mutations in nuclear genes encoding mitochondrial proteins that are essential for mitochondrial functions can disturb mitochondrial homeostasis.

Considering that mitochondria have a crucial role in the maintenance of cellular homeostasis, decline in mitochondrial function could have devastating consequences in the human body functioning, leading to a broad spectrum of human mitochondrial diseases[1,6].

In the past, mitochondrial diseases were considered rare, of purely academic interest. Currently, they are among the most common genetic human diseases.

In fact, approximately 1,700 proteins are present in the mitochondrion. Most of them are required for the maintenance of the organelle itself (organellar morphology and integrity; replication, transcription and translation of mtDNA; import of proteins; transporters and carriers for small molecules), while the remaining proteins have more specialized functions (lipid and amino acid metabolism; OXPHOS; cell signalling and apoptosis) associated with the cell homeostasis[2]. Thus, mitochondrial diseases may result from a mutation in any of these hundreds genes. Currently, mutations in the 37 mtDNA encoded genes and, at least, in 240 nuclear genes have been identified in association with the development of mitochondrial human disease, making these disorders the most heterogeneous group of metabolic diseases[29,163].

Mitochondrial diseases are associated with the genetic control of bioenergetics, dynamics, quality control and intracellular communication. Accordingly, these diseases can be divided into these four groups, despite there is considerable overlap between them.

In this section, the term OXPHOS diseases will be used to define the pathologies related to mitochondrial bioenergetics, which are a genetically and clinically heterogeneous group of disorders caused by primary defects in the mitochondrial ATP production by OXPHOS. Although the common feature of OXPHOS diseases is MRC deficiency, they occur due to defects of different proteins and enzymes. An impairment of MRC function leads to a variety of metabolic consequences that are relevant for disease pathophysiology. The clinical manifestations (Figure 1.3) of patients are quite heterogeneous, involving isolated organ deficiency or affecting several organs, leading to multisystemic clinical presentations, being the nervous system, skeletal muscle and heart the most affected tissues[28], which are reliant on mitochondrial energy, with less capacity to upregulate the glycolysis rates[12]. However,

the tissue specificity associated with specific mitochondrial genotypes is a key point that is still unclear[28].

Many classic syndromes have been described over the last decades. The age of onset range from the neonatal period to late adulthood[3,26]. The most common syndromes with neonatal and childhood onset include Leigh syndrome (LS), Pearson syndrome and Alpers syndrome. In contrast, examples of clinical syndromes with adulthood onset include Kearns-Sayre syndrome (KSS), myoclonic epilepsy with ragged-red fibres (MERRF), neuropathy, ataxia and retinitis pigmentosa (NARP), mitochondrial encephalopathy, lactic acidosis with stroke-like episodes (MELAS), mitochondrial neuro-gastrointestinal involvement and encephalopathy (MNGIE), and chronic progressive external ophthalmoplegia (CPEO)[29]. In some syndromes, such as in Leber's Hereditary Optic Neuropathy (LHON), the symptoms may occur at any age between the adolescence and late adulthood[3], with exceptions in childhood[164].

However, most of patients do not fit in defined syndromes. Instead, many other symptoms, common in the population, such as diabetes, deafness, myopathy, cardiomyopathy, liver and renal dysfunctions and gastrointestinal symptoms, may appear combined in the same individual, associated with mitochondrial disease[29,135,161,165,166]. In order to clarify the diagnosis, detailed investigations are mandatory to identify other signals such as cardiac involvement, short stature, sensorineural deafness, optic atrophy, epilepsy, pigmentary retinopathy and others[29].

CI deficiency is a frequent cause of mitochondrial diseases, and the main clinical features are hypotonia, antenatal and post-natal growth retardation and encephalopathy[167,168].

In contrast, CIII impairment is a relatively rare cause of MRC dysfunction, and the clinical presentation is highly heterogeneous, including myopathy, encephalomyopathy, cardiomyopathy, multisystem disorders, intrauterine growth retardation and tubulopathy[169].

CIV deficiency is associated with phenotypes such as encephalomyopathy, myopathy, hepatic failure, and Leigh syndrome[170–172].

Finally, CV deficiency is mainly related to cardiomyopathy and neuropathy[173–175].

However, deficiency of more than one MRC enzyme is a common finding, since combined defects are found in 49% of the known disease-causing genes of

mitochondrial energy metabolism[163]. The clinical presentations are heterogeneous concerning tissue involvement, severity and onset, presenting classical encephalomyopathy but also nephropathy, hepatopathy, hematologic findings, or Perrault Syndrome – ovarian dysgenesis (female) and sensorineural deafness[163].

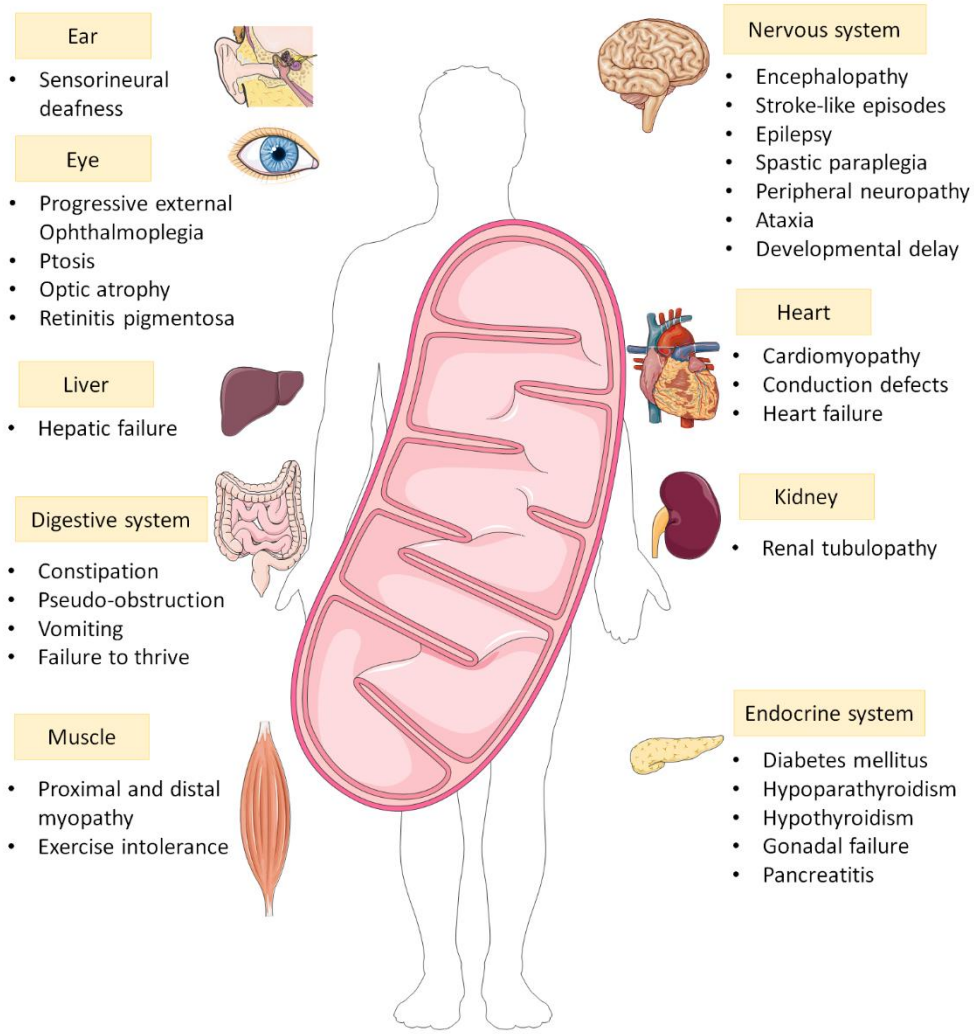

Figure 1.3 - Range of clinical manifestations identified in patients presenting OXPHOS diseases, according to the affected organ.

The inheritance pattern of OXPHOS diseases is dependent on the genetic mutations, including maternal, autosomal recessive, dominant or X-linked inheritance. In addition, sporadic cases due to *de novo* mutations may occur. Therefore, mitochondrial diseases are associated with mutations in either mtDNA and/or nDNA[176]. Primary mtDNA mutations have predominantly been identified in adults, compared with mutations in nuclear genes that are more often found in childhood,

associated to severe and progressive diseases[28]. However, over the last years, it has become clear that the mtDNA mutations can present throughout life and that nuclear genes mutations can also be present in adult life of patients with recessive, dominant or X-linked OXPHOS diseases[177]. The establishment of genotype-phenotype correlation has been difficult, since only few patients have been described with the same genetic mutation; moreover, different mutations can give rise to the same syndrome and, conversely, the same genetic mutation can be associated with different syndromes[178]. Therefore, the disease-causing mutation is identified in a limited number of patients[3].

The clinical and genetic heterogeneity bring difficulties in establishing the precise prevalence of OXPHOS diseases. Recent studies looking at the prevalence in children suggest a range from 5 to 15 cases per 100,000 individuals[26]. In centre Portugal, the prevalence in children up to 10 years of age was estimated to be 15:100,000[179]. In adults, OXPHOS disorders has been estimated to be approximately 1:4,300 of the population affected or at risk of developing disease, in North East England[26]. These recent studies support the view that mtDNA mutations are the major cause of OXPHOS disease in adults, since 40% of patients present one of the three point mutations causing LHON (m.11778G>A, m.3460G>A and m.14484T>C), against 23% of adults that had a known nuclear gene mutation[180–182].

1.8.1 Genetic causes

To date, mitochondrial proteomics analysis reveals that, in addition to the 13 proteins encoded by the mtDNA, more than 200 proteins encoded by nDNA are essential pieces for OXPHOS, including the majority of MRC subunits and the assembly factors of OXPHOS complexes, the substrates, and all the proteins involved in maintenance, expression, transcription and translation of mtDNA[2,161]. Therefore, it is not surprising that mutations in any of these components could lead to OXPHOS dysfunction.

1.8.1.1 mtDNA mutations

Pathogenic alterations in the mitochondrial genome were not reported until 1988[23,183]. Since then, several mtDNA mutations have been described, giving the notion that they are more common than it was previously thought, as they have been found in 0.5-1% of the population, at heteroplasmy levels higher than 1%[184]. In most cases, mtDNA pathogenic mutations are heteroplasmic, and the phenotype is a reflection of the proportion of mutant mtDNA molecules load[185]. Pathogenic homoplasmic mutations were thought to be a rare cause of diseases. However, in addition to the LHON mutation m.11778G>A[183] and the mutation m.1555A>G associated to maternally inherited deafness[186], several cases of multi-system disease have been described due to homoplasmic mutations[187–189].

The mtDNA mutations fall into three major classes: point mutations, rearrangements (insertions and deletions) and copy number reduction (depletions).

In the last years, the "morbidity map" of mtDNA has gone from the one pathogenic point mutation identified in 1988 to more than 60 (Table 1.1) mtDNA point mutations confirmed to be associated with a wide variety of human diseases (http://www.mitomap.org; accessed on July, 2017). Point mutations in mtDNA can be further divided into those that affect the expression or the function of any of the 13 respiratory chain subunits encoded by mtDNA, since they are present in mtDNA genes coding for MRC peptides, and those that impair mitochondrial protein synthesis, caused by mutations affecting tRNA or rRNA[178,190]. According to Mitomap, 29 confirmed pathogenic mutations have been found in RNA genes and 35 confirmed pathogenic mutations in protein encoding genes.

The most common mutations affecting mitochondrial genes encoding proteins have been reported in LHON and NARP/LS. These mutations are frequent, and have been identified in non-related patients. Other mutations have also been reported in numerous genes, more often restricted to a specific patient or family[3]. Approximately one-third of the mtDNA mutations were found only in single cases, according to a recent epidemiological study[26]. Frequently, NARP occurs due to the mutation m.8993T>G in the *mt-ATP6* gene, changing an amino acid in the ATP6 protein[191]. To date, LHON has been associated with three primary mutations (m.3460G>A,

m.11778G>A and m.14484T>C), although several other mtDNA alterations can act synergistically, leading to different effects according to the haplogroup of each individual[192,193].

Table 1.1 Mitochondrial DNA point mutations identified in OXPHOS diseases, according to MITOMAP (www.mitomap.org, accessed on July, 2017).

Mutation	Locus	Pathology/phenotype	Homoplasmy	Heteroplasmy
m.583G>A	*MT-TF*	MELAS / mitochondrial myopathy / exercise intolerance	-	+
m.1494C>T	*MT-RNR1*	Maternally inherited deafness	+	-
m.1555A>G	*MT-RNR1*	Maternally inherited deafness	+	-
m.1606G>A	*MT-TV*	Ataxia, myoclonus and deafness	-	+
m.1644G>A	*MT-TV*	MELAS and hypertrophic cardiomyopathy	-	+
m.3243A>G	*MT-TL1*	MELAS / LS / Diabetes mellitus and deafness / Maternal inherited diabetes and deafness/ Sensorineural Hearing Loss / CPEO/ Mitochondrial myopathy /Cardiac and multi-organ dysfunction	-	+
m.3256C>T	*MT-TL1*	MELAS	-	+
m.3260A>G	*MT-TL1*	MELAS / Maternal myopathy and cardiomyopathy	-	+
m.3271T>C	*MT-TL1*	MELAS/ Diabetes Mellitus	-	+
m.3291T>C	*MT-TL1*	MELAS/ Myopathy /Deafness and cognitive impairment	-	+
m.3302A>G	*MT-TL1*	Mitochondrial myopathy	-	+
m.3303C>T	*MT-TL1*	Mitochondrial myopathy and cardiomyopathy	+	+
m.3376G>A	*MT-ND1*	LHON-MELAS overlap syndrome	+	+
m.3460G>A	*MT-ND1*	LHON	+	+
m.3635G>A	*MT-ND1*	LHON	+	-
m.3697G>A	*MT-ND1*	MELAS / LS / LHON and dystonia	+	+
m.3700G>A	*MT-ND1*	LHON	+	-
m.3733G>A	*MT-ND1*	LHON	+	+
m.3890G>A	*MT-ND1*	LS / optic atrophy / progressive encephalomyopathy	-	+
m.4171C>A	*MT-ND1*	LHON	+	+
m.4298G>A	*MT-TI*	CPEO	-	+
m.4300A>G	*MT-TI*	Maternally inherited cardiomyopathy	+	+
m.4308G>A	*MT-TI*	CPEO	-	+
m.4332G>A	*MT-TQ*	Encephalopathy / MELAS	-	+
m.5537A>T	*MT-TW*	LS	-	+
m.5650G>A	*MT-TA*	Myopathy	-	+
m.5703G>A	*MT-TN*	CPEO / Myopathy	-	+
m.7445A>G	*MT-CO1*	Sensorineural hearing loss	+	+
m.7497G>A	*MT-TS1*	Mitochondrial Myopathy / Exercise intolerance	+	+
m.7511T>C	*MT-TS1*	Sensorineural hearing loss	+	+

Mutation	Locus	Pathology/phenotype	Homoplasmy	Heteroplasmy
m.8344A>G	*MT-TK*	MERRF / Depressive mood disorder / leukoencephalopathy/ hypertrophic cardiomyopathy	-	+
m.8356T>C	*MT-TK*	MERRF	-	+
m.8363G>A	*MT-TK*	MERRF / Autism / LS / Maternally inherited cardiomyopathy and deafness	-	+
m.8528T>C	*MT-ATP8/6*	Infantile cardiomyopathy	+	+
m.8993T>C	*MT-ATP6*	NARP / LS / Maternally inherited LS	-	+
m.8993T>G	*MT-ATP6*	NARP / LS/ Maternally inherited LS	-	+
m.9176T>C	*MT-ATP6*	LS / Familial bilateral striatal necrosis	+	+
m.9176T>G	*MT-ATP6*	LS / Spastic paraplegia	-	+
m.9185T>C	*MT-ATP6*	LS / ataxia / NARP-like disease	+	+
m.10010T>C	*MT-TG*	Progressive encephalopathy	-	+
m.10158T>C	*MT-ND3*	LS	+	+
m.10191T>C	*MT-ND3*	LS/ Leigh-like disease / Epilepsy, strokes, optic atrophy and cognitive decline	-	+
m.10197G>A	*MT-ND3*	LS / dystonia / stroke / LHON and dystonia	+	+
m.10663T>C	*MT-ND4L*	LHON	+	-
m.11777C>A	*MT-ND4*	LS	-	+
m.11778G>A	*MT-ND4*	LHON / progressive dystonia	+	+
m.12147G>A	*MT-TH*	MERRF and MELAS / encephalopathy	-	+
m.12315G>A	*MT-TL2*	CPEO / KSS	-	+
m.12706T>C	*MT-ND5*	LS	-	+
m.13051G>A	*MT-ND5*	LHON	+	-
m.13513G>A	*MT-ND5*	LS / MELAS / LHON-MELAS overlap syndrome	-	+
m.13514A>G	*MT-ND5*	LS / MELAS	-	+
m.14459G>A	*MT-ND6*	LS / LHON and dystonia	+	+
m.14482C>A	*MT-ND6*	LHON	+	+
m.14482C>G	*MT-ND6*	LHON	+	+
m.14484T>C	*MT-ND6*	LHON	+	+
m.14487T>C	*MT-ND6*	Dystonia / LS / Ataxia / Ptosis / Epilepsy	-	+
m.14495A>G	*MT-ND6*	LHON	-	+
m.14568C>T	*MT-ND6*	LHON	+	-
m.14674T>C	*MT-TE*	Reversible COX deficiency myopathy	+	-
m.14709T>C	*MT-TE*	Mitochondrial myopathy, Diabetes Mellitus and deafness / encephalomyopathy /dementia, diabetes and ophthalmoplegia	+	+
m.14849T>C	*MT-CYB*	Exercise intolerance / Septo-optic dysplasia	-	+
m.14864T>C	*MT-CYB*	MELAS	-	+
m.15579A>G	*MT-CYB*	Multisystem disorder, exercise intolerance	-	+

(+) Present; (-) Absent.

There are common mutations in tRNA or rRNA genes, such as the m.3243A>G in the *MT-TL* gene *(*mt-tRNA^{Leu}) and the m.8344A>G in *MT-TK* gene (mt-tRNA^{Lys}), causing MELAS and MERRF, respectively[194,195]. Yet, several other mutations in these genes have been reported in non-related individuals or families. Mutations in any component of the translation apparatus, including tRNA and rRNA genes, cause proteins synthesis anomalies resulting in generalized OXPHOS deficiency.

Other category of mtDNA mutations are rearrangements. The most frequent rearrangements causing disease are single, large-scale deletions. Although the position and size of the deletion may differ among patients, they usually eliminate several genes, encoding proteins and tRNAs. Large-scale deletions are usually heteroplasmic, and occur between directly repeated sequences[3,196–198]. Large-scale heteroplasmic mtDNA deletions are frequently detected in patients presenting KSS, PEO and Pearson syndrome[3,197]. The most common deletion (4,977bp) was the first mutation to be identified in mtDNA[23], and it has been found in 30% of patients harbouring a unique deletion, flanked by 13-bp direct repeats. The “common deletion” has been described in both diseases, therefore, no correlation can be found between clinical presentation and the size or nature of the rearrangements[3].

Multiple mtDNA deletions and mtDNA depletion (deficiency in mtDNA content) are secondary anomalies in mtDNA due to mutations in nuclear genes responsible for the mtDNA replication and/or maintenance and transcription. Mitochondrial depletion syndrome is usually associated with early childhood onset and multi-system disease, while multiple deletions generally result in later onset and milder disease burden[29].

Mitochondrial depletion syndrome includes several diseases; it was initially described as congenital myopathy or hepatopathy[199]. Currently, many patients with mitochondrial depletion have demonstrated different clinical manifestations, caused by a drastic decrease in mtDNA copy number.

1.8.1.1.1 Pathogenicity criteria for mtDNA mutations

Novel mutations are still being reported, especially in genes encoding proteins. However, as mtDNA is highly polymorphic, and interpretation of mtDNA variants is

complex and remains challenging, the pathogenic significance of a novel variant needs to be determined using a series of criteria before a diagnosis can be established with confidence[200,201]. After DiMauro and Schon (2001) have succinctly described the canonical pathogenic criteria for mtDNA point mutations, some adjustments were made because some well-established pathogenic mutations fail to meet these criteria[202]. In 2004, the first scoring criteria applied to mitochondrial-tRNA mutations was published[203]. A comparison between canonical criteria and weighted criteria[204] evaluates the scoring system as more precise by improving the accuracy of pathogenicity assignment. Currently, there are two scoring systems: the pathogenicity scoring system applied to mutations affecting mt-tRNA[205] and a scoring criterion for pathogenicity of mutations in mitochondrial protein coding genes[200]. Recently, González-Vioque and co-workers[206] proposed to include a negative scoring for mutations which fail to show any mitochondrial defect in functional studies, in addition to the scoring system proposed by Yarham and colleagues (2011).

Succinctly, the criteria available in the literature are based on the genetic characterisation of mtDNA variants, namely the mode of inheritance and the presence of the variant in unrelated patients, on the histochemical and biochemical evidences of disease and on the functional studies.

Histochemical and biochemical evidences have been important indicators of mitochondrial involvement in pathology[186,207–211].

For histochemical evaluation, several staining approaches have been applied on skeletal muscle[212,213], revealing a mosaic pattern of normal and deficient muscle fibres[186,207,210,214–216]. Furthermore, TEM has demonstrated to be a useful tool to identify mitochondrial morphological alterations in muscle[217]. However, muscle unavailability is often a limitation.

The analysis of MRC enzymatic activity using the spectrophotometry assay has been the gold standard for the evaluation of bioenergetics status of mitochondria from several tissues[107]. This approach is useful for verifying whether there are single or multiple respiratory complex enzyme deficiencies in order to get a correlation with the genetic mutations identified, i.e., a specific complex deficiency related to the presence of a mtDNA-encoded subunit mutation or multiple complexes affected in the presence of a tRNA mutation[218]. Furthermore, immunocytochemical staining for identification of

OXPHOS defects can be achieved in cultured skin fibroblasts, using specific antibodies against proteins for each complex[219].

Other parameters have been evaluated mainly on patients' cells (e.g. skin fibroblasts), in order to confirm the mitochondrial dysfunction, namely mitochondrial membrane potential (ΔΨm), intracellular ATP levels, ROS production[220,221] and oxygen consumption[208]. More recently, the Seahorse Bioscience® technology allowed to determine several bioenergetics parameters of intact cells, with real-time monitoring, using the oxygen consumption rate (OCR) – respiration – and the extracellular acidification rate (ECAR) – glycolysis[222].

In addition to the histochemical and biochemical data, functional evidences of pathogenicity for novel or rare mtDNA variants can be achieved applying additional methods.

BN-PAGE has been used as an extra tool for evaluating the single or multiple deficiency of complexes' assembly[173,207,208,210,211]. Native proteins and complexes can be identified, allowing the evaluation of mitochondrial complexes and supercomplexes assembly. The experimental procedure can be challenging since the use of several detergents and buffers is required and numerous steps need to be performed[223]. Moreover, this method is time-consuming. In accordance with the tissue available to perform BN-PAGE, some modifications to the protocols are needed. For example, blue bands are perceived after the BN-PAGE for muscle, but in the case of fibroblasts it is often necessary to complement with the immunoblot followed by specific antibodies incubation, in order to detect the MRC complexes[224].

In order to verify if a sequence variation affects the level of a specific mitochondrial protein or the steady-state level of a mt-tRNA, western-blot or northern-blot hybridization can be performed, respectively. Furthermore, single-fibre studies have been used to investigate the segregation of the mutation with the affected muscle fibres[208,214–216]. However, this method is only applicable to heteroplasmic variants.

Mitochondrial cybrid system is useful to study the impact of a mtDNA mutation by eliminating the nuclear background of the patient, for excluding the influence of nuclear variants[225]. Despite being widely used for pathogenicity studies of mtDNA mutations, cybrids present numerous disadvantages. The ρ0 cells have an unstable

nuclear background since in most of studies they were created from tumour cell lines[225,226]. Moreover, these tumour cell lines are anaerobic at baseline which may influence the mtDNA genotype-phenotype correlation[226]. The cybridization procedure is time-consuming and requires multi-step control of efficiency, namely the control of the absence of mtDNA in ρ0 cells, control of the presence of mtDNA mutation in cybrid cells and the control of nuclear background. Furthermore, transcriptomic changes may be caused by the cybridization multi-stage procedure[227]. Therefore, caution must be taken to interpret the results obtained, which could be different according to the methodology and cell line used to perform the technique, leading to conflicting and irrelevant findings[226].

In addition to the criteria established in the literature, an extra tool for evaluating mtDNA variants significance is the haplogroup determination. This investigation allows to distinguish which variants are private or global mutations or haplogroup-specific polymorphisms, using the phylogenetic analysis[228]. Additionally, a variety of *in silico* tools are available in order to predict the functional impact of a novel sequence variant[228]. Each tool use different algorithms to determinate the effect of the alteration; therefore, the results obtained from the combination of several different tools may be used as supplementary evidence to interpret the pathogenicity. Taking into account these parameters, an integrated approach for classifying mitochondrial DNA variants has been suggested based on clinical diagnostic laboratory's experience[218].

In accordance with the overall principals available in literature, the criteria for the classification of mitochondrial variants pathogenicity are represented in the Figure 1.4.

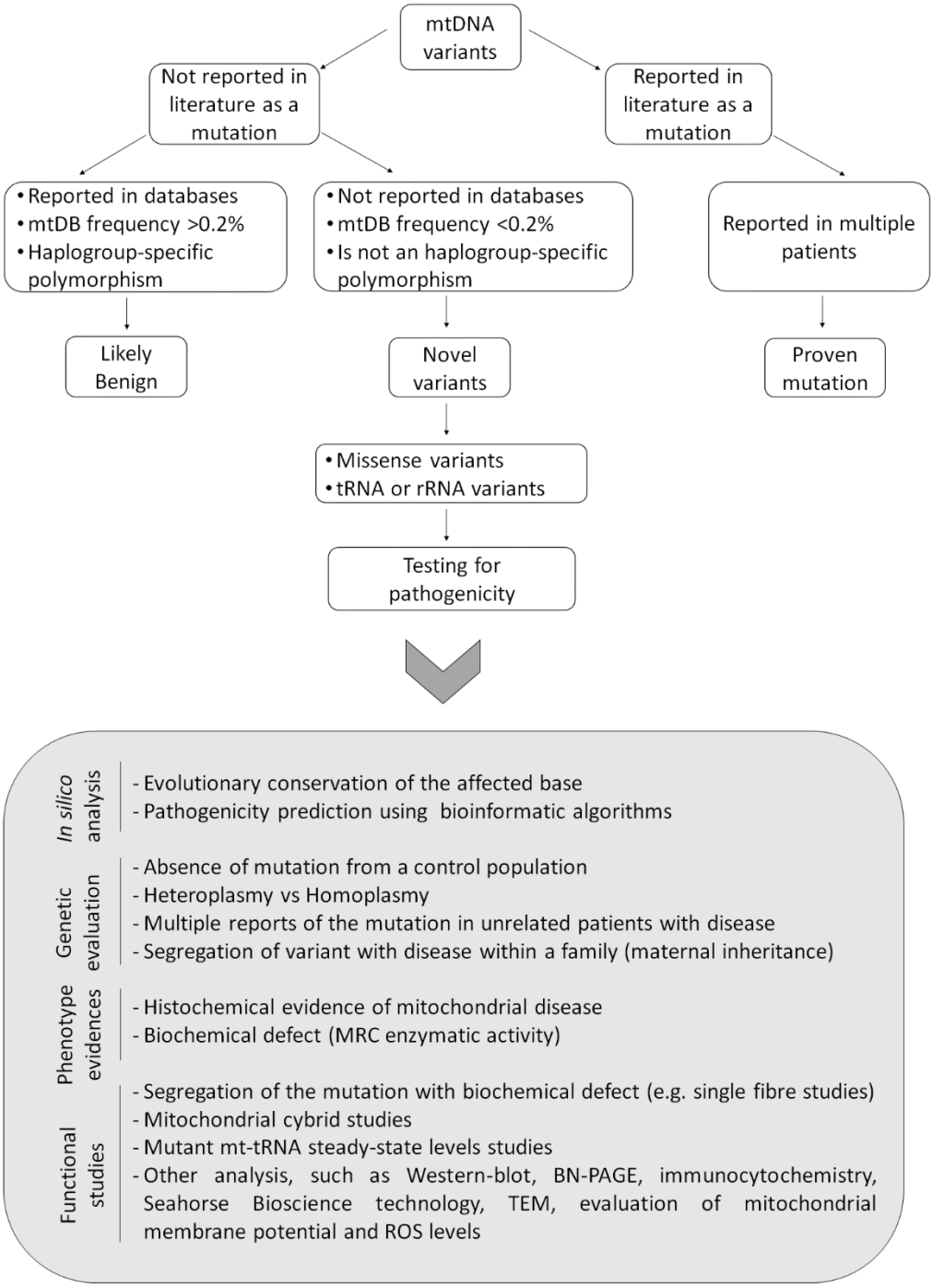

Figure 1.4 - Schematic diagram for the classification and prediction of the pathogenicity for mtDNA variants.

1.8.1.2 Nuclear DNA mutations

The number of disease-causing mutations in nuclear genes is growing, and the vast majority of MRC deficiencies are caused by these mutations. The nDNA mutations can be divided into several groups, according to the pathways: those that are present in structural genes coding subunits for MRC complexes; in genes involved in MRC complexes assembly; genes responsible for mtDNA transcription, translation, stability and maintenance; genes coding several enzymes involved in mtDNA metabolism[3].

Mutations in several nuclear genes encoding MRC subunits have been identified in patients with a range of clinical presentations. Most of mutations have been found in CI genes (Figure 1.5), leading to CI deficiency[3]. The predominant clinical presentation of patients harbouring these mutations has been LS or Leigh-like syndrome, although cardiomyopathy has also been reported[3]. The first mutation in a gene encoding a MRC subunit was identified in the *SDHA* gene, encoding for a CII subunit[229]. Mutations in this gene have been later reported in patients presenting LS[230,231], although mutations in the other genes encoding for CII subunits have been associated with carcinogenesis[232]. Mutations in nuclear genes encoding CIII subunits (for example, *UQCRB* and *UQCRQ*), CIV subunits (e.g., *COX4I2*, *COX6B1* and *COX7B*) and CV subunits (*ATP5A1* and *ATP5E*) have been described in association with a wide range of different phenotypes[175,233–238].

In addition to mutations in nuclear genes coding for MRC subunits, disruption in any of the mechanisms allowing structural integrity of the MRC complexes may result in catalytic dysfunction or instability of the complex. Then, these mechanisms include the assembly of complexes' subunits, incorporation of cofactors, translation of specific subunits and *haem*, iron or copper assembly[3].

Mutations in various genes responsible for CI assembly (e. g., *NDUFAF1*, *NDUFAF2* and *NDUFAF6*) have been related to various clinical phenotypes, namely LS and cardiomyopathy[239–242].

CII deficiency represents a rare cause of mitochondrial diseases, although mutations in two assembly factors (*SDHAF1 and SDHAF2*) have been identified in patients with infantile leukoencephalopathy[243] and paragangliomas[244].

Mutations in *BCS1L* gene responsible for CIII assembly caused a wide range of clinical presentations in non-related patients, including tubulopathy and hepatic failure[245], GRACILE syndrome – Growth retardation, amino aciduria, cholestasis, iron overload, lactic acidosis, and early death[246] and Björnstad syndrome – Pili torti and nerve deafness[247]. Mutations in another factor for CIII assembly (*TTC19*) were described as a cause for severe neurological abnormalities[248].

Several genes encoding assembly proteins of CIV have been described as disease-causing. Mutations in *SURF1* gene are the main cause of LS associated with COX deficiency[249–251]. Many other assembly factors of CIV, such as *COX10*, *COX15* and *TACO1*, have been also reported with mutations causing disease. However, patients harbouring these mutations presented several different clinical manifestations, such as tubulopathy and leukodystrophy[252,253], cardiomyopathy or LS[254–256], and late onset LS[257], respectively. In addition, other clinical manifestations have been identified in patients harbouring mutations in other genes responsible for CIV assembly. Thereby, no genotype-phenotype correlation has been assigned.

The majority of the CV deficiency is caused by mtDNA mutations; only two mutations in nuclear genes encoding CV assembly factors have been reported. A mutation in the *ATPAF2* gene resulted in dysmorphic features, neurological involvement and methylglutaconic aciduria in one patient[258], while neonatal encephalocardiomyopathy and isolated CV were reported in a large kindred of gipsy origin harbouring a mutation in TMEM70 gene[259].

Whereas several MRC proteins have iron-sulphur clusters, deficiencies in its assembly have been reported, resulting in dysfunction of CI, CII and CIII. Friedreich's ataxia is due to a mutation of *FXN* gene that codes a mitochondrial protein involved in iron-sulphur protein biogenesis[260]. Other mutations in genes coding for iron-sulphur cluster proteins, such as *ISCU*, *NFU1*, *BOLA3*, *GLRX5* and *LYRM4*, have been identified in association with a wide variety of clinical presentations. For example, mutations in the *ISCU* gene lead to myopathy, with exercise intolerance and myoglobinuria[261,262].

Theoretically, defects in proteins involved in mtDNA replication can affect mtDNA content level, leading to deficiencies of multiple MRC complexes. Mutations in some particular genes can give rise to multiple mtDNA deletions or depletion, such as mutations in *DGUOK*[263–265] and *TYMP*[266]. Mutations in *POLG1, POLG2*, *TWNK* and *OPA1*

genes cause multiple deletions in muscle of patients presenting autosomal-dominant external ophthalmoplegia[267–270], between other clinical manifestations.

Mutations in several nuclear genes involved in mitochondrial translation (Figure 1.5), affecting ribosomal proteins[271–275], aminoacyl-tRNA synthetases[276–285], initiation, elongation and termination factors[286–292], have been reported in patients presenting multiple MRC deficiency and various clinical manifestations.

Interestingly, it is becoming more evident and clear that the heterogeneity and unpredictability associated to mtDNA mutations are also present in nuclear gene mutations coding mitochondrial proteins. Therefore, mutations in the same nuclear gene can be associated with different clinical manifestations, causing either quantitative or qualitative mtDNA abnormalities, and the inheritance pattern of the associated diseases can be either dominant or recessive[3].

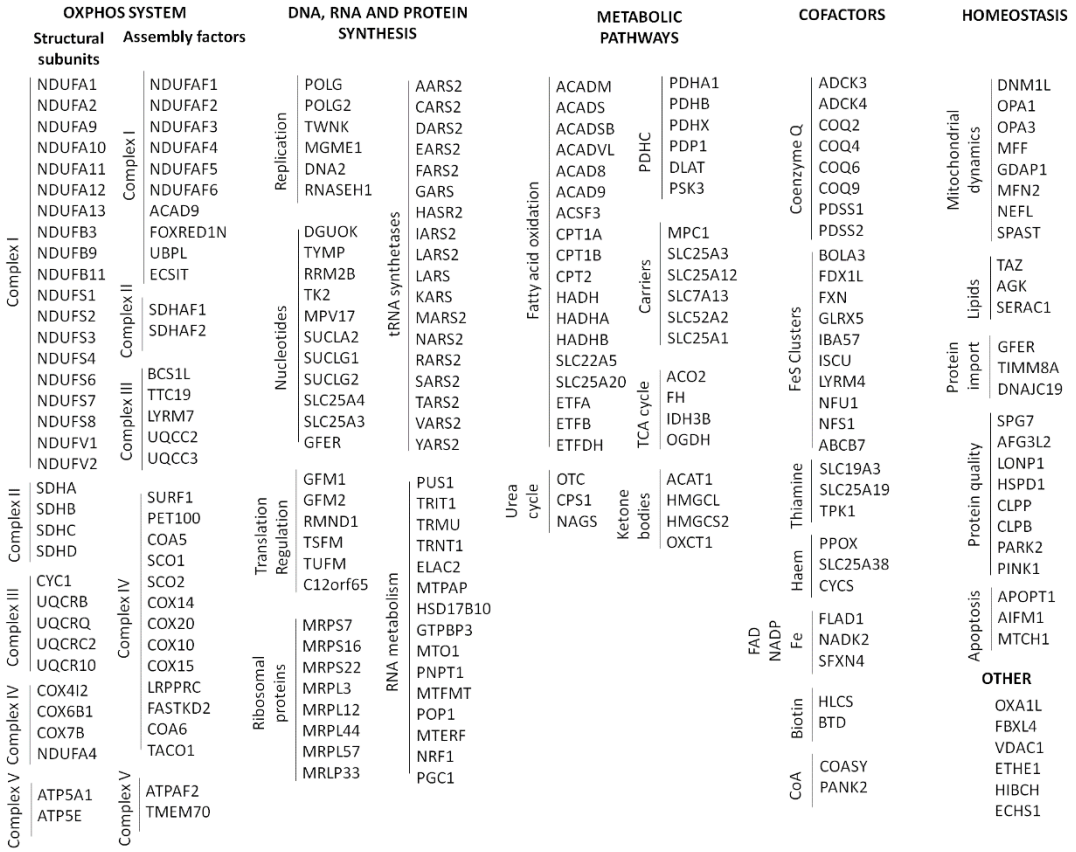

Figure 1.5 - Nuclear genes defects in which mutations causing mitochondrial diseases have been identified.

1.8.1.2.1 Pathogenicity criteria for nDNA mutations

Clinical molecular laboratories are increasingly detecting novel sequence variants in the course of testing patient samples, mostly due to the use of Next generation sequencing (NGS). In this context, the use of standards and guidelines for the interpretation of sequence variations using specific criteria are mandatory. Currently, sequence variations of nuclear genes are interpreted and reported according to the American College of Medical Genetics and Genomics (ACMG) recommendations[293].

First, search for variations in the literature and population databases is useful to verify the frequency in large populations. However, careful must be taken because population databases do not include only healthy individuals, they also contain pathogenic variants and, in some cases, variants that are incorrectly classified. Second, also in the case of nDNA variants, the *in silico* tools available are used to predict the pathogenicity of a variant, with some limitations related to the fact that it only allows the prediction of results. A detailed list of available databases and *in silico* tools are referred in Richards *et al*, 2015 and Wong, 2013[293,294].

In general, the evaluation of the segregation, the identification for *de novo* variations, the allelic data, and finally, the performance of functional studies are mandatory criteria, in addition to population data and computational and predictive analysis.

Accordingly, two sets of criteria were proposed by Richard and co-workers (2015), in order to classify and distinguish variants as pathogenic or likely pathogenic and as benign or likely benign. Then, each pathogenic criteria is categorized as “very strong”, “strong”, “moderate” and “supporting”, and each benign criteria is classified as “stand-alone”, “strong” and “supporting”. At that point, using the rules for combining criteria is possible to classify variants as “pathogenic”, “likely pathogenic”, “benign”, “likely benign” and “uncertain significance”[293]. Confirmation studies are recommended for all sequence variations that are classified as “pathogenic” or “likely pathogenic” for a Mendelian disorder.

1.9 Therapeutic strategies for mitochondrial diseases

In addition to the diagnostic challenge, progress in treatments and therapies for OXPHOS diseases is slow due to the complexity of mitochondrial dysfunction. Thus, an effective disease-modifying therapy is lacking, since management of mitochondrial disease is extremely difficult[28,29]. However, a number of symptomatic measures can greatly improve the outcome of these patients, while the investigation of disease modifying treatments are increasing[295].

Currently, different strategies, including lifestyle, pharmacological interventions, and molecular-based (gene) therapy, have been proposed in order to relieve the mitochondrial dysfunction, by targeting oxidative stress or mitochondrial quality control system, by increasing the efficiency of OXPHOS, by manipulating the mtDNA heteroplasmy, among others[28,295–297]. However, the number of properly controlled clinical trials has been limited[177,298], due to the reduced number of patients presenting the same clinical phenotype and genotype[28].

Although further advances will be required in all these areas, these strategies are the cornerstone for the development of novel therapies targeting mitochondrial diseases. The challenge that remains is the association of positive laboratory findings into safe and effective therapies for patients. Still, it is critical that our understanding of the pathogenic mechanisms involved in mitochondrial diseases became more clear, allowing the development of new potential therapeutic strategies.

Chapter 2 – Aims

The present study aimed to evaluate the impact of four unclassified mitochondrial DNA variants, detected in four unrelated patients suspected of OXPHOS disease, in order to establish a genetic diagnosis and clarify the underlying pathogenic mechanism.

In this regard, we addressed the following specific objectives:

1. Clarify the functional impact of a novel mtDNA mutation (m.8418T>C) in *MT-ATP8* gene and elucidate the association with bioenergetics dysfunction, in order to establish the role of a molecular genetic defect linked to mtDNA in a patient with severe optic neuropathy.
2. Investigate the functional influence of the unclassified mitochondrial DNA sequence variation m.14771C>A, at the *MT-CYB* gene, in a patient presenting with severe intellectual disability, cerebellar atrophy, severe ataxia, course face, relative macrocephaly, congenital hypotonia, absent speech, and other features such as clinodactyly.
3. Clarify the molecular genetic defect and elucidate the cellular mechanisms that are affected in a patient presenting chronic progressive external ophthalmoplegia and harbours a novel mt-tRNA$^{Ser(UCN)}$ variant (m.7486G>A) in addition to the mtDNA “common deletion”.
4. Elucidate the functional consequences of an unclassified mt-tRNA variant (m.14706A>G, *MT-TE*), in order to clarify the cause of incomplete penetrance of the cardiomyopathy presented in a familial case of sudden death.

Chapter 3 – Case Reports

3.1 CASE REPORT I

An unclassified mitochondrial *ATP8* gene variant in a patient with severe bilateral optic neuropathy: a functional genomics' approach

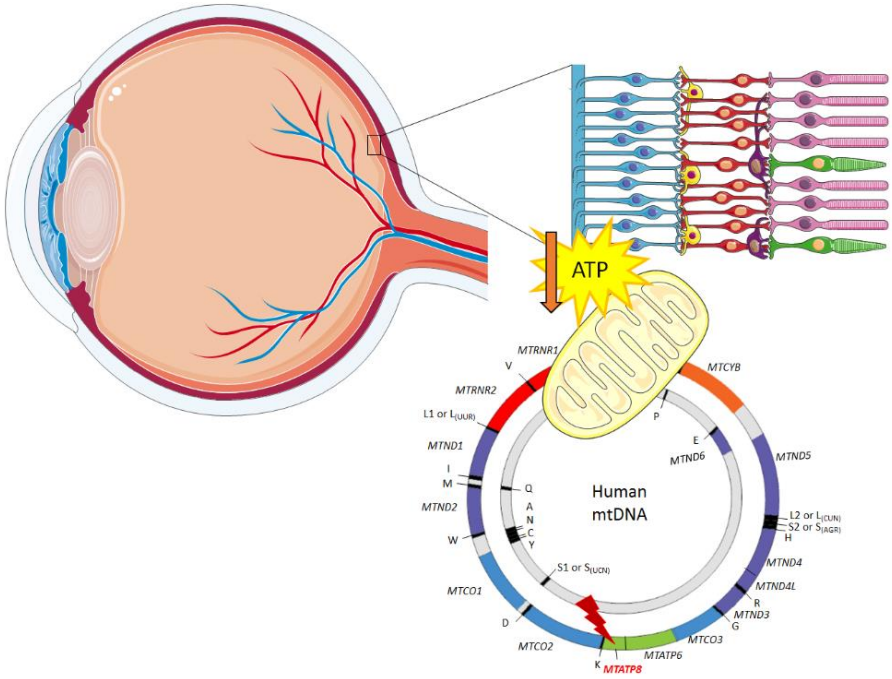

Abstract

Optic neuropathy is a frequent cause of vision loss. Leber's hereditary optic neuropathy (LHON) is a hereditary form of optic neuropathy, involving mitochondrial dysfunction, and one of the most frequent mitochondrial diseases. Most of clinically suspected LHON patients remain without a genetic diagnosis. In a previous study, screening of mtDNA revealed an unclassified probably pathogenic homoplasmic alteration in the *MT-ATP8* gene (m.8418T>C, p.Leu18Pro) of complex V (CV) in DNA samples from patient's lymphocytes and fibroblasts. The whole exome sequencing did not reveal other relevant variants. Accordingly, the present work aimed to investigate the biomolecular alterations related to the genetic variant, in a patient with severe optic neuropathy, and to clarify its association with the bioenergetics failure. Biochemical analysis demonstrated CV deficiency and hyperpolarization of mitochondrial membrane potential. There was impaired assembly of CV and reduced ATP synthase subunit 8 expression. Intracellular ATP levels were diminished, even with the increased glycolysis rate. Moreover, ultrastructural changes of endoplasmic reticulum were observed. Taken together, the results showed that m.8418T>C is linked to a pathogenic effect, presenting a range of functional consequences to the cells, suggesting that bioenergetics failure is the most probable cause of severe optic neuropathy in this patient.

Keywords: LHON; *MT-ATP8*; mtDNA variant; Complex V; bioenergetics failure.

3.1.1 Introduction

Optic neuropathy is mainly characterized by reduced visual acuity, dyschromatopsia, defect of visual field and abnormal pupillary response. There are several types of optic neuropathy, according to the aetiology. Therefore, the mode of onset is an essential clue in identifying the type of optic neuropathy[299].

Leber's hereditary optic neuropathy (LHON) is one of the most common mitochondrial respiratory chain diseases, and presents with painless and acute or subacute onset loss of central vision in one eye, followed by similar involvement of the other eye, within days, months or years[300]. Mitochondrial dysfunction has been pointed as the cause for selective death of retinal ganglion cells occurring in this pathology. It is estimated that 90% of LHON cases with a genetic mutation identified are due to three pathogenic mutations in mtDNA, involving genes of CI (m.11778G>A, *MT-ND4*; m.3460G>A, *MT-ND1*; m.14484T>C, *MT-ND6*)[300]. Nevertheless, the majority of the clinically suspected LHON patients remain without genetic diagnosis. Moreover, several mtDNA sequence variations have been described in association with mitochondrial neuropathy[301], namely in *MT-ATP6/8* genes[173,175].

ATP synthase (also named F_1F_0-ATP synthase or complex V) is a crucial component for mitochondrial energy production in the mammalians, using the energy of an electrochemical gradient across the IMM to catalyse the ATP synthesis, in the final step of OXPHOS. This enzyme is a multisubunit complex containing two functional domains, a hydrophilic F_1 and a hydrophobic F_0 domain, connected by a central stalk and a peripheral stalk (stator). The soluble component F_1 acts as the catalytic domain, in the mitochondrial matrix, where ADP is phosphorylated to ATP. The F_0 domain is embedded in the IMM, being essential to transfer protons from the intermembrane space to the matrix[83]. CV is composed predominantly by subunits encoded by nuclear genes; only two F_0 subunits, ATP synthase protein 6 (or a) and 8 (or A6L), are encoded by mtDNA genes, *MT-ATP6* and *MT-ATP8* respectively. These two subunits are among the last subunits to be assembled in CV[81,82,302].

Deficiency of ATP synthase could be associated with mutations in genes encoding either subunits or essential proteins for CV assembly[303]. To date, several mtDNA mutations associated to CV have been described related to mitochondrial defects,

mainly in *MT-ATP6* gene, as reviewed from Kucharczyk and colleagues[83]. To our knowledge, only four pathogenic mutations have been published in *MT-ATP8* gene associated with improper assembly and reduced activity of CV[173–175,304]. Given its function, it is not surprising that defects affecting CV may result in mitochondrial diseases. However, the underlying pathogenic mechanisms are not clearly understood, being more complex than a simple decrease in ATP supply[83]. Other processes in cells are likely to contribute for pathogenesis, such as ROS production, altered mitochondrial membrane potential, metabolic acidosis and possibly other unrecognized dysfunctions[303].

The present work aims to clarify the functional impact of an unclassified mtDNA variant (m.8418T>C, *MT-ATP8*, p.Leu18Pro, ATP synthase protein 8) and elucidate the association with bioenergetics dysfunction, in order to establish the role of a molecular genetic defect linked to mtDNA in a patient with severe optic neuropathy.

3.1.2. Samples and methods

3.1.2.1 Case report

A 42-year-old previously healthy man (patient 1, P1) presented with painless subacute visual loss in the right eye (RE), started to be followed in the Neurology and Ophthalmology Departments of Coimbra University Hospitals (CHUC). On neuro-ophthalmological examination, visual acuity was 20/30 in the RE and 20/20 in the left eye (LE). Colour vision was 1/17 (Ishihara plates) in the RE and 17/17 in the LE. There was a relative afferent pupillary defect and optic disc oedema in the RE on funduscopy. On standard automated perimetry there was an arcuate inferior scotoma in the RE. Neurologic exam was normal. Magnetic resonance imaging (MRI), that included fat-suppressed thin sections of the orbits with contrast, was unremarkable. Serologic studies and lumbar puncture were normal. He underwent intravenous methylprednisolone (1g for 3 days) followed by oral prednisone (60mg for 11 days). Over the following months there was no significant visual acuity or visual field improvement. Nine months after the onset of symptoms in the RE there was painless

loss of vision in the LE. Visual acuity was 20/30 in the RE and 20/50 in the LE. Colour vision was 2/17 Ishihara plates in the RE and 3/17 in the LE. On funduscopy there was optic atrophy in the RE and optic disc oedema in the LE. Standard automated perimetry showed an inferior arcuate scotoma in the RE and a central scotoma in the LE. The MRI of the orbits and brain with contrast was normal. Intravenous methylprednisolone (1g for 5 days) was offered but there was no clinical improvement with treatment. Over the following years, the patient was visually stable and there were no new episodes of optic neuropathy or other neurological symptoms. There is no family history of the disease and unfortunately, no sample from maternal lineage was available.

Skin biopsies of patient and controls were collected in the CHUC. Skin biopsies from three healthy Portuguese individuals without clinical evidence of a mitochondrial disorder, collected in the context of other medical interventions (surgery), were used as control samples in the experiments of functional analysis.

The DNA samples of 200 healthy subjects of the same ethnic background were used as controls.

Informed consent was obtained from the participants, as recommended by the local Ethics Committee (CE-032/2014), following the Tenets of the Helsinki Declaration.

3.1.2.2 Skin derived cultured fibroblasts

Fibroblasts were grown in complete medium – Ham's F-10 (Gibco, Life Technologies) supplemented with 20% FBS (Gibco, Life Technologies), 4mM GlutaMAX (Gibco, Life Technologies), 2.5mM sodium pyruvate (Gibco, Life Technologies), 65µg/ml uridine (Sigma-Aldrich, 250U/ml penicillin (Gibco, Life Technologies), 250µg/ml streptomycin (Gibco, Life Technologies), 250µg/ml kanamycin (Sigma-Aldrich), 2.5µg/ml amphotericin B (Gibco, Life Technologies), 2% Ultroser G (Gibco, Life Technologies) – and incubated at 37^{o}C and 5% CO_2, with 95% humidity. All handling procedures were conducted in aseptic conditions in a laminar flow cabinet, using sterile instruments and reagents.

3.1.2.3 Molecular genetic screening

Total DNA was extracted from fibroblasts and blood using the phenol-chloroform method according to standard protocols[305,306].

The entire mitochondrial genome was sequenced in patient through the NGS in the two available tissues (skin fibroblasts and blood), enriched by a single amplicon long-range PCR followed by massively parallel sequencing[307], on HiSeq2000 equipment from Illumina technology, at the mitochondrial laboratory, department of molecular and human genetics at Baylor College of Medicine, Houston. The haplogroup of the patient was determined using the Haplogrep® tool[308]. The unclassified mtDNA variant detected has been submitted to ClinVar (http://www.ncbi.nlm.nih.gov/clinvar/).

In order to verify the involvement of possible alterations in nuclear genes, the NGS exome was performed by Nextera Exome Capture methodology Illumina Nextera Rapid Capture Exome v1.2 PE100, from Illumina, totalizing around 200 thousand exons, followed by sequencing accomplished using the Illumina HiSeq2500 equipment. Data analysis was performed using the software Ingenuity® Variant Analysis.

3.1.2.4 Total RNA extraction and reverse transcriptase

RNA from controls and patients' fibroblasts was obtained with RNeasy Mini Kit (Qiagen) according to the manufacturer's protocol. Briefly, pelleted fibroblasts (~$3x10^6$ cells) were lysed by buffer RLT plus β-mercaptoethanol as indicated in the protocol and were mixed to homogenize. The RNA was precipitated with 70% ethanol. Sample was transferred to an RNeasy spin column placed in a 2ml collection tube, and centrifuged for 15 sec at ≥8,000 x*g*. In order to eliminate genomic DNA contamination, two different on-column DNase (RNase-Free DNase set, Qiagen) digestion steps were performed. After washing, RNase-free water was added directly to the spin column membrane, and the tube was centrifuged for 1 min at ≥8,000 x*g* to elute the RNA.

Before performing the reverse transcriptase reaction, the concentration and quality of RNA were verified by digital electrophoresis using the Agilent 2100 Bioanalyser to check the rRNA ratio and the presence of degradation products. In

order to match the quality criteria, only the RNA samples presenting RNA integrity number (RIN) higher than 8 (range: 0-10) were used in the following steps.

The transcription of RNA into cDNA was performed using a High-Capacity cDNA Reverse Transcription Kit (Applied Biosystems), according to the manufacturer's protocol. The reaction was conducted as follows: 10 min at 25°C and 120 min at 37°C, for primer annealing and cDNA synthesis, respectively, and 5 min at 85°C, for denaturation of reverse transcriptase, and then the samples were cooled to 4°C. In this step a duplicate without reverse transcriptase (RT-) for all samples and controls was included in order to check for DNA contamination during the Real-time PCR reaction.

The cDNA was sequenced by automated Sanger sequencing, according to the manufacturer's instructions (3130 ABI Prism sequencing system), using BigDye® Terminator Ready Reaction Mix v3.1 (Applied Biosystems), in order to verify the presence of the novel sequence variation previously found.

3.1.2.5 Quantification of MT-ATP8 mRNA levels

In order to use the most stable genes to normalization, a TaqMan Array Fast plate (Applied Biosystems, USA) was tested to the cDNA fibroblasts samples. The stability of the amplified products of ten different genes was verified using different tools (NormFinder: http://moma.dk/normfinder-software; Genorm: http://medgen.ugent.be/~jvdesomp/genorm/; and BestKeeper: http://genex.gene-quantification.info/). Accordingly, the best housekeeping genes for our samples were *TBP* and *HMBS*.

The cDNA of each patient's sample and three controls was amplified in a 7500 Fast Real-Time PCR system (Applied Biosystems, USA), using the specific TaqMan gene expression assay (Applied Biosystems) and TaqMan Universal Master Mix II (Applied Biosystems) following the manufacturer's protocol. The qPCR reactions were performed in triplicate and using three independent cDNAs from each sample. The thermal cycling conditions included 10 min at 95°C, proceeding with 40 cycles of 95°C for 15 sec and 60°C for 1 min. Before the analysis, Ct values were corrected with the RT-values for each sample using the GenEx V.6 software (MultiD Analyses AB).

Quantification of mt-ATP8 mRNA levels was obtained using the $2^{-\Delta\Delta Ct}$ method, where $\Delta Ct = Ct^{mt\text{-}ATP8} - Ct^{HMBS\ and\ TBP\ mean}$ and $\Delta\Delta Ct = \Delta Ct^{sample} - \Delta Ct^{Control}$.

3.1.2.6 Detection of ATP synthase protein 8 levels

Human primary fibroblasts were grown to confluence. After being washed and scraped from the culture flasks, cells were homogenized at 4°C using a glass/Teflon homogenizer in isolation buffer (20mM HEPES, 10mM KCl, 1.5mM $MgCl_2$, 250mM sucrose, 1mM EDTA, 1mM EGTA, pH 7.4) containing protease inhibitors (1mM DTT, 1µg/ml chymostatin, 1µg/ml leupeptin, 1µg/ml antipain, 1µg/ml pepstatin A and 0.1mM PMSF). The lysate was centrifuged at 700 x*g* for 12 min at 4°C in order to sediment mainly intact cells, cell debris and nuclei. The supernatant was then centrifuged at 12,000 x*g* for 20 min at 4°C, for obtaining the crude mitochondrial pellet, which was solubilized in a solution containing 10mM Tris-acetate, pH 8.0, 5mM $CaCl_2$, 0.5% Nonidet P40, 1mM DTT, 1µg/ml chymostatin, 1µg/ml leupeptin, 1µg/ml antipain, 1µg/ml pepstatin A and 0.1mM PMSF, prior to storage at -80°C.

Samples were analysed by SDS-PAGE according to a method previously described[309]. Total protein content of mitochondria-enriched fractions was quantified using the Bradford method. Volumes were adjusted according to the total protein concentration of each sample and 30µg of total protein were loaded per lane into a 10% polyacrylamide gel. After electrophoresis, proteins were electrotransferred (Mini PROTEAN® tetra cell system, BioRad) to PVDF membranes (Hybond P 0.5µm, Amersham) for 2 h at 0.75A, at 4°C. Afterwards, the membranes were blocked for 1 h in Tris-buffered saline solution (50mM Tris and 150mM NaCl) with 0.1% Tween-20 (TBS-T) and 5% skimmed milk, followed by an incubation overnight, at 4°C, with rabbit monoclonal anti-human citrate synthase (CS, ab129095, Abcam) at 1:5,000, or rabbit polyclonal anti-human ATP8 (sc-84231, Santa Cruz Biotechnology) at 1:200. After washing the membranes in TBS-T, they were incubated with the appropriate HRP-conjugated secondary antibody solution (1:5,000, Bio-Rad) for 90 min at room temperature.

Afterwards, membranes were incubated with chemiluminescence substrate (Clarity Western ECL Substrate, Bio-Rad) and detection was carried out using the

VersaDoc Imaging System 3000 (Bio-Rad). Protein band intensities were calculated by using Quantity One® 1-D software (Bio-Rad) from at least 3 independent experiments, with values expressed as mean±SEM. Relative quantification of A6L subunit (ATP synthase protein 8) was performed using the citrate synthase (CS) as a normalizing protein.

3.1.2.7 Relative quantification of MRC complexes

Samples were processed according to the protocol described[224]. Firstly, cells were sedimented by centrifugation at 800 x*g* for 10 min at 4°C. After discarding the supernatant, samples were solubilized with digitonin (4 mg/mL in PBS) for 10 min at 4°C. Following centrifugation at 12,000 x*g* for 10 min at 4°C, pellets were washed with cold PBS and centrifuged at 12,000 x*g* for 5 min at 4°C. Crude mitochondrial pellets were suspended in ACBT buffer (1.5mM aminocaproic acid and 75mM Tris-glycine, pH 7.0) and incubated with 10% n-Dodecyl-D-maltoside (DDM) on ice for 10 min. Suspensions were centrifuged at 12,000 x*g* at 4°C, for 30 min, and the protein concentration in the supernatant was measured by the Bradford method. Samples were supplemented with BN-sample buffer (5% Coomassie Blue G-250, 750mM 6-aminocaproic acid, 50mM Tris-glycine/HCl and 0.5mM EDTA). A molecular weight marker (NativeMARK Unstained Protein Standard, Life Technologies) and 30µg of each sample were loaded into polyacrylamide gels (4-15% Mini-PROTEAN TGX Precast gel, Bio-Rad) and run for 30 min at 30V, 4°C. The run extended for 4 h at 80V, 4°C. One anode buffer (50mM Tris-glycine, pH 7.0) and two cathode buffers were used; deep blue cathode buffer A (15mM Tris-glycine, 50mM tricine, 0.02% Coomassie Blue G-250, pH 7.0) was replaced by cathode buffer B (15mM Tris-glycine and 50mM tricine, pH 7.0) when the running front reached 1/2 of the total running length.

Polyacrylamide gel with the native marker was cut and stained. Firstly, gel was incubated in fixing solution (50% methanol, 10% acetic acid, 100nM ammonium acetate) for 15-30 min, stained (0.025% Coomassie Blue G, 10% acetic acid) for 30-60 min and washed (10% acetic acid) twice for 15-60 min. The gel containing the proteins of interest was eletrotransferred (Mini PROTEAN® tetra cell system, BioRad) to a PVDF membrane (Hybond P 0.5µm, Amersham) for 2 h at 0.2A, at 4°C.

Blocking was carried out using 5% skimmed milk in TBS-T for 1 h, at room temperature. Afterwards, membranes were incubated with monoclonal primary antibodies [anti-NDUFA9 (ab14713, Abcam) at 1:1,000 for CI; anti-SDHA (ab14715, Abcam) at 1:5,000 for CII; anti-UQCRC2 (ab14745, Abcam) at 1:1,000 for CIII; anti-COX IV (ab14744, Abcam) at 1:750 for CIV; and anti-ATP5A (ab14748, Abcam) at 1:1,000 for CV] overnight, at 4^{o}C. After washing the membranes in TBS-T, they were incubated with the anti-mouse HRP-conjugated secondary antibody solution (1:5,000, Bio-Rad), for 1 h at room temperature. Detection was carried out using a chemiluminescence substrate (Clarity Western ECL Substrate, Bio-Rad), through the ChemiDocTM XRS+ System (Bio-Rad). Protein band intensities were calculated by Quantity One® 1-D software (Bio-Rad) from at least 3 independent experiments, with values expressed as mean±SEM. Relative semi-quantification of each complex assembled was performed in comparison to CII levels.

3.1.2.8 MRC enzymatic activity evaluation

Primary fibroblasts obtained from the patient biopsy were pelleted from six T_{25} culture flasks and washed with PBS prior to resuspension in the same buffer; samples were stored at -80^{o}C for 8 days. Ended this standardized period of time, samples were submitted to two freeze-thaw cycles. The spectrophotometric determination of the catalytic activity of the MRC complexes and segments was performed as previously described[107] using a SLM AMINCO DW2000 UV-VIS spectrophotometer. The enzymatic activities of all respiratory complexes and segments were normalised for total protein mass, determined by the Bradford method, and CS activity to correct for variations in mitochondrial content. All measurements were performed at 37^{o}C using a temperature-controlled cuvette jacket. The MRC deficiency criterion was considered when enzymatic activity ≤40% of reference mean value corrected to CS[107]. The MRC screening of the controls' fibroblasts was carried out by spectrophotometric bioanalytical evaluation to confirm the absence of mitochondrial energy dysfunction indicators.

3.1.2.9 ATP levels measurement

Intracellular ATP levels were measured in patient's and control's fibroblasts by using the luciferin/luciferase assay with ATPlite kit (Perkin Elmer), according to the manufacturer's instructions with minor modifications. In brief, a volume of 100µl suspension with cells was mixed with 50µl of mammalian cell lysis solution to release the intracellular ATP. One third of the cells' lysates were used to protein quantification by PierceTM BCA protein assay kit (ThermoScientific), following the manufacturer's indications. The remaining mixture was then transferred into a white walled solid bottom 96-well plate, 33.3µl of substrate solution were added and the luminescence intensity was measured by a Synergy™ HT-BioTek® Microplate Reader. Previously ATP standard solutions were prepared and treated in parallel with lysates, in order to calculate the ATP concentration in samples through the ATP standard curve. The ATP levels (nmol) were normalised to the protein content.

3.1.2.10 Mitochondrial respiratory rate and glycolytic activity evaluation

Oxygen consumption rate (OCR) and extracellular acidification rate (ECAR) were measured in adherent fibroblasts with a XF24 Extracellular Flux Analyser (Seahorse Bioscience, Billerica, MA, USA).

Each of the three controls' and patient's fibroblast cell lines were seeded in XF24 cell culture microplates (Seahorse Bioscience) at a density of 2×10^4 cells/well in normal culture medium and incubated for 24 h at 37°C in 5% CO_2 atmosphere. The OCR assays were conducted after replacing the growth medium in each well of unbuffered DMEM with the same glucose, glutamine and pyruvate concentrations as normal culture medium, pre-warmed at 37°C. The cells were pre-incubated for 1 h to allow temperature and pH equilibration in a CO_2-free environment, before starting the assay procedure. Baseline measurements of OCR were followed by the sequential addition to each well of oligomycin, FCCP and rotenone plus antimycin A (final concentrations: 1µM), with measurements between them.

At the end of each experiment, total protein quantification of individual wells was measured by Bradford method. Results were expressed as pmol of O_2 per minute per mg of protein. The bioenergetics parameters that were evaluated included: basal

respiration, maximum respiration, spare respiratory capacity, ATP production capacity and proton leak.

By directly measuring the ECAR, the XF Glycolysis Stress Test allows to assess the key parameters of glycolytic flux: glycolysis, glycolytic capacity, glycolytic reserve, as well as non-glycolytic acidification. Similarly to OCR evaluations, ECAR assays were performed after cells incubation in unbuffered DMEM without glucose or pyruvate, pre-warmed at 37^{o}C for 1 h in a CO_2-free incubator. After ECAR baseline measurements, referred to as non-glycolytic acidification, a saturating concentration of glucose caused a rapid increase in ECAR (glycolysis under basal conditions). The second injection was of oligomycin, with the subsequent increase in ECAR, revealing the cellular maximum glycolytic capacity. The final injection was of 2-deoxy-glucose (2-DG), a glucose analogue, resulting in ECAR decrease. The difference between glycolytic capacity and glycolysis rate defines the glycolytic reserve. At the end of each assay, protein determination was performed using Bradford method. Data units are mpH (index of the acidification of the medium surrounding the cells as protons are produced and extruded) per minute per mg of protein.

All determinations were performed in 9-12 replicates for each sample.

3.1.2.11 Analysis of mitochondrial membrane potential

Mitochondrial membrane potential was determined using the cationic fluorescent probe rhodamine 123 (Molecular probes, Invitrogen), which accumulates predominantly in polarized mitochondria. The variation of rhodamine 123 (positively charged) cellular retention was studied in order to estimate changes in $\Delta\Psi_m$. Following a washing step with Krebs medium (132mM NaCl, 4mM KCl, 1mM $CaCl_2.2H_2O$, 1.2mM NaH_2PO_4, 1.4mM $MgCl_2$, 6mM D-glucose, and 10mM HEPES) pH 7.4, dermal fibroblasts were incubated in the same medium containing 1.5µM rhodamine 123 for 1 h at 37^{o}C. Basal fluorescence (λ=540nm for excitation and λ=590nm for emission) was measured using a Microplate Spectrofluorometer Gemini EM (Molecular Devices, USA) for 5 min, followed by the addition of inhibitors of MRC (8µM rotenone – inhibitor of CI, 20µM antimycin A – inhibitor or CIII, or 2µg/ml oligomycin – inhibitor of CV) *per* well, and measured for 3 min at 37^{o}C. Carbonyl cyanide-p-trifluoromethoxyphenylhydrazone (FCCP, 2µM), a mitochondrial uncoupler, was added to the cells and the fluorescence

values were collected for another 3 min. In order to correct the rhodamine 123 fluorescence, values for variations in total intracellular protein content in each well were quantified by the Bradford method. Results were expressed as the difference between the basal fluorescence values and the increase of rhodamine 123 fluorescence levels upon addition of OXPHOS inhibitors or FCCP.

3.1.2.12 Measurement of mitochondrial superoxide anion ($O_2^{\bullet-}$)

Mitochondrial $O_2^{\bullet-}$ levels in fibroblasts from controls and patient were measured by using the fluorescent probe MitoSOX Red (Molecular Probes, Invitrogen). Briefly, dermal fibroblasts were washed in Krebs medium (132mM NaCl, 4mM KCl, 1mM $CaCl_2.2H_2O$, 1.2mM NaH_2PO_4, 1.4mM $MgCl_2$, 6mM D-glucose, and 10mM HEPES) at pH 7.4, and then incubated with 10µM MitoSOX Red in Krebs medium for 30 min, at 37°C. The basal fluorescence was taken for 20 min at 37°C with λ=510nm for excitation and λ=560nm for emission, followed by the addition of 8µM rotenone or 20µM antimycin A and measured for 40 min at 37°C, using a Microplate Spectrofluorometer Gemini EM (Molecular Devices, USA).In order to correct the MitoSOX Red fluorescence, values for variations in total intracellular protein content in each well were quantified by the Bradford method. The values were obtained as RFU (relative fluorescence units) per minute per milligram of protein, for each condition and then normalised to the basal (untreated) conditions.

3.1.2.13 Transmission electron microscopy (TEM)

Fibroblasts were collected and centrifuged at 775 *xg* for 5 min. The supernatant was discarded and pellet cells were fixed with 2.5% glutaraldehyde in 0.1M sodium cacodylate buffer (pH 7.2) supplemented with 1mM calcium chloride for 2 h. Following rinsing in the same buffer, post-fixation was performed using 1% osmium tetroxide for 1 h. After rinsing in buffer, buffer and distilled water and a final rinsing step in distilled water, 1% aqueous uranyl acetate was added to the cells, for contrast enhancement during for 1 h in the dark. After rinsing in distilled water, samples were dehydrated in a graded acetone series (30–100%), impregnated and embedded in Epoxy resin (Fluka

Analytical). Ultrathin sections (70nm) were mounted on copper grids and stained with lead citrate 0.2%, for 7 min. Observations were carried out on a FEI-Tecnai G2 Spirit Bio Twin at 80kV and images were acquired using the software AnalySIS 3.2.

3.1.2.14 Statistical analysis

Results were analysed using GraphPad Prism version 5.0 software for Windows, San Diego, California, USA. Normality tests were applied in order to verify the Gaussian distribution of the results. Statistical significance of differences between patient and controls was assessed by Student's *t*-test (or nonparametric Mann-Whitney test).

Statistical significance is represented as * for $p \leq 0.05$, ** for $p \leq 0.01$ and *** for $p \leq 0.001$.

3.1.3 Results

3.1.3.1 Genetic screening confirmed the unclassified mtDNA variant

The presence of the sequence variation in the *MT-ATP8* gene (m.8418T>C [228], p.Leu18Pro, ClinVar accession number: SCV000484519), haplogroup markers and polymorphisms were confirmed by NGS through the sequencing of the whole-mitochondrial genome (Table 3.1.1) and rearrangements were excluded. The patient belongs to the haplogroup T2b21. The unclassified alteration in *MT-ATP8* gene was detected in the cDNA of patient's fibroblasts (results not shown), but it was absent in the 200 controls screened (results not shown).

The exome sequencing results showed polymorphisms, variants with uncertain significance and unknown variants. After the analysis, there was no evidence that the nuclear variants represented a potential cause of the presented clinical phenotype of the patient (Table 3.1.2).

Table 3.1.1 Mitochondrial variants detected in the patient with severe optic neuropathy through the whole mitochondrial genome sequencing by NGS.

Nucleotide Change	Amino acid change	Locus	Previously described
m.73A>G	-	*HV2*	Yes
m.152T>C	-	*HV2*	Yes
m.263A>G	-	*HV2*	Yes
m.709G>A	-	*MT-RNR1 (12S)*	Yes
m.750A>G	-	*MT-RNR1 (12S)*	Yes
m.930G>A	-	*MT-RNR1 (12S)*	Yes
m.1438A>G	-	*MT-RNR1 (12S)*	Yes
m.1888G>A	-	*MT-RNR2 (16S)*	Yes
m.2706A>G	-	*MT-RNR2 (16S)*	Yes
m.4216T>C	Y304H	*MT-ND1*	Yes
m.4769A>G	Syn (M100M)	*MT-ND2*	Yes
m.4917A>G	N150D	*MT-ND2*	Yes
m.5147G>A	Syn (T226T)	*MT-ND2*	Yes
m.7028C>T	Syn (A375A)	*MT-COI*	Yes
m.8418T>C	**L18P**	***MT-ATP8***	**No**
m.8697G>A	Syn (M57M)	*MT-ATP6*	Yes
m.8860A>G	T112A	*MT-ATP6*	Yes
m.9278C>T	Syn (A24A)	*MT-COIII*	Yes
m.10057T>C	-	*MT-TG*	Yes
m.10463T>C	-	*MT-TR*	Yes
m.11251A>G	Syn (L164L)	*MT-ND4*	Yes
m.11719G>A	Syn (G320G)	*MT-ND4*	Yes
m.11812A>G	Syn (L351L)	*MT-ND4*	Yes
m.13368G>A	Syn (G344G)	*MT-ND5*	Yes
m.14233A>G	Syn (D147D)	*MT-ND6*	Yes
m.14766C>T	T7I	*MT-CYB*	Yes
m.14836A>G	Syn (W30W)	*MT-CYB*	Yes
m.14905G>A	Syn (M53M)	*MT-CYB*	Yes
m.15326A>G	T194A	*MT-CYB*	Yes
m.15452C>A	L236I	*MT-CYB*	Yes
m.15607A>G	Syn (K287K)	*MT-CYB*	Yes
m.15928G>A	-	*MT-TT*	Yes
m.16126T>C	-	*HV1, D-loop*	Yes
m.16294C>T	-	*HV1*	Yes
m.16304T>C	-	*HV1*	Yes
m.16519T>C	-	*D-loop*	Yes

Table 3.1.2 Variants selected after filtering the exome results for variant calling and low frequency (<1%).

Gene	Sequence variation	Amino acid change	dbSNP ID	Zygosity	Clinical Significance
HSPG2	c.8685G>C	p.A2869P	139838884	Heterozygous	Unknown
HSPG2	c.6624G>A	p.A2182T	143109401	Heterozygous	Unknown
TCAF2	c.876C>T	p.R265W	62486260	Homozygous	Unknown
MT-ATP8	m.8418T>C	p.L18P	-	Homoplasmic	Unknown

3.1.3.2 Transcript and protein levels assessment point to a significant decrease in the ATP synthase protein 8 subunit of CV

In order to verify whether the ATP synthase protein 8 is destabilized by the present variant, transcript and protein levels were determined. The transcript level was similar to controls (p=0.5495) (Figure 3.1.1A), but the protein levels were significantly decreased compared to controls (**p= 0.0015) (Figure 3.1.1B).

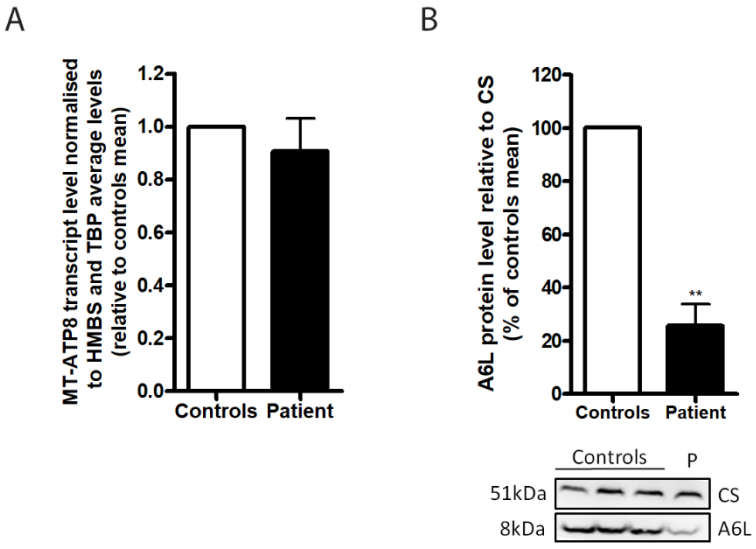

Figure 3.1.1 - Mitochondrial *ATP8* transcript and A6L protein level quantification in patient's fibroblasts. (**A**) Transcript level was evaluated from three independent RNA extractions and cDNA synthesis, in triplicate for each sample, normalised to the mean of the housekeeping genes HMBS and TBP. Data is representative of the mean±SEM, analysed with unpaired Student's *t*-test. (**B**) A6L protein levels were normalised to citrate synthase (CS). Results are representative of three independent determinations, run in duplicate, and presented as the mean±SEM. Statistical significance was determined by Mann-Whitney test, **p<0.01.

3.1.3.3 Complex I and V fully assembled are impaired

Concerning the assembly of MRC complexes (Figure 3.1.2A), a statistical significant reduction was verified for the fully assembled CI and V (**p*=0.0188 and ***p*=0.0010, respectively) in comparison to controls (Figure 3.1.2B and E, respectively). The CIII and CIV analysis did not present statistical significant alterations (Figures 3.1.2C and D, respectively).

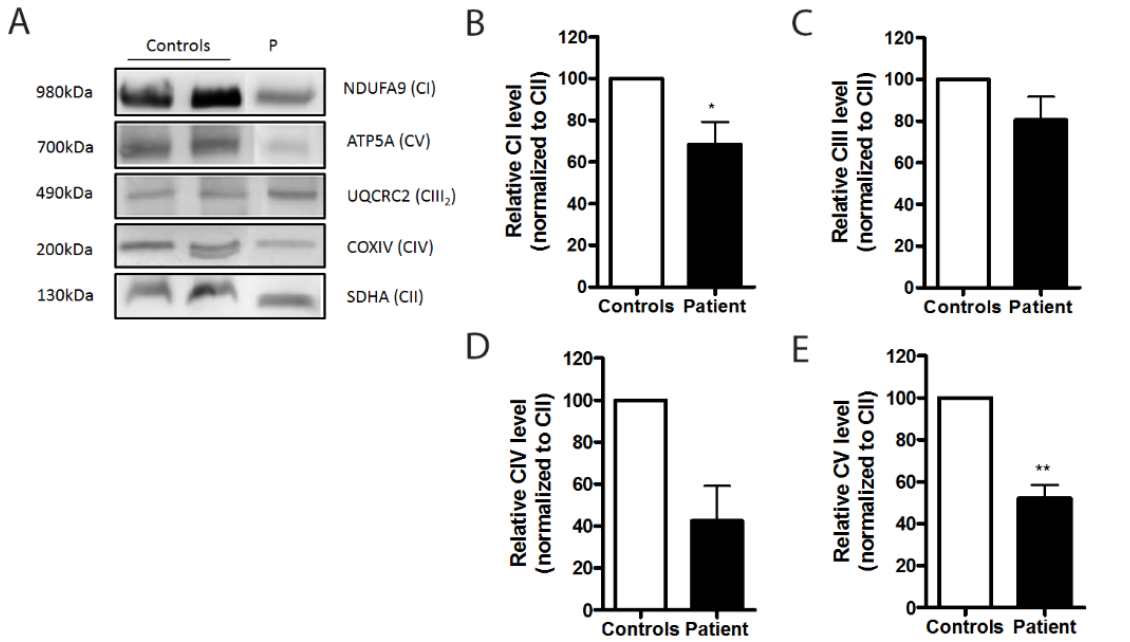

Figure 3.1.2 - **Quantification of the fully assembled complexes of MRC in fibroblasts of controls and patient with m.8418T>C.** Error bars are representative of the mean±SEM based on at least three independent experiments in duplicates. (**A**) Native electrophoresis followed by Western-blot analysis for complexes I to V in controls and patient, represented by P; (**B**) Relative level of fully assembled CI, Mann-Whitney test: **p*=0.0188; (**C**) Relative level of fully assembled CIII; (**D**) Relative level of fully assembled CIV; (**E**) Relative level of fully assembled CV, unpaired Student's *t*-test, ***p*=0.0010.

3.1.3.4 OXPHOS activity is impaired and intracellular ATP levels are decreased

Assessment of MRC enzymatic activities revealed that in patient's fibroblasts, when compared to the controls, complexes I, II and IV activities were not affected (Figures 3.1.3B-C and E), in contrast to the CIII activity that was diminished (49.5% in relation to controls, **p*=0.0234) (Figure 3.1.3D). Moreover, a significant decrease in CV activity (36% in comparison to control, ***p*=0.0078) was observed (Figure 3.1.3F).

Concerning the intracellular ATP levels, these were significantly decreased (*p=0.472) in patient's fibroblasts, in comparison with the controls (Figure 3.1.3I).

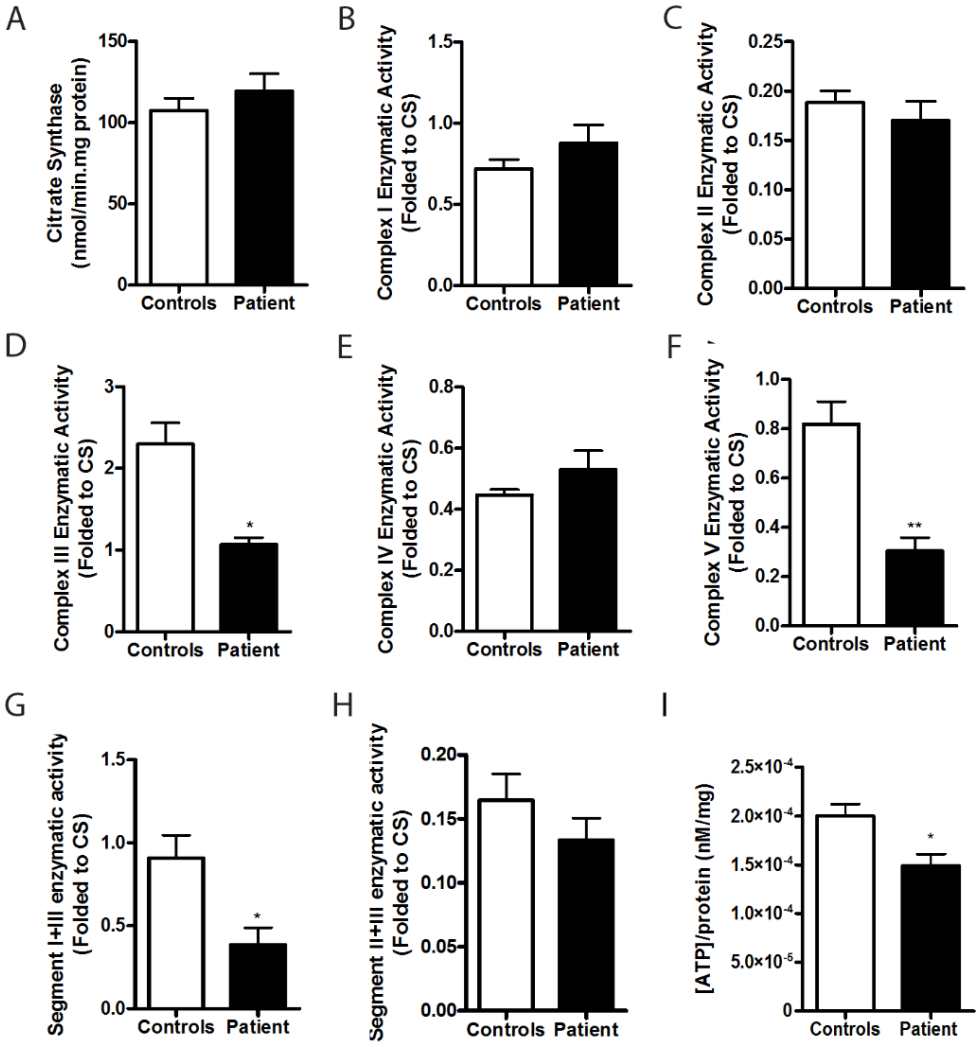

Figure 3.1.3 - **Mitochondrial enzymatic activity and ATP levels in patient and controls** of (**A**) citrate synthase, (**B**) CI; (**C**) CII; (**D**) CIII, Mann-Whitney test (*p=0.0234); (**E**) CIV; (**F**) CV, Unpaired t-test (**p=0.0010); (**G**) segment I+III, Mann-Whitney test (*p=0.0142); (**H**) segment II+III. Data are presented as the mean±SEM from at least three independent measurements; (**I**) Intracellular ATP levels determination in patient harbouring the m.8418T>C variation and controls (*p=0.0472). Results are derived of three independent measurements, run in triplicate.

3.1.3.5 OCR and ECAR evaluation indicated a decrease in ATP production and increase in glycolysis

OCR and ECAR were evaluated in cells of the patient and controls using Seahorse Bioscience technologies, allowing the evaluation of important bioenergetics parameters (Figure 3.1.4). In accordance with the OCR evaluation, mitochondrial respiration of patient's cells was deteriorated (Figure 3.1.4A), showing reduced ATP production (Figure 3.1.4G).

In order to compensate the reduced mitochondrial ATP production, glycolysis and the glycolytic capacity were significantly increased (**p=0.0028 and *p=0.0424, respectively) (Figure 3.1.4H and I, respectively). The glycolytic reserve presented similar results of controls' values (Figures 3.1.4J).

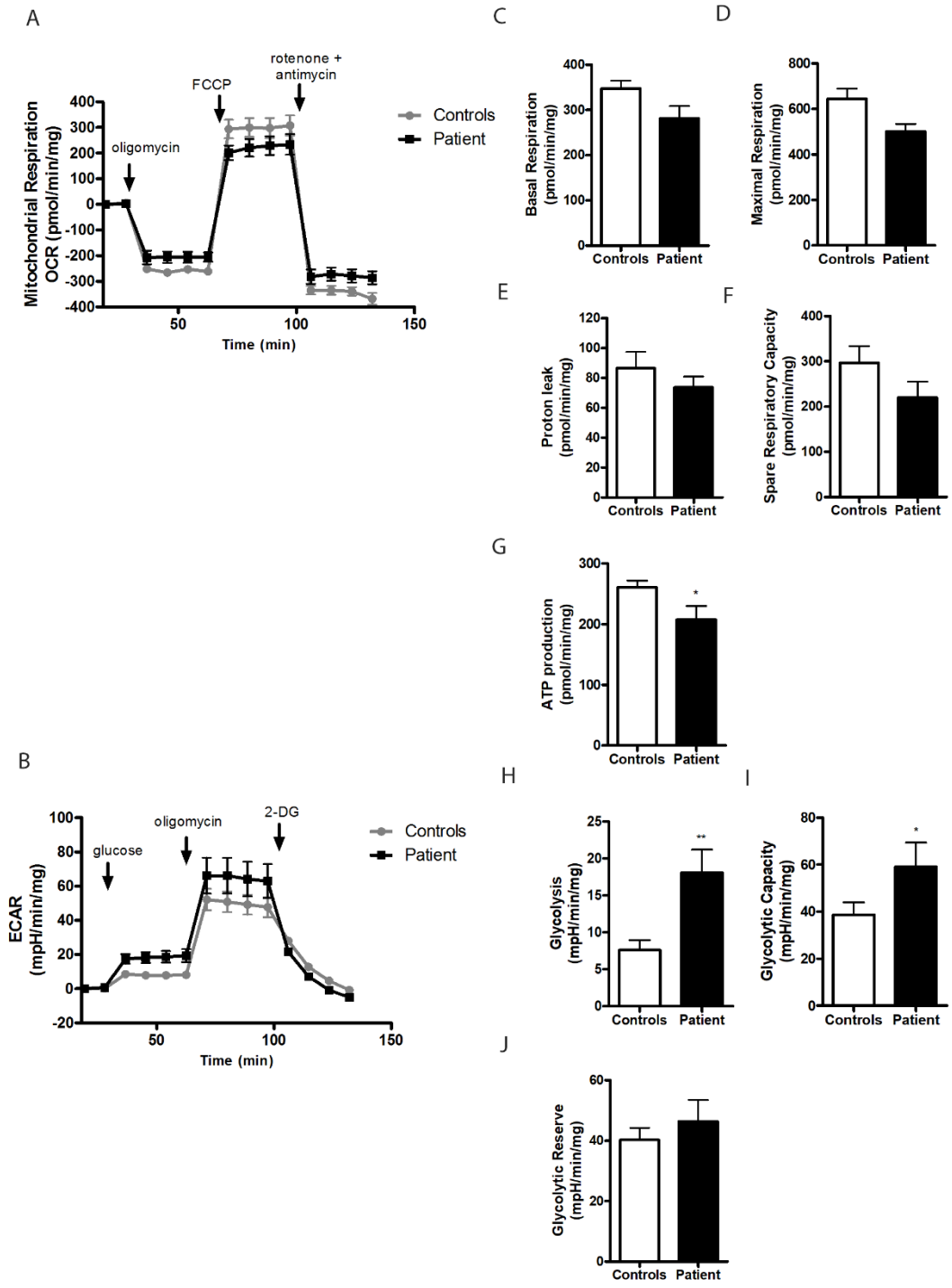

Figure 3.1.4 - **Respiration rate and glycolytic function measured by Seahorse Bioscience® technology**. Errors bars represent the standard error of mean based on three independent experiments in triplicates. **(A)** Mitochondrial respiration profile; **(B)** Acidification profile; **(C)** Basal respiration; **(D)** Maximal respiration; **(E)** Proton leak; **(F)** Spare respiratory capacity; **(G)** ATP production, Mann-Whitney test, **p*=0.0151; **(H)** Glycolysis, Mann-Whitney test, ***p*=0.0028; **(I)** Glycolytic Capacity, Mann-Whitney test, **p*=0.0424; **(J)** Glycolytic reserve.

3.1.3.6 Mitochondrial membrane potential evaluation showed hyperpolarization

Accumulation of rhodamine 123 probe in polarized mitochondria allowed the detection of significant changes in $\Delta\Psi_m$ of patient's cells, compared to control group. After the inhibition of complex I and III activities with rotenone and antimycin A, respectively, an increase of fluorescence was observed, which was further significantly increased after addition of FCCP (***p=0.0008 and **p=0.0019, respectively). The increase in fluorescence was more pronounced in patient's cells than in control (Figure 3.1.5A and B). Similar results were obtained after simulation of the maximal depolarization (oligomycin plus FCCP), where the difference between patient and controls was even more significant (***p=0.0002) (Figure 3.1.5C). A higher retention of rhodamine 123 in patient's fibroblasts highly suggests mitochondrial membrane hyperpolarization.

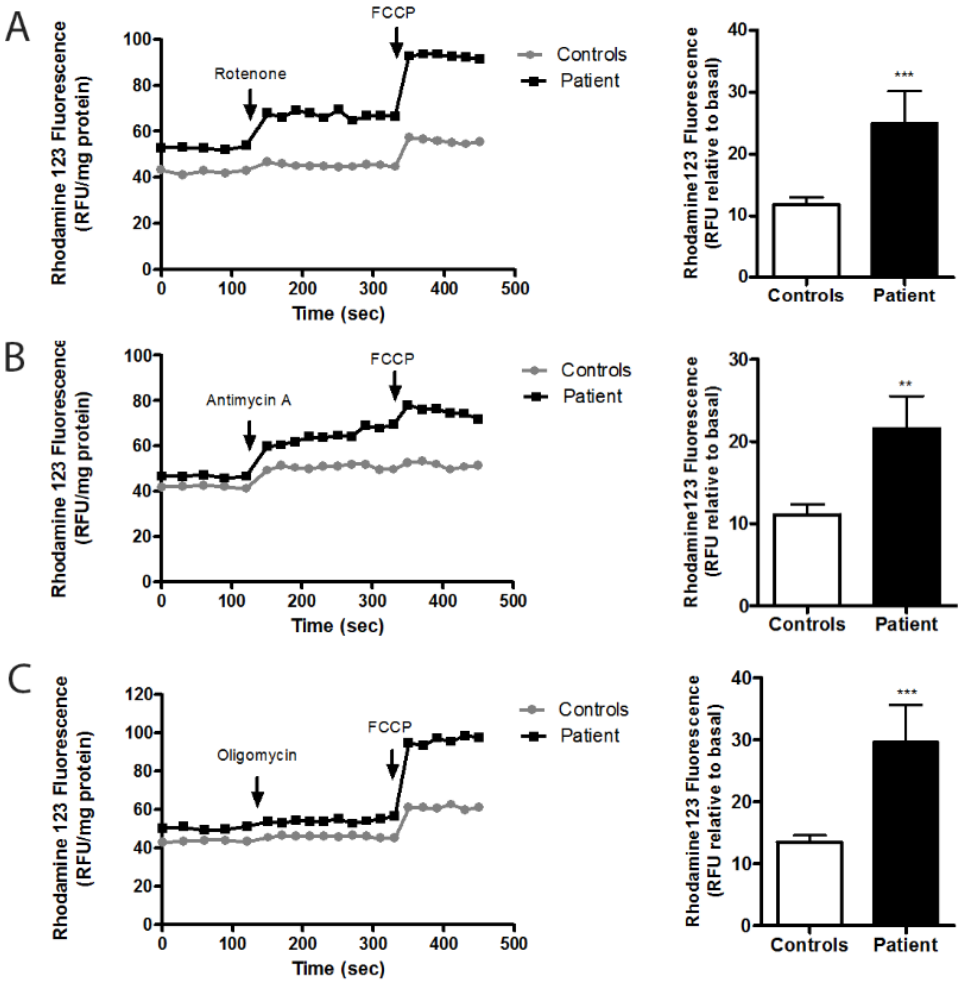

Figure 3.1.5 - Mitochondrial membrane potential in fibroblasts of patient and controls. Membrane potential evaluation after **(A)** CI inhibition with rotenone followed by uncoupling with FCCP (left), represented by the difference between the basal and rotenone plus FCCP-induced levels of rhodamine123 (***p=0.0008) (right); **(B)** CIII inhibition with antimycin-A followed by uncoupling with FCCP (left), represented by the difference between the basal and antimycin A plus FCCP-induced levels of rhodamine123 (**p=0.0019) (right); **(C)** CV inhibition with oligomycin followed by uncoupling with FCCP (left), represented by the difference between the basal and oligomycin plus FCCP-induced levels of rhodamine123 (***p=0.0002) (right); Data are presented as the mean±SEM based on three independent measurements in triplicates. Statistical significance was evaluated by Unpaired Student's *t*-test.

3.1.3.7 Superoxide anion production increased upon inhibition of complex I

Mitochondrial $O_2^{\bullet-}$ basal levels were not changed in patients' cells when compared to control values (Figure 3.1.6A). However, a significant increase in superoxide production was observed after the addition of rotenone (*p=0.0351) (Figure 3.1.6B). Otherwise, the complex III inhibition did not affect the $O_2^{\bullet-}$ production (Figure 3.1.6C).

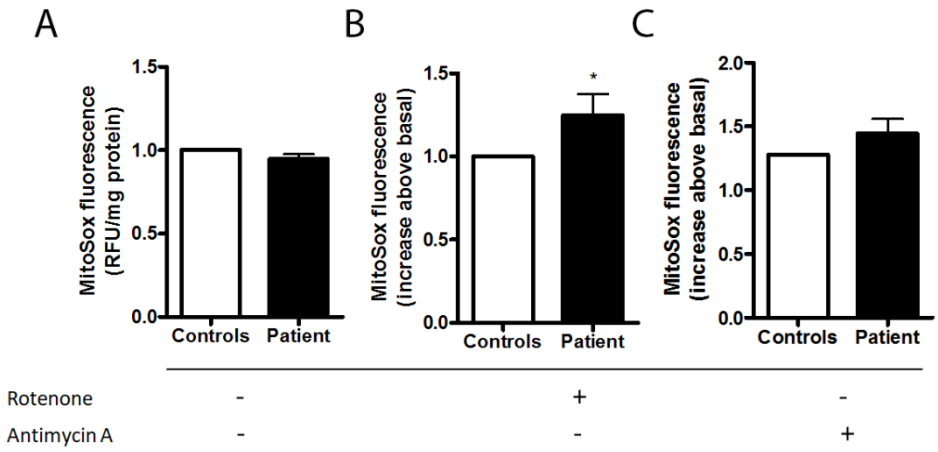

Figure 3.1.6 - **Levels of superoxide anion production in fibroblasts of patient harbouring the m.8418T>C and controls. (A)** Basal levels of superoxide anion; **(B)** Superoxide anion levels after inhibition of CI with rotenone (**p*=0.0351); **(C)** Superoxide anion levels after inhibition of CIII with antimycin A. Results are from three independent measurements in triplicates. Errors bars represent the mean±SEM and the statistical significance was verified by unpaired Student's *t*-test, ****p*<0.0001.

3.1.3.8 Ultrastructural and morphological investigation

In the images obtained by TEM (Figure 3.1.7), the comparison between controls' (Figure 3.1.7A-C) and patient's fibroblasts (Figure 3.1.7D) disclosed rough endoplasmic reticulum (RER) morphology alterations, namely a marked dilation was detected in the patient. Regarding the mitochondrial morphology, no visible changes were observed. Moreover, the presence of Golgi apparatus was rarely detected in patient's cells.

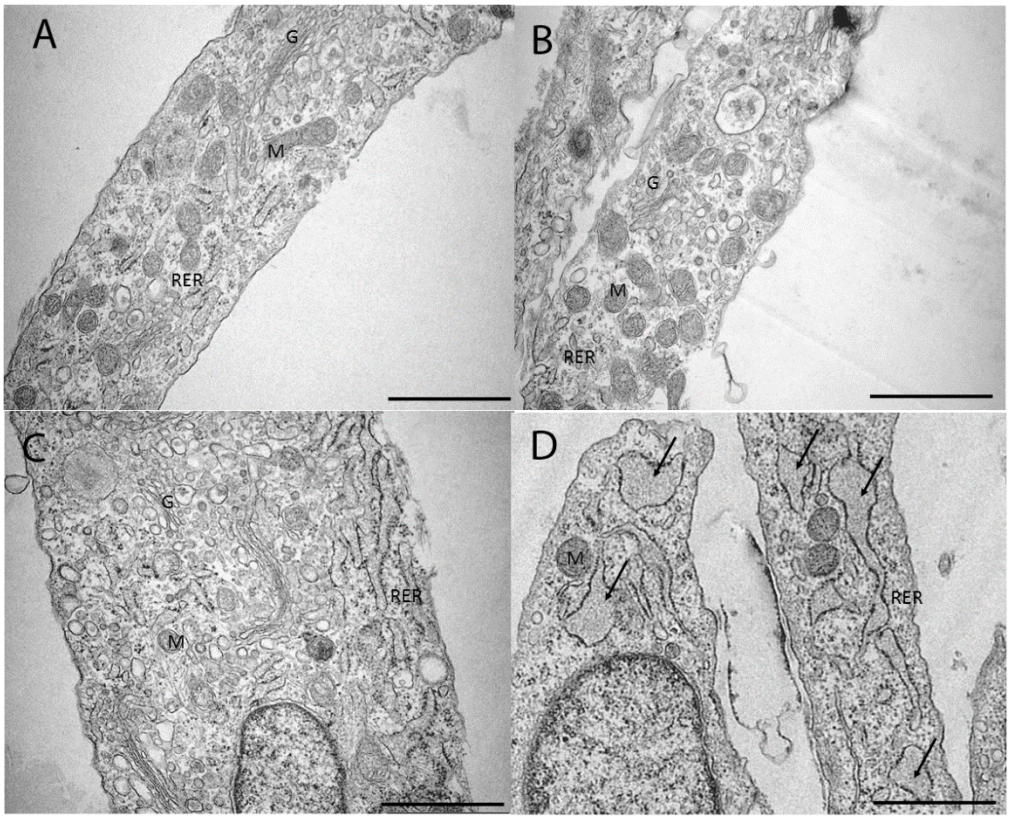

Figure 3.1.7 - Study of primary fibroblasts by transmission electron microscopy. Ultrastructural aspects of (**A**) Control 1, (**B**) Control 2, (**C**) Control 3, (**D**) Patient. Dilation of RER in patient's cells is assigned with arrows. G – Golgi, M – Mitochondrion, RER – Rough Endoplasmic Reticulum. Scale bar: 1 μm.

3.1.4 Discussion

Alterations in the content, structure and function of human ATP synthase have been associated with severe pathological conditions (hypertrophic cardiomyopathy, cerebellar ataxia, neuropathy, diabetes mellitus, sensorineural hearing impairment, and hypergonadotropic hypogonadism), resulting in mitochondrial disorders, as previously reported[173–175,304].

In this case report, the exome and whole mitochondrial genome analysis confirm the presence of a novel mtDNA alteration in the *MT-ATP8* gene (m.8418T>C, p.Leu18Pro) in the patient's DNA samples. The sequence variation was detected in homoplasmy in blood and dermal fibroblasts. Accordingly, and reinforcing our results, the sequence variation was not detected in the 5140 human mitochondrial genomes presented in the mtDNA-GeneSyn tool[310]. These data suggest that the novel variant

does not occur in the general population and provides further evidence for its possible pathogenicity.

Besides, the sequence variation changes the aliphatic amino acid Leucine to Proline, a cyclic amino acid, in a transmembrane domain; this may cause abnormal ATP synthase protein 8 structure. Moreover, the majority of the mutations detected in the other mitochondrial gene of ATP synthase (*MT-ATP6*) alters Leucine to Proline on subunit 6, causing a range of mitochondrial diseases[311–313]. An attractive hypothesis is that mutations in these residues modify proton movement indirectly by changing the secondary structure[314]. Additionally, the sequence variation under study is present in a conserved position and it was predicted to be deleterious by five freely available bioinformaticss tools, as previously described by our group[228].

Since the transcript level of *MT-ATP8* gene was not affected (Figure 3.1.1A), it is likely that post-translational mechanism, including increased proteolysis, lead to ATP synthase protein 8 reduction to less than 50% of controls levels (Figure 3.1.1B). A mechanism of quality control involved in the correction of translation defects in mitochondria has been described, which is composed by chaperones that interact with unfolded and misfolded proteins, and recruit these proteins to a mitochondrial protease complex for degradation[57]. Therefore, one hypothesis is that structural changes of ATP synthase protein 8 are causing protein degradation by the protein quality control machinery in mitochondria.

In addition, the CV fully assembled is approximately 50% of control value (Figure 3.1.2E), which is in accordance with the ATP synthase protein 8 quantification (Figure 3.1.1B). It is not totally clear how ATP synthase is assembled in human mitochondria. However, recent studies have suggested that the pore-forming complex, composed by the c-ring and the subunit 6, is assembled in the last step, in order to avoid a proton efflux and simultaneously the dissipation of the mitochondrial membrane potential without ATP synthesis[82,83,86,302]. Moreover, the two mitochondrial encoded subunits of ATP synthase (6 and 8) are proposed to be assembled together in the membrane in this final step, when the subunit 6, in close arrangement with the c-ring, constitute an integral membrane proton channel, and the subunit 8 provide a physical link between the proton channel and the stator. Consequently, the 6 and 8 subunits have a very important role in the structural stabilization of the ATP synthase holocomplex[82,83,86,302].

Furthermore, the association of the two subunits seems to be essential to stabilize the formation of dimers, through the link of accessory subunits (e and g)[302]. Accordingly, it seems reasonable to suggest that the reduction in the assembly of holocomplex V can be ascribed to a decrease in the 8 subunit. This consequence, and the fact that subunits 6 and 8 are assembled together, could cause changes in F_0 function, leading to inhibition in the transport of protons from the intermembrane space to the matrix. In addition, blocking of proton transport creates a high protonic potential in the intermembrane space, causing mitochondrial membrane hyperpolarization (Figure 3.1.5). Similar results were obtained for alterations in *MT-ATP6* gene affecting subunit 6[220,303,315].

The loss of F_0 function restricts the F_1 rotor movement and the activity of CV may be compromised. Accordingly, the biochemical evaluation of the MRC catalytic activity in patient's fibroblasts demonstrated a deficit (37% of control values) in CV activity (Figure 3.1.3F). Currently, it is not clear how CV deficiency would affect the activity of other complexes, namely CIII, as presented in our study and reported by Ware and colleagues[174].

The final consequence of ATP synthase dysfunction in patient's fibroblasts is a reduction in intracellular ATP levels (Figure 3.1.3I). In order to verify the general mitochondrial bioenergetics capacity, OXPHOS and glycolytic function were compared. As represented in Figure 3.1.4, the OXPHOS capacity to produce ATP (Figure 3.1.4G) is reduced as expected. Contrariwise, glycolysis and glycolytic capacity (Figure 3.1.4H and I) are significantly increased. These results suggest that the cells are trying to compensate the decrease in mitochondrial ATP production increasing glycolysis, even so this compensatory mechanism is not enough to reach the normal intracellular ATP levels.

A predictable effect of impaired energy would be an increase in ROS production, since the electron transfer compounds in the respiratory chain become over-reduced. In this study, in the basal conditions, the MitoSox fluorescence was not altered in comparison to controls (Figure 3.1.6A). These results suggest unaltered levels of superoxide anion in skin fibroblasts of patient, similar to a recent study in a patient presenting mitochondrial syndrome with ataxia, peripheral neuropathy, diabetes mellitus, and hypergonadotropic hypogonadism, caused by a novel mutation in *MT-*

ATP6/8 gene[173]. One cannot exclude that superoxide dismutase enzymes activity (Cu/Zn-SOD and Mn-SOD) might be up-regulated[220], which may mask a possible slight increase in ROS production. However, the increase production of superoxide anion after the inhibition of complex I suggests an augmented susceptibility to generate excessive ROS in such conditions, what could be the case of retinal ganglion cells of patient.

Since the formation and decay of supramolecular structures (oligomers) of ATP synthase are dynamic processes linked to formation and loss of cristae[83,316], and because the subunit 8 seems to be essential to the stabilization of ATP synthase oligomerization[82,302], the morphology of mitochondria was investigated by TEM. However, no dramatic changes were observed in mitochondrial ultrastructure, contrarily to RER cisternae (Figure 3.1.7D). Similarly, Signorini and colleagues described RER dilation in skin fibroblasts of patients presenting Rett Syndrome[317]. Recently, a network involving ER-mitochondria contact sites were reported to play a role in protein and lipid biogenesis, bioenergetics, membrane architecture and organellar dynamics[318]. According to other studies, decreased cellular ATP levels could lead to ER stress, defined as an accumulation of unfolded or misfolded proteins in ER lumen, that could cause ER dilation[153,319]. Therefore, mitochondrial dysfunction in patient's fibroblasts may be an inducer of ER stress. It has been described that, under stress conditions, the contact sites between these two organelles amplify, triggering multiple and synergistic responses, namely autophagosome formation, apoptosis activation and a decrease in mitochondrial biogenesis[153,154,320]. Further investigation will be necessary in order to understand the impact of ER-mitochondria crosstalk in the pathophysiology of the disease.

In conclusion, the present results are the first report to characterize the structural and functional role of p.Leu18Pro of the ATP synthase protein 8 of the human mitochondrial ATP synthase. In this study, we report a novel homoplasmic mutation m.8418T>C in the *MT-ATP8* gene of a patient suspected of LHON. The mutation is possibly affecting the protein structure, causing protein degradation and impaired assembly of CV. Besides, hyperpolarization of mitochondrial membrane potential was demonstrated. The biochemical analysis showed decreased CV activity and ATP production, and increased glycolysis. Moreover, the reported ultrastructural changes

are to be considered as a new finding to be investigated in LHON disease. Additionally, the variant may be identified in other independent families with the same phenotype in order to reinforce the pathogenicity.

Taken together, the results suggest that m.8418T>C is pathogenic, presenting a range of consequences to cells, affecting the bioenergetics and being the probable cause for disease pathogenesis in the P1.

3.2 CASE REPORT II

Mitochondrial dysfunction in a lysosomal storage disorder: a spinocerebellar ataxia case report

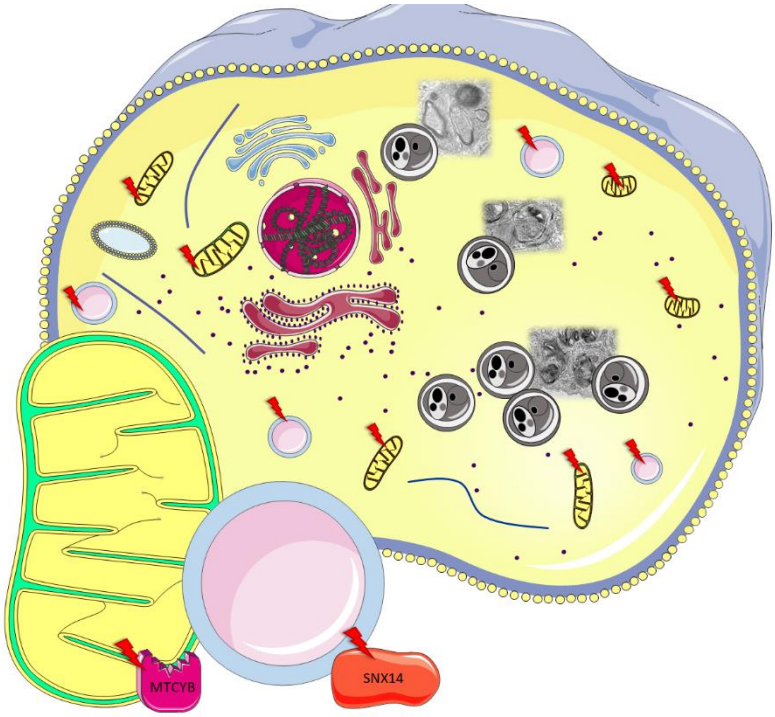

Abstract

Mutations in the *SNX14* gene have been identified in association with spinocerebellar ataxia, autosomal recessive 20, a lysosomal storage disorder (LSD), affecting the lysosomal function, with impact on the recycling of cellular components. However, the mechanism leading to cell death remains unclear in this disorder. Recently, mitochondrial dysfunction has been implicated in LSDs. In the present study, a novel maternal inherited homoplasmic mtDNA variant (m.14771C>A) in *MT-CYB* was identified in a patient with spinocerebellar ataxia, autosomal recessive 20, in whom a homozygous mutation in the *SNX14* gene was previously found. Other mutations causing mitochondrial diseases were excluded by NGS of the entire mtDNA and the nuclear panel Mitome500. The functional impact of the unclassified mtDNA variant was investigated in cultured fibroblasts of the patient, in order to clarify the mitochondrial involvement in this pathology. *In silico* analysis predicted that the sequence variation is likely pathogenic. The assessment of MTCYB protein level showed a significant decrease. There was an impairment in catalytic activity of mitochondrial respiratory chain complexes I, III and V. The evaluation of oxygen consumption revealed a respiration deficit, in agreement with the significant decrease of intracellular ATP levels detected. Concordantly, the mitochondrial membrane was depolarized. These results indicate mitochondrial dysfunction, strongly suggesting a possible deleterious role for the unclassified mtDNA variant identified. Multilamellar bodies had been previously identified in patient's skin fibroblasts, corroborating the lysosomal dysfunction. The impact on the recycling of cellular components has been considered the main cause of the clinical phenotype. The clear evidence of bioenergetics dysfunction herein presented suggests an important contribution of mitochondrial impairment for the clinical manifestation, as recently described for other LSDs.

Keywords: Spinocerebellar ataxia; mtDNA variant; bioenergetics dysfunction; lysosomal dysfunction.

3.2.1 Introduction

OXPHOS diseases are a group of disorders with a heterogeneous clinical presentation, affecting several organs and tissues[28,29,163]. Therefore, the identification of a specific syndrome or phenotype is often difficult. In addition, lysosomal storage disorders (LSD) also present heterogeneous clinical manifestations, which can overlap with those observed in mitochondrial disorders[321], as in the case of the patient in study (patient 2, P2).

The patient's phenotype included coarse face, relative macrocephaly, short stature, severe intellectual disability with absent speech, severe ataxia and cerebellar atrophy. Recently, the set of these clinical manifestations was designated as spinocerebellar ataxia, autosomal recessive 20 (OMIM: #616354)[322], in association with *SNX14* mutations[323,324]. The authors hypothesized that *SNX14* gene product might be implicated in the recycling of cellular components in human cerebellar development and maintenance[323], and that the SNX14 protein mediates the fusion of lysosomes with autophagosomes, consistent with a defect in autophagosome clearance[324]. Moreover, the activation of apoptosis in neural tissue was observed by the dramatic increase in caspase 3 signal, explaining the neuronal cell death occurring in the disease[324]. Accordingly, mutations in *SNX14*, being associated to a defect in the elimination of cellular components, would define these genetic abnormalities as the cause of this new LSD. However, the specific molecular mechanisms leading to neurodegeneration in LSDs are still not clear.

Recently, the presence of mitochondrial dysfunction has been established in LSDs[325], but the molecular mechanism underlying the association of lysosomal dysregulation and mitochondrial damage remains uncertain. On the other hand, there are evidences that mitochondrial damage may cause lysosomal dysfunction, suggesting a crosstalk between the two organelles[326,327].

Therefore, the present work aimed to investigate the functional impact of a novel mtDNA sequence variation (m.14771C>A) in the *MT-CYB* gene identified in a patient presenting spinocerebellar ataxia, autosomal recessive 20 (OMIM: #616354), harbouring a *SNX14* mutation (c.2596C>T, p.Gln866*).

3.2.2 Samples and methods

3.2.2.1 Case report

The patient is a 16-year-old Portuguese female (P2) (Figure 3.2.1A, II6), followed at the Paediatric Hospital – Centro Hospitalar e Universitário de Coimbra (CHUC). Parents (Figure 3.2.1A, I1 and I2) are consanguineous (first cousins), healthy, with normal IQ. She and her healthy non-identical twin (Figure 3.2.1A, II7) are the youngest of seven siblings, two boys and five females. The older sister (Figure 3.2.1A, II3) presents a similar clinical phenotype. This family was analysed in detail[322], allowing the definition of a novel spinocerebellar ataxia phenotype. According to the study, the mutation c.2596C>T in the *SNX14* gene was identified in homozygosity only in the two affected sisters. Nevertheless, as the hypothesis of a mitochondrial disease was previously considered, the investigation has been carried out, allowing the identification of an unclassified mtDNA variant.

Mitochondrial bioenergetics' characterisation was further performed on skin fibroblasts from the patient and lymphocytes of the proband, the affected sister, and their parents.

The DNA samples of 200 healthy subjects of the same ethnic background were used as controls. Skin biopsies from three Portuguese individuals without any clinical evidence of a mitochondrial disorder, collected in the context of other medical interventions, were used as control samples in the experiments of functional analysis.

Informed consent was obtained from the participants, as recommended by the local Ethics Committee (CE-032/2014), following the Tenets of the Helsinki Declaration.

3.2.2.2 Skin derived cultured fibroblasts

Skin biopsy was collected in the hospital under local anaesthesia and the culture of fibroblasts was carried out as described in the case report I of this chapter (section 3.1.2.2).

3.2.2.3 Molecular genetics screening

The entire mitochondrial genome of patient's DNA derived from fibroblasts and lymphocytes was sequenced using the NGS, as previously described[307]. Haplogroup of the patient was determined using the Haplogrep® tool[308], based in mtDNA sequence variations detected. Automated Sanger sequencing analysis was performed according to the manufacturer's instructions (3130 ABI Prism sequencing system), using BigDye® Terminator Ready Reaction Mix v3.1 (Applied Biosystems), for investigation of the mtDNA region (14420-14855) in DNA from patient's fibroblasts and lymphocytes. The genetic screening of the 200 controls' samples was carried out by the same method in order to verify the absence of the novel genetic variant. A screening for the m.14771C>A sequence variation using DNA from parents, the affected sister and the twin sister was also performed by Sanger sequencing.

To analyse potential nuclear gene involvement, coding exons of 513 (Appendix) candidate genes related to mitochondrial structure and function (Mitome500) were hybridized with customized oligonucleotide probe library, captured and then massively sequenced using the HiSeq2000 platform (Illumina technology®).

3.2.2.4 *In silico* Analysis

The *in silico* analysis included the evolutionary conservation of the *MT-CYB* gene and MTCYB amino acid sequence from different species [human (*Homo Sapiens*, NC_012920), chimpanzee (*Pan troglodytes*, NC_001643), bonobo (*Pan paniscus*, NC_001644), orangutan (*Pongo pygmaeus*, NC_001646), gorilla (*Gorilla gorilla*, NC_001645), mouse (*Mus musculus*, NC_005089), rat (*Rattus norvegicus*, NC_001665), bovine (*Bos taurus*, NC_006853), chicken (*Gallus gallus*, NC_001323), frog (*Xenopus laevis*, NC_001573), urchin (*Strongylocentrotus purpuratos*, NC_001453) and fruit fly (*Drosophila melanogaster*, NC_001709)] using ClustalOmega|EBI®[328]. In addition, the impact of the amino acid substitution in protein function was predicted by five bioinformatics tools: PolyPhen® v2[329], SIFT®[330], Mutation Assessor®[331], Provean®[332] and PredictProtein®[333].

3.2.2.5 Quantification of MT-CYB mRNA levels

RNA from controls and patients' fibroblasts was obtained with RNeasy Mini Kit (Qiagen) and the transcription of RNA into cDNA was performed using a High-Capacity cDNA Reverse Transcription Kit (Applied Biosystems), according to the manufacturer's protocol, as described in the section 3.1.2.4 of the case report I. Also, cDNA of patient was sequenced in order to verify the presence of the novel sequence variation previously found.

The cDNA from patient's sample and three controls was amplified in a 7500 Fast Real-Time PCR system (Applied Biosystems, USA), using the *MT-CYB* TaqMan gene expression assay (Applied Biosystems), the *TBP* and *HMBS* TaqMan gene expression assays (Applied Biosystems) as housekeeping genes, as previously determined in the section 3.1.2.5 of the chapter 3.1, and the TaqMan Universal Master Mix II (Applied Biosystems), following the manufacturer's protocol.

The qPCR reactions were performed in triplicate, using three independent cDNAs from each sample. Quantification of MT-CYB mRNA levels was obtained using the $2^{-\Delta\Delta Ct}$ method, where $\Delta Ct = Ct^{\text{mt-CYB}} - Ct^{\text{HMBS and TBP mean}}$ and $\Delta\Delta Ct = \Delta Ct^{\text{sample}} - \Delta Ct^{\text{Control}}$.

3.2.2.6 Detection of MTCYB protein levels

Human primary fibroblasts were grown to confluence, and scraped from the culture flasks for obtaining the mitochondrial-enriched fraction, after a series of centrifugations, as previously described in case report I of this chapter (section 3.1.2.6).

Samples were analysed by SDS-PAGE according to a method previously described[309]. Total protein content of mitochondria-enriched fractions was quantified using the Bradford method, and 30µg of total protein were loaded per lane into a 10% polyacrylamide gel. After electrophoresis, proteins were electrotransferred (Mini PROTEAN® tetra cell system, BioRad) to PVDF membranes (Hybond P 0.5µm, Amersham) for 2 h at 0.75A, at 4°C. After the blocking step, membranes were incubated overnight, at 4°C, with mouse monoclonal anti-human HSP60 (Millipore) at 1:1,000, or rabbit polyclonal anti-human CYB (sc-84231, Santa Cruz Biotechnology) at 1:200. Then, membranes were incubated with the appropriate HRP-conjugated

secondary antibody solution (1:5,000, Bio-Rad) for 90 min at room temperature. Membranes were incubated with chemiluminescence substrate (Clarity Western ECL Substrate, Bio-Rad) and detection was carried out using the VersaDoc Imaging System 3000 (Bio-Rad). Protein band intensities were calculated by using Quantity One® 1-D software (Bio-Rad) from at least 3 independent experiments, with values expressed as mean±SEM. Relative quantification of MTCYB subunit was performed using HSP60 as the normalising protein.

3.2.2.7 MRC enzymatic activity evaluation

Catalytic activity of MRC complexes and segments was performed for patient's fibroblasts, as previously described and the results were corrected to citrate synthase activity, used as a mitochondrial reference enzyme[107].

3.2.2.8 Mitochondrial respiratory rate and glycolytic activity evaluation

OCR and ECAR were measured in fibroblasts of patient and three controls using a XF24 Extracellular Flux Analyser (Seahorse Bioscience, Billerica, MA, USA), as previously described in the section 3.1.2.10 of the case report I (chapter 3.1).

3.2.2.9 ATP levels measurement

Intracellular ATP levels were measured in patient's and control's fibroblasts by using the luciferin/luciferase assay with ATPlite kit (Perkin Elmer), according to the manufacturer's instructions with minor modifications described previously in the section 3.1.2.9 of the case report I. ATP concentration, using an ATP standard curve, was normalised to the protein content.

3.2.2.10 Analysis of mitochondrial membrane potential

Mitochondrial membrane potential was determined using the cationic fluorescent probe Rhodamine 123 (Molecular probes, Invitrogen), which accumulates mostly in polarized mitochondria. The variation of rhodamine 123 retention was studied as in

the case report I (section 3.1.2.11), in order to estimate changes in $\Delta\Psi_m$. Results were expressed as the difference between the basal fluorescence values and the increase of Rhodamine 123 fluorescence levels upon addition of mitochondrial complexes inhibitors or uncoupler FCCP, normalised to protein content.

3.2.2.11 Measurement of mitochondrial superoxide anion

The mitochondrial $O_2^{\bullet-}$ basal levels and mitochondrial $O_2^{\bullet-}$ production after CI or CIII inhibition were measured in fibroblasts from controls and patient using the fluorescent probe MitoSOX Red (Molecular Probes, Invitrogen), as described in the case report I (section 3.1.2.12).

The values were obtained as RFU (relative fluorescence units) *per* min, *per* mg of protein, for each condition and then normalised to the basal (untreated) conditions.

3.2.2.12 Transmission electron microscopy

TEM procedure was performed as described in the case report I (section 3.1.2.13) of this chapter.

3.2.2.13 Statistical analysis

Results were analysed using GraphPad Prism® software version 5.0 for Windows, San Diego, California, USA. Normality tests were applied in order to verify the Gaussian distribution of the results. Statistical significance of differences between patient and controls was assessed by a Student's *t*-test (or nonparametric Mann-Whitney test).

Results of the statistical significance are represented as *$p \leq 0.050$, **$p \leq 0.010$ and ***$p \leq 0.001$.

3.2.3 Results

3.2.3.1 Genetic screening revealed an unclassified mtDNA variant

The analysis of the entire mitochondrial genome by NGS revealed previously reported polymorphisms and a novel homoplasmic sequence variation in the *MT-CYB* (m.14771C>A, p.Pro9Thr; ClinVar accession number: SCV000492501) (Table 3.2.1) in patient's fibroblasts and lymphocytes. A previous analysis allowed determining that the patient belongs to the haplogroup H3+152.

Table 3.2.1 Mitochondrial variants detected in the patient through the NGS for whole mitochondrial genome

Nucleotide Change	Amino acid change	Locus	Previously described
m.152T>C	-	*HV2, OH*	Yes
m.263A>G	-	*HV2*	Yes
m.750A>G	-	*MT-RNR1 (12S)*	Yes
m.1438A>G	-	*MT-RNR1 (12S)*	Yes
m.4769A>G	Syn (M100M)	*MT-ND2*	Yes
m.6776T>C	Syn (H291H)	*MT-COI*	Yes
m.7391T>C	Syn (Y496Y)	*MT-COI*	Yes
m.8860A>G	T112A	*MT-ATP6*	Yes
m.13635T>C	Syn (G433G)	*MT-ND5*	Yes
m.14771C>A	**P9T**	***MT-CYB***	**No**
m.15326A>G	T194A	*MT-CYB*	Yes
m.15608C>T	Syn (L288L)	*MT-CYB*	No
m.16519T>C	-	*D-Loop*	Yes

Sanger sequencing of the mtDNA region of interest (14420-14855) confirmed the presence of the variant (m.14771C>A) in DNA from lymphocytes (Figure 3.2.1B, II6 .a) and skin fibroblasts (Figure 3.2.1B, II6 .b), as well as in cDNA from fibroblasts of patient (Figure 3.2.1B, II6 .c). The same alteration was detected in homoplasmy in DNA from lymphocytes of parents (Figures 3.2.1B I1 and I2), and the two sisters, affected (Figure 3.2.1B, II3) and unaffected twin (Figure 3.2.1B, II7). However, the sequence variation was absent in the 200 controls screened (data not shown).

The Mitome500 panel allowed the identification of novel nuclear variants in heterozygosity without relevance (Table 3.2.2).

The evaluation of evolutionary conservation shows that the nucleotide and the amino acid are 100% conserved in the different species (Figure 3.2.1C-D, respectively).

PolyPhen®, SIFT®, MutationAssessor® and Provean® predict that the variant, p.Pro9Thr, is likely deleterious. PredictProtein® foresees that the variation is located in a helix α conformation, being an exposed residue.

Table 3.2.2 List of the sequence variations detected in nuclear genes in patient's samples, after filtering for variant calling and excluding known polymorphisms.

Gene	Sequence variation	Amino acid change	NCBI ClinVar	% allele mutant	Clinical Significance
COX5A	c.115C>G	p.R39G	rs200811470	47.01	Unknown
GBE1	c.839G>A	p.G280D	rs28763902	46.81	Likely benign
MARS2	c.369G>T	p.Q123H	-	47.96	Unknown
PGM1	c.794A>G	p.N265S	-	51.77	Unknown
SLC37A4	c.594A>T	p.N198I	rs34203644	42.60	Likely benign
SUCLG2	c.832G>A	p.D278N	rs200619917	44.28	Unknown

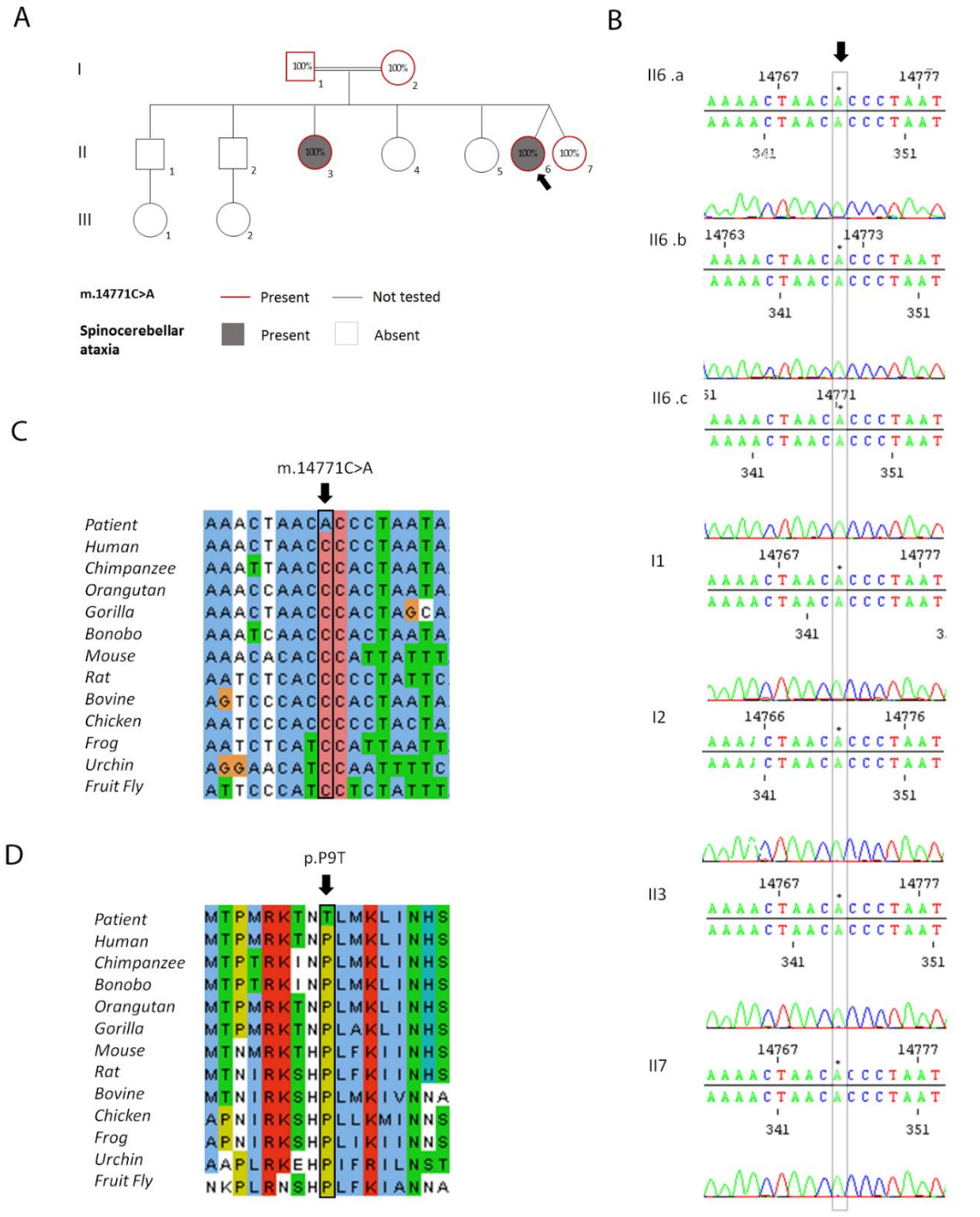

Figure 3.2.1 - **Detection of m.14771C>A, *MT-CYB***. **(A)** Pedigree of the family in study showing the percentage of the novel sequence variation in tested individuals. The arrow indicates the proband (patient 2); **(B)** Electropherograms showing the m.14771C>A variant in DNA from patient's (II6 .a) lymphocytes, (II6 .b) skin fibroblasts, (I1) father's lymphocytes, (I2) mother's lymphocytes, (II3) affected sister's lymphocytes, (II7) unaffected twin-sister's lymphocytes, and (II6 .c) cDNA from patient's fibroblasts; **(C)** Evolutionary conservation of the nucleotide position m.14771 in *MT-CYB* gene; **(D)** Evolutionary conservation of the amino acid position 9 in MTCYB protein.

3.2.3.2 Decreased protein levels of MTCYB subunit of CIII

The levels of MT-CYB transcript and protein were analysed in order to verify the impact of the novel variant detected in *MT-CYB* gene. The transcript levels were similar to those obtained for controls (Figure 3.2.2A), but the protein levels were significantly decreased (**p=0.004) (Figure 3.2.2B).

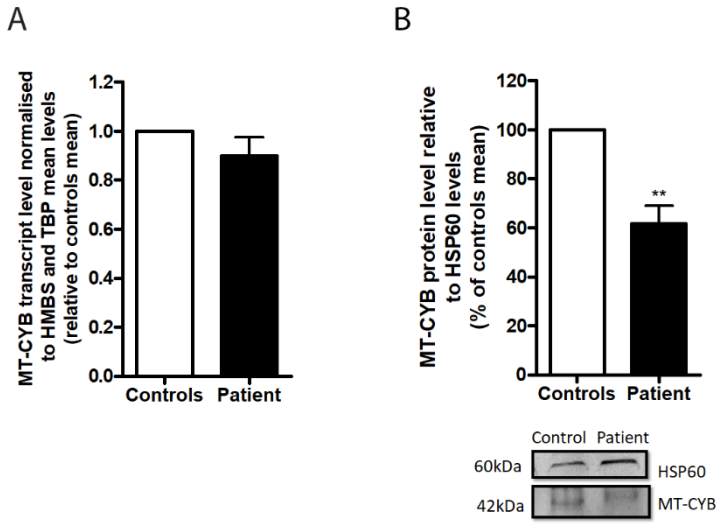

Figure 3.2.2 - **Mitochondrial cytochrome b transcript and protein levels quantification in patient's fibroblasts. (A)** Transcript level was evaluated from three independent RNA extractions and cDNA synthesis, in triplicate for each sample, normalised to the mean of the housekeeping genes *HMBS* and *TBP*. Data is representative of the mean±SEM, analysed with unpaired Student's *t*-test. **(B)** MTCYB protein level normalised to HSP60. Results are representative of three independent procedures in duplicate, presented as the mean±SEM. Statistical significance was determined by Mann-Whitney test, **p=0.004.

3.2.3.3 Reduced OXPHOS activity and decreased ATP levels

Assessment of mitochondrial respiratory chain enzymatic activities in patient's fibroblasts revealed a significant reduction of CI (**p=0.0016) and CV (*p=0.018) activities (Figure 3.2.3B and F). Also, CIII activity was significantly decreased (49% in comparison to controls) (Figure 3.2.3D), in contrast to complexes II, IV and segments I+III and II+III activities that were normal, when compared to the controls (Figure3.2.3C, E and G-H).

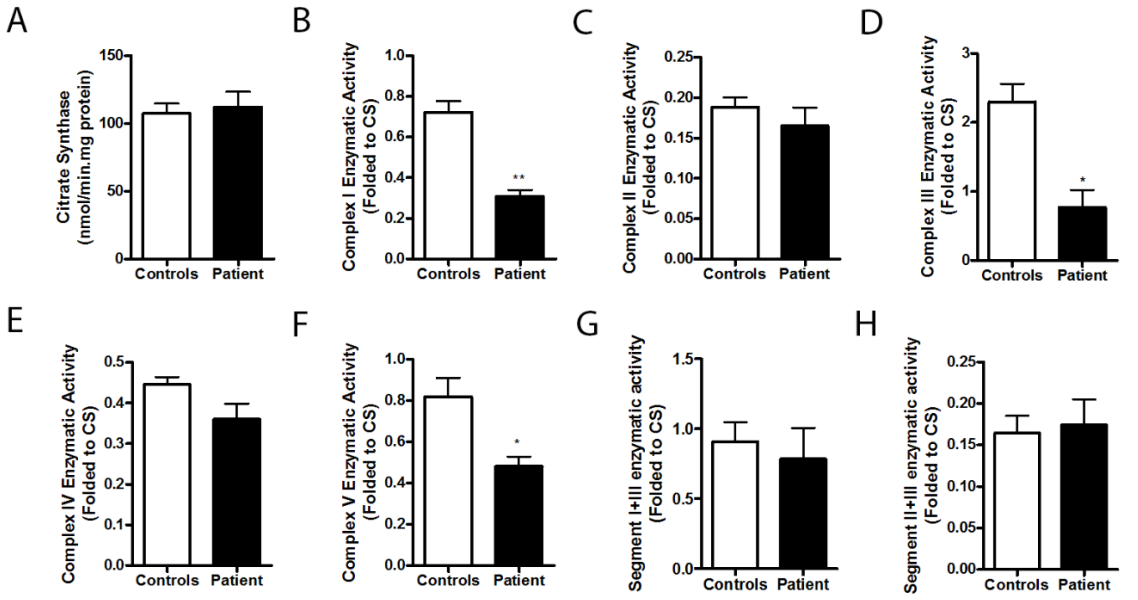

Figure 3.2.3 - **Mitochondrial enzymatic activity in fibroblasts of patient and controls** of **(A)** Citrate Synthase, **(B)** Complex I (**p=0.0016); **(C)** Complex II; **(D)** Complex III (*p=0.0314); **(E)** Complex IV; **(F)** Complex V (*p=0.018); **(G)** Segment I+III; **(H)** Segment II+III. Data are presented as the mean±SEM from at least three independent measurements. Statistical significance was determined by Mann-Whitney test.

In accordance with the OCR evaluation (Figure 3.2.4A), the basal mitochondrial respiration of patient's cells presents a significant decrease (***p=0.0006) (Figure 3.2.4C), showing that the ATP produced using the oxygen consumption is statistically reduced (***p<0.0001) (Figure 3.2.4G). Also, the stimulation of maximal respiration reveals a reduced capacity in patient's cells (***p=0.0009) (Figure 3.2.4D).

Glycolytic function was evaluated through the extracellular acidification (Figure 3.2.4B), showing that glycolysis, glycolytic reserve and capacity are significantly increased (**p=0.0019, **p=0.0930, and *p=0.0213, respectively) (Figure 3.2.4H-J), in order to compensate the reduced mitochondrial respiration.

Intracellular ATP levels measurement revealed a significant decrease (***p<0.0001) in patient's fibroblasts (Figure 3.2.4K).

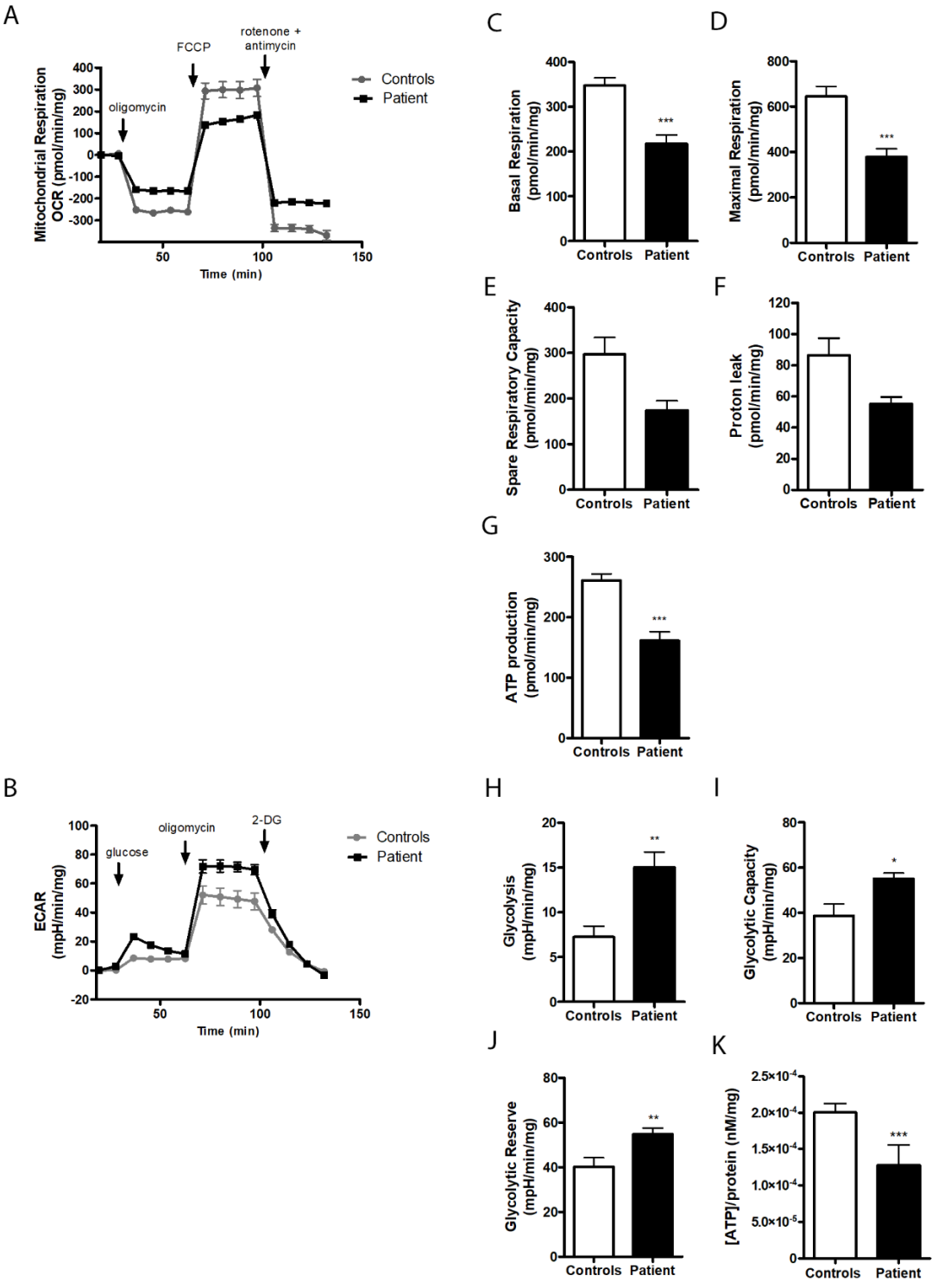

Figure 3.2.4 - **Bioenergetics parameters**. Error bars represent the standard error of mean based on three independent experiments in triplicates. **(A)** Mitochondrial respiration profile; **(B)** Acidification profile; **(C)** Basal respiration (Unpaired Student's *t*-test, ***p=0.0006); **(D)** Maximal respiration (Mann-Whitney test, ***p=0.0009); **(E)** Spare respiratory Capacity; **(F)** Proton leak; **(G)** ATP production (Unpaired Student's *t*-test, ***p<0.0001); **(H)** Glycolysis (Mann-Whitney test, **p=0.0019); **(I)** Glycolytic capacity (Mann-Whitney test, *p=0.0213); **(J)** Glycolytic reserve (Mann-Whitney test, **p=0.0093); **(K)** Intracellular ATP level (Mann-Whitney test, ***p<0.0001).

3.2.3.4 Decreased mitochondrial membrane potential

Accumulation of rhodamine 123 probe in polarized mitochondria allowed the detection of significant changes in $\Delta\Psi_m$ of patient's cells, compared to control group. After inhibition of complexes I and III with rotenone and antimycin A, respectively, an increase in fluorescence was observed, more significant after the addition of FCCP (Figure 3.2.5A-B). The increase in fluorescence was more pronounced in control's cells than in patient's cells, especially after the inhibition of CI plus FCCP (**p*=0.0318) (Figure 3.2.5A). Similar results were obtained after simulation of the maximal depolarization (with oligomycin plus FCCP), where the difference between patient and controls was also significant (**p*=0.0478) (Figure 3.2.5C).

These results indicate mitochondrial membrane depolarization in patient's fibroblasts.

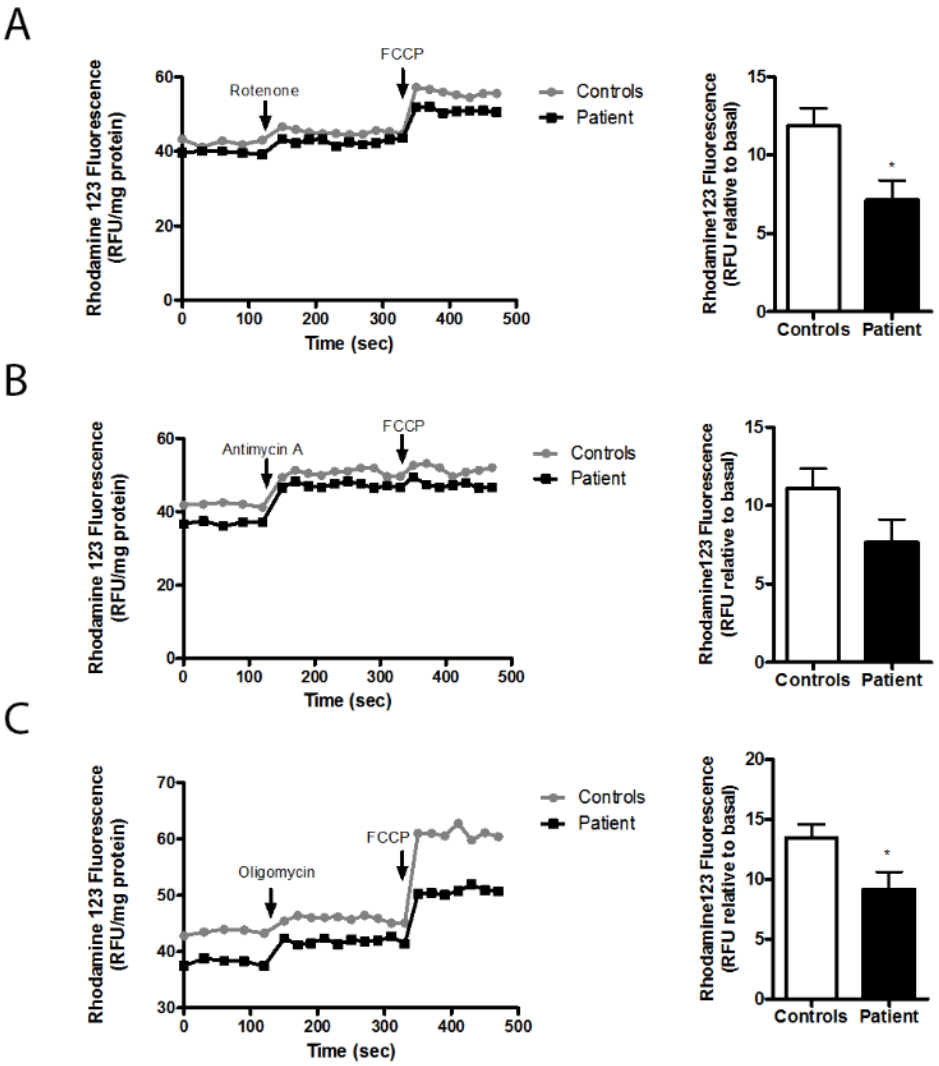

Figure 3.2.5 - **Mitochondrial membrane potential measurements in fibroblasts of patient and controls**. **(A)** Uncoupling with FCCP after complex I inhibition with rotenone (left), graphical representation of the difference between the basal and rotenone plus FCCP-induced levels of rhodamine123 (**p*=0.0318) (right), **(B)** Complex III inhibition followed by uncoupling with FCCP (left), graphical representation of the difference between the basal and antimycin A plus FCCP-induced levels of rhodamine123 (right) **(C)** Complex V inhibition followed by uncoupling with FCCP (left), graphical representation of the difference between the basal and oligomycin plus FCCP-induced levels of rhodamine123 (**p*=0.0478) (right). Data are presented as the mean±SEM based on three independent measurements in triplicates. Statistical significance was evaluated by unpaired Student's *t*-test.

3.2.3.5 Increased production of mitochondrial superoxide anion

Mitochondrial $O_2^{\bullet-}$ basal levels were decreased in patients' cells when compared to control values (***p<0.0001) (Figure 3.2.6A). However, a significant increase in mitochondrial superoxide anion levels was observed, after addition of rotenone to inhibit CI activity (*p=0.0367) or antimycin A to inhibit CIII (***p<0.0001) (Figure 3.2.6B-C), suggesting that further decrease in these complexes activities is able to exacerbate the production of mitochondrial reactive oxygen species.

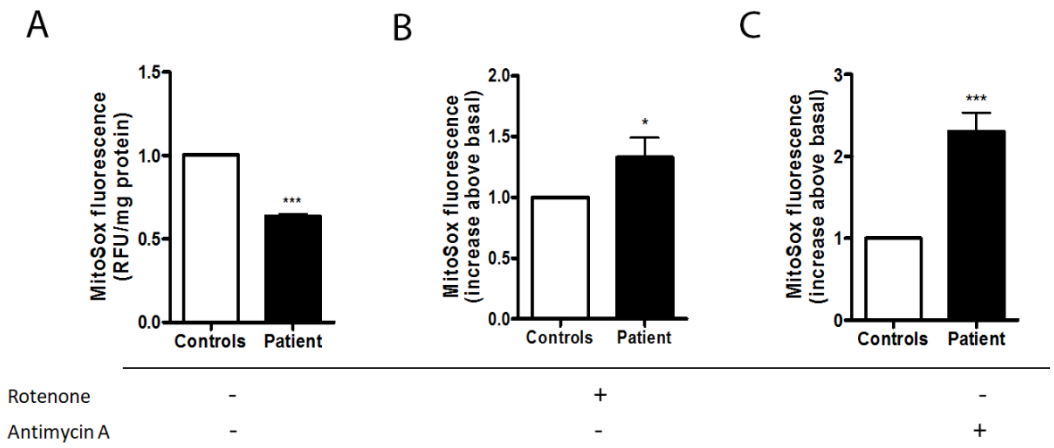

Figure 3.2.6 - **Superoxide anion levels in fibroblasts of patient with m.14771C>A variant and in controls**. **(A)** Basal levels (***p<0.0001) or following **(B)** complex I inhibition with rotenone (*p=0.0367) or **(C)** complex III inhibition with antimycin A (***p<0.0001). Results derive from three independent measurements in triplicates. Errors bars represent the mean±SEM and the statistical significance was verified by unpaired Student's *t*-test.

3.2.3.6 Ultrastructural investigation showed abnormal cellular structures

In the images obtained by TEM (Figure 3.2.7), the comparison between controls' (Figure 3.2.7A) and patient's (Figure 3.2.7B) fibroblasts disclosed the presence of several multilamellar bodies (MLB) in patient's cells, but no visible changes were observed regarding mitochondrial morphology.

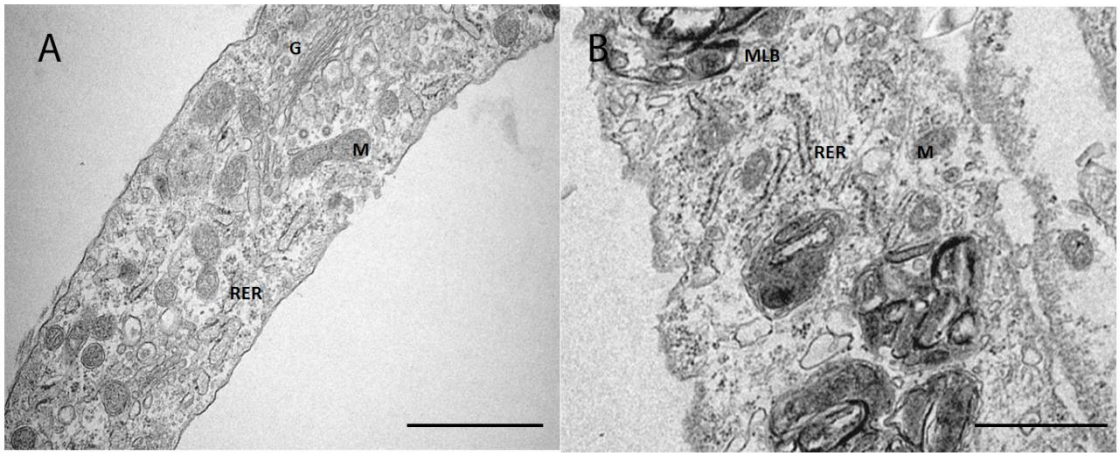

Figure 3.2.7 - **Morphological study of primary fibroblasts by transmission electron microscopy.** Ultrastructural aspects of **(A)** control and **(B)** patient. G – Golgi, M – Mitochondrion, RER – Rough Endoplasmic Reticulum, MLB – Multilamellar Bodies. Scale bar: 1 µm.

3.2.4 Discussion

Mitochondrial cytochrome b is a highly conserved protein and the only one encoded by mtDNA in complex III. The conservation of the protein reflects its importance in mitochondrial energy production. Additionally, MTCYB is involved in the first step of CIII assembly[79], and it is part of the catalytic redox core of this complex[69]. Therefore, mutations in this protein may affect the complex assembly or stability, or instead, inhibit the catalytic activity without impairing its assembly[334]. Indeed, several sequence variations are reported in *MT-CYB* gene related to diverse mitochondrial diseases, being exercise intolerance, mitochondrial myopathy, encephalomyopathy, optic neuropathy and hypertrophic cardiomyopathy the most frequent clinical manifestations (MITOMAP: A Human Mitochondrial Genome Database. http://www.mitomap.org, 2017).

In the present work, an unclassified maternal inherited variant (m.14771C>A) in *MT-CYB* is reported in a patient with spinocerebellar ataxia (P2), autosomal recessive 20 (OMIM: #616354). PredictProtein shows that p.Pro9Thr (MTCYB) variation is located in a helix α conformation and it is an exposed residue. However, proline is totally conserved in this position for the species analysed and, as proline is a cyclic and non-polar amino acid, the substitution for threonine, which is polar, could lead to

structural consequences in the protein, since the hydroxyl group of threonine is fairly reactive, being able to form hydrogen bonds with a variety of polar substrates. In addition to structural consequences, others *in silico* tools used to predict the pathogenicity are in agreement, revealing scores indicative of pathogenicity.

The determination of haplogroup allows to verify that the variant is not a haplogroup marker, since it is reported in GenBank only in one individual (KM101785.1) that belongs to a different haplogroup (H5a) of the patient presented herein.

In order to verify the functional impact of the novel variant, transcript and protein levels were measured, as well as bioenergetics parameters evaluated. As predicted, the variant is causing a significant decrease in protein levels, and the catalytic activity of complex III is significantly reduced (36% of control). In addition, activities of complexes I and V are significantly decreased, showing generalized changes in OXPHOS. This hypothesis is supported by the decrease in basal respiration, maximal respiration and ATP production measured through oxygen consumption in intact cells. Moreover, the intracellular ATP content is significantly decreased, despite the increased glycolytic flux, which may try to compensate the energy demand. Furthermore, the mitochondrial membrane is depolarized and the production of superoxide anion is significantly increased after inhibition of complexes I and III, which are deficient, suggesting that a more pronounced decline of activities can lead to an excessive production of superoxide anion, and consequently, a potential increase of damaged proteins and nucleic acids.

Overall, the results are indicative of mitochondrial dysfunction in patient's cells. Thus, the novel mtDNA variant presented in this study seems to be a good candidate for mitochondrial dysfunction occurring in this patient.

Meanwhile, the recently described phenotype[323] occurring in this family was later identified in other two unrelated consanguineous families with similar clinical phenotypes and different mutations in the *SNX14* gene[323]. Only the affected individuals presented the mutations in homozygosity. The authors have identified MLB in all patients of different families, similar to the MLB identified in the present study, and a granular pattern for immunostaining of p62 in skin fibroblasts of patients, suggesting a defect in the autophagy pathway[323].

Mutations in *SNX14* have been associated to a defect in the elimination of cellular components[324] causing this LSD; however, the specific molecular mechanisms leading to neurodegeneration in LSDs are still not clear.

In the present study, we have demonstrated a mitochondrial dysfunction in skin fibroblasts of this patient harbouring a *SNX14* pathogenic mutation causing spinocerebellar ataxia. This evidences corroborate the previously mentioned studies suggesting a crosstalk between mitochondria and lysosome[325–327]. We can argue that the mitochondrial dysfunction contributes for the patient's phenotype, since energy production by OXPHOS is essential in all human tissues, especially during brain development and maintenance.

The accumulation of p62 in patient's cells[323] corroborates the hypothesis that mitochondria are probably among the cellular components that are not being efficiently removed. In fact, p62 has been involved in selective degradation of depolarized mitochondria (mitophagy)[336]. As a consequence, defective mitochondria would accumulate within cells with lower capacity to produce ATP. The consequent excessive generation of ROS and calcium imbalance could cause the activation of apoptosis, and cell death.

In summary, a defect in the elimination of damaged cellular components seems to be an important pathogenic mechanism in spinocerebellar ataxia, autosomal recessive 20. The novel mitochondrial variant (m.14771C>A) found in patient 2 can be the trigger for mitochondrial dysfunction. Additionally, dysfunctional mitochondria, as other cellular components, cannot be correctly eliminated due to lysosomal dysfunction[323]. Our results proved a mitochondrial dysfunction occurring in spinocerebellar ataxia, autosomal recessive 20, as recently described in other LSDs, suggestive of a metabolic disease with bigenomic origin. This opens a new perspective on the molecular mechanisms underlying the LSDs.

3.3. CASE REPORT III

Disclosing the functional changes of two genetic alterations in a patient with chronic progressive external ophthalmoplegia: report of the novel mtDNA m.7486G>A variant

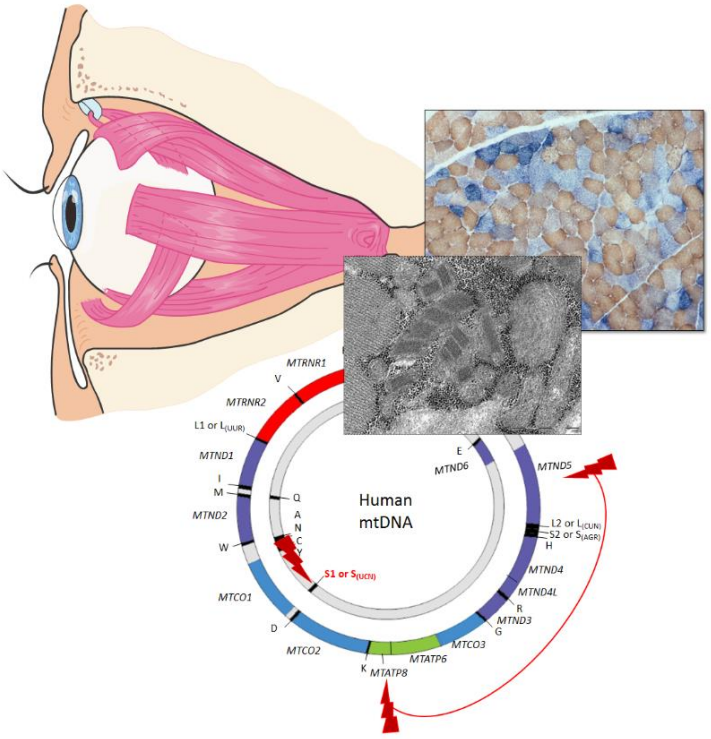

Abstract

Chronic progressive external ophthalmoplegia (CPEO) is characterized by ptosis and ophthalmoplegia and is usually caused by mtDNA deletions or mt-tRNA mutations. The aim of the present work was to clarify the genetic defect in a CPEO patient (P3) and elucidate the pathogenic mechanism. The patient presented ragged-red fibres, a mosaic pattern of COX-deficient fibres in muscle and combined deficiency of respiratory chain complexes I and IV. Genetic investigation revealed the "common deletion" in patient's muscle and fibroblasts. Moreover, a novel heteroplasmic mt-tRNA$^{Ser(UCN)}$ variant (m.7486G>A) in the anticodon loop was detected in muscle homogenate (~50%), fibroblasts (~11%) and blood (~4%). Single-fibre analysis showed segregation with COX-deficient fibres for both genetic alterations. Assembly defects of mtDNA-encoded complexes were demonstrated in fibroblasts. Functional analyses showed significant bioenergetics dysfunction, reduction in respiration rate and ATP production, up-regulation of glycolysis and mitochondrial depolarization. Multilamellar bodies were detected by electron microscopy, suggesting disturbance in autophagy. In conclusion, we report a CPEO patient with two possible genetic origins, both segregating with biochemical and histochemical defect. The "common mtDNA deletion" is the most likely cause, yet the potential pathogenic effect of a novel mt-tRNA$^{Ser(UCN)}$ variant cannot be fully excluded.

Keywords: CPEO; mtDNA common deletion; mt-tRNA variant (m.7486G>A); bioenergetics dysfunction; translation defect.

3.3.1 Introduction

Mitochondrial diseases are among the most heterogeneous disorders known to date, with respect to the mode of inheritance, clinical presentations, age of onset, and biochemical and genetic defects. One of the most common presentations of mtDNA-associated disease in adulthood is chronic progressive external ophthalmoplegia (CPEO), which is characterized by progressive paralysis of the extraocular muscles (EOMs) leading to ptosis and impaired eye movement (ophthalmoplegia)[337].

CPEO is commonly caused by either primary mitochondrial genetic defects such as single, large-scale mtDNA deletions[196,337–341] and mt-tRNA point mutations[214,342–353], or multiple mtDNA deletions, which are secondary abnormalities due to primary mutations in nuclear genes responsible for the maintenance of mitochondrial genome integrity[354,355]. The single 4,977bp deletion, known as the "common deletion", is present in one-third of the patients with Kearns-Sayre Syndrome (KSS)/CPEO and Pearson syndrome, and is the most frequent genetic defect found in patients with CPEO[23,356].

Muscle biopsies of CPEO patients typically comprise subsarcolemmal accumulation of abnormal mitochondria known as ragged-red fibres (RRF) and a mosaic pattern of COX-deficient fibres showing abnormal COX activity. The amount and tissue distribution of mutated mtDNA molecules are the most important factors in determining the clinical symptoms. Indeed, mitochondrial dysfunction occurs in a tissue when a critical number of mutated mtDNA accumulates and exceeds a biochemical threshold (threshold effect), which has been shown to vary for different types of mutation, namely 50-80% for single, large-scale mtDNA deletions and 70-95% for tRNA point mutations[215,357]. Currently, more than half of disease-related mtDNA point mutations have been reported within mt-tRNA genes that cause defective translation and, consequently, combined respiratory chain deficiency. While the size and exact breakpoints of mtDNA deletions are highly variable, any deletion that eliminates a mt-tRNA gene causes the same impairment of overall mitochondrial-encoded proteins.

Studies reporting single, large-scale mtDNA deletions have rarely provided functional evidences of the genetic defect[317,339,341,358–362]; therefore, deeper investigation regarding the affected cellular mechanisms is still needed.

The aim of the present work was to: (i) clarify the molecular genetic defect and (ii) elucidate which cellular mechanisms are affected in a CPEO patient (P3) that harbours a novel mt-tRNA$^{Ser(UCN)}$ variant (m.7486G>A, ClinVar accession number: SCV000492500) in addition to the "common deletion".

3.3.2 Samples and Methods

3.3.2.1 Case report

The patient 3 is a 62-year-old Portuguese Caucasian female followed at the Neurology Department of the Coimbra Hospital University Centre. The first clinical signs started at the age of 12 years old with slowly progressive ptosis of the right eyelid and later involvement of the other eyelid at the age of 45 years old. At this point, she was observed in the context of a corneal ulcer and complaints that she had "difficulties to maintain the eyes open". The disease maintained a slow progression and she was diagnosed with CPEO at the age of 55 years old, with the neurological examination revealing severe bilateral eyelid ptosis, ophthalmoplegia and dysphonia. There was no reported family history of CPEO or any other mitochondrial disorder.

Biological samples (peripheral blood, skin and muscle biopsies) were collected from the patient investigated in the present study during diagnostic laboratory investigation conducted at the Laboratory of Biochemical Genetics (LBG).

The DNA samples of 200 adult healthy subjects of the same ethnic background were used as controls.

Informed consent was obtained from the participants, as recommended by the local Ethics Committee (CE-032/2014), following the Tenets of the Helsinki Declaration.

3.3.2.2 Histology, histochemistry and quadruple immunofluorescence in muscle

Routine histological (Haematoxylin & Eosin – H&E, modified Gomori trichrome staining) and histochemical (cytochrome *c* oxidase [COX], succinate dehydrogenase [SDH], and sequential COX/SDH) analysis of the patient's skeletal muscle was performed, by following standard methods[213].

Quadruple immunofluorescence was performed on cryosectioned patient skeletal muscle (n=1,022) using antibodies detecting subunits of OXPHOS complexes: anti-NDUFB8 for CI and anti-COXI for CIV, as described[212]. Mitochondrial mass was quantified using an antibody to Porin and the myofibre boundaries were labelled with the antibody to Laminin.

Brightfield and fluorescent images were acquired using a Zeiss Axio Imager M1 and Zen 2011 (blue edition) software, with a monochrome Digital Camera (AxioCam MRm) and filter cubes for Alexa Fluor dyes at 405nm (laminin), 488nm (COX-I), 546nm (porin) and 647nm (NDUFB8) wavelengths. Image analysis was performed using IMARIS software, allowing measurement of optical densities of different channels in single muscle fibres. Statistical analysis was performed as previously described whereby the Z_scores for COX-I, NDUFB8 and porin were derived using the standard values recorded in normal controls.

3.3.2.3 Skin derived cultured fibroblasts

Fibroblasts from skin biopsies of the patient and three healthy Portuguese individuals (control group), without clinical evidence of mitochondrial disease, were grown in complete medium supplemented with 20% FBS (Gibco, Life Technologies) and antibiotics, as in case report I (section 3.1.2.2).

3.3.2.4 Genetic investigation in different tissues

Total DNA was extracted from several tissues including blood, dermal fibroblasts and muscle homogenate according to standard protocols[305,363].

Individual COX-positive and COX-deficient muscle fibres were isolated by laser microcapture, using a PALM Laser Capture Microdissection system, and lysed to obtain total cellular DNA, as previously described[364]. The stained sections were then used for single-cell molecular analyses.

3.3.2.4.1 Whole mitochondrial genome sequencing

The presence of sequence variants and rearrangements were detected by subjecting the patient's mitochondrial genome to NGS in all available tissues, enriched by a single amplicon long-range PCR followed by massively parallel sequencing[307], using the HiSeq2000 platform (Illumina technology).

Haplogroup of patient was determined using the Haplogrep® tool[308].

3.3.2.4.2 Confirmation of the mt-tRNA novel sequence variation

Automated Sanger sequencing analysis was performed, according to the manufacturer's instructions (3130 ABI Prism sequencing system), using BigDye® Terminator Ready Reaction Mix v3.1 (Applied Biosystems), for investigating the region 7241-7644, in the available tissues of the patient. The genetic screening of the 200 controls' samples was carried out by the same method to check for the presence of the novel mtDNA sequence variation (m.7486G>A) detected in the patient.

3.3.2.4.3 *In silico* analysis

The *in silico* analysis included the evolutionary conservation of the *MT-TS1* gene (mt-tRNA$^{Ser(UCN)}$) from mtDNA of different species, according to the proposed consensus panel[365] using ClustalOmega|EBI®[328]. The location of the m.7486G>A sequence variation in the cloverleaf structure of mt-tRNA$^{Ser(UCN)}$ was verified from Mamit-tRNA® database[366].

3.3.2.4.4 Screening for mtDNA rearrangements

The presence of rearrangements in mtDNA was confirmed in DNA derived from muscle homogenate, using an established triplicate long PCR approach for multiple deletions and single deletion, amplifying approximately 10, 13 and 16 kb of the mtDNA in three separate reactions. For ~10kb amplification PCR forward-F (m.6122-6139) and reverse-R (m.16133-16153) primers were used. For ~13kb amplification PCR F (m.13965-13984) and R (m.129-110) primers were used and for ~16kb amplification

PCR F (m.1157-1167) and R (m.19-1) were employed. Cycling conditions were: 94°C, 2 min.; 35 cycles of 94°C, 30 sec and 65°C, 16 min; 72°C,16 min. Amplifying PCR products were separated in 0.7% agarose gels.

3.3.2.4.5 Single fibre studies

The m.7486G>A mt-tRNA mutation load was assessed by pyrosequencing technology, in all available tissues and in individual COX-positive and COX-deficient muscle fibres. The PyroMark Assay Design Software v.2.0. (Qiagen) was used to design locus-specific PCR and sequencing primers for the m.7486G>A variant (biotinylated forward primer: m.7466-7485; reverse primer: m.7583-7600; sequence primer: m.7488-7502) and pyrosequencing was performed on the Pyromark Q24 platform, according to the manufacturer's protocol. Pyromark Q24 software was used to quantify the m.7486G>A heteroplasmy levels by directly comparing the peak heights of both wild-type and mutant nucleotides at this position[367].

The multiplex *MTND1/MTND4* real-time PCR assay was performed using DNA from individual COX-deficient and COX-positive isolated muscle fibres and muscle homogenate and the mtDNA deletion level was calculated from the proportion of wild-type (*MTND4*) to total (*MTND1*) copy number by the established $\Delta\Delta C_t$ method[368]. PCR amplification was completed in a 25µl reaction in triplicate for each sample, with each plate containing a serial dilution of p7D1 plasmid for standard curve generation, as reported previously[369].

3.3.2.4.6 Nuclear panel investigation

Mitome500 panel was performed by NGS, as described in the case report II (section 3.2.2.3), in order to identify possible alterations in nuclear genes encoding mitochondrial proteins.

3.3.2.5 Quantification of mt-tRNA$^{Ser(UCN)}$ steady-state level by high-resolution Northern blot

The steady-state levels of mt-tRNA$^{Ser(UCN)}$ were determined using the RNA extracted from muscle specimens of the patient and unaffected controls by high-resolution Northern Blot analysis, as described[208], using probes for mt-tRNA$^{Ser(UCN)}$ and mt-tRNA$^{Leu(UUR)}$. Following PhosphorImager analysis, the radioactive signal for the mt-tRNA$^{Ser(UCN)}$ probe was normalised to the mt-tRNA$^{Leu(UUR)}$ probe.

3.3.2.6 MRC enzymatic activity evaluation

Spectrophotometric determination of the catalytic activity of the MRC complexes and segments was performed as previously described[107].

3.3.2.7 Mitochondrial respiratory rate, glycolytic activity and intracellular ATP levels evaluation

OCR and ECAR were measured in adherent fibroblasts with a XF24 Extracellular Flux Analyser (Seahorse Bioscience, Billerica, MA, USA) as described in the case report I (3.1.2.10) of this chapter.

Intracellular ATP levels were measured in fibroblasts of patient and controls using the luciferin/luciferase assay with ATPlite kit (Perkin Elmer), according to the manufacturer's instructions with minor modifications described in the section 3.1.2.9 of the case report I. Determined ATP concentration, using an ATP standard curve, was normalised to the protein content.

3.3.2.8 Analysis of mitochondrial membrane potential

Mitochondrial membrane potential was determined as described in the section 3.1.2.11 of the case report I in the chapter 3.1.

3.3.2.9 Determination of superoxide anion levels

The measurement of superoxide anion levels was performed as described in the case report I (section 3.1.2.12).

3.3.2.10 Relative quantification of MCR complexes

Samples were processed according to the protocol described elsewhere[224] with minor alterations described in the case report I, section 3.1.2.7.

3.3.2.11 Transmission electron microscopy

Muscle fibres from a fresh biopsy were fixed with 4% glutaraldehyde in 0.2M sodium cacodylate buffer (pH 7.2) for 4 h. After rinsing twice in the same buffer, fibres were post-fixed in 1% osmium tetroxide for 2 h. Following rinsing in buffer, samples were then dehydrated in a grade ethanol series (75-100%) before being embedded in Epoxy resin (Fluka Analytical). Semi-thin sections (2µm) were obtained and stained with toluidine blue for light microscopy in order to identify the area of interest.

Fibroblasts were collected and centrifuged at 775 x*g* for 5 min. The supernatant was discarded and pellet cells were fixed with 2.5% glutaraldehyde in 0.1M sodium cacodylate buffer (pH 7.2) supplemented with 1mM calcium chloride for 2 h. Following rinsing in the same buffer, post-fixation was performed using 1% osmium tetroxide for 1 h. After rinsing twice in buffer, and distilled water and, 1% aqueous uranyl acetate was added to the cells, for contrast enhancement during 1 h in the dark. After rinsing in distilled water, samples were dehydrated in a graded acetone series (30–100%), impregnated and embedded in Epoxy resin (Fluka Analytical).

Finally, for both preparations, ultrathin sections (70nm) were mounted on copper grids (300 mesh) and stained with lead citrate 0.2%, for 7 min. Observations were carried out on a FEI-Tecnai G2 Spirit Bio Twin at 100kV and images were acquired using the software AnalySIS 3.2.

3.3.2.12 Statistical analysis

Data were analysed using GraphPad Prism version software 5.00 for Windows, San Diego, California, USA. Normality tests were applied in order to assure the Gaussian distribution of the results. Statistical analysis of the patient's vs. controls' results was assessed by a Student's *t*-test (or nonparametric Mann-Whitney test).

Statistical significance is represented as * for $0.050 \geq p > 0.010$, ** for $0.010 \geq p > 0.001$ and *** for $p \leq 0.001$.

3.3.3 Results

3.3.3.1 Histochemistry and quadruple immunofluorescence in muscle

Histological and histochemical examination of cryosectioned patient skeletal muscle revealed the presence of approximately 10% RRF as a result of mitochondria subsarcolemmal accumulation (Figure 3.3.1A,B) and a significant proportion (40%-50%) of COX-deficient fibres (Figure 3.3.1C-E), being both usually used as biomarkers of mitochondrial dysfunction. Assessment by quadruple immunofluorescence (Figure 3.3.2A) showed an equal down regulation (43%) of both CI and CIV levels in individual fibres (Figure 3.3.2B); the mitochondrial respiratory chain profile (Figure 3.3.2B) was similar to the profiles previously reported for single, large-scale deletion[212].

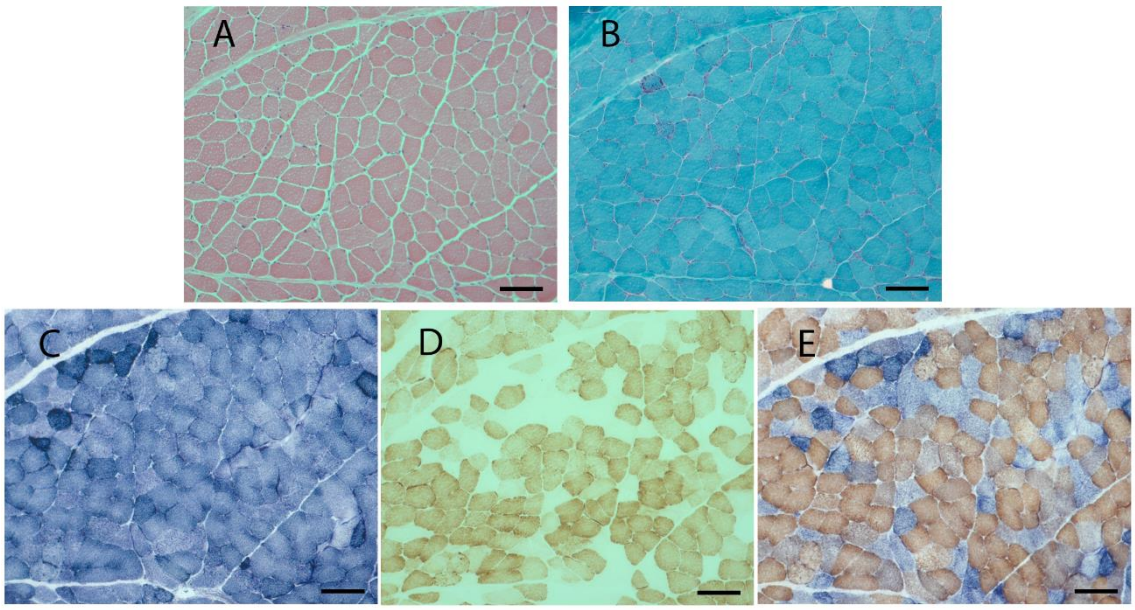

Figure 3.3.1 - Histopathological features associated with mtDNA disease in patient's skeletal muscle. (A) H&E staining showing general muscle morphology; **(B)** modified Gomori trichrome staining highlighting muscle RRF; **(C)** SDH staining, which reveals subsarcolemmal accumulation of mitochondrial activity; **(D)** COX-deficient fibres and COX-positive fibres; **(E)** sequential COX/SDH histochemistry emphasizing individual COX-deficient fibres which retain SDH activity. Scale bar: 100µm.

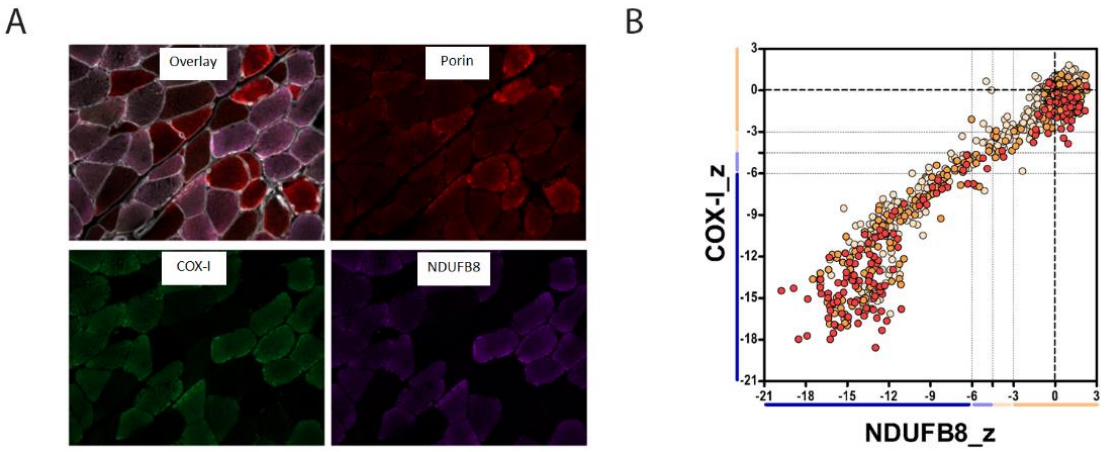

Figure 3.3.2 - **Mitochondrial respiratory chain profile in patient's muscle biopsy. (A)** Representative image of quadruple immunofluorescence (laminin – white (405nm), NDUFB8 – purple (647 nm), COX-I – green (488 nm) and porin – red (546 nm)) performed in patient's muscle section. **(B)** Mitochondrial respiratory chain profile showing CI, CIV and porin levels in patient (n=1022 fibres). Each dot represents an individual muscle fibre color coded according to its mitochondrial mass (very low: blue, low: light blue, normal: light orange, high: orange and very high: red). Thin black dashed lines indicate the SD limits for the classification of fibres, lines next to x and y axis indicate the levels of NDUFB8 and COX-I respectively (beige: normal, light beige: intermediate(+), light blue: intermediate(-) and blue: negative), bold dashed lines indicate the mean expression level of normal fibres.

3.3.3.2 Genetic investigations in different tissues

The entire mitochondrial genome analysis by NGS revealed previously reported polymorphisms and a novel heteroplasmic variant in the *MT-TS1* gene (m. 7486G>A, mt-tRNA$^{Ser(UCN)}$, ClinVar accession number: SCV000492500) (Table 3.3.1) in the patient's muscle homogenate (~90%), fibroblasts (~11%) and lymphocytes (~4%). Besides, a heteroplasmic single, large-scale deletion was detected in muscle homogenate and fibroblasts of patient, but not in blood, with the sequence breakpoints determined as 8482-13447, corresponding to the "common deletion".

Table 3.3.1 Mitochondrial sequence variations detected by whole mitochondrial genome sequencing in the patient presenting CPEO.

Nucleotide Change	Amino acid change	Locus	Previously described
m.263A>G	-	*HV2*	Yes
m.1438A>G	-	*MT-RNR1 (12S)*	Yes
m.2706A>G	-	*MT-RNR2 (16S)*	Yes
m.7028C>T	Syn (A375A)	*MT-COI*	Yes
m.7486G>A	**-**	***MT-TS1***	**No**
m.8860A>G	T112A	*MT-ATP6*	Yes
m.15326A>G	T194A	*MT-CYB*	Yes
m.16311T>C	-	*HV1*	Yes

The previous analysis allowed determining that the patient belongs to the haplogroup H+16311.

The evolutionary conservation showed that cytosine is conserved throughout evolution (Figure 3.3.3A). The sequence variation was present at residue 32 in the anticodon loop of *mt*-tRNA$^{Ser(UCN)}$ affecting a 3-methylcytidine post-transcriptional position (Figure 3.3.3B). Moreover, the same alteration was not detected in the 200 controls screened by Sanger sequencing (data not shown).

Heteroplasmy quantification of the mt-tRNA$^{Ser(UCN)}$ variant (m.7486G>A) was obtained by pyrosequencing in fibroblasts (~10%) and about 50% in muscle homogenate was recorded.

Long-Range PCR for ~10kb amplification presented a product size band with ~10kb (*wild type*) and also ~5kb, confirming the presence of the single, large-scale deletion (Figure 3.3.4A), which is in agreement with the deletion size detected by NGS.

The Mitome500 panel revealed some polymorphisms and unknown variants in heterozygosity (Table 3.3.2). A number of candidate genes involved in mtDNA replication and maintenance, including *POLG*, *TWNK* (formerly *PEO1*), *MPV17*, *TK2*, *SLC25A4* (*ANT1*), *OPA1*, *TYMP*, *DGUOK*, *SURF1* and *RRM2B,* were investigated, but the variants found could not explain the mtDNA rearrangement.

Table 3.3.2 List of the sequence variations detected in nuclear genes in patient's samples, after filtering for variant calling and excluding known polymorphisms.

Gene	Sequence variation	Amino acid change	NCBI ClinVar	% allele mutant	Clinical Significance
COX18	c.10C>T	p.R4W	rs187930178	49.86	Unknown
MRLP39	c.925C>T	p.H309Y	rs138089183	45.52	Unknown
MTFMT	c.172T>A	p.F58I	rs188718836	51.35	Unknown
NARS2	c.688G>C	p.G230R	rs190014304	52.35	Unknown

3.3.3.3 mt-tRNA$^{Ser(UCN)}$ steady-state level presented normal values

Concerning the investigation of the processing of mt-tRNA$^{Ser(UCN)}$, the steady-state level of this tRNA was determined in the patient's muscle by Northern blot hybridization. Levels of the mature mt-tRNA$^{Ser(UCN)}$ transcript were almost unchanged when compared to controls (Figure 3.3.3C).

3.3.3.4 Single fibre studies revealed the segregation of the m.7486G>A variant and the "common deletion" with the biochemical defect

Single muscle fibre analysis was performed to determine whether heteroplasmy levels of the m.7486G>A variant segregated with the observed biochemical defect in this tissue. The results revealed significantly higher levels (***p<0.0001, Mann-Whitney test) of heteroplasmy in COX-deficient fibres (92.24±0.58%, n=29), compared to COX-positive fibres (14.96±2.98%, n=26) (Figure 3.3.3D).

The same approach was completed to analyse the common deletion load showing significantly higher levels (***p<0.0001, Mann-Whitney test) in COX- deficient fibres (89.58±2, n=27) and the absence of deletion in most of COX-positive muscle fibres (-2±3.3, n=17), (Figure 3.3.4B). Accordingly, muscle homogenate presents 57% to 61% of deletion in the three independent experiments performed.

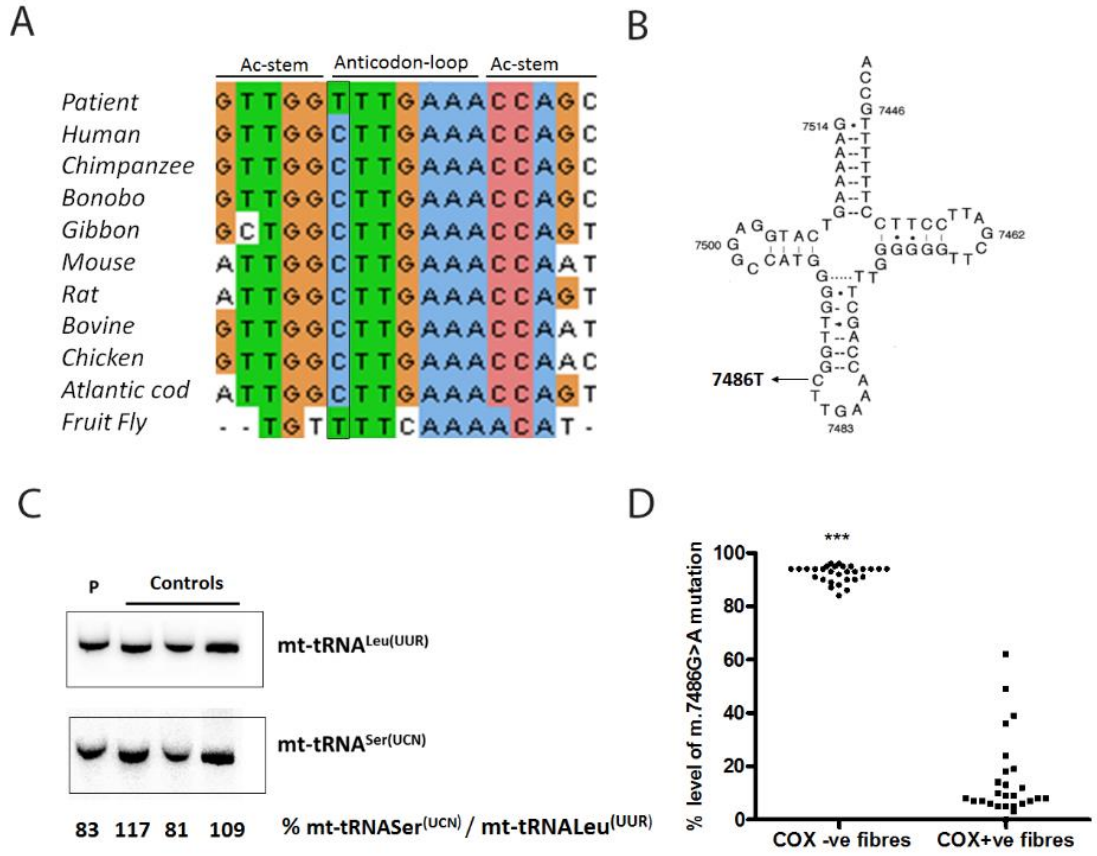

Figure 3.3.3 - **Investigation of the m.7486G>A sequence variation. (A)** Evolutionary conservation of m.7486G>A change in mt-tRNA$^{Ser(UCN)}$ in different species. **(B)** Proposed secondary structure of mt-tRNA$^{Ser(UCN)}$. The gene is encoded in the light strand and thus the base change at position 7486 is shown as C to T. **(C)** Representation of mt-tRNA$^{Ser(UCN)}$ steady-state levels by high-resolution northern blot in skeletal muscle, without significant differences between patient and controls. **(D)** Single-fibre analysis by pyrosequencing of the m.7486G>A mutation in individual COX-deficient and COX-positive muscle fibres, showing a clear segregation of high mutation load with the biochemical defect. Mann-Whitney test, ***p<0.0001.

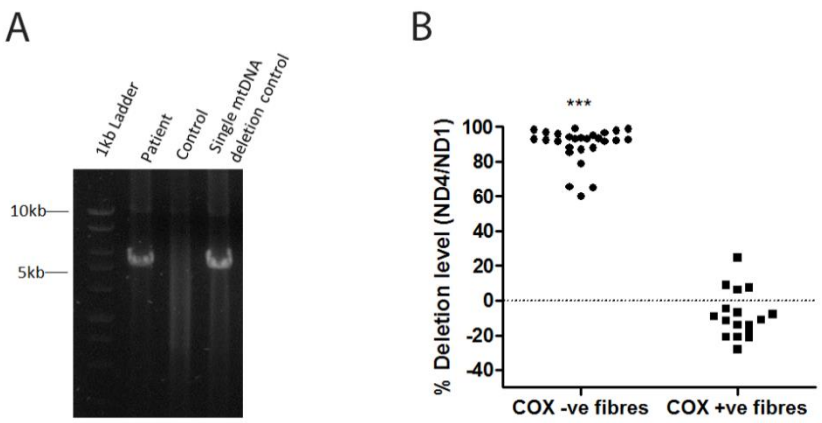

Figure 3.3.4 - Study of the "common deletion". (A) Long-range PCR for detection of the "common deletion", amplifying approximately 10kb of the mtDNA, producing a product size of approximately 5kb. **(B)** Single fibre study for the presence of the "common deletion" in individual COX-deficient and COX-positive muscle fibres after Real-time PCR analysis, showing a clear segregation of high mutant load with the biochemical defect. Mann-Whitney test, ***p<0.0001.

3.3.3.5 Assembly of MRC complexes was impaired

Concerning the assembly of the MRC complexes, a statistical significant reduction was found in all fully assembled complexes, in comparison to controls (Figure 3.3.5A). The results are similar for the four complexes with mitochondrial subunits: CI (Figure 3.3.5B, *p=0.0162, Mann-Whitney test); CIII (Figure 3.3.5C, *p=0.0127), CIV (Figure 3.3.5D, *p=0.0357) and CV (Figure 3.3.5E, *p=0.0216).

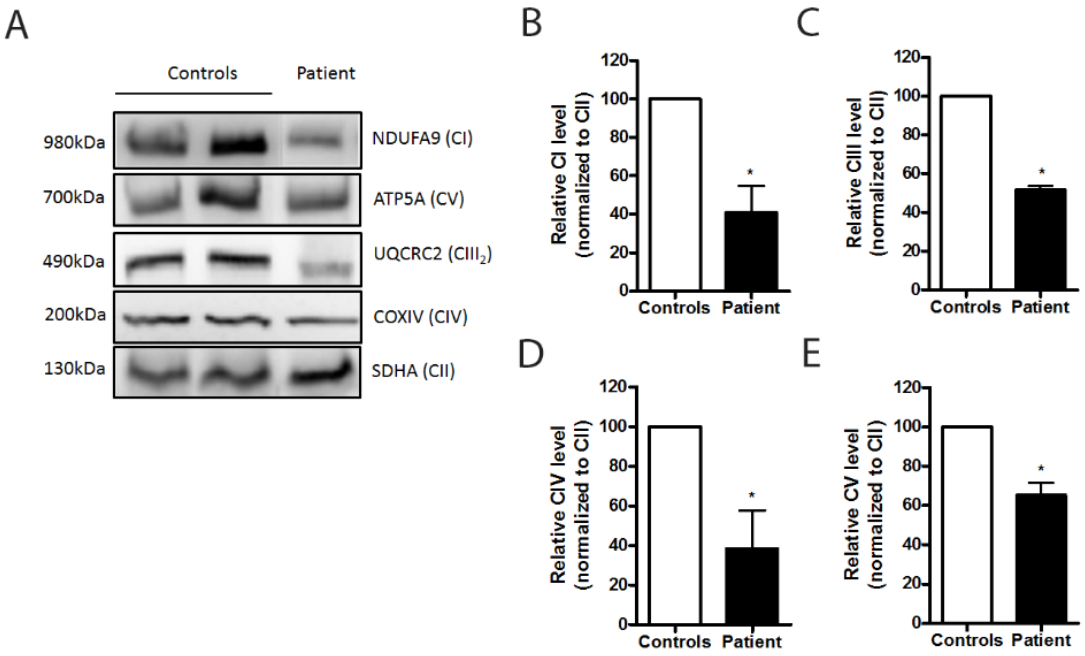

Figure 3.3.5 - **Quantification of the fully assembled complexes of MRC in fibroblasts of controls and patient 3. (A)** Blue-native PAGE followed by immunoblot with antibodies directed against specific individual subunits, in order to quantify the fully assembled OXPHOS complexes. Complex II was used as loading control. **(B)** Relative fully assembled complex I level, **p*=0.0162; **(C)** Relative fully assembled complex III level, **p*=0.0127; **(D)** Relative fully assembled complex IV level, **p*=0.0357; **(E)** Relative fully assembled complex V level, **p*=0.0226. The analysis was performed using Mann-Whitney test. Results are representative of the mean±SEM based on at least three independent experiments in duplicate. C – Complex.

3.3.3.6 Biochemical analysis showed decreased MRC enzymatic activity

Assessment of respiratory enzymatic activity in muscle homogenate and skin fibroblasts of patient revealed a reduction in CIV activity (44.8% and 88.9% of controls, respectively), being more pronounced in the muscle. The activity of the other complexes was not totally concordant between the different tissues (Table 3.3.3). However, CV activity was diminished in muscle (69.0% of the controls' mean) and in skin fibroblasts (66.3%). CI activity is slightly reduced only in muscle (Table 3.3.3).

Table 3.3.3 Assessment of enzymatic activity of the mitochondrial respiratory chain complexes. Results are expressed as nmol of substrate per min per mg of protein normalised to Citrate Synthase. Patient values are presented as the mean of replicates. Control values are shown as mean±SD.

	Patient's muscle	Reference values (*n*=32)	Patient's fibroblasts	Reference values (n=3)
	Mean (% of controls)	Mean ± SD (min – max)	Mean (% of controls)	Mean ± SD (min – max)
Citrate Synthase (CS) (nmol/min/mg)	156.18 (137%)	113.6 ± 27.6 (70.0 - 165.1)	107.19 (102%)	105.40 ± 13.34 (92.70 - 119.45)
Complex I/CS	0.14 (88%)	0.16 ± 0.09 (0.02 - 0.39)	0.85 (116%)	0.73 ± 0.14 (0.64 - 0.89)
Complex II/CS	0.21 (66%)	0.32 ± 0.21 (0.07 - 1.13)	0.13 (68%)	0.19 ± 0.02 (0.17 - 0.20)
Complex III/CS	1.85 (153%)	1.21 ± 0.68 (0.30 - 2.94)	1.60 (78%)	2.06 ± 0.92 (1.03 - 2.77)
Complex IV/CS	0.77 (44%)	1.72 ± 1.35 (0.40 - 7.54)	0.40 (89%)	0.45 ± 0.02 (0.43 - 0.48)
Complex V/CS	0.58 (69%)	0.84 ± 0.55 (0.18 - 2.90)	0.55 (66%)	0.83 ± 0.15 (0.71 - 1.00)
Complexes II+III/CS	0.10 (36%)	0.28 ± 0.19 (0.10 - 0.74)	0.11 (65%)	0.17 ± 0.06 (0.12 - 0.23)
Complexes I+III/CS	0.34 (109%)	0.31* ± 0.21 (0.05 - 0.85)	0.43 (49%)	0.88 ± 0.24 (0.67 - 1.14)

**n*=22

3.3.3.7 Mitochondrial respiration was significantly reduced

The OCR results revealed a significant reduction in mitochondrial respiration of patient's cells compared to controls (Figure 3.3.6A); there were evident differences in basal respiration (Figure 3.3.6C, ****p*=0.0008), maximal respiration (Figure 3.3.6D, ****p*=0.0008) and ATP production (Figure 3.3.6E, ****p*<0.0001). In order to compensate the reduced mitochondrial respiration rate, glycolysis and glycolytic capacity are enhanced, although not significantly (Figure 3.3.6H, I). Also, intracellular ATP levels were not significantly changed (Figure 3.3.6K).

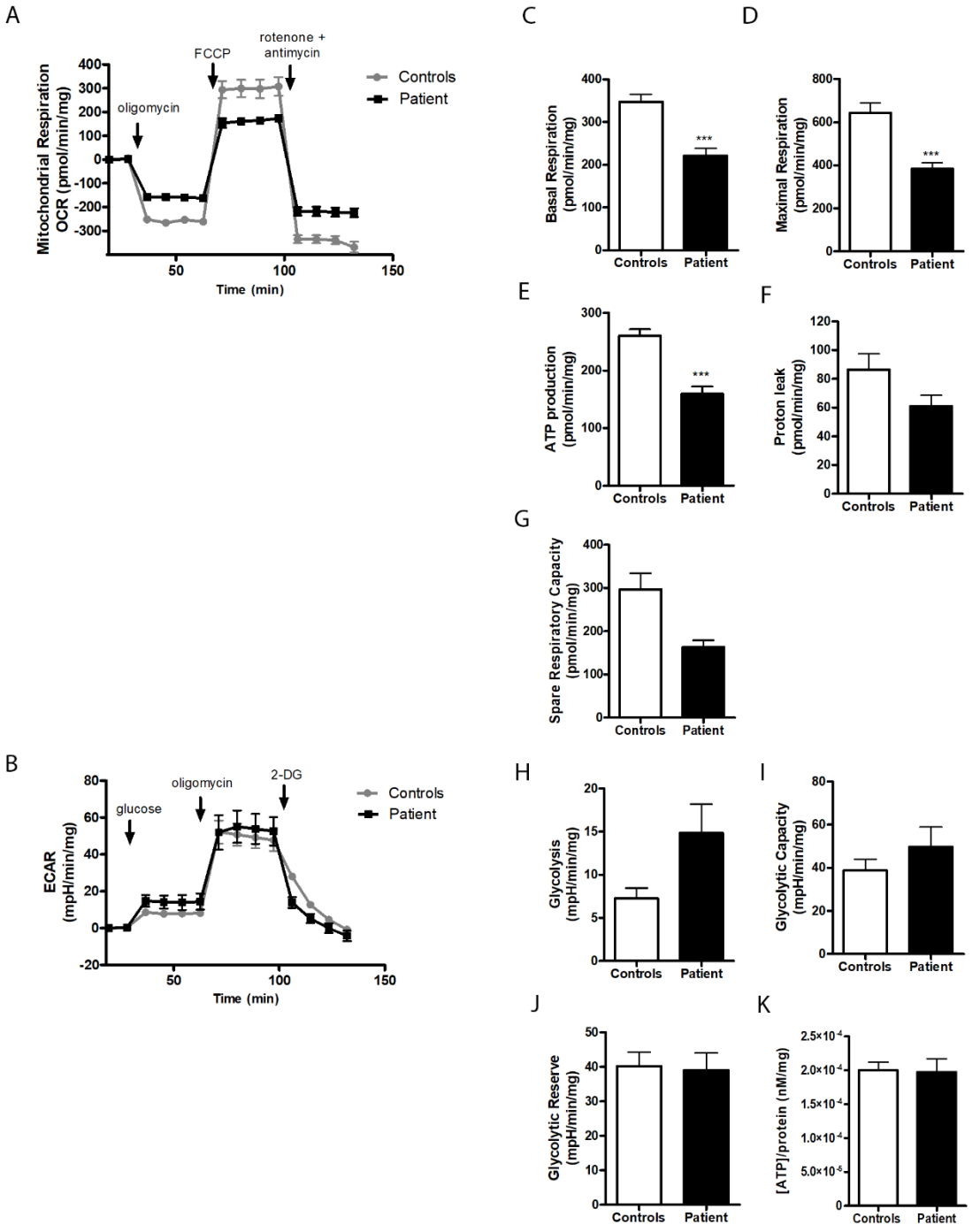

Figure 3.3.6 - **Bioenergetics parameters. (A)** Mitochondrial Respiration Profile; **(B)** Acidification profile; **(C)** Basal respiration, Unpaired t-test, ***p=0.0008; **(D)** Maximal respiration, Mann Whitney test, ***p=0.0008; **(E)** ATP production, Unpaired t-test, ***p<0.0001; **(F)** Proton leak; **(G)** Spare respiratory Capacity; **(H)** Glycolysis; **(I)** Glycolytic Capacity; **(J)** Glycolytic Reserve. **(K)** Intracellular ATP levels. Data are representative of the mean±SEM.

3.3.3.8 Mitochondrial membrane potential evaluation disclosed depolarization

Differential accumulation of rhodamine 123 probe in mitochondria allowed the detection of significant changes in the $\Delta\psi_m$ of patient's dermal fibroblasts compared to the control group (Figure 3.3.7). Indeed, addition of the uncoupler FCCP in cells pre-exposed to rotenone (Figure 3.3.7A), antimycin A (Figure 3.3.7B) or oligomycin (Figure 3.3.7C) caused a rise in rhodamine 123 fluorescence that was significantly lower in patient's cells than in controls. The results suggest mitochondrial membrane depolarization in patient's fibroblasts.

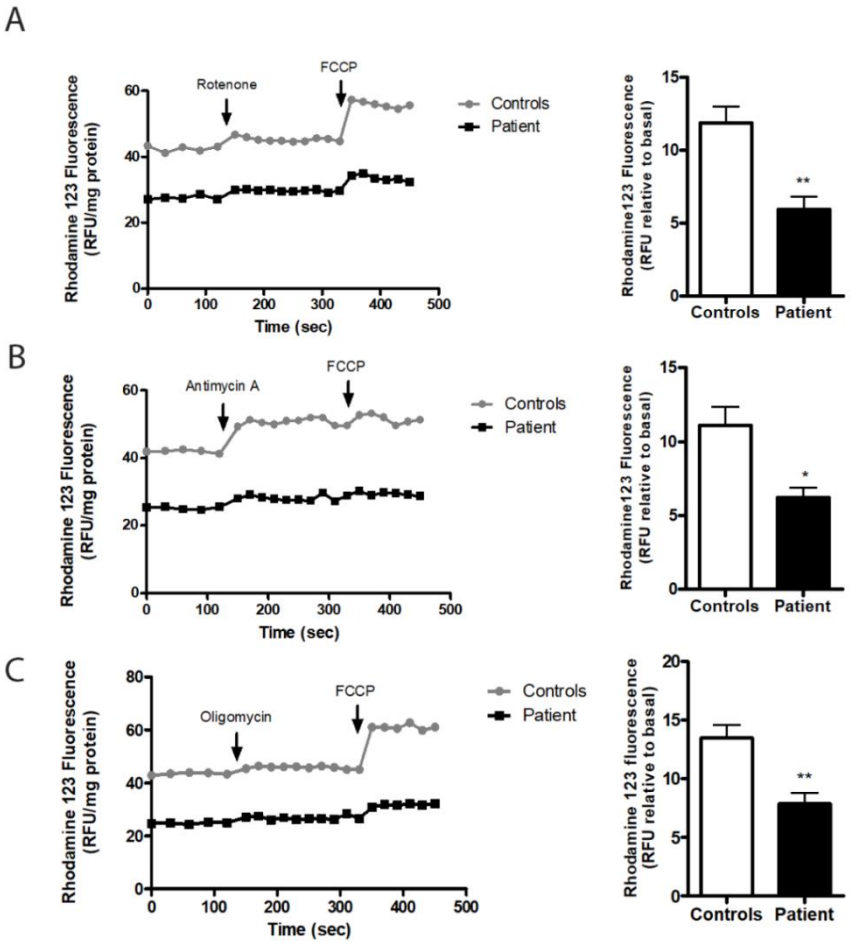

Figure 3.3.7 - Mitochondrial membrane potential measurement in patient's skin fibroblasts and control group. **(A)** Complex I inhibition followed by uncoupling with FCCP (left), graphical representation of the difference between the basal and rotenone plus FCCP-induced levels of rhodamine123 (***p*=0.0068) (right); **(B)** Complex III inhibition followed by uncoupling with FCCP (left), graphical representation of the difference between the basal and antimycin A plus-FCCP induced levels of rhodamine123 (**p*=0.0369) (right), **(C)** Complex V inhibition followed by uncoupling with FCCP to induce the maximal depolarization (left), graphical representation of the difference between the basal and oligomycin plus FCCP-induced levels of rhodamine123 (***p*=0.0084) (right) .Results are the mean±SEM of three independent measurements run in triplicates. Statistical analysis was performed using the Unpaired Student's *t*-test.

3.3.3.9 Superoxide anion presented normal levels in skin fibroblasts of the patient

Regarding the superoxide anion production, the results showed normal basal levels compared to controls (Figure 3.3.8A). However, mitochondrial superoxide production increased significantly ($p<0.0001$) after the inhibition of CI (Figure 3.3.8B). The same result was not observed after the inhibition of CIII (Figure 3.3.8C).

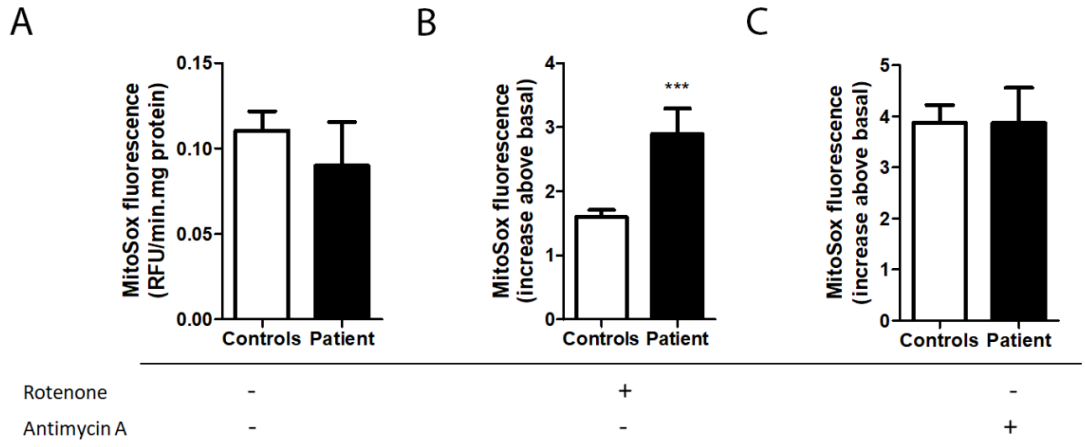

Figure 3.3.8 - Levels of superoxide anion production in fibroblasts of patient and controls. (**A**) basal levels; (**B**) after complex I inhibition with rotenone; (**C**) after complex III inhibition with antimicyn A. Results are from three independent measurements in triplicates. Errors bars represent the mean±SEM and the statistical significance was verified by Unpaired Student's *t*-test, ****p*<0.0001.

3.3.3.10 Mitochondrial morphology in fibroblasts and muscle

Regarding TEM analysis remarkable morphological and ultrastructural differences were observed between control's (Figure 3.3.9A) and patient's (Figure 3.3.9B) skin fibroblasts. Indeed, skin fibroblasts derived from the patient showed the presence of large multilamellar bodies (MLB) (Figure 3.3.9B), suggesting impaired autophagy. Mitochondrial hyperproliferation, enlarged mitochondria and mitochondria presenting structural alterations of cristae such as paracrystalline inclusions and concentric "onion-shaped" cristae, were observed in patient's muscle (Figure 3.3.9C-E).

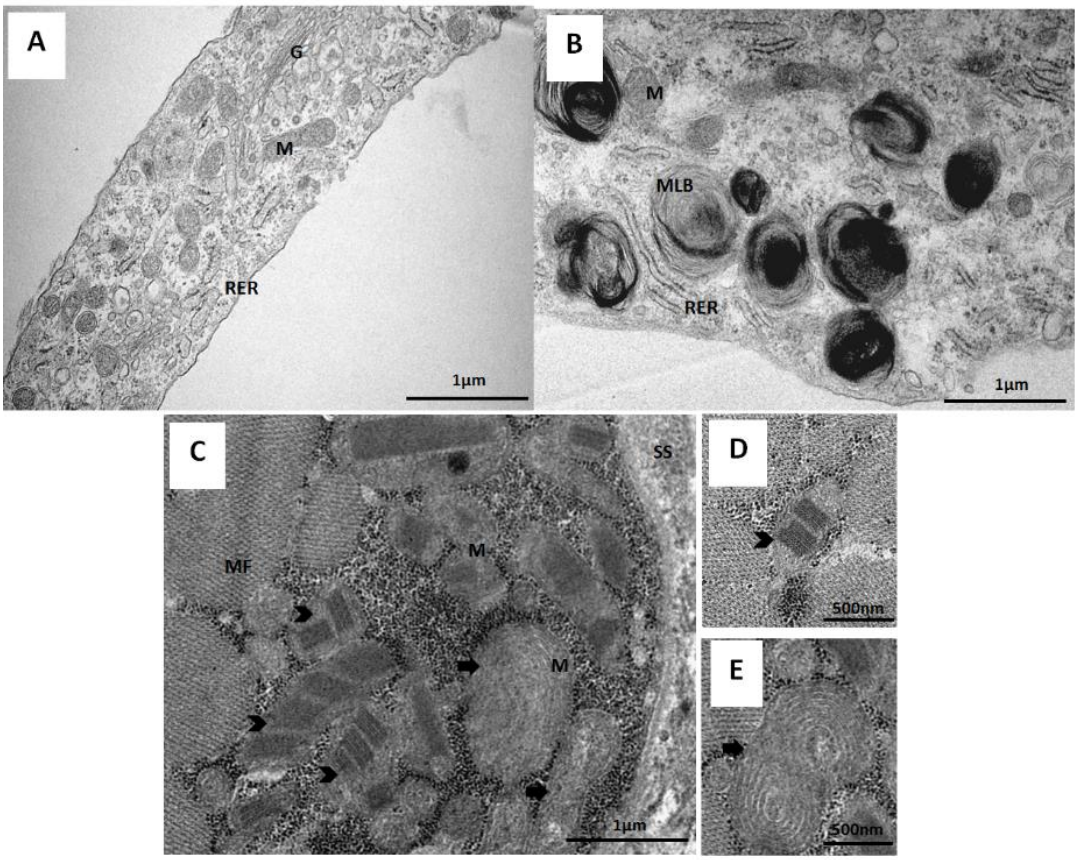

Figure 3.3.9 – Ultrastructural study of primary fibroblasts and skeletal muscle by transmission electron microscopy. **(A)** Control's fibroblasts, **(B)** Patient's fibroblasts showing multilamellar bodies (MLB), **(C-E)** Myofibres of patient's skeletal muscle in the transverse plane, presenting abnormal mitochondria with paracrystalline inclusions (arrowhead) and concentric cristae (arrows). G – Golgi, M – Mitochondrion, RER – Rough Endoplasmic Reticulum, MF – myofibrils, SS – Subsarcolemmal space.

3.3.4 Discussion

In the present report, the P3 showed histological and histochemical changes in muscle that were indicative of OXPHOS dysfunction and mitochondrial-related disease. Both immunofluorescence and MRC evaluation revealed decreased levels and activity of multiple complexes in muscle sections and homogenate, respectively, likely due to the defective translation.

Deep genetic investigation allowed identification of the "common deletion" in muscle (60% of heteroplasmy and segregation with COX-deficient fibres) and fibroblasts, and a novel mt-tRNA$^{Ser(UCN)}$ variation (m.7486G>A) in muscle, fibroblasts and blood. The percentage of deleted molecules is probably enough to cause a clinical

phenotype, while the presence of a novel heteroplasmic (50% in muscle homogenate) variant in the anticodon loop of the mt-tRNA$^{Ser(UCN)}$ was also relevant.

There are numerous examples of disease-causing mutations in *mt-tRNA* genes and more than 20 variants, in 13 different *mt-tRNA* genes, were reported in association with CPEO and/or myopathy[301]. Three of them have been reported in *MT-TS1* gene: m.7506G>A[370], m.7451A>T[216] and m.7458G>A[209]. Nevertheless, the interpretation of pathogenicity for mtDNA variants is complex and challenging. The pathogenic variants in mt-tRNA genes may impair transcription termination and tRNA maturation, reduce the aminoacylation, abolish post-transcriptional modification of tRNA, decrease the binding to translation factors or the mitoribosome, alter the structure, perturb the stability, and disturb codon reading, ultimately leading to loss of function[30,57]. The novel variation m.7486G>A (*MT-TS1*) affects a highly conserved nucleotide and alters the first base of the anticodon loop adjacent to the anticodon stem (position 32 of mt-tRNA$^{Ser(UCN)}$), disturbing a 3-methylcytidine (m^3C) post-transcriptional modification position[30,371–374]. Little is known about the function of this type of modification, although a role in accurate codon recognition and translation efficiency has been suggested[375,376].Thus, the m.7486G>A variation could affect the conformation of the anticodon loop by creating a U32 pair with A38, that may disturb the interaction with mitoribosome, thus reducing the contact time for codon recognition. Similar defects in the conformation of the anticodon loop were suggested for the m.7480T>C variation, reported as pathogenic and causing mitochondrial myopathy, located in the anticodon loop of mt-tRNA$^{Ser(UCN)}$ at position 38 (opposite to 32)[377]. The novel variation herein reported was identified (about 90%) in COX-deficient fibres of the affected tissue (muscle) by single fibre studies, segregating with the biochemical phenotype (Figure 3.3.3D) but maintaining the mt-tRNA$^{Ser(UCN)}$ steady-state levels.

According to the scoring criteria[205] for characterisation of the pathogenicity for the novel m.7486G>A variant, the score totals 11 points, out of 20, as follows: (1) the variant was heteroplasmic in different tissues (2 points); (2) the base is conserved throughout evolution (2 points); (3) there was a strong histochemical evidence of mitochondrial disease (2 points); (4) biochemical defects were detected in complexes I, III or IV (2 points); and (5) the variant segregated with the biochemical phenotype (3 points). Some of these criteria were certainly influenced by the presence of the

"common deletion". However, the specific criterion for the segregation with the biochemical defect suggested that the sequence variation is "probably pathogenic".

The defective mitochondrial translation is predicted to be the primary consequence of mutations affecting *mt-tRNA* genes, leading to OXPHOS deficiency. The "common deletion" would be expected to have a similar detrimental effect on translation of all subunits encoded by mitochondrial genome. Therefore, the most likely genetic cause of CPEO in this patient is the "common deletion", even though the m.7486G>A sequence variation holds a huge pathogenic potential associated to the disease.

Since the first report[23], the consequences of the "common deletion" have been characterised[339,341,358–362], namely the decrease in MRC activity[339,341,359,361], mitochondrial protein synthesis[360], mitochondrial membrane potential and ATP synthesis[362].

In order to corroborate the functional cellular consequences of the "common deletion" and explore other mechanisms, a functional analysis was conducted in skin fibroblasts of the patient. A significant decrease in all fully-assembled complexes with mtDNA-encoded subunits was found, highlighting the effect in mitochondrial translation. The oxygen consumption in patient's cells was significantly compromised, compared to controls, impairing the cellular response to further energetic demands. A decrease in $\Delta\Psi_m$ was also observed, confirming previous results[362]. Regarding the increased superoxide anion production noticed upon CI activity inhibition, it seems reasonable to assume that the mitochondrial $O_2^{\bullet-}$ production may reach higher levels in the affected tissue (muscle), since CI presented a normal activity in fibroblasts but a reduction in the enzymatic activity in muscle of the patient.

Concerning ultrastructural alterations, the most relevant finding in fibroblasts was the presence of large MLB, which could be interpreted as an expression of cellular damage, suggesting alterations of autophagy, similarly to the hypothesis proposed by Signorini and colleagues in skin fibroblasts of patients affected with Rett syndrome[317] and Thomas and co-workers in fibroblasts of patients presenting Spinocerebellar ataxia, autosomal recessive 20[323]. The accumulation of abnormal mitochondria in patient's skeletal muscle, presenting paracrystalline inclusions and concentric cristae, reinforces the mitochondrial dysfunction observed in this tissue, as previously

described for myopathy caused by large-scale single mtDNA deletion or mt-tRNA mutations[217]. These results strongly suggest that defects in the proteolytic systems, namely mitophagy, responsible for the elimination of damaged or dysfunctional mitochondria, can be implicated in the disease.

In conclusion, we describe the first report of a patient with CPEO presenting two genetic alterations, probably leading to the phenotype: a single, large-scale mtDNA deletion and one *mt-tRNA* sequence variation. Since both alterations show high levels in muscle, segregate with the biochemical defect and they may promote inefficient mitochondrial translation, it is difficult to assign the isolated impact of the novel *mt-tRNA* sequence variation. The "common deletion" is the most likely genetic cause. However, the potential pathogenic effect of the novel mt-tRNA$^{Ser(UCN)}$ sequence variation cannot be ignored, and it may be valuable in evaluating further cases. Concerning the cellular consequences, functional evidences were gathered, demonstrating the inability to produce mtDNA-encoded proteins, leading to incomplete fully assembled OXPHOS complexes and resulting in electron transport deficiency, inefficient respiration and depolarization of mitochondrial membrane. Nonetheless, more investigation will be required to fully understand the molecular pathways that contribute to CPEO expression.

3.4 CASE REPORT IV

An unclassified mtDNA variant in a familial case of sudden death associated to a *MYBPC3* mutation

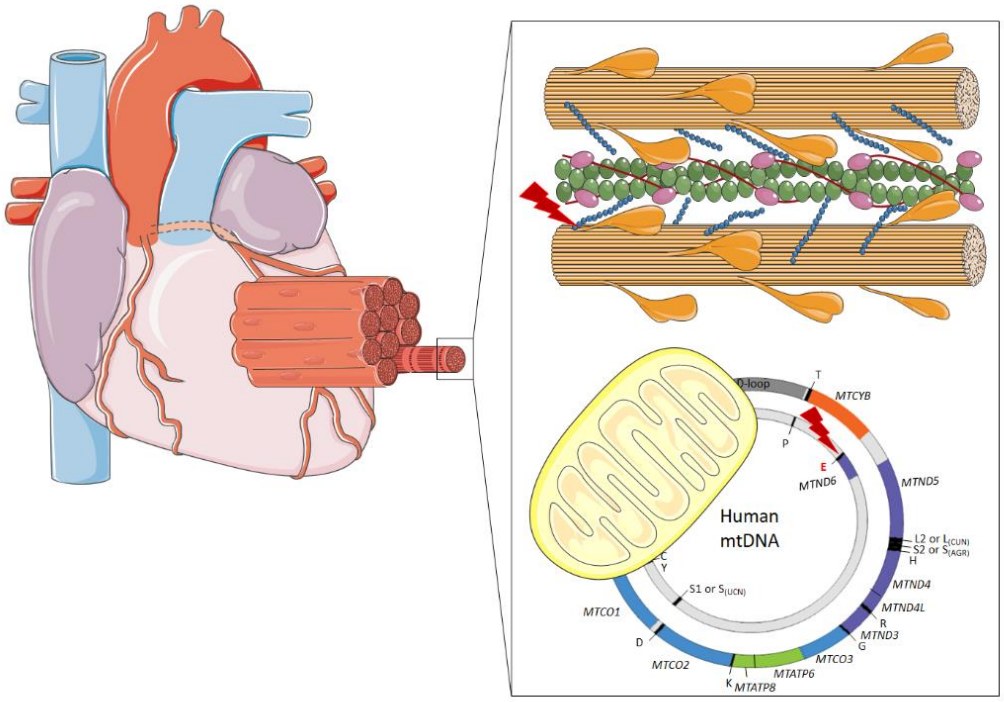

Abstract

Cardiomyopathies are a frequent cause of sudden death. Familial cardiomyopathies are often autosomal dominant diseases with incomplete penetrance, presenting heterogeneity in genetic causes. These range from mutations in genes encoding sarcomere proteins to mitochondrial DNA mutations. Herein, a familial case of sudden cardiac death harbouring a heterozygous sarcomere mutation in *MYBPC3* gene and a homoplasmic mitochondrial sequence variation (m.14706A>G) is reported (patient 4, P4). The present work aimed to elucidate the functional impact of the unclassified mtDNA variant (m.14706A>G) detected in homoplasmy in muscle, liver and fibroblasts of the proband. In spite of the m.14706A>G alteration do not segregate with the disease, this maternal inherited sequence variation changes a conserved wobble base pair at the penultimate base pair before the anticodon loop of the mt-tRNA^{Glu}, possibly resulting in a functional and/or structural perturbation of the mt-tRNA, usually involving defects in the translation of oxidative phosphorylation subunits. Indeed, a drastic decrease of complexes fully assembled was observed in patient's fibroblasts. A severe multiple mitochondrial respiratory chain complexes' deficiency was observed in liver and muscle. In accordance with the tissue specificity, we suggest that mitochondrial dysfunction is probably caused by the unclassified mtDNA variant m.14706A>G, acting synergistically with the *MYBPC3* gene mutation, leading to severe defects in the contractile function of sarcomere, and, consequently, to heart failure. Nevertheless, the hypothesis that another nuclear variant could be modulating the severity of phenotype, explaining the incomplete penetrance associated to cardiomyopathy verified for the two sequence variations detected, cannot be excluded.

Keywords: Cardiomyopathy; sudden death; mtDNA variant; MYBPC3.

3.4.1 Introduction

Sudden unexplained death is generally caused by hereditary conditions, mostly cardiovascular diseases[378,379]. Cardiomyopathies, such as hypertrophic cardiomyopathy (HCM), dilated cardiomyopathy (DCM) and left ventricular noncompaction (LVNC) are a frequent cause of sudden cardiac death (SCD)[378,379].

Familial cardiomyopathies are often autosomal dominant diseases with incomplete penetrance[380,381]. The clinical manifestations are highly heterogeneous, varying from asymptomatic cases to sudden death. Mutations in genes encoding proteins of the sarcomere are the most common genetic cause of cardiomyopathies[382–384]. In addition, in the last years, some reports of compound or double mutations in sarcomere genes have been described in more severe cases[385–390]. Other genetic causes of SCD are lysosomal storage diseases and mitochondrial disorders[382].

The mtDNA mutations causing cardiomyopathies were associated to clinical heterogeneity in the severity and age of presentation[391,392].

This work aimed to elucidate the functional impact of an unclassified mtDNA variant (m.14706A>G) detected in the patient 4 (P4), in order to clarify the incomplete penetrance of cardiomyopathy in this family.

3.4.2 Patient and methods

3.4.2.1 Case report

The P4 is the third son of healthy non-consanguineous parents (Figure 3.4.1A, II-3). He died suddenly, at the age of 21 months old. Cardiac alterations were not detected in the autopsy, as mild congestion of the liver was the only finding detected.

Family history investigation (Figure 3.4.1A) revealed that the eldest brother (II-1) had died unexpectedly, at the age of 6 months. The study of the maternal lineage revealed deafness in the grandmother and her two sisters. Father's family presented diabetes type II in six individuals (the grandmother and her three sisters and two

brothers). The lack of more evidences crucial to obtain clues related to the genetic cause of sudden death led to mtDNA investigation.

Meanwhile, the youngest brother (II-4) presented transitory septal hypertrophy, at birth. However, so far he does not present cardiac abnormalities. Furthermore, in the other older brother (II-2), LVNC was diagnosed at the age of 12 years old and a cardioverter-defibrillator was implanted, after a syncope episode.

Accordingly, a genetic evaluation for a panel of genes involved in cardiomyopathy (including *MYH7*, *MYBCP3*, *TNNT2*, *TNNT3* and *MYL2*) was performed, using DNA samples from the parents (I-1,2), the patient (II-3) and his two brothers (II-2 and II-4), at the Medical Genetics Department of Paediatric Hospital of Coimbra – CHUC. A mutation in exon 6 of *MYBCP3* gene (c.772G>A, p.Glu258Lys) was identified in heterozygosity in all samples, except for II-4.

Biological samples (skin, muscle and liver biopsies) were collected from the patient in the first hours after post-mortem and blood from parents and the two brothers were collected for genetic investigation.

The DNA samples of 200 healthy subjects of the same ethnic background were used as controls for screening the mtDNA sequence variation. Skin biopsies from three healthy Portuguese individuals without clinical evidence of mitochondrial disorder, collected in the context of other medical interventions (e.g. surgery), were used as control samples in the experiments of functional analysis.

Informed consent was obtained from the participants, as recommended and approved by the local Ethics Committee (CE-032/2014), following the Tenets of the Helsinki Declaration.

3.4.2.2 Skin derived cultured fibroblasts

Skin biopsy was collected post-mortem and immediately placed in sterile Mg^{2+}/Ca^{2+}-free HBSS. Fibroblasts were grown in complete medium as described in case report I (section 3.1.2.2).

3.4.2.3 Molecular genetic screening

The entire mitochondrial genome of patient´s fibroblasts and liver was sequenced through the NGS, as previously described[307]. Haplogroup of the patient was determined using the Haplogrep® tool[308], based on the mtDNA sequence variations detected. Automated Sanger sequencing analysis was performed, according to the manufacturer's instructions (3130 ABI Prism sequencing system), using BigDye® Terminator Ready Reaction Mix v3.1 (Applied Biosystems), for investigation of the mtDNA region (14420-14855) in DNA from patient's fibroblasts, muscle and lymphocytes. The genetic screening of the 200 controls' samples was carried out by the same method in order to verify the absence of the novel genetic variant. A DNA screening for investigating the presence of the m.14706A>G sequence variation in lymphocytes from other relatives (parents, affected brother and healthy brother) was also performed by Sanger sequencing.

Coding exons of 513 candidate nuclear genes related to mitochondrial structure and function (Mitome500 panel) were hybridized with customized oligonucleotide probe library, captured and then massively sequenced using the HiSeq2000 platform (Illumina technology®), in order to verify the involvement of possible alterations in nuclear genes encoding mitochondrial proteins

3.4.2.4 *In silico* analysis

The *in silico* analysis included the evolutionary conservation of the *MT-TE* gene from mtDNA of different species, according to the proposed consensus panel[365] using ClustalOmega|EBI®[328]. The location of the m.14706A>G sequence variation in the cloverleaf structure of mt-tRNA^{Glu} was verified from Mamit-tRNA® database[366].

3.4.2.5 MRC enzymatic activity evaluation

Catalytic activity of MRC complexes and segments was performed in patient's fibroblasts, muscle and liver as previously described[107]. The results were corrected to CS, used as a mitochondrial reference enzyme[107].

3.4.2.6 Mitochondrial respiratory rate, glycolytic activity and intracellular ATP levels measurement

OCR and ECAR were measured in patient's fibroblasts and three controls using a XF24 Extracellular Flux Analyser (Seahorse Bioscience, Billerica, MA, USA), as described in detail in the case report I (section 3.1.2.10).

Intracellular ATP levels were measured in patient's and control's fibroblasts by using the luciferin/luciferase assay with ATPlite kit (Perkin Elmer), according to the manufacturer's instructions with minor modifications described in the section 3.1.2.9 of the case report I. Determined ATP concentration, using an ATP standard curve, was normalised to the protein content.

3.4.2.7 Analysis of mitochondrial membrane potential

Mitochondrial membrane potential was determined using the cationic fluorescent probe rhodamine 123 (Molecular probes, Invitrogen) and the variation of rhodamine 123 retention was studied as in the section 3.1.2.11 of the case report I, in order to estimate changes in mitochondrial membrane potential ($\Delta\Psi_m$). Results were expressed as the difference between the basal fluorescence values and the increase of rhodamine 123 fluorescence levels upon addition of inhibitors or uncoupler FCCP, normalised to protein content.

3.4.2.8 Measurement of mitochondrial superoxide anion

Determination of mitochondrial $O_2^{\bullet-}$ basal levels and mitochondrial $O_2^{\bullet-}$ production after CI or CIII inhibition were measured in fibroblasts from controls and

patient using the fluorescent probe MitoSox Red (Molecular Probes, Invitrogen), as described in the case report I (section 3.1.2.12).

The values were obtained as RFU (relative fluorescence units) per minute per milligram of protein, for each condition and then normalised to the basal (untreated) conditions.

3.4.2.9 Transmission electron microscopy

Fibroblasts were collected and the procedure for TEM was performed as described in detail in the section 3.1.2.13 of the case report I.

3.4.2.10 Statistical analysis

Results were analysed using GraphPad Prism version 5.0 software for Windows, San Diego, California, USA. Normality tests were applied in order to verify the Gaussian distribution of the results. Statistical significance of differences between patient and controls was assessed by a Student's *t*-test (or nonparametric Mann-Whitney test).

Results of the statistical significance are represented as * for $p \leq 0.050$, ** for $p \leq 0.010$ and *** for $p \leq 0.001$.

3.4.3 Results

3.4.3.1 Genetic screening confirmed an unclassified mtDNA variant

The presence of the homoplasmic sequence variation in the *MT-TE* gene (m.14706A>G [228], mt-tRNA^{Glu}, ClinVar accession number: SCV000484537), previously detected by Sanger sequencing in muscle (Figure 3.4.1B – II3.a), liver (Figure 3.4.1B – II3.b) and skin fibroblasts (Figure 3.4.1B – II3.c), as well as the haplogroup markers and polymorphisms were confirmed by NGS through the sequencing of the whole-mitochondrial genome (Table 3.4.1), and rearrangements were excluded. The patient belongs to the haplogroup T1a1.

The *in silico* analysis previously performed[393], classified the variant as possibly pathogenic. The affected position is highly conserved in evolution (Figure 3.4.1C), and the nucleotide alteration disrupts a Wobble base pair in the anti-codon stem of mt-tRNA^{Glu} (Figure 3.4.1D).

Moreover, the unclassified sequence variation was not detected in the 200 controls screened (data not shown).

The MITOME500 panel revealed some polymorphisms, variants with uncertain significance and unknown variants (Table 3.4.2).

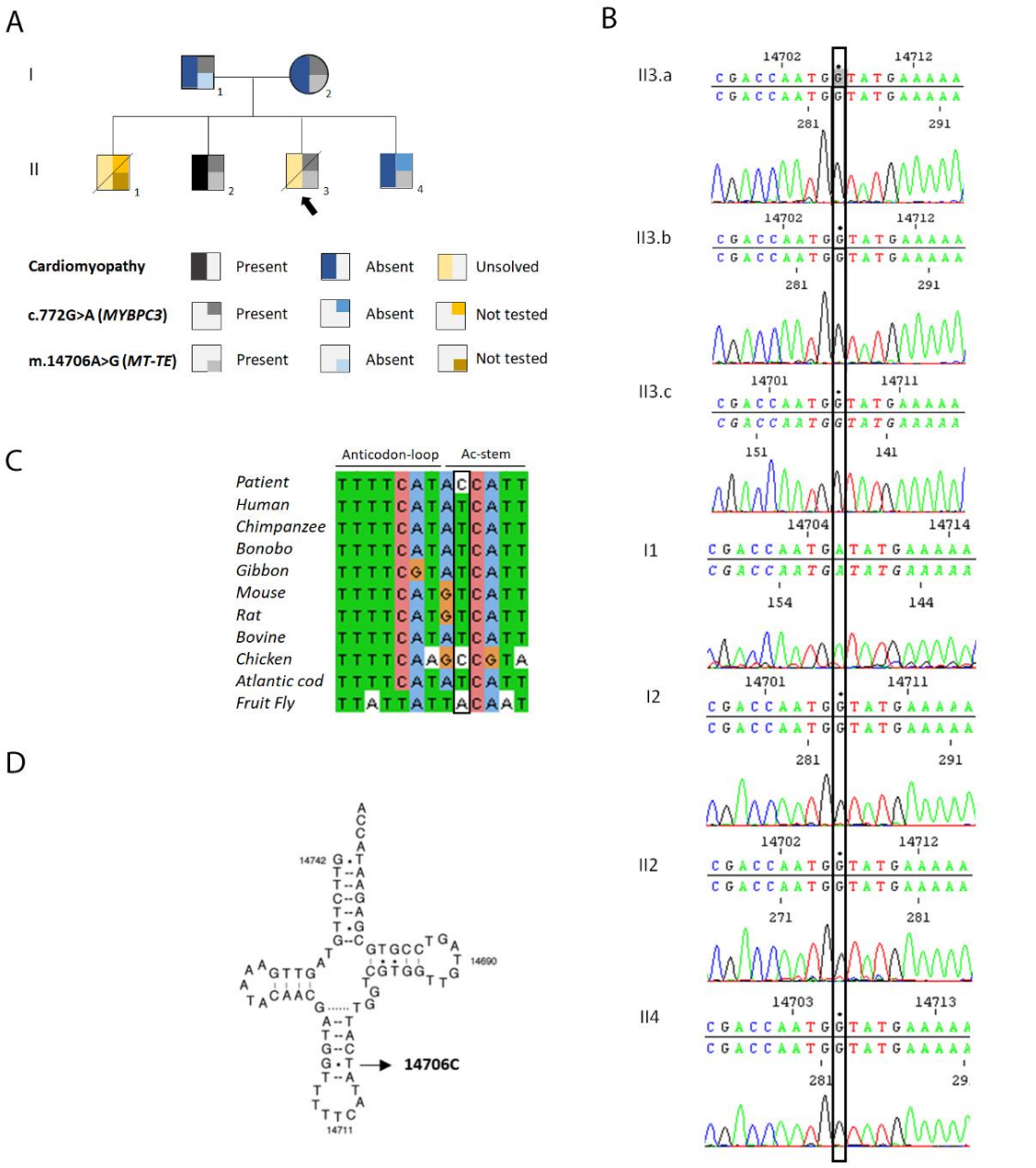

Figure 3.4.1 - **Identification and analysis of m.14706A>G, *MT-TE*. (A)** Pedigree of the presented family. Generations are indicated on the left in Roman numerals and the numbers under the individuals represent identification for each generation. The arrow indicates the P4 of the present study (proband). **(B)** Electropherograms showing the m.14706A>G variant in DNA from patient's muscle (II3.a), liver (II3.b) and fibroblasts (II3.c), and in DNA from lymphocytes of father (I1), mother (I2), the affected brother (II2) and the youngest brother (II4). **(C)** Evolutionary conservation of the nucleotide position m.14706 in *MT-TE* gene. **(D)** Proposed secondary structure of mt-tRNA^{Glu}. The gene is encoded in the light strand of mtDNA and thus the base change at position 14706 is shown as T to C.

Table 3.4.1 Mitochondrial variants detected in P4 samples through the whole mitochondrial genome sequencing by NGS.

Nucleotide Change	Amino acid change	Locus	Previously described
m.73A>G	-	*HV2*	Yes
m.152T>C	-	*HV2, OH*	Yes
m.195T>C	-	*HV2, OH*	Yes
m.263A>G	-	*HV2*	Yes
m.709G>A	-	*MT-RNR1 (12S)*	Yes
m.750A>G	-	*MT-RNR1 (12S)*	Yes
m.1438A>G	-	*MT-RNR1 (12S)*	Yes
m.1888G>A	-	*MT-RNR2 (16S)*	Yes
m.2706A>G	-	*MT-RNR2 (16S)*	Yes
m.3213A>G	-	*MT-RNR2 (16S)*	No
m.4216T>C	Y304H	*MT-ND1*	Yes
m.4769A>G	Syn (M100M)	*MT-ND2*	Yes
m.4917A>G	N150D	*MT-ND2*	Yes
m.7028C>T	Syn (A375A)	*MT-CO1*	Yes
m.8697G>A	Syn (M57M)	*MT-ATP6*	Yes
m.8860A>G	T112A	*MT-ATP6*	Yes
m.9899T>C	Syn (H231H)	*MT-CO3*	Yes
m.10463T>C	-	*MT-TR*	Yes
m.11251A>G	Syn (L164L)	*MT-ND4*	Yes
m.11719G>A	Syn (G320G)	*MT-ND4*	Yes
m.12633C>A	Syn (S99S)	*MT-ND5*	Yes
m.13368G>A	Syn (G344G)	*MT-ND5*	Yes
m.14706A>G	**-**	***MT-TE***	**No**
m.14766C>T	T7I	*MT-CYB*	Yes
m.14905G>A	Syn (M53M)	*MT-CYB*	Yes
m.15326A>G	T194A	*MT-CYB*	Yes
m.15452C>A	L236I	*MT-CYB*	Yes
m.15607A>G	Syn (K287K)	*MT-CYB*	Yes
m.15928G>A	-	*MT-TT*	Yes
m.16126T>C	-	*HV1, D-loop*	Yes
m.16163A>G	-	*HV1, D-loop*	Yes
m.16172T>C	-	*HV1, D-loop*	Yes
m.16186C>T	-	*HV1, D-loop*	Yes

m.16189T>C	-	*HV1, D-loop*	Yes
m.16294C>T	-	*HV1*	Yes
m.16519T>C	-	*D-loop*	Yes

Table 3.4.2 List of the sequence variations detected in nuclear genes in patient's samples, after filtering for variant calling and excluding known polymorphisms.

Gene	Sequence variation	Amino acid change	NCBI ClinVar	% allele mutant	Clinical Significance
AMPD1	c.1029G>T	p.R23C	rs61752478	53.41	Adenosine monophosphate deaminase deficiency (autosomal recessive)
MTRF1L	c.191T>C	p.L64S	-	25.17	Unknown
TOP1MT	c.479A>T	p.K160M	-	46.66	Unknown
MRPL11	c.424C>T	p.R14C	rs145756140	55.99	Unknown
TSFM	c.269G>A	G90D	rs371076990	50.42	Unknown

3.4.3.2 Bioenergetics evaluation showed tissue-specific alterations

The enzymatic activity of each complex was measured in the available tissues, showing differences between the three tissues of patient (Table 3.4.3). The liver and muscle presented a decrease in the activity of several complexes, more pronounced in liver in which the reduction was above 50% of reference values in the five complexes (CI: 20.6%; CII: 39.9%; CIII: 48.3%; CIV: 31.9% and CV: 34.4) (Table 3.4.3). The activity of CI and CIV was the most affected in muscle (31% and 47.1%, respectively). In patient's fibroblasts, only the CIII activity was decreased (59% of controls mean).

Oxygen consumption rate (Figure 3.4.2A) in patient's fibroblasts was similar to controls, in all conditions tested (Figure 3.4.2C-G), as well as the intracellular ATP levels (Figure 3.4.2K).

The ECAR is increased in patient 4 (Figure 3.4.2B, H-J), particularly after the addition of oligomycin, representing a significantly increased glycolytic reserve in the patient compared to controls (***p=0.0004) (Figure 3.4.2J).

Table 3.4.3 Assessment of enzymatic activity of the MRC complexes. Results are expressed as nmol of substrate per min per mg of protein normalised to citrate synthase (CS). Patient values are presented as the mean of replicates. Control values are shown as mean±SD.

	Patient's muscle	Reference values (*n*=32)	Patient's fibroblasts	Reference values (*n*=3)	Patient's liver	Reference values (*n*=18)
	Mean (% of controls)	Mean ± SD (min – max)	Mean (% of controls)	Mean ± SD (min – max)	Mean (% of controls)	Mean ± SD (min – max)
CS (nmol/min/mg)	111.40 (98%)	113.6 ± 27.6 (70.0 - 165.1)	81.96 (77%)	105.4 ± 13.3 (92.7 - 119.5)	106.76 (107%)	99.5 ± 33.5 (49.0 - 156.0)
Complex I/CS	0.05 (31%)	0.16 ± 0.09 (0.02 - 0.39)	0.80 (109%)	0.73 ± 0.14 (0.64 - 0.89)	0.07 (21%)	0.34 ± 0.15 (0.19 - 0.65)
Complex II/CS	0.18 (56%)	0.32 ± 0.21 (0.07 - 1.13)	0.19 (100%)	0.19 ± 0.02 (0.17 - 0.20)	0.75 (40%)	1.88 ± 0.97 (0.79 - 4.20)
Complex III/CS	0.88 (73%)	1.21 ± 0.68 (0.30 - 2.94)	1.22 (59%)	2.06 ± 0.92 (1.03 - 2.77)	1.14 (48%)	2.36 ± 1.02 (1.37 - 4.25)
Complex IV/CS	0.81 (47%)	1.72 ± 1.35 (0.40 - 7.54)	0.50 (111%)	0.45 ± 0.02 (0.43 - 0.48)	0.86 (32%)	2.70 ± 1.16 (1.57 - 5.11)
Complex V/CS	1.61 (192%)	0.84 ± 0.55 (0.18 - 2.90)	0.79 (95%)	0.83 ± 0.15 (0.71 - 1.00)	0.42 (34%)	1.22 ± 0.44 (0.67 - 2.02)
Complexes II+III/CS	0.18 (64%)	0.28 ± 0.19 (0.10 - 0.74)	0.20 (118%)	0.17 ± 0.06 (0.12 - 0.23)	0.66 (70%)	0.94 ± 0.42 (0.31 - 1.62)
Complexes I+III/CS	0.42 (135%)	0.31 ± 0.21 (0.05 - 0.85)*	0.50 (57%)	0.88 ± 0.24 (0.67 - 1.14)	1.12 (138%)	0.81 ± 0.38 (0.07 - 1.43)

**n*=22

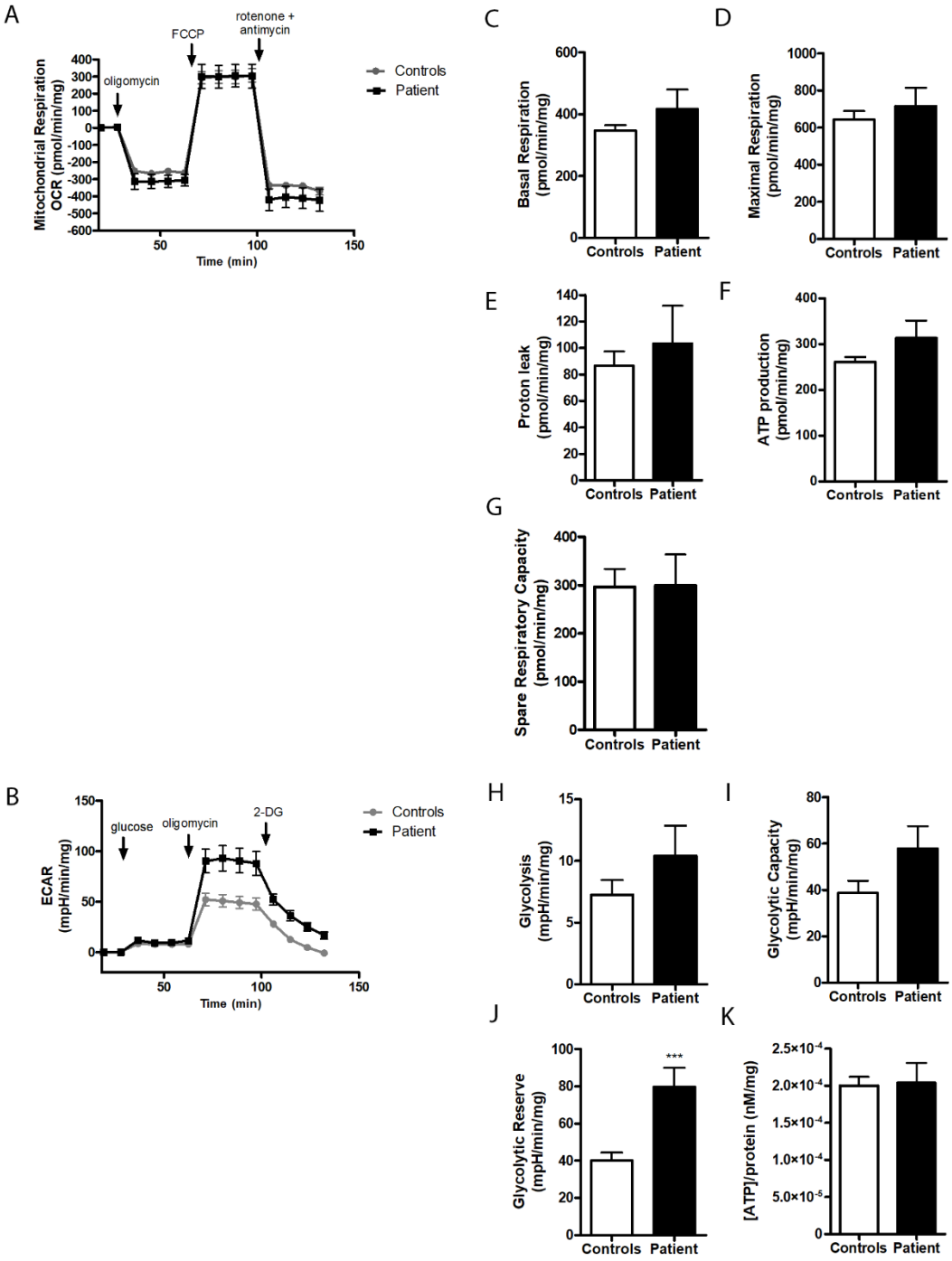

Figure 3.4.2 - **Bioenergetics parameters analysis in the patient harbouring the m.14706A>G variant and controls.** Error bars represent the standard error of mean based on three independent experiments in triplicates. (**A**) Mitochondrial respiration profile; (**B**) Acidification profile; (**C**) Basal respiration; (**D**); Maximal respiration (**E**) Proton leak; (**F**) ATP production; (**G**) Spare respiratory capacity; (**H**) Glycolysis; (**I**) Glycolytic Capacity; **(J)** Glycolytic reserve, Mann-Whitney test, ***p=0.0004; **(K)** Intracellular ATP levels.

3.4.3.3 Mitochondrial membrane potential and superoxide anion presented normal levels in patient´s fibroblasts

Rhodamine 123 release was similar in patient and controls' fibroblasts, in all conditions (Figure 3.4.3), showing that the mitochondrial membrane potential is maintained in patient's cells.

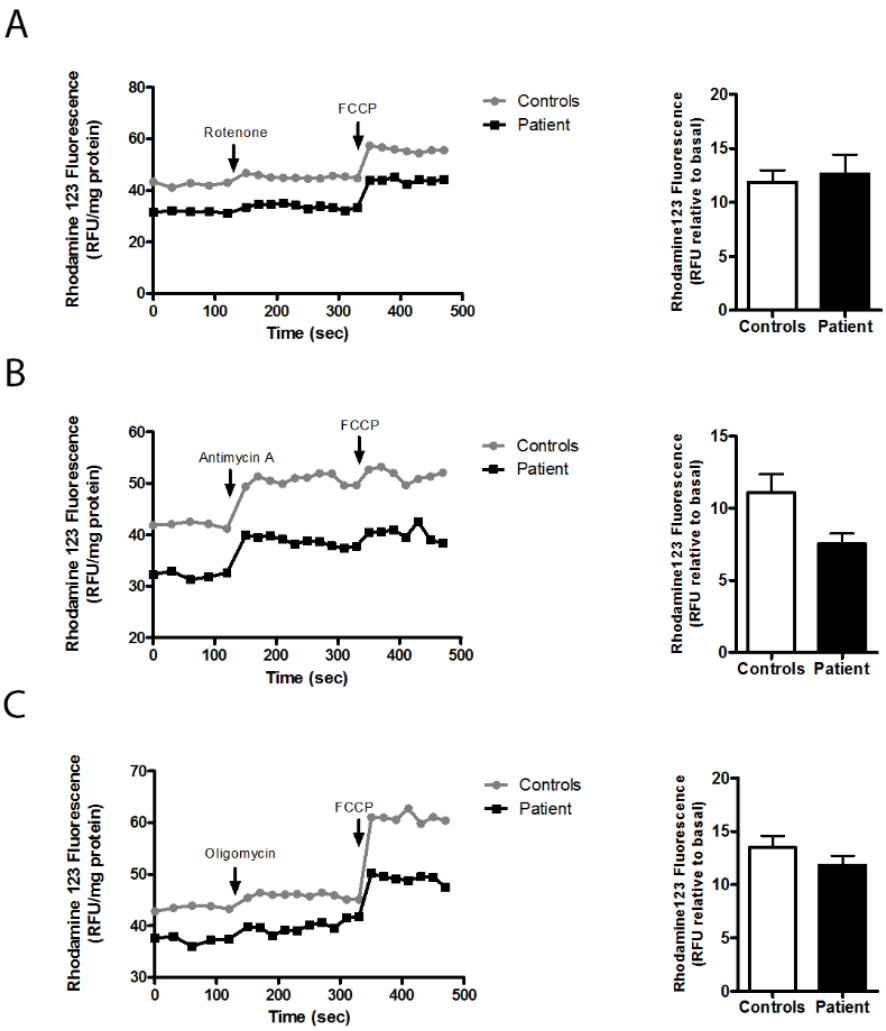

Figure 3.4.3 - **Mitochondrial membrane potential measurements in fibroblasts of patient 4 and controls**. (**A**) Complex I inhibition followed by uncoupling with FCCP (left), graphical representation of the difference between the basal and rotenone plus FCCP-induced levels of rhodamine123 (right); (**B**) Complex III inhibition followed by uncoupling with FCCP (left), graphical representation of the difference between the basal and antimycin A plus FCCP-induced levels of rhodamine123 (right); (**C**) Complex V inhibition followed by uncoupling with FCCP (left), graphical representation of the difference between the basal and oligomycin plus FCCP-induced levels of rhodamine123 (right). Data are presented as the mean±SEM based on three independent measurements in triplicates.

The superoxide anion levels in basal condition (Figure 3.4.4A), as well as after the inhibition of CI (Figure 3.4.4B) were normal. After the inhibition of CIII with antimycin A, a significant increase in the production of superoxide anion was observed in patient's cells compared to controls (Figure 3.4.4C; ***p*=0.0035).

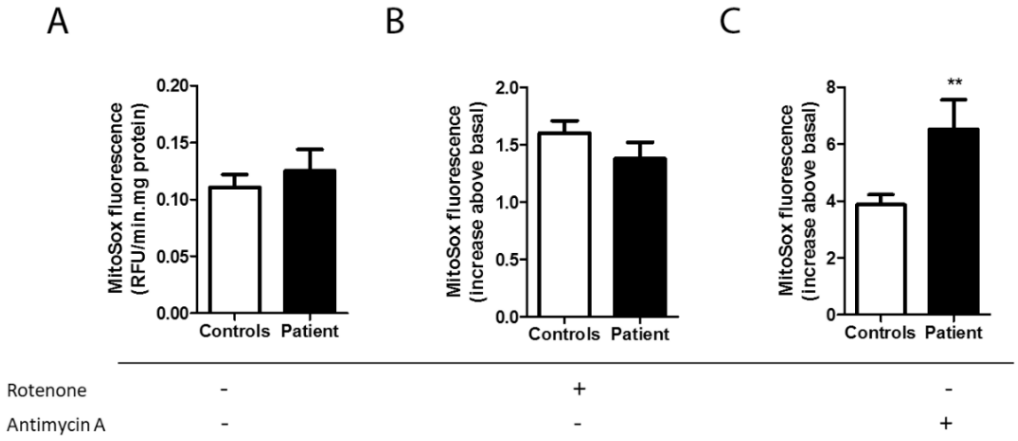

Figure 3.4.4 - Levels of superoxide anion production in fibroblasts of patient 4 with the m.14706A>G variant and in controls (**A**) at basal levels; (**B**) after complex I inhibition with rotenone; (**C**) after complex III inhibition with antimycin A. Results are from three independent measurements in triplicates. Errors bars represent the mean±SEM and the statistical significance was verified by Unpaired t-test, ***p*<0.035.

3.4.3.4 The assembly of OXPHOS complexes presented significant alterations

The assembly of OXPHOS complexes was verified by native electrophoresis followed by Western-blotting. The four complexes harbouring mtDNA encoded subunits presented a significant decrease in patient's fibroblasts in comparison to controls (Figure 3.4.5; **p*=0.0485 – CI; ***p*=0.0047 – CIII; ****p*<0.0001 – CIV; **p*=0.0138 – CV).

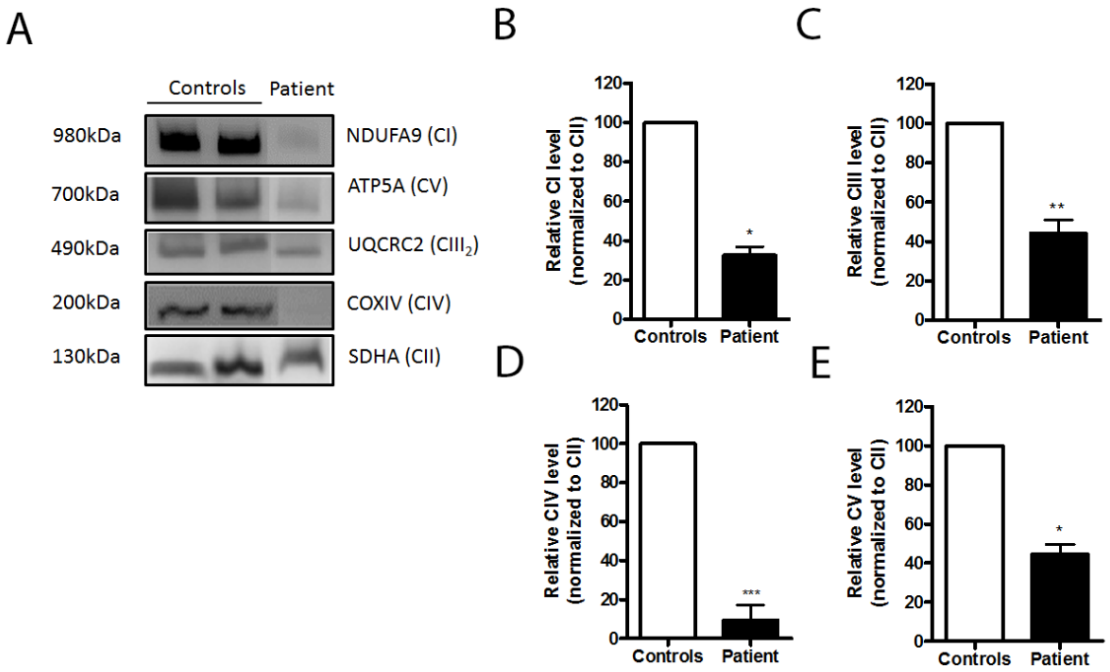

Figure 3.4.5 - **Quantification of the fully assembled complexes of MRC in fibroblasts of patient with m.14706A>G variant and controls**. Error bars are representative of the mean±SEM based on at least three independent experiments in duplicates. (**A**) Native electrophoresis followed by Western-blot analysis for Complexes I to V in controls and patient, represented by P; Relative level of fully assembled; (**B**) CI (Mann-Whitney test: **p*=0.0485); (**C**) CIII (Mann-Whitney test: ***p*=0.0047); (**D**) CIV (Student's *t*-test: ****p*<0.0001); (**E**) CV (Mann-Whitney test: **p*=0.0138).

3.4.3.5 TEM investigation revealed mitochondrial morphological changes

Analysis of fibroblasts from controls (Figure 3.4.6A) and patient 4 (Figure 3.4.6B) by TEM showed that mitochondria of patient's fibroblasts are larger compared to controls.

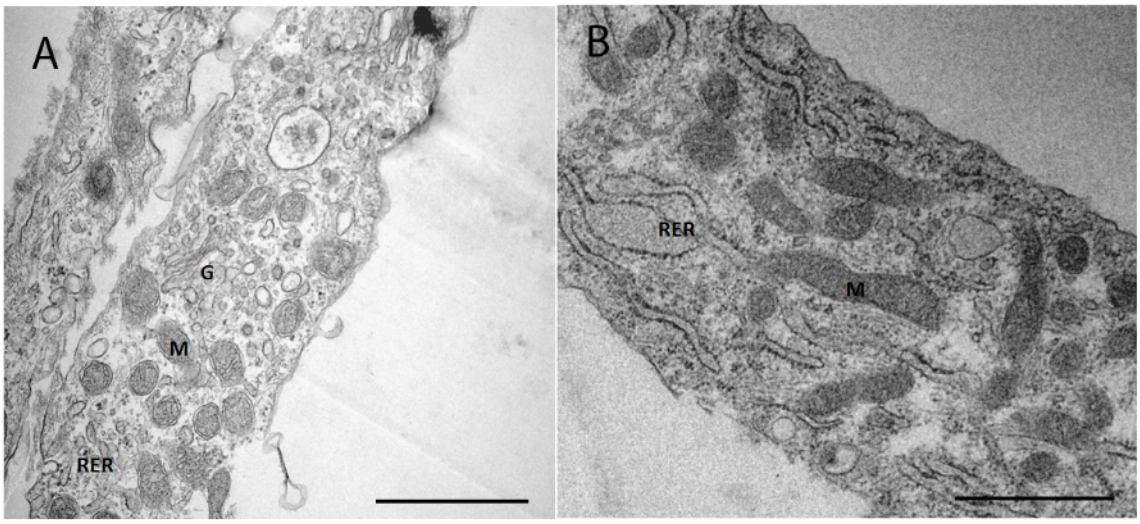

Figure 3.4.6 - **Morphological study of primary fibroblasts by transmission electron microscopy.** Ultrastructural aspects of (**A**) Control and (**B**) Patient. G – Golgi, M – Mitochondrion, RER – Rough Endoplasmic Reticulum. Scale bar: 1 µm.

3.4.4 Discussion

Left ventricular noncompaction is a rare and potentially progressive cardiomyopathy, whose aetiology is not fully understood. The clinical spectrum ranges from no symptoms to heart failure, in both children and adults[394]. Genetic heterogeneity is observed, and the identification of few genes with known mutations in comparison with the higher proportion of familial cases suggests that other genetic factors remain to be identified[395].

In the present familial case, a mutation in exon 6 of *MYBPC3* gene (c.772G>A, p.Glu258Lys) was identified in heterozygosity in all individuals (both parents and offspring, except II-4). Mutations in this gene, which encodes the cardiac myosin binding protein C (cMyBP-C) that regulates the contractility and alters sarcomere energetics, are among the most frequent causes of HCM, usually leading to milder phenotypes and presenting with later onset of HCM[383,388]. This pathogenic mutation is the most studied and prevalent *MYBPC*3 mutation[386], being associated to a severe phenotype, a poor prognosis and high penetrance[396]. In addition to HCM, mutations in the *MYBPC3* gene have been associated with other cardiomyopathies, namely LVNC[390]. However, to our knowledge, this is the first report to describe this mutation in a familial case of LVNC. Additionally, the incomplete penetrance observed in this family

do not correspond to the high penetrance described in HCM. Moreover, intrafamilial differences, or a more severe or early phenotype have been explained by the presence of a second causal mutation in the families[381], namely in a LVNC case[390]. However, the presence of compound or double heterozygosity, or homozygosity, in sarcomere genes was not observed in the family under study.

The incomplete penetrance associated to cardiomyopathy has also been reported for maternal inherited homoplasmic pathogenic mtDNA mutations[186,397,398], in addition to the same effect related to the *MYBPC3* mutation.

Since the mechanical demands never cease and the provision of energy must be continuous, OXPHOS is a critical process for producing sufficient levels of ATP in order to safeguard the cardiac function[399]. For this reason, mitochondrial dysfunction caused by mtDNA or nuclear DNA mutations may result in mitochondrial cardiomyopathies and heart failure[392], occurring in approximately one-third of children with mitochondrial diseases, leading to an increase of mortality in these children[399]. Approximately twenty variants in mt-tRNA and mt-rRNA genes have been associated to cardiomyopathy, according to Mitomap[335].

The homoplasmic maternally inherited mitochondrial variant detected in the present study, m.14706A>G (*MT-TE*), changes a conserved U-G Wobble base pair at the penultimate base pair before the anticodon loop of the mt-tRNA^{Glu}. These Wobble base pair has unique chemical, structural, dynamic and ligand-binding properties, which can only be partially mimicked by Watson-Crick base pairs, and it is an essential unit of RNA secondary structure[400]. For this reason, the substitution of a G-U Wobble base pair can result in a functional and/or structural perturbation of the mt-tRNA^{Glu}.

According to Mitomap and Mamit-tRNA databases, there are approximately fifteen sequence variations in *MT-TE* gene associated to disease, mainly myopathy and encephalomyopathy. One of them, m.14674T>C, detected in patients with myopathy [401] and infantile reversible respiratory chain deficiency[210], was confirmed in homoplasmy, similarly to the variant described in the present study. Furthermore, one of the reported variants (m.14696A>G), causing progressive encephalopathy, is also located in a Wobble base pair[402].

Taking into account the important function of mt-tRNAs in translation of OXPHOS subunits, and the fact that a mutated mt-tRNA is unlikely to be compensated by other

tRNAs, since each mitochondrial genome bears a single copy of only 22 mt-tRNAs[374], it seems reasonable to suggest that the variant m.14706A>G may have consequences in the efficient translation of the mitochondrial proteins. Indeed, a drastic decrease of complexes I, III, IV and V fully assembled was observed in the patient's fibroblasts.

The defect in the assembly of OXPHOS complexes may also lead to a decrease in the activity of complexes. In fact, the activity of complexes is reduced in liver and muscle of patient, but the reduction in fibroblasts was only observed in CIII. However, the percentage of cases with an OXPHOS deficiency detected is lower in fibroblasts, compared to muscle, despite functional studies are more easily performed in fibroblasts[403]. Intracellular ATP levels, oxygen consumption, mitochondrial membrane potential and basal levels of superoxide production did not present significant alterations in patient's fibroblasts. However, the superoxide production showed a significant increase after the inhibition of the CIII activity, suggesting that oxidative stress can increase in case of a more severe reduction of CIII activity, as in the case of the liver and muscle of patient, which has been demonstrated to contribute for the development of cardiomyopathy[404]. Besides the translational defect and the increase in ROS production, the observation of the increased size of mitochondria in patient's fibroblasts was also indicative of mitochondrial involvement in the pathogenesis of cardiomyopathy, as verified in a case of HCM caused by a mtDNA mutation in the 16S rRNA[397].

The ECAR analysis showed an increased capacity for the response to the energy demand by revealing an improved glycolytic reserve in patient's fibroblasts. Therefore, it is possible that this compensatory mechanism is sufficient to maintain the energy requirements in skin fibroblasts of the patient, which might be more difficult in tissues with higher energy needs, as the skeletal muscle, liver and heart, as previously described[399]. Moreover, homoplasmic pathogenic mtDNA mutations have been reported in association with a differential phenotypic expression[183,186], which could be related to tissue-specific nuclear modifier genes[186,403,405].

Thus, taking into account the pathogenic role that the mt-tRNA variant may have in cardiac cells, we propose that this sequence variation is causing mitochondrial dysfunction that may contribute to or potentiate the severity of the phenotype. Indeed, Sacoto *et al.* (2015)[406] had also reported the synergistic effect of a *MYBPC3*

mutation plus a mitochondrial tRNA mutation in a familial case of dilated cardiomyopathy, long QT syndrome and hearing loss, and ultimately sudden death[406]. Then, abnormalities in cMyBP-C causing alterations in the contractile function of cardiomyocytes may act synergistically with mitochondrial variants causing energy deficits and increased ROS production, leading to a more severe heart failure and sudden cardiac death. Nevertheless, one cannot exclude the hypothesis that another nuclear variant could be modulating the severity of phenotype, explaining the incomplete penetrance associated to cardiomyopathy verified for the two sequence variations detected.

Together, these reports demonstrate the importance of taking into account the clinical manifestations in order to unveil the genetic mechanisms involved in heterogeneous and complex diseases, such as cardiomyopathies.

Chapter 4 – Conclusions

Despite remarkable progress in defining the genetic basis of the mitochondrial diseases, the molecular diagnosis remains difficult due to the complexity, heterogeneity and the multisystem involvement presented in these group of disorders.

The identification of the disease-causing genes is of extreme importance for diagnosis, genetic counselling, prenatal diagnosis and for better understanding the pathophysiology of these diseases in order to develop new and effective treatments for patients.

In the last few years, the NGS technology became an indispensable tool for the genetic investigation of mitochondrial diseases, allowing the sequencing of the whole mitochondrial DNA, some panels of multiple nuclear genes, and whole exome/genome sequencing (WES/WGS) in a time- and cost-effective manner compared to the standard methods[407]. These approaches provide valuable information on the genes implicated in these diseases, allowing the identification of novel sequence variations that can clarify the involvement of mitochondrial dysfunction in the pathogenesis and, therefore, bringing the possibility to obtain a molecular diagnosis for several unresolved cases. In spite of the fact that NGS offers a robust platform for comprehensive analysis of mtDNA, the interpretation of rare or novel mitochondrial variants is complex and remains challenging[218,293].

In accordance with the current systems described in the literature, the overall criteria for classifying the pathogenicity of novel mitochondrial variants are represented in the Figure 1.4. Some criterion may be difficult to accomplish, leading to an inappropriate classification of novel variants that would not reach the status of definite diagnosis (in terms of pathogenicity), which is what happens when the functional analysis is not available, since these systems assign a major importance for functional studies. Also, it is widely accepted that heteroplasmy is one marker of pathogenicity of a mtDNA sequence variation, in opposition to the variants detected in homoplasmy, considered as polymorphisms. However, the rule is broken in the m.11778G>A mutation leading to LHON[183] as well as for many other clinical presentations, demonstrating that homoplasmic variants can also be a cause of disease.

In addition, other factors are crucial to achieve a fast and correct genetic diagnosis, such as the tissue selected for functional studies and the molecular genetic

investigation of the family. Muscle is often the favourite tissue for screening the mtDNA because in some cases (e.g. pure myopathy) the molecular defect is not present in other tissues. Despite this, a muscle biopsy is invasive and it is often not available. As an alternative, less invasive tissues could also be used for experimental studies, such as skin fibroblasts. Fibroblasts cell culture is widely used in functional analysis, since it allows to observe cellular events with the presence of a mtDNA mutation and the nuclear background of the patient. Moreover, as primary cells, they do not require transformation, representing more realistically what is occurring *in vivo*[227].

Concerning the segregation of the variant within the family members, it is not possible to get samples from relatives for all cases, increasing the difficulty in assigning the pathogenicity for a novel mtDNA variant.

At last, the existence of more than one independent report with the same variant, in order to perform a correlation between the genotype and phenotype, is one of the most difficult parameters to assign the pathogenicity of rare and novel variants, even with the considerable advances obtained with the NGS. Notwithstanding, it is important to report the novel mtDNA sequence variations, predicted as probably pathogenic, in order to expand the knowledge, enabling independent groups, to report the same mtDNA variant detected, to confirm the pathogenicity.

Thus, it is of extreme importance to check all available parameters and use the new technologies in order to get the more precise classification for mtDNA pathogenicity and improve the efficiency of the genetic diagnosis. Additionally, the role of clinician is essential, since clinical manifestations and family history remain crucial clues to make an earlier diagnosis, and to decrease the large number of unsolved sporadic cases of mitochondrial diseases.

Accordingly, in the present work it was not possible to achieve some of the criteria established due to limitations concerning each case.

The major issue in the attempt to prove the pathogenicity of the mtDNA variants studied was its presence in only one individual/family. Also, when the published criteria are applied to determinate the pathogenicity in the case of patients 1, 2 and 4, the presence of the sequence variation in homoplasmy decreases the significance for disease causality.

The molecular genetic investigation of the family is important to check the segregation of the variant but it also allows to understand the inheritance pattern. However, the availability of samples from maternal relatives may not exist in the cases of adult patients, which was the case of patients 1 and 3.

Other frequent difficulty is the heterogeneity of clinical manifestations that complicates the disease identification, such as in the case of patient 2, in which a new syndrome was identified during this study. Also, the peculiar family history is often a challenge, and at the same time, it is an example of the extraordinary complexity found in the genetic investigation. Indeed, in the case report II of the chapter 3.2, it is presented a case of two girls, non-identical twins, one affected and the other healthy; and also in the case report IV, the transitory symptom of cardiomyopathy in the only one healthy brother, so far, was the clue to achieve the diagnosis in the brothers.

Regarding the functional analysis, several studies were performed with different approaches in accordance with the type of sequence variation, particularly in protein-encoding or tRNA genes. Each case revealed different challenges in the analysis and correlation of the overall results. In a general view, the approaches evaluated the mitochondrial function, namely the energetic state of cells, and some parameters related to the cellular consequences of the variants, in an attempt to circumvent the limitations in manipulating mtDNA. The evidences observed in each case suggested that the mtDNA variants are possibly involved in the mitochondrial dysfunction observed in all cases. However, the patient 4 seems to be the most affected by the limitation of tissue specificity for functional analysis, in which the fibroblasts did not demonstrate significant functional changes, in most of the assays.

In addition to the bioenergetics dysfunction, several cellular mechanisms seem to be altered in patients' cells, opening new insights for the investigation of mitochondrial diseases. For instance, ER stress may be a possible explanation for the enlargement of ER lumen observed in patient 1 and macroautophagy alterations caused by loss of lysosomal function is the most probable cause for the new syndrome described for patient 2.

Furthermore, OXPHOS diseases may be caused by a double genetic origin, besides the known depletion or deletion-associated syndromes. A good example of this interaction is the case of patient 2. Also, other diseases, namely cardiomyopathies,

could be related to different inheritance mode, and sometimes, the combination of several variants (nuclear and mitochondrial) is the explanation for the more severe phenotype and incomplete penetrance of the disease between individuals within the same family, as in the case report IV.

Moreover, the presence of two alterations in mtDNA (the "common" deletion and a novel heteroplasmic mt-tRNA sequence variation, m.7486G>A) that segregate together within the affected tissue in patient 3, gives the idea that other similar cases must exist, most probably in whom the evaluation of point mutations was not performed after the discovery of the "common" deletion. It is expected that the NGS for sequencing the whole mtDNA will help to identify other cases, and clarify the significance of this finding.

Despite the advances in the genetic diagnosis, these disorders are amazingly complex and the identification of a link between genotype and phenotype is frequently a challenge. The increasing number of genes leading to MRC deficiency suggests that mitochondria are involved in a wide range of processes associated with disease, namely other types of disorders in which the MRC deficiency may be secondary to various cellular processes[408,409].

Although considerable progress in understanding mitochondrial function has been made during the last years, much remains to be understood and many questions remain unanswered.

The list of mtDNA variants will expand continuously, but factors such like heteroplasmy, complex inheritance, variable "penetrance" and interactions with modifier genes make difficult to verify its pathogenicity and to understand how they lead to disease. Also, the genetic counselling is a challenging area for woman with mtDNA mutations due to the bottleneck effect and tissue segregation, as well as the understanding of the mechanism involved in tissue specificity, and predicting disease progression.

Expanding our knowledge about mitochondrial biology, namely the processes such as mtDNA replication, transcription, translation, repair, degradation, mtRNA metabolism, assembly of complexes, mitochondrial quality control, mito-nuclear signalling, its regulation and its interplay with the rest of the cell, will provide crucial

clues to define human diseases caused by mitochondrial dysfunction and develop effective therapeutic strategies.

Further research is urgent to disclose the answers to these questions.

In conclusion, the classification of the pathogenicity for mtDNA variants is not "black or white", instead they present several "scales of grey".

If applying the scoring criteria for determining the pathogenicity of the mtDNA variants under study, several limitations difficult the assignment of a result, and important aspects are missing. For instance, in the case of patient 1 was not possible to measure the biochemical activity of MRC in the affected tissue (retinal ganglion cells in eyes), being not possible to ascribe 8 points; for patients 1 and 3, samples from maternal relatives were not available to check the segregation; 5 points (patients 1 and 2) and 2 points (patient 4) were not referred because of the fact that the variants have been detected in homoplasmy; and in all independent reports, 5 or 2 points (tRNA variant or protein-encoding gene, respectively) will not be included until someone reports another unrelated case. Then, the score obtained for each sequence variation under study (Table 4.1 – see score) is not enough to reach the definitive status of "pathogenic" due to the limitations described above.

However, if one checks the overall of important criteria without assigning a score, it is evident that most of the criteria were fulfilled (Table 4.1). Furthermore, in the case of the m.14706A>G, the scoring classification pointed the sequence variation as a "polymorphism", even when the variant accomplishes several other criteria that are not usually scored. Thus, the pathogenicity of novel or rare mtDNA variants should be determined carefully, evaluating all available aspects in order to do a fair classification, not excluding variants with milder effect that may be reported later by other individual groups.

Overall, the present work allowed to:

(i) confirm the high pathogenic potential of the four unclassified mtDNA variants;

(ii) report the variants showing functional evidences for its pathogenicity;

(iii) include these sequence variations in the genetic investigation of other patients presenting similar phenotypes;

(iv) contribute for significant developments in the field of mitochondrial diseases pathogenicity, namely the idea that the interorganellar crosstalk is an essential process for cell homeostasis;

(v) clarify the molecular genetic diagnosis of the patients under study.

Table 4.1. Summary of the pathogenicity evaluation of the four unclassified mtDNA variants studied.

	m.8418T>C	***m.14771C>A***	***m.7486G>A***	***m.14706A>G***
Evolutionary conservation	+	+	+	+
Pathogenicity prediction (probably deleterious)	+	+	+	+
Absence from a control population	+	+	+	+
Heteroplasmy	-	-	+	-
Multiple reports	-	-	-	-
Segregation with disease	Not tested	-	Not tested	-
Histochemical evidence	Not tested	Not tested	+	Not tested
Biochemical defect	+	+	+	+
Positive functional study*	+	+	+	+
Score of pathogenicity	24 out of 40 "probably pathogenic"	24 out of 40 "probably pathogenic"	11 out of 20 "probably pathogenic"	3 out of 20 "polymorphism"

*At least one of the functional assays showing significant alterations, suggesting a pathogenic role for the mtDNA variant; (+) the criterion was fulfilled; (-) the criterion was not fulfilled.

Chapter 5 – Future Perspectives

Further investigation will be necessary to understand some unclear aspects and to answer the still open questions, such as:

- It will be crucial to evaluate the crosstalk between mitochondria-ER and mitochondria-lysosome, in cells from the patients mentioned in case reports I and II, respectively, in order to understand in which way the inter-organelle crosstalk is involved in the pathophysiology of these complexes diseases.
- The development of new technology in order to manipulate mitochondria will be essential to test the pathogenicity of the sequence variation detected in P3.
- Performing the WEG for samples of P4 and his family will certainly help to clarify the genetic diagnosis and the incomplete penetrance associated to cardiomyopathy and to the nuclear mutation identified.
- The report of these sequence variations by independent laboratories will be decisive for corroborating its pathogenicity.

Chapter 6 – References

1. Schapira AH V. Mitochondrial disease. *Lancet (London, England)*. 2006;368(9529):70-82. doi:10.1016/S0140-6736(06)68970-8.
2. Area-Gomez E, Schon EA. Mitochondrial genetics and disease. *J Child Neurol*. 2014;29(9):1208-1215. doi:10.1177/0883073814539561.
3. Rotig A. Genetics of mitochondrial respiratory chain deficiencies. *Rev Neurol (Paris)*. 2014;170(5):309-322. doi:10.1016/j.neurol.2013.11.006.
4. Kulawiak B, Hopker J, Gebert M, Guiard B, Wiedemann N, Gebert N. The mitochondrial protein import machinery has multiple connections to the respiratory chain. *Biochim Biophys Acta*. 2013;1827(5):612-626. doi:10.1016/j.bbabio.2012.12.004.
5. Hatefi Y. The mitochondrial electron transport and oxidative phosphorylation system. *Annu Rev Biochem*. 1985;54:1015-1069. doi:10.1146/annurev.bi.54.070185.005055.
6. Sun N, Youle RJ, Finkel T. The Mitochondrial Basis of Aging. *Mol Cell*. 2016;61(5):654-666. doi:10.1016/j.molcel.2016.01.028.
7. Quiros PM, Mottis A, Auwerx J. Mitonuclear communication in homeostasis and stress. *Nat Rev Mol Cell Biol*. 2016;17(4):213-226. doi:10.1038/nrm.2016.23.
8. Shokolenko IN, Alexeyev MF. Mitochondrial DNA: A disposable genome? *Biochim Biophys Acta*. 2015;1852(9):1805-1809. doi:10.1016/j.bbadis.2015.05.016.
9. Lloyd RE, McGeehan JE. Structural analysis of mitochondrial mutations reveals a role for bigenomic protein interactions in human disease. *PLoS One*. 2013;8(7):e69003. doi:10.1371/journal.pone.0069003.
10. Hamanaka RB, Chandel NS. Mitochondrial reactive oxygen species regulate cellular signaling and dictate biological outcomes. *Trends Biochem Sci*. 2010;35(9):505-513. doi:10.1016/j.tibs.2010.04.002.
11. Jouaville LS, Pinton P, Bastianutto C, Rutter GA, Rizzuto R. Regulation of mitochondrial ATP synthesis by calcium: evidence for a long-term metabolic priming. *Proc Natl Acad Sci U S A*. 1999;96(24):13807-13812.
12. Osellame LD, Blacker TS, Duchen MR. Cellular and molecular mechanisms of mitochondrial function. *Best Pract Res Clin Endocrinol Metab*. 2012;26(6):711-723. doi:10.1016/j.beem.2012.05.003.

13. Bhatti JS, Bhatti GK, Reddy PH. Mitochondrial dysfunction and oxidative stress in metabolic disorders - A step towards mitochondria based therapeutic strategies. *Biochim Biophys Acta*. November 2016. doi:10.1016/j.bbadis.2016.11.010.

14. Newmeyer DD, Ferguson-Miller S. Mitochondria: releasing power for life and unleashing the machineries of death. *Cell*. 2003;112(4):481-490. doi:10.1016/S0092-8674(03)00116-8.

15. Rodriguez J, Lazebnik Y. Caspase-9 and APAF-1 form an active holoenzyme. Genes Dev. 1999;13(24):3179-3184. PMCID:PMC317200.

16. Xiong S, Mu T, Wang G, Jiang X. Mitochondria-mediated apoptosis in mammals. *Protein Cell*. 2014;5(10):737-749. doi:10.1007/s13238-014-0089-1.

17. Nass mm, Nass s. Intramitochondrial fibers with dna characteristics. I. Fixation and electron staining reactions. *J Cell Biol*. 1963;19:593-611. doi:10.1083/jcb.19.3.613.

18. Schatz G. The isolation of possible mitochondrial precursor structures from aerobically grown baker's yeast. *Biochem Biophys Res Commun*. 1963;12:448-451. doi:10.1016/0006-291X(63)90313-9.

19. Anderson S, Bankier AT, Barrell BG, et al. Sequence and organization of the human mitochondrial genome. *Nature*. 1981;290(5806):457-465. doi:10.1038/29045790.

20. Attardi G, Chomyn A, Montoya J, Ojala D. Identification and mapping of human mitochondrial genes. *Cytogenet Cell Genet*. 1982;32(1-4):85-98. doi:10.1159/000131689.

21. Chen XJ, Butow RA. The organization and inheritance of the mitochondrial genome. *Nat Rev Genet*. 2005;6(11):815-825. doi:10.1038/nrg1708.

22. Kang D, Kim SH, Hamasaki N. Mitochondrial transcription factor A (TFAM): roles in maintenance of mtDNA and cellular functions. *Mitochondrion*. 2007;7(1-2):39-44. doi:10.1016/j.mito.2006.11.017.

23. Holt IJ, Harding AE, Morgan-Hughes JA. Deletions of muscle mitochondrial DNA in patients with mitochondrial myopathies. *Nature*. 1988;331(6158):717-719. doi:10.1038/331717a0.

24. Macmillan C, Lach B, Shoubridge EA. Variable distribution of mutant mitochondrial DNAs (tRNA(Leu[3243])) in tissues of symptomatic relatives with

MELAS: the role of mitotic segregation. *Neurology*. 1993;43(8):1586-1590. doi:10.1212/WNL.43.8.1586.

25. Schon EA, Bonilla E, DiMauro S. Mitochondrial DNA mutations and pathogenesis. *J Bioenerg Biomembr*. 1997;29(2):131-149. doi:10.1023/A:1022685929755.
26. Gorman GS, Schaefer AM, Ng Y, et al. Prevalence of nuclear and mitochondrial DNA mutations related to adult mitochondrial disease. *Ann Neurol*. 2015;77(5):753-759. doi:10.1002/ana.24362.
27. Hutchison CA 3rd, Newbold JE, Potter SS, Edgell MH. Maternal inheritance of mammalian mitochondrial DNA. *Nature*. 1974;251(5475):536-538. doi:10.1038/251536a0.
28. Lightowlers RN, Taylor RW, Turnbull DM. Mutations causing mitochondrial disease: What is new and what challenges remain? *Science*. 2015;349(6255):1494-1499. doi:10.1126/science.aac7516.
29. Ng YS, Turnbull DM. Mitochondrial disease: genetics and management. *J Neurol*. 2016;263(1):179-191. doi:10.1007/s00415-015-7884-3.
30. Tuppen HAL, Blakely EL, Turnbull DM, Taylor RW. Mitochondrial DNA mutations and human disease. *Biochim Biophys Acta*. 2010;1797(2):113-128. doi:10.1016/j.bbabio.2009.09.005.
31. Fox TD. Mitochondrial protein synthesis, import, and assembly. *Genetics*. 2012;192(4):1203-1234. doi:10.1534/genetics.112.141267.
32. McKinney EA, Oliveira MT. Replicating animal mitochondrial DNA. *Genet Mol Biol*. 2013;36(3):308-315. doi:10.1590/S1415-47572013000300002.
33. Holt IJ, Jacobs HT. Unique features of DNA replication in mitochondria: a functional and evolutionary perspective. *Bioessays*. 2014;36(11):1024-1031. doi:10.1002/bies.201400052.
34. Pohjoismaki JLO, Goffart S. Of circles, forks and humanity: Topological organisation and replication of mammalian mitochondrial DNA. *Bioessays*. 2011;33(4):290-299. doi:10.1002/bies.201000137.
35. Bogenhagen DF, Clayton DA. The mitochondrial DNA replication bubble has not burst. *Trends Biochem Sci*. 2003;28(7):357-360. doi:10.1016/S0968-0004(03)00132-4.
36. Holt IJ, Lorimer HE, Jacobs HT. Coupled leading- and lagging-strand synthesis of

mammalian mitochondrial DNA. *Cell*. 2000;100(5):515-524. doi:10.1016/S0092-8674(00)80688-1.

37. Yasukawa T, Reyes A, Cluett TJ, et al. Replication of vertebrate mitochondrial DNA entails transient ribonucleotide incorporation throughout the lagging strand. *EMBO J*. 2006;25(22):5358-5371. doi:10.1038/sj.emboj.7601392.
38. Reyes A, Kazak L, Wood SR, Yasukawa T, Jacobs HT, Holt IJ. Mitochondrial DNA replication proceeds via a "bootlace" mechanism involving the incorporation of processed transcripts. *Nucleic Acids Res*. 2013;41(11):5837-5850. doi:10.1093/nar/gkt196.
39. Van Haute L, Pearce SF, Powell CA, D'Souza AR, Nicholls TJ, Minczuk M. Mitochondrial transcript maturation and its disorders. *J Inherit Metab Dis*. 2015;38(4):655-680. doi:10.1007/s10545-015-9859-z.
40. Rorbach J, Minczuk M. The post-transcriptional life of mammalian mitochondrial RNA. *Biochem J*. 2012;444(3):357-373. doi:10.1042/BJ20112208.
41. Ojala D, Montoya J, Attardi G. tRNA punctuation model of RNA processing in human mitochondria. *Nature*. 1981;290(5806):470-474. doi:10.1038/290470a0.
42. Park CB, Larsson N-G. Mitochondrial DNA mutations in disease and aging. *J Cell Biol*. 2011;193(5):809-818. doi:10.1083/jcb.201010024.
43. Litonin D, Sologub M, Shi Y, et al. Human mitochondrial transcription revisited: only TFAM and TFB2M are required for transcription of the mitochondrial genes in vitro. *J Biol Chem*. 2010;285(24):18129-18133. doi:10.1074/jbc.C110.128918.
44. Sologub M, Litonin D, Anikin M, Mustaev A, Temiakov D. TFB2 is a transient component of the catalytic site of the human mitochondrial RNA polymerase. *Cell*. 2009;139(5):934-944. doi:10.1016/j.cell.2009.10.031.
45. Martin M, Cho J, Cesare AJ, Griffith JD, Attardi G. Termination factor-mediated DNA loop between termination and initiation sites drives mitochondrial rRNA synthesis. *Cell*. 2005;123(7):1227-1240. doi:10.1016/j.cell.2005.09.040.
46. Blomain ES, McMahon SB. Dynamic regulation of mitochondrial transcription as a mechanism of cellular adaptation. *Biochim Biophys Acta*. 2012;1819(9-10):1075-1079. doi:10.1016/j.bbagrm.2012.06.004.
47. Yakubovskaya E, Mejia E, Byrnes J, Hambardjieva E, Garcia-Diaz M. Helix

unwinding and base flipping enable human MTERF1 to terminate mitochondrial transcription. *Cell*. 2010;141(6):982-993. doi:10.1016/j.cell.2010.05.018.

48. Jourdain AA, Koppen M, Wydro M, et al. GRSF1 regulates RNA processing in mitochondrial RNA granules. *Cell Metab*. 2013;17(3):399-410. doi:10.1016/j.cmet.2013.02.005.
49. Antonicka H, Sasarman F, Nishimura T, Paupe V, Shoubridge EA. The mitochondrial RNA-binding protein GRSF1 localizes to RNA granules and is required for posttranscriptional mitochondrial gene expression. *Cell Metab*. 2013;17(3):386-398. doi:10.1016/j.cmet.2013.02.006.
50. Lee K-W, Okot-Kotber C, LaComb JF, Bogenhagen DF. Mitochondrial ribosomal RNA (rRNA) methyltransferase family members are positioned to modify nascent rRNA in foci near the mitochondrial DNA nucleoid. *J Biol Chem*. 2013;288(43):31386-31399. doi:10.1074/jbc.M113.515692.
51. Hallberg BM, Larsson N-G. Making proteins in the powerhouse. *Cell Metab*. 2014;20(2):226-240. doi:10.1016/j.cmet.2014.07.001.
52. Ruzzenente B, Metodiev MD, Wredenberg A, et al. LRPPRC is necessary for polyadenylation and coordination of translation of mitochondrial mRNAs. *EMBO J*. 2012;31(2):443-456. doi:10.1038/emboj.2011.392.
53. Agrawal RK, Sharma MR. Structural aspects of mitochondrial translational apparatus. *Curr Opin Struct Biol*. 2012;22(6):797-803. doi:10.1016/j.sbi.2012.08.003.
54. Richman TR, Davies SMK, Shearwood A-MJ, et al. A bifunctional protein regulates mitochondrial protein synthesis. *Nucleic Acids Res*. 2014;42(9):5483-5494. doi:10.1093/nar/gku179.
55. Boczonadi V, Horvath R. Mitochondria: impaired mitochondrial translation in human disease. *Int J Biochem Cell Biol*. 2014;48:77-84. doi:10.1016/j.biocel.2013.12.011.
56. Mai N, Chrzanowska-Lightowlers ZMA, Lightowlers RN. The process of mammalian mitochondrial protein synthesis. *Cell Tissue Res*. 2017;367(1):5-20. doi:10.1007/s00441-016-2456-0.
57. Smits P, Smeitink J, van den Heuvel L. Mitochondrial translation and beyond: processes implicated in combined oxidative phosphorylation deficiencies. *J*

Biomed Biotechnol. 2010;2010:737385. doi:10.1155/2010/737385.

58. Christian BE, Spremulli LL. Mechanism of protein biosynthesis in mammalian mitochondria. *Biochim Biophys Acta*. 2012;1819(9-10):1035-1054. doi:10.1016/j.bbagrm.2011.11.009.
59. Gruschke S, Ott M. The polypeptide tunnel exit of the mitochondrial ribosome is tailored to meet the specific requirements of the organelle. *Bioessays*. 2010;32(12):1050-1057. doi:10.1002/bies.201000081.
60. Richter R, Pajak A, Dennerlein S, Rozanska A, Lightowlers RN, Chrzanowska-Lightowlers ZMA. Translation termination in human mitochondrial ribosomes. *Biochem Soc Trans*. 2010;38(6):1523-1526. doi:10.1042/BST0381523.
61. Copeland WC, Longley MJ. Mitochondrial genome maintenance in health and disease. *DNA Repair (Amst)*. 2014;19:190-198. doi:10.1016/j.dnarep.2014.03.010.
62. Brown WM, George MJ, Wilson AC. Rapid evolution of animal mitochondrial DNA. *Proc Natl Acad Sci U S A*. 1979;76(4):1967-1971.
63. Alexeyev M, Shokolenko I, Wilson G, LeDoux S. The maintenance of mitochondrial DNA integrity--critical analysis and update. *Cold Spring Harb Perspect Biol*. 2013;5(5):a012641. doi:10.1101/cshperspect.a012641.
64. Muftuoglu M, Mori MP, de Souza-Pinto NC. Formation and repair of oxidative damage in the mitochondrial DNA. *Mitochondrion*. 2014;17:164-181. doi:10.1016/j.mito.2014.03.007.
65. Cline SD. Mitochondrial DNA damage and its consequences for mitochondrial gene expression. *Biochim Biophys Acta*. 2012;1819(9-10):979-991. doi:10.1016/j.bbagrm.2012.06.002.
66. Vogel RO, Smeitink JAM, Nijtmans LGJ. Human mitochondrial complex I assembly: a dynamic and versatile process. *Biochim Biophys Acta*. 2007;1767(10):1215-1227. doi:10.1016/j.bbabio.2007.07.008.
67. Yankovskaya V, Horsefield R, Tornroth S, et al. Architecture of succinate dehydrogenase and reactive oxygen species generation. *Science*. 2003;299(5607):700-704. doi:10.1126/science.1079605.
68. Sun F, Huo X, Zhai Y, et al. Crystal structure of mitochondrial respiratory membrane protein complex II. *Cell*. 2005;121(7):1043-1057.

doi:10.1016/j.cell.2005.05.025.

69. Ghezzi D, Zeviani M. Assembly factors of human mitochondrial respiratory chain complexes: physiology and pathophysiology. *Adv Exp Med Biol*. 2012;748:65-106. doi:10.1007/978-1-4614-3573-0_4.

70. Xia D, Esser L, Tang W-K, et al. Structural analysis of cytochrome bc1 complexes: implications to the mechanism of function. *Biochim Biophys Acta*. 2013;1827(11-12):1278-1294. doi:10.1016/j.bbabio.2012.11.008.

71. Kadenbach B, Huttemann M. The subunit composition and function of mammalian cytochrome c oxidase. *Mitochondrion*. 2015;24:64-76. doi:10.1016/j.mito.2015.07.002.

72. Tsukihara T, Aoyama H, Yamashita E, et al. The whole structure of the 13-subunit oxidized cytochrome c oxidase at 2.8 A. *Science*. 1996;272(5265):1136-1144. doi:10.1126/science.242.5265.1136.

73. Fernandez-Vizarra E, Tiranti V, Zeviani M. Assembly of the oxidative phosphorylation system in humans: what we have learned by studying its defects. *Biochim Biophys Acta*. 2009;1793(1):200-211. doi:10.1016/j.bbamcr.2008.05.028.

74. Alcazar-Fabra M, Navas P, Brea-Calvo G. Coenzyme Q biosynthesis and its role in the respiratory chain structure. *Biochim Biophys Acta*. 2016;1857(8):1073-1078. doi:10.1016/j.bbabio.2016.03.010.

75. Ow Y-LP, Green DR, Hao Z, Mak TW. Cytochrome c: functions beyond respiration. *Nat Rev Mol Cell Biol*. 2008;9(7):532-542. doi:10.1038/nrm2434.

76. Vartak R, Deng J, Fang H, Bai Y. Redefining the roles of mitochondrial DNA-encoded subunits in respiratory Complex I assembly. *Biochim Biophys Acta*. 2015;1852(7):1531-1539. doi:10.1016/j.bbadis.2015.04.008.

77. Sanchez-Caballero L, Guerrero-Castillo S, Nijtmans L. Unraveling the complexity of mitochondrial complex I assembly: A dynamic process. *Biochim Biophys Acta*. 2016;1857(7):980-990. doi:10.1016/j.bbabio.2016.03.031.

78. Na U, Yu W, Cox J, et al. The LYR factors SDHAF1 and SDHAF3 mediate maturation of the iron-sulfur subunit of succinate dehydrogenase. *Cell Metab*. 2014;20(2):253-266. doi:10.1016/j.cmet.2014.05.014.

79. Fernandez-Vizarra E, Zeviani M. Nuclear gene mutations as the cause of

mitochondrial complex III deficiency. *Front Genet*. 2015;6:134. doi:10.3389/fgene.2015.00134.

80. Soto IC, Fontanesi F, Liu J, Barrientos A. Biogenesis and assembly of eukaryotic cytochrome c oxidase catalytic core. *Biochim Biophys Acta*. 2012;1817(6):883-897. doi:10.1016/j.bbabio.2011.09.005.
81. Fujikawa M, Sugawara K, Tanabe T, Yoshida M. Assembly of human mitochondrial ATP synthase through two separate intermediates, F1-c-ring and b-e-g complex. *FEBS Lett*. 2015;589(19 Pt B):2707-2712. doi:10.1016/j.febslet.2015.08.006.
82. Wittig I, Meyer B, Heide H, et al. Assembly and oligomerization of human ATP synthase lacking mitochondrial subunits a and A6L. *Biochim Biophys Acta*. 2010;1797(6-7):1004-1011. doi:10.1016/j.bbabio.2010.02.021.
83. Kucharczyk R, Zick M, Bietenhader M, et al. Mitochondrial ATP synthase disorders: molecular mechanisms and the quest for curative therapeutic approaches. *Biochim Biophys Acta*. 2009;1793(1):186-199. doi:10.1016/j.bbamcr.2008.06.012.
84. Wittig I, Schagger H. Supramolecular organization of ATP synthase and respiratory chain in mitochondrial membranes. *Biochim Biophys Acta*. 2009;1787(6):672-680. doi:10.1016/j.bbabio.2008.12.016.
85. Kuhlbrandt W. Structure and function of mitochondrial membrane protein complexes. *BMC Biol*. 2015;13:89. doi:10.1186/s12915-015-0201-x.
86. Ruhle T, Leister D. Assembly of F1F0-ATP synthases. *Biochim Biophys Acta*. 2015;1847(9):849-860. doi:10.1016/j.bbabio.2015.02.005.
87. Keilin D, Hartree EF. Activity of the cytochrome system in heart muscle preparations. *Biochem J*. 1947;41(4):500-502. doi:10.1042/bl0410500.
88. CHANCE B, WILLIAMS GR. A method for the localization of sites for oxidative phosphorylation. *Nature*. 1955;176(4475):250-254. doi:10.1038/176250a0.
89. HATEFI Y, HAAVIK AG, GRIFFITHS DE. Studies on the electron transfer system. XL. Preparation and properties of mitochondrial DPNH-coenzyme Q reductase. *J Biol Chem*. 1962;237:1676-1680. PMID:13905327.
90. Green DE, Tzagoloff A. The mitochondrial electron transfer chain. *Arch Biochem Biophys*. 1966;116(1):293-304. doi:10.1016/0003-9861(66)90036-1.

91. Berry EA, Trumpower BL. Isolation of ubiquinol oxidase from Paracoccus denitrificans and resolution into cytochrome bc1 and cytochrome c-aa3 complexes. *J Biol Chem*. 1985;260(4):2458-2467. PMID:2982819.

92. Sone N, Sekimachi M, Kutoh E. Identification and properties of a quinol oxidase super-complex composed of a bc1 complex and cytochrome oxidase in the thermophilic bacterium PS3. *J Biol Chem*. 1987;262(32):15386-15391. PMID:2824457.

93. Iwasaki T, Matsuura K, Oshima T. Resolution of the aerobic respiratory system of the thermoacidophilic archaeon, Sulfolobus sp. strain 7. I. The archaeal terminal oxidase supercomplex is a functional fusion of respiratory complexes III and IV with no c-type cytochromes. *J Biol Chem*. 1995;270(52):30881-30892. doi:10.1074/jbc.270.52.30881.

94. Boumans H, Grivell LA, Berden JA. The respiratory chain in yeast behaves as a single functional unit. *J Biol Chem*. 1998;273(9):4872-4877. doi:10.1074/jbc.273.9.4872.

95. Bruel C, Brasseur R, Trumpower BL. Subunit 8 of the Saccharomyces cerevisiae cytochrome bc1 complex interacts with succinate-ubiquinone reductase complex. *J Bioenerg Biomembr*. 1996;28(1):59-68. doi:10.1007/BF02109904.

96. Schagger H, Pfeiffer K. The ratio of oxidative phosphorylation complexes I-V in bovine heart mitochondria and the composition of respiratory chain supercomplexes. *J Biol Chem*. 2001;276(41):37861-37867. doi:10.1074/jbc.M106474200.

97. Acin-Perez R, Fernandez-Silva P, Peleato ML, Perez-Martos A, Enriquez JA. Respiratory active mitochondrial supercomplexes. *Mol Cell*. 2008;32(4):529-539. doi:10.1016/j.molcel.2008.10.021.

98. Lapuente-Brun E, Moreno-Loshuertos R, Acin-Perez R, et al. Supercomplex assembly determines electron flux in the mitochondrial electron transport chain. *Science*. 2013;340(6140):1567-1570. doi:10.1126/science.1230381.

99. Moreno-Loshuertos R, Enriquez JA. Respiratory supercomplexes and the functional segmentation of the CoQ pool. *Free Radic Biol Med*. 2016;100:5-13. doi:10.1016/j.freeradbiomed.2016.04.018.

100. Moreno-Lastres D, Fontanesi F, Garcia-Consuegra I, et al. Mitochondrial complex

I plays an essential role in human respirasome assembly. *Cell Metab*. 2012;15(3):324-335. doi:10.1016/j.cmet.2012.01.015.

101. Lenaz G, Genova ML. Structural and functional organization of the mitochondrial respiratory chain: a dynamic super-assembly. *Int J Biochem Cell Biol*. 2009;41(10):1750-1772.
102. Vartak R, Porras CA-M, Bai Y. Respiratory supercomplexes: structure, function and assembly. *Protein Cell*. 2013;4(8):582-590. doi:10.1007/s13238-013-3032-y.
103. McKenzie M, Lazarou M, Thorburn DR, Ryan MT. Mitochondrial respiratory chain supercomplexes are destabilized in Barth Syndrome patients. *J Mol Biol*. 2006;361(3):462-469. doi:10.1016/j.jmb.2006.06.057.
104. Chen Y-C, Taylor EB, Dephoure N, et al. Identification of a protein mediating respiratory supercomplex stability. *Cell Metab*. 2012;15(3):348-360. doi:10.1016/j.cmet.2012.02.006.
105. Dienhart MK, Stuart RA. The yeast Aac2 protein exists in physical association with the cytochrome bc1-COX supercomplex and the TIM23 machinery. *Mol Biol Cell*. 2008;19(9):3934-3943. doi:10.1091/mbc.E08-04-0402.
106. Ryan MT, Hoogenraad NJ. Mitochondrial-nuclear communications. *Annu Rev Biochem*. 2007;76:701-722. doi:10.1146/annurev.biochem.76.052305.091720.
107. Grazina MM. Mitochondrial respiratory chain: biochemical analysis and criterion for deficiency in diagnosis. *Methods Mol Biol*. 2012;837:73-91. doi:10.1007/978-1-61779-504-6_6.
108. Caito SW, Aschner M. Mitochondrial Redox Dysfunction and Environmental Exposures. *Antioxid Redox Signal*. 2015;23(6):578-595. doi:10.1089/ars.2015.6289.
109. Brand MD, Affourtit C, Esteves TC, et al. Mitochondrial superoxide: production, biological effects, and activation of uncoupling proteins. *Free Radic Biol Med*. 2004;37(6):755-767. doi:10.1016/j.freeradbiomed.2004.05.034.
110. Griparic L, van der Bliek AM. The many shapes of mitochondrial membranes. *Traffic*. 2001;2(4):235-244. doi:10.1034/j.1600-0854.2001.1r008.x.
111. Parone PA, Da Cruz S, Tondera D, et al. Preventing mitochondrial fission impairs mitochondrial function and leads to loss of mitochondrial DNA. *PLoS One*. 2008;3(9):e3257. doi:10.1371/journal.pone.0003257.

112. McInnes J. Mitochondrial-associated metabolic disorders: foundations, pathologies and recent progress. *Nutr Metab (Lond)*. 2013;10(1):63. doi:10.1186/1743-7075-10-63.

113. Nunnari J, Suomalainen A. Mitochondria: in sickness and in health. *Cell*. 2012;148(6):1145-1159. doi:10.1016/j.cell.2012.02.035.

114. Yoon Y, Pitts KR, McNiven MA. Mammalian dynamin-like protein DLP1 tubulates membranes. *Mol Biol Cell*. 2001;12(9):2894-2905. doi:10.1091/mbc.12.9.2894.

115. Ingerman E, Perkins EM, Marino M, et al. Dnm1 forms spirals that are structurally tailored to fit mitochondria. *J Cell Biol*. 2005;170(7):1021-1027. doi:10.1083/jcb.200506078.

116. Waterham HR, Koster J, van Roermund CWT, Mooyer PAW, Wanders RJA, Leonard J V. A lethal defect of mitochondrial and peroxisomal fission. *N Engl J Med*. 2007;356(17):1736-1741. doi:10.1056/NEJMoa064436.

117. Ashrafian H, Docherty L, Leo V, et al. A mutation in the mitochondrial fission gene Dnm1l leads to cardiomyopathy. *PLoS Genet*. 2010;6(6):e1001000. doi:10.1371/journal.pgen.1001000.

118. Friedman JR, Lackner LL, West M, DiBenedetto JR, Nunnari J, Voeltz GK. ER tubules mark sites of mitochondrial division. *Science*. 2011;334(6054):358-362. doi:10.1126/science.1207385.

119. Zuchner S, Mersiyanova I V, Muglia M, et al. Mutations in the mitochondrial GTPase mitofusin 2 cause Charcot-Marie-Tooth neuropathy type 2A. *Nat Genet*. 2004;36(5):449-451. doi:10.1038/ng1341.

120. Delettre C, Lenaers G, Griffoin JM, et al. Nuclear gene OPA1, encoding a mitochondrial dynamin-related protein, is mutated in dominant optic atrophy. *Nat Genet*. 2000;26(2):207-210. doi:10.1038/79936.

121. Amati-Bonneau P, Milea D, Bonneau D, et al. OPA1-associated disorders: phenotypes and pathophysiology. *Int J Biochem Cell Biol*. 2009;41(10):1855-1865. doi:10.1016/j.biocel.2009.04.012.

122. Wang X, Schwarz TL. The mechanism of Ca2+ -dependent regulation of kinesin-mediated mitochondrial motility. *Cell*. 2009;136(1):163-174. doi:10.1016/j.cell.2008.11.046.

123. Cagin U, Enriquez JA. The complex crosstalk between mitochondria and the

nucleus: What goes in between? *Int J Biochem Cell Biol*. 2015;63:10-15. doi:10.1016/j.biocel.2015.01.026.

124. Mottis A, Jovaisaite V, Auwerx J. The mitochondrial unfolded protein response in mammalian physiology. *Mamm Genome*. 2014;25(9-10):424-433. doi:10.1007/s00335-014-9525-z.

125. Bezawork-Geleta A, Brodie EJ, Dougan DA, Truscott KN. LON is the master protease that protects against protein aggregation in human mitochondria through direct degradation of misfolded proteins. *Sci Rep*. 2015;5:17397. doi:10.1038/srep17397.

126. Quiros PM, Langer T, Lopez-Otin C. New roles for mitochondrial proteases in health, ageing and disease. *Nat Rev Mol Cell Biol*. 2015;16(6):345-359. doi:10.1038/nrm3984.

127. Nolden M, Ehses S, Koppen M, Bernacchia A, Rugarli EI, Langer T. The m-AAA protease defective in hereditary spastic paraplegia controls ribosome assembly in mitochondria. *Cell*. 2005;123(2):277-289. doi:10.1016/j.cell.2005.08.003.

128. Casari G, De Fusco M, Ciarmatori S, et al. Spastic paraplegia and OXPHOS impairment caused by mutations in paraplegin, a nuclear-encoded mitochondrial metalloprotease. *Cell*. 1998;93(6):973-983. doi:10.1016/S0092-8674(00)81203-9.

129. Zhao Q, Wang J, Levichkin I V, Stasinopoulos S, Ryan MT, Hoogenraad NJ. A mitochondrial specific stress response in mammalian cells. *EMBO J*. 2002;21(17):4411-4419. doi:10.1093/emboj/cdf445.

130. Martinus RD, Garth GP, Webster TL, et al. Selective induction of mitochondrial chaperones in response to loss of the mitochondrial genome. *Eur J Biochem*. 1996;240(1):98-103. doi:10.1111/j.1432-1033.1996.0098h.x.

131. Schulz AM, Haynes CM. UPR(mt)-mediated cytoprotection and organismal aging. *Biochim Biophys Acta*. 2015;1847(11):1448-1456. doi:10.1016/j.bbabio.2015.03.008.

132. Nargund AM, Fiorese CJ, Pellegrino MW, Deng P, Haynes CM. Mitochondrial and nuclear accumulation of the transcription factor ATFS-1 promotes OXPHOS recovery during the UPR(mt). *Mol Cell*. 2015;58(1):123-133. doi:10.1016/j.molcel.2015.02.008.

133. Rugarli EI, Langer T. Mitochondrial quality control: a matter of life and death for neurons. *EMBO J*. 2012;31(6):1336-1349. doi:10.1038/emboj.2012.38.

134. Grisolia S, Knecht E, Hernandez-Yago J, Wallace R. Turnover and degradation of mitochondria and their proteins. *Ciba Found Symp*. 1979;(75):167-188. doi:10.1002/9780470720585.ch11.

135. Lasserre J-P, Dautant A, Aiyar RS, et al. Yeast as a system for modeling mitochondrial disease mechanisms and discovering therapies. *Dis Model Mech*. 2015;8(6):509-526. doi:10.1242/dmm.020438.

136. Sugiura A, McLelland G-L, Fon EA, McBride HM. A new pathway for mitochondrial quality control: mitochondrial-derived vesicles. *EMBO J*. 2014;33(19):2142-2156. doi:10.15252/embj.201488104.

137. McLelland G-L, Soubannier V, Chen CX, McBride HM, Fon EA. Parkin and PINK1 function in a vesicular trafficking pathway regulating mitochondrial quality control. *EMBO J*. 2014;33(4):282-295. doi:10.1002/embj.201385902.

138. Suliman HB, Piantadosi CA. Mitochondrial Quality Control as a Therapeutic Target. *Pharmacol Rev*. 2016;68(1):20-48. doi:10.1124/pr.115.011502.

139. Ashrafi G, Schwarz TL. The pathways of mitophagy for quality control and clearance of mitochondria. *Cell Death Differ*. 2013;20(1):31-42. doi:10.1038/cdd.2012.81.

140. Ding W-X, Yin X-M. Mitophagy: mechanisms, pathophysiological roles, and analysis. *Biol Chem*. 2012;393(7):547-564. doi:10.1515/hsz-2012-0119.

141. Thomas RE, Andrews LA, Burman JL, Lin W-Y, Pallanck LJ. PINK1-Parkin pathway activity is regulated by degradation of PINK1 in the mitochondrial matrix. *PLoS Genet*. 2014;10(5):e1004279. doi:10.1371/journal.pgen.1004279.

142. Sahin E, Colla S, Liesa M, et al. Telomere dysfunction induces metabolic and mitochondrial compromise. *Nature*. 2011;470(7334):359-365. doi:10.1038/nature09787.

143. Luo Y, Bond JD, Ingram VM. Compromised mitochondrial function leads to increased cytosolic calcium and to activation of MAP kinases. *Proc Natl Acad Sci U S A*. 1997;94(18):9705-9710.

144. Arnould T, Vankoningsloo S, Renard P, et al. CREB activation induced by mitochondrial dysfunction is a new signaling pathway that impairs cell

proliferation. *EMBO J*. 2002;21(1-2):53-63. doi: 10.1093/emboj/21.1.53.

145. Amuthan G, Biswas G, Ananadatheerthavarada HK, Vijayasarathy C, Shephard HM, Avadhani NG. Mitochondrial stress-induced calcium signaling, phenotypic changes and invasive behavior in human lung carcinoma A549 cells. *Oncogene*. 2002;21(51):7839-7849. doi:10.1038/sj.onc.1205983.
146. Amuthan G, Biswas G, Zhang SY, Klein-Szanto A, Vijayasarathy C, Avadhani NG. Mitochondria-to-nucleus stress signaling induces phenotypic changes, tumor progression and cell invasion. *EMBO J*. 2001;20(8):1910-1920. doi:10.1093/emboj/20.8.1910.
147. Biswas G, Anandatheerthavarada HK, Zaidi M, Avadhani NG. Mitochondria to nucleus stress signaling: a distinctive mechanism of NFkappaB/Rel activation through calcineurin-mediated inactivation of IkappaBbeta. *J Cell Biol*. 2003;161(3):507-519. doi:10.1083/jcb.200211104.
148. Kops GJPL, Dansen TB, Polderman PE, et al. Forkhead transcription factor FOXO3a protects quiescent cells from oxidative stress. *Nature*. 2002;419(6904):316-321. doi:10.1038/nature01036.
149. Chen X-L, Kunsch C. Induction of cytoprotective genes through Nrf2/antioxidant response element pathway: a new therapeutic approach for the treatment of inflammatory diseases. *Curr Pharm Des*. 2004;10(8):879-891.
150. Lu W, Chen Z, Zhang H, Wang Y, Luo Y, Huang P. ZNF143 transcription factor mediates cell survival through upregulation of the GPX1 activity in the mitochondrial respiratory dysfunction. *Cell Death Dis*. 2012;3:e422. doi:10.1038/cddis.2012.156.
151. Chae S, Ahn BY, Byun K, et al. A systems approach for decoding mitochondrial retrograde signaling pathways. *Sci Signal*. 2013;6(264):rs4. doi:10.1126/scisignal.2003266.
152. Eisenberg-Bord M, Schuldiner M. Ground control to major TOM: mitochondria-nucleus communication. *FEBS J*. June 2016. doi:10.1111/febs.13778.
153. van Vliet AR, Verfaillie T, Agostinis P. New functions of mitochondria associated membranes in cellular signaling. *Biochim Biophys Acta*. 2014;1843(10):2253-2262. doi:10.1016/j.bbamcr.2014.03.009.
154. Marchi S, Patergnani S, Pinton P. The endoplasmic reticulum-mitochondria

connection: one touch, multiple functions. *Biochim Biophys Acta*. 2014;1837(4):461-469. doi:10.1016/j.bbabio.2013.10.015.

155. Hamasaki M, Furuta N, Matsuda A, et al. Autophagosomes form at ER-mitochondria contact sites. *Nature*. 2013;495(7441):389-393. doi:10.1038/nature11910.

156. Hailey DW, Rambold AS, Satpute-Krishnan P, et al. Mitochondria supply membranes for autophagosome biogenesis during starvation. *Cell*. 2010;141(4):656-667. doi:10.1016/j.cell.2010.04.009.

157. Wiley SE, Andreyev AY, Divakaruni AS, et al. Wolfram Syndrome protein, Miner1, regulates sulphydryl redox status, the unfolded protein response, and Ca2+ homeostasis. *EMBO Mol Med*. 2013;5(6):904-918. doi:10.1002/emmm.201201429.

158. Schon EA, Area-Gomez E. Is Alzheimer's disease a disorder of mitochondria-associated membranes? *J Alzheimers Dis*. 2010;20 Suppl 2:S281-92. doi:10.3233/JAD-2010-100495.

159. Giorgi C, Ito K, Lin H-K, et al. PML regulates apoptosis at endoplasmic reticulum by modulating calcium release. *Science*. 2010;330(6008):1247-1251. doi:10.1126/science.1189157.

160. Neuspiel M, Schauss AC, Braschi E, et al. Cargo-selected transport from the mitochondria to peroxisomes is mediated by vesicular carriers. *Curr Biol*. 2008;18(2):102-108. doi:10.1016/j.cub.2007.12.038.

161. Vafai SB, Mootha VK. Mitochondrial disorders as windows into an ancient organelle. *Nature*. 2012;491(7424):374-383. doi:10.1038/nature11707.

162. Brand MD, Nicholls DG. Assessing mitochondrial dysfunction in cells. *Biochem J*. 2011;435(2):297-312. doi:10.1042/BJ20110162.

163. Mayr JA, Haack TB, Freisinger P, et al. Spectrum of combined respiratory chain defects. *J Inherit Metab Dis*. 2015;38(4):629-640. doi:10.1007/s10545-015-9831-y.

164. Grazina MM, Diogo LM, Garcia PC, et al. Atypical presentation of Leber's hereditary optic neuropathy associated to mtDNA 11778G>A point mutation--A case report. *Eur J Paediatr Neurol*. 2007;11(2):115-118. doi:10.1016/j.ejpn.2006.11.015.

165. Zeviani M, Carelli V. Mitochondrial disorders. *Curr Opin Neurol*. 2007;20(5):564-571. doi:10.1097/WCO.0b013e3282ef58cd.

166. DiMauro S, Schon EA. Mitochondrial respiratory-chain diseases. *N Engl J Med*. 2003;348(26):2656-2668. doi:10.1056/NEJMra022567.

167. Distelmaier F, Koopman WJH, van den Heuvel LP, et al. Mitochondrial complex I deficiency: from organelle dysfunction to clinical disease. *Brain*. 2009;132(Pt 4):833-842. doi:10.1093/brain/awp058.

168. Benit P, Chretien D, Kadhom N, et al. Large-scale deletion and point mutations of the nuclear NDUFV1 and NDUFS1 genes in mitochondrial complex I deficiency. *Am J Hum Genet*. 2001;68(6):1344-1352. doi:10.1086/320603.

169. Valnot I, Kassis J, Chretien D, et al. A mitochondrial cytochrome b mutation but no mutations of nuclearly encoded subunits in ubiquinol cytochrome c reductase (complex III) deficiency. *Hum Genet*. 1999;104(6):460-466. doi: 10.1007/s004390050988.

170. DiMauro S. Mitochondrial myopathies. *Curr Opin Rheumatol*. 2006;18(6):636-641. doi:10.1097/01.bor.0000245729.17759.f2.

171. Cormier V, Rustin P, Bonnefont JP, et al. Hepatic failure in disorders of oxidative phosphorylation with neonatal onset. *J Pediatr*. 1991;119(6):951-954. doi:10.1016/S0022-3476(05)83054-9.

172. Rahman S, Blok RB, Dahl HH, et al. Leigh syndrome: clinical features and biochemical and DNA abnormalities. *Ann Neurol*. 1996;39(3):343-351. doi:10.1002/ana.410390311.

173. Kytovuori L, Lipponen J, Rusanen H, Komulainen T, Martikainen MH, Majamaa K. A novel mutation m.8561C>G in MT-ATP6/8 causing a mitochondrial syndrome with ataxia, peripheral neuropathy, diabetes mellitus, and hypergonadotropic hypogonadism. *J Neurol*. 2016;263(11):2188-2195. doi:10.1007/s00415-016-8249-2.

174. Ware SM, El-Hassan N, Kahler SG, et al. Infantile cardiomyopathy caused by a mutation in the overlapping region of mitochondrial ATPase 6 and 8 genes. *J Med Genet*. 2009;46(5):308-314. doi:10.1136/jmg.2008.063149.

175. Jonckheere AI, Hogeveen M, Nijtmans LGJ, et al. A novel mitochondrial ATP8 gene mutation in a patient with apical hypertrophic cardiomyopathy and

neuropathy. *J Med Genet*. 2008;45(3):129-133. doi:10.1136/jmg.2007.052084.

176. DiMauro S, Schon EA. Nuclear power and mitochondrial disease. *Nat Genet*. 1998;19(3):214-215. doi:10.1038/883.
177. Chinnery PF. Mitochondrial disease in adults: what's old and what's new? *EMBO Mol Med*. 2015;7(12):1503-1512. doi:10.15252/emmm.201505079.
178. Rotig A. Human diseases with impaired mitochondrial protein synthesis. *Biochim Biophys Acta*. 2011;1807(9):1198-1205. doi:10.1016/j.bbabio.2011.06.010.
179. Diogo L, Grazina M, Garcia P, et al. Pediatric mitochondrial respiratory chain disorders in the Centro region of Portugal. *Pediatr Neurol*. 2009;40(5):351-356. doi:10.1016/j.pediatrneurol.2008.11.012.
180. Y-W-Man P, Griffiths PG, Brown DT, Howell N, Turnbull DM, Chinnery PF. The epidemiology of Leber hereditary optic neuropathy in the North East of England. *Am J Hum Genet*. 2003;72(2):333-339. doi:10.1086/346066.
181. Yu-Wai-Man P, Griffiths PG, Burke A, et al. The prevalence and natural history of dominant optic atrophy due to OPA1 mutations. *Ophthalmology*. 2010;117(8):1538-46, 1546.e1. doi:10.1016/j.ophtha.2009.12.038.
182. Pfeffer G, Pyle A, Griffin H, et al. SPG7 mutations are a common cause of undiagnosed ataxia. *Neurology*. 2015;84(11):1174-1176. doi:10.1212/WNL.0000000000001369.
183. Wallace DC, Singh G, Lott MT, et al. Mitochondrial DNA mutation associated with Leber's hereditary optic neuropathy. *Science*. 1988;242(4884):1427-1430. doi:10.1126/Science.2201231.
184. Elliott HR, Samuels DC, Eden JA, Relton CL, Chinnery PF. Pathogenic mitochondrial DNA mutations are common in the general population. *Am J Hum Genet*. 2008;83(2):254-260. doi:10.1016/j.ajhg.2008.07.004.
185. Rotig A, Munnich A. Genetic features of mitochondrial respiratory chain disorders. *J Am Soc Nephrol*. 2003;14(12):2995-3007. doi:10.1097/01.ASN.0000065481.24091.C9.
186. Taylor RW, Giordano C, Davidson MM, et al. A homoplasmic mitochondrial transfer ribonucleic acid mutation as a cause of maternally inherited hypertrophic cardiomyopathy. *J Am Coll Cardiol*. 2003;41(10):1786-1796. doi:10.1016/S0735-1097(03)00300-0.

187. Tiranti V, Corona P, Greco M, et al. A novel frameshift mutation of the mtDNA COIII gene leads to impaired assembly of cytochrome c oxidase in a patient affected by Leigh-like syndrome. *Hum Mol Genet*. 2000;9(18):2733-2742. doi:10.1093/hmg/9.18.2733.

188. Limongelli A, Schaefer J, Jackson S, et al. Variable penetrance of a familial progressive necrotising encephalopathy due to a novel tRNA(Ile) homoplasmic mutation in the mitochondrial genome. *J Med Genet*. 2004;41(5):342-349. doi:10.1136/jmg.2003.016048

189. McFarland R, Clark KM, Morris AAM, et al. Multiple neonatal deaths due to a homoplasmic mitochondrial DNA mutation. *Nat Genet*. 2002;30(2):145-146. doi:10.1038/ng819.

190. DiMauro S. Mitochondrial DNA medicine. *Biosci Rep*. 2007;27(1-3):5-9. doi:10.1007/s10540-007-9032-5.

191. Holt IJ, Harding AE, Petty RK, Morgan-Hughes JA. A new mitochondrial disease associated with mitochondrial DNA heteroplasmy. *Am J Hum Genet*. 1990;46(3):428-433.

192. Yu D, Jia X, Zhang A-M, et al. Mitochondrial DNA sequence variation and haplogroup distribution in Chinese patients with LHON and m.14484T>C. *PLoS One*. 2010;5(10):e13426. doi:10.1371/journal.pone.0013426.

193. Ji Y, Zhang A-M, Jia X, et al. Mitochondrial DNA haplogroups M7b1'2 and M8a affect clinical expression of leber hereditary optic neuropathy in Chinese families with the m.11778G-->a mutation. *Am J Hum Genet*. 2008;83(6):760-768. doi:10.1016/j.ajhg.2008.11.002.

194. Shoffner JM, Lott MT, Lezza AM, Seibel P, Ballinger SW, Wallace DC. Myoclonic epilepsy and ragged-red fiber disease (MERRF) is associated with a mitochondrial DNA tRNA(Lys) mutation. *Cell*. 1990;61(6):931-937. doi:10.1016/0092-8674(90)90059-N.

195. Goto Y, Nonaka I, Horai S. A mutation in the tRNA(Leu)(UUR) gene associated with the MELAS subgroup of mitochondrial encephalomyopathies. *Nature*. 1990;348(6302):651-653. doi:10.1038/348651a0.

196. Lopez-Gallardo E, Lopez-Perez MJ, Montoya J, Ruiz-Pesini E. CPEO and KSS differ in the percentage and location of the mtDNA deletion. *Mitochondrion*.

2009;9(5):314-317. doi:10.1016/j.mito.2009.04.005.

197. Pitceathly RDS, Rahman S, Hanna MG. Single deletions in mitochondrial DNA--molecular mechanisms and disease phenotypes in clinical practice. *Neuromuscul Disord*. 2012;22(7):577-586. doi:10.1016/j.nmd.2012.03.009.

198. Krishnan KJ, Reeve AK, Samuels DC, et al. What causes mitochondrial DNA deletions in human cells? *Nat Genet*. 2008;40(3):275-279. doi:10.1038/ng.f.94.

199. Moraes CT, Shanske S, Tritschler HJ, et al. mtDNA depletion with variable tissue expression: a novel genetic abnormality in mitochondrial diseases. *Am J Hum Genet*. 1991;48(3):492-501.

200. Wong L-JC. Pathogenic mitochondrial DNA mutations in protein-coding genes. *Muscle Nerve*. 2007;36(3):279-293. doi:10.1002/mus.20807.

201. Dimauro S, Davidzon G. Mitochondrial DNA and disease. *Ann Med*. 2005;37(3):222-232. doi:10.1080/07853890510007368.

202. DiMauro S, Schon EA. Mitochondrial DNA mutations in human disease. *Am J Med Genet*. 2001;106(1):18-26. doi:10.1002/ajmg.1392.

203. McFarland R, Elson JL, Taylor RW, Howell N, Turnbull DM. Assigning pathogenicity to mitochondrial tRNA mutations: when “definitely maybe” is not good enough. *Trends Genet*. 2004;20(12):591-596. doi:10.1016/j.tig.2004.09.014.

204. Yarham JW, Elson JL, Blakely EL, McFarland R, Taylor RW. Mitochondrial tRNA mutations and disease. *Wiley Interdiscip Rev RNA*. 2010;1(2):304-324. doi:10.1002/wrna.27.

205. Yarham JW, Al-Dosary M, Blakely EL, et al. A comparative analysis approach to determining the pathogenicity of mitochondrial tRNA mutations. *Hum Mutat*. 2011;32(11):1319-1325. doi:10.1002/humu.21575.

206. Gonzalez-Vioque E, Bornstein B, Gallardo ME, Fernandez-Moreno MA, Garesse R. The pathogenicity scoring system for mitochondrial tRNA mutations revisited. *Mol Genet genomic Med*. 2014;2(2):107-114. doi:10.1002/mgg3.47.

207. McCann BJ, Tuppen HAL, Kusters B, et al. A novel mitochondrial DNA m.7507A>G mutation is only pathogenic at high levels of heteroplasmy. *Neuromuscul Disord*. 2015;25(3):262-267. doi:10.1016/j.nmd.2014.11.002.

208. Swalwell H, Blakely EL, Sutton R, et al. A homoplasmic mtDNA variant can

influence the phenotype of the pathogenic m.7472Cins MTTS1 mutation: are two mutations better than one? *Eur J Hum Genet*. 2008;16(10):1265-1274. doi:10.1038/ejhg.2008.65.

209. Souilem S, Kefi M, Mancuso M, Nesti C, Hentati F, Amouri R. A novel heteroplasmic tRNA Ser(UCN) mtDNA point mutation associated with progressive ophthalmoplegia and dysphagia. *Diagn Mol Pathol*. 2010;19(1):28-32. doi:10.1097/PDM.0b013e3181b00f02.
210. Mimaki M, Hatakeyama H, Komaki H, et al. Reversible infantile respiratory chain deficiency: a clinical and molecular study. *Ann Neurol*. 2010;68(6):845-854. doi:10.1002/ana.22111.
211. Jonckheere AI, Hogeveen M, Nijtmans L, et al. A novel mitochondrial ATP8 gene mutation in a patient with apical hypertrophic cardiomyopathy and neuropathy. *BMJ Case Rep*. 2009;2009. doi:10.1136/bcr.07.2008.0504.
212. Rocha MC, Grady JP, Grunewald A, et al. A novel immunofluorescent assay to investigate oxidative phosphorylation deficiency in mitochondrial myopathy: understanding mechanisms and improving diagnosis. *Sci Rep*. 2015;5:15037. doi:10.1038/srep15037.
213. Old SL, Johnson MA. Methods of microphotometric assay of succinate dehydrogenase and cytochrome c oxidase activities for use on human skeletal muscle. *Histochem J*. 1989;21(9-10):545-555. doi:10.1007/BF01753355.
214. Alston CL, Lowe J, Turnbull DM, Maddison P, Taylor RW. A novel mitochondrial tRNAGlu (MTTE) gene mutation causing chronic progressive external ophthalmoplegia at low levels of heteroplasmy in muscle. *J Neurol Sci*. 2010;298(1-2):140-144. doi:10.1016/j.jns.2010.08.014.
215. Greaves LC, Yu-Wai-Man P, Blakely EL, et al. Mitochondrial DNA defects and selective extraocular muscle involvement in CPEO. *Invest Ophthalmol Vis Sci*. 2010;51(7):3340-3346. doi:10.1167/iovs.09-4659.
216. Blakely EL, Yarham JW, Alston CL, et al. Pathogenic mitochondrial tRNA point mutations: nine novel mutations affirm their importance as a cause of mitochondrial disease. *Hum Mutat*. 2013;34(9):1260-1268. doi:10.1002/humu.22358.
217. Vincent AE, Ng YS, White K, et al. The Spectrum of Mitochondrial Ultrastructural

Defects in Mitochondrial Myopathy. *Sci Rep*. 2016;6:30610. doi:10.1038/srep30610.

218. Wang J, Schmitt ES, Landsverk ML, et al. An integrated approach for classifying mitochondrial DNA variants: one clinical diagnostic laboratory's experience. *Genet Med*. 2012;14(6):620-626. doi:10.1038/gim.2012.4.
219. de Paepe B, Smet J, Leroy JG, et al. Diagnostic value of immunostaining in cultured skin fibroblasts from patients with oxidative phosphorylation defects. *Pediatr Res*. 2006;59(1):2-6. doi:10.1203/01.pdr.0000191294.34122.ab.
220. Baracca A, Sgarbi G, Mattiazzi M, et al. Biochemical phenotypes associated with the mitochondrial ATP6 gene mutations at nt8993. *Biochim Biophys Acta*. 2007;1767(7):913-919. doi:10.1016/j.bbabio.2007.05.005.
221. Sikorska M, Sandhu JK, Simon DK, et al. Identification of ataxia-associated mtDNA mutations (m.4052T>C and m.9035T>C) and evaluation of their pathogenicity in transmitochondrial cybrids. *Muscle Nerve*. 2009;40(3):381-394. doi:10.1002/mus.21355.
222. Zhang J, Nuebel E, Wisidagama DRR, et al. Measuring energy metabolism in cultured cells, including human pluripotent stem cells and differentiated cells. *Nat Protoc*. 2012;7(6):1068-1085. doi:10.1038/nprot.2012.048.
223. Wittig I, Braun H-P, Schagger H. Blue native PAGE. *Nat Protoc*. 2006;1(1):418-428. doi:10.1038/nprot.2006.62.
224. Calvaruso MA, Smeitink J, Nijtmans L. Electrophoresis techniques to investigate defects in oxidative phosphorylation. *Methods*. 2008;46(4):281-287. doi:10.1016/j.ymeth.2008.09.023.
225. Swerdlow RH. Mitochondria in cybrids containing mtDNA from persons with mitochondriopathies. *J Neurosci Res*. 2007;85(15):3416-3428. doi:10.1002/jnr.21167.
226. Wilkins HM, Carl SM, Swerdlow RH. Cytoplasmic hybrid (cybrid) cell lines as a practical model for mitochondriopathies. *Redox Biol*. 2014;2:619-631. doi:10.1016/j.redox.2014.03.006.
227. Jankauskaite E, Bartnik E, Kodron A. Investigating Leber's hereditary optic neuropathy: Cell models and future perspectives. *Mitochondrion*. 2017;32:19-26. doi:10.1016/j.mito.2016.11.006.

228. Bacalhau M, Pratas J, Simoes M, et al. In silico analysis for predicting pathogenicity of five unclassified mitochondrial DNA mutations associated with mitochondrial cytopathies' phenotypes. *Eur J Med Genet*. 2017;60(3):172-177. doi:10.1016/j.ejmg.2016.12.009.

229. Bourgeron T, Rustin P, Chretien D, et al. Mutation of a nuclear succinate dehydrogenase gene results in mitochondrial respiratory chain deficiency. *Nat Genet*. 1995;11(2):144-149. doi:10.1038/ng1095-144.

230. Parfait B, Chretien D, Rotig A, Marsac C, Munnich A, Rustin P. Compound heterozygous mutations in the flavoprotein gene of the respiratory chain complex II in a patient with Leigh syndrome. *Hum Genet*. 2000;106(2):236-243. doi:10.1007/s004399900218.

231. Horvath R, Abicht A, Holinski-Feder E, et al. Leigh syndrome caused by mutations in the flavoprotein (Fp) subunit of succinate dehydrogenase (SDHA). *J Neurol Neurosurg Psychiatry*. 2006;77(1):74-76. doi:10.1136/jnnp.2005.067041.

232. Baysal BE. Clinical and molecular progress in hereditary paraganglioma. *J Med Genet*. 2008;45(11):689-694. doi:10.1136/jmg.2008.058560.

233. Indrieri A, van Rahden VA, Tiranti V, et al. Mutations in COX7B cause microphthalmia with linear skin lesions, an unconventional mitochondrial disease. *Am J Hum Genet*. 2012;91(5):942-949. doi:10.1016/j.ajhg.2012.09.016.

234. Massa V, Fernandez-Vizarra E, Alshahwan S, et al. Severe infantile encephalomyopathy caused by a mutation in COX6B1, a nucleus-encoded subunit of cytochrome c oxidase. *Am J Hum Genet*. 2008;82(6):1281-1289. doi:10.1016/j.ajhg.2008.05.002.

235. Shteyer E, Saada A, Shaag A, et al. Exocrine pancreatic insufficiency, dyserythropoeitic anemia, and calvarial hyperostosis are caused by a mutation in the COX4I2 gene. *Am J Hum Genet*. 2009;84(3):412-417. doi:10.1016/j.ajhg.2009.02.006.

236. Haut S, Brivet M, Touati G, et al. A deletion in the human QP-C gene causes a complex III deficiency resulting in hypoglycaemia and lactic acidosis. *Hum Genet*. 2003;113(2):118-122. doi:10.1007/s00439-003-0946-0.

237. Barel O, Shorer Z, Flusser H, et al. Mitochondrial complex III deficiency associated with a homozygous mutation in UQCRQ. *Am J Hum Genet*.

2008;82(5):1211-1216. doi:10.1016/j.ajhg.2008.03.020.

238. Mayr JA, Havlickova V, Zimmermann F, et al. Mitochondrial ATP synthase deficiency due to a mutation in the ATP5E gene for the F1 epsilon subunit. *Hum Mol Genet*. 2010;19(17):3430-3439. doi:10.1093/hmg/ddq254.
239. Pagliarini DJ, Calvo SE, Chang B, et al. A mitochondrial protein compendium elucidates complex I disease biology. *Cell*. 2008;134(1):112-123. doi:10.1016/j.cell.2008.06.016.
240. Dunning CJR, McKenzie M, Sugiana C, et al. Human CIA30 is involved in the early assembly of mitochondrial complex I and mutations in its gene cause disease. *EMBO J*. 2007;26(13):3227-3237. doi:10.1038/sj.emboj.7601748.
241. Fassone E, Taanman J-W, Hargreaves IP, et al. Mutations in the mitochondrial complex I assembly factor NDUFAF1 cause fatal infantile hypertrophic cardiomyopathy. *J Med Genet*. 2011;48(10):691-697. doi:10.1136/jmedgenet-2011-100340.
242. Herzer M, Koch J, Prokisch H, et al. Leigh disease with brainstem involvement in complex I deficiency due to assembly factor NDUFAF2 defect. *Neuropediatrics*. 2010;41(1):30-34. doi:10.1055/s-0030-1255062.
243. Ghezzi D, Goffrini P, Uziel G, et al. SDHAF1, encoding a LYR complex-II specific assembly factor, is mutated in SDH-defective infantile leukoencephalopathy. *Nat Genet*. 2009;41(6):654-656. doi:10.1038/ng.378.
244. Hao H-X, Khalimonchuk O, Schraders M, et al. SDH5, a gene required for flavination of succinate dehydrogenase, is mutated in paraganglioma. *Science*. 2009;325(5944):1139-1142. doi:10.1126/science.1175689.
245. de Lonlay P, Valnot I, Barrientos A, et al. A mutant mitochondrial respiratory chain assembly protein causes complex III deficiency in patients with tubulopathy, encephalopathy and liver failure. *Nat Genet*. 2001;29(1):57-60. doi:10.1038/ng706.
246. Visapaa I, Fellman V, Vesa J, et al. GRACILE syndrome, a lethal metabolic disorder with iron overload, is caused by a point mutation in BCS1L. *Am J Hum Genet*. 2002;71(4):863-876. doi:10.1086/342773.
247. Hinson JT, Fantin VR, Schonberger J, et al. Missense mutations in the BCS1L gene as a cause of the Bjornstad syndrome. *N Engl J Med*. 2007;356(8):809-819.

doi:10.1056/NEJMoa055262.

248. Ghezzi D, Arzuffi P, Zordan M, et al. Mutations in TTC19 cause mitochondrial complex III deficiency and neurological impairment in humans and flies. *Nat Genet*. 2011;43(3):259-263. doi:10.1038/ng.761.

249. Kovarova N, Pecina P, Nuskova H, et al. Tissue- and species-specific differences in cytochrome c oxidase assembly induced by SURF1 defects. *Biochim Biophys Acta*. 2016;1862(4):705-715. doi:10.1016/j.bbadis.2016.01.007.

250. Ribeiro C, do Carmo Macario M, Viegas AT, et al. Identification of a novel deletion in SURF1 gene: Heterogeneity in Leigh syndrome with COX deficiency. *Mitochondrion*. 2016;31:84-88. doi:10.1016/j.mito.2016.10.004.

251. Zhu Z, Yao J, Johns T, et al. SURF1, encoding a factor involved in the biogenesis of cytochrome c oxidase, is mutated in Leigh syndrome. *Nat Genet*. 1998;20(4):337-343. doi:10.1038/3804.

252. Valnot I, von Kleist-Retzow JC, Barrientos A, et al. A mutation in the human heme A:farnesyltransferase gene (COX10) causes cytochrome c oxidase deficiency. *Hum Mol Genet*. 2000;9(8):1245-1249. doi:10.1093/hmg/9.8.1245.

253. Antonicka H, Leary SC, Guercin G-H, et al. Mutations in COX10 result in a defect in mitochondrial heme A biosynthesis and account for multiple, early-onset clinical phenotypes associated with isolated COX deficiency. *Hum Mol Genet*. 2003;12(20):2693-2702. doi:10.1093/hmg/ddg284.

254. Bugiani M, Tiranti V, Farina L, Uziel G, Zeviani M. Novel mutations in COX15 in a long surviving Leigh syndrome patient with cytochrome c oxidase deficiency. *J Med Genet*. 2005;42(5):e28. doi:10.1136/jmg.2004.029926.

255. Oquendo CE, Antonicka H, Shoubridge EA, Reardon W, Brown GK. Functional and genetic studies demonstrate that mutation in the COX15 gene can cause Leigh syndrome. *J Med Genet*. 2004;41(7):540-544.

256. Antonicka H, Mattman A, Carlson CG, et al. Mutations in COX15 produce a defect in the mitochondrial heme biosynthetic pathway, causing early-onset fatal hypertrophic cardiomyopathy. *Am J Hum Genet*. 2003;72(1):101-114. doi:10.1086/345489.

257. Weraarpachai W, Antonicka H, Sasarman F, et al. Mutation in TACO1, encoding a translational activator of COX I, results in cytochrome c oxidase deficiency and

late-onset Leigh syndrome. *Nat Genet*. 2009;41(7):833-837. doi:10.1038/ng.390.

258. De Meirleir L, Seneca S, Lissens W, et al. Respiratory chain complex V deficiency due to a mutation in the assembly gene ATP12. *J Med Genet*. 2004;41(2):120-124. doi:10.1136/jmg.2003.012047.
259. Cizkova A, Stranecky V, Mayr JA, et al. TMEM70 mutations cause isolated ATP synthase deficiency and neonatal mitochondrial encephalocardiomyopathy. *Nat Genet*. 2008;40(11):1288-1290. doi:10.1038/ng.246.
260. Rotig A, de Lonlay P, Chretien D, et al. Aconitase and mitochondrial iron-sulphur protein deficiency in Friedreich ataxia. *Nat Genet*. 1997;17(2):215-217. doi:10.1038/ng1097-215.
261. Olsson A, Lind L, Thornell L-E, Holmberg M. Myopathy with lactic acidosis is linked to chromosome 12q23.3-24.11 and caused by an intron mutation in the ISCU gene resulting in a splicing defect. *Hum Mol Genet*. 2008;17(11):1666-1672. doi:10.1093/hmg/ddn057.
262. Mochel F, Knight MA, Tong W-H, et al. Splice mutation in the iron-sulfur cluster scaffold protein ISCU causes myopathy with exercise intolerance. *Am J Hum Genet*. 2008;82(3):652-660. doi:10.1016/j.ajhg.2007.12.012.
263. Dimmock DP, Zhang Q, Dionisi-Vici C, et al. Clinical and molecular features of mitochondrial DNA depletion due to mutations in deoxyguanosine kinase. *Hum Mutat*. 2008;29(2):330-331. doi:10.1002/humu.9519.
264. Brahimi N, Jambou M, Sarzi E, et al. The first founder DGUOK mutation associated with hepatocerebral mitochondrial DNA depletion syndrome. *Mol Genet Metab*. 2009;97(3):221-226. doi:10.1016/j.ymgme.2009.03.007.
265. Nobre S, Grazina M, Silva F, Pinto C, Goncalves I, Diogo L. Neonatal liver failure due to deoxyguanosine kinase deficiency. *BMJ Case Rep*. 2012;2012. doi:10.1136/bcr.12.2011.5317.
266. Rotig A, Poulton J. Genetic causes of mitochondrial DNA depletion in humans. *Biochim Biophys Acta*. 2009;1792(12):1103-1108. doi:10.1016/j.bbadis.2009.06.009.
267. Amati-Bonneau P, Valentino ML, Reynier P, et al. OPA1 mutations induce mitochondrial DNA instability and optic atrophy “plus” phenotypes. *Brain*. 2008;131(Pt 2):338-351. doi:10.1093/brain/awm298.

268. Longley MJ, Clark S, Yu Wai Man C, et al. Mutant POLG2 disrupts DNA polymerase gamma subunits and causes progressive external ophthalmoplegia. *Am J Hum Genet*. 2006;78(6):1026-1034. doi:10.1086/504303.

269. Van Goethem G, Dermaut B, Lofgren A, Martin JJ, Van Broeckhoven C. Mutation of POLG is associated with progressive external ophthalmoplegia characterized by mtDNA deletions. *Nat Genet*. 2001;28(3):211-212. doi:10.1038/90034.

270. Spelbrink JN, Li FY, Tiranti V, et al. Human mitochondrial DNA deletions associated with mutations in the gene encoding Twinkle, a phage T7 gene 4-like protein localized in mitochondria. *Nat Genet*. 2001;28(3):223-231. doi:10.1038/90058.

271. Menezes MJ, Guo Y, Zhang J, et al. Mutation in mitochondrial ribosomal protein S7 (MRPS7) causes congenital sensorineural deafness, progressive hepatic and renal failure and lactic acidemia. *Hum Mol Genet*. 2015;24(8):2297-2307. doi:10.1093/hmg/ddu747.

272. Carroll CJ, Isohanni P, Poyhonen R, et al. Whole-exome sequencing identifies a mutation in the mitochondrial ribosome protein MRPL44 to underlie mitochondrial infantile cardiomyopathy. *J Med Genet*. 2013;50(3):151-159. doi:10.1136/jmedgenet-2012-101375.

273. Galmiche L, Serre V, Beinat M, et al. Exome sequencing identifies MRPL3 mutation in mitochondrial cardiomyopathy. *Hum Mutat*. 2011;32(11):1225-1231. doi:10.1002/humu.21562.

274. Smits P, Saada A, Wortmann SB, et al. Mutation in mitochondrial ribosomal protein MRPS22 leads to Cornelia de Lange-like phenotype, brain abnormalities and hypertrophic cardiomyopathy. *Eur J Hum Genet*. 2011;19(4):394-399. doi:10.1038/ejhg.2010.214.

275. Miller C, Saada A, Shaul N, et al. Defective mitochondrial translation caused by a ribosomal protein (MRPS16) mutation. *Ann Neurol*. 2004;56(5):734-738. doi:10.1002/ana.20282.

276. Oliveira R, Sommerville EW, Thompson K, et al. Lethal Neonatal LTBL Associated with Biallelic EARS2 Variants: Case Report and Review of the Reported Neuroradiological Features. *JIMD Rep*. 2017;33:61-68. doi:10.1007/8904_2016_581.

277. Pierce SB, Gersak K, Michaelson-Cohen R, et al. Mutations in LARS2, encoding mitochondrial leucyl-tRNA synthetase, lead to premature ovarian failure and hearing loss in Perrault syndrome. *Am J Hum Genet*. 2013;92(4):614-620. doi:10.1016/j.ajhg.2013.03.007.

278. Pierce SB, Chisholm KM, Lynch ED, et al. Mutations in mitochondrial histidyl tRNA synthetase HARS2 cause ovarian dysgenesis and sensorineural hearing loss of Perrault syndrome. *Proc Natl Acad Sci U S A*. 2011;108(16):6543-6548. doi:10.1073/pnas.1103471108.

279. Belostotsky R, Ben-Shalom E, Rinat C, et al. Mutations in the mitochondrial seryl-tRNA synthetase cause hyperuricemia, pulmonary hypertension, renal failure in infancy and alkalosis, HUPRA syndrome. *Am J Hum Genet*. 2011;88(2):193-200. doi:10.1016/j.ajhg.2010.12.010.

280. Riley LG, Cooper S, Hickey P, et al. Mutation of the mitochondrial tyrosyl-tRNA synthetase gene, YARS2, causes myopathy, lactic acidosis, and sideroblastic anemia--MLASA syndrome. *Am J Hum Genet*. 2010;87(1):52-59. doi:10.1016/j.ajhg.2010.06.001.

281. Elo JM, Yadavalli SS, Euro L, et al. Mitochondrial phenylalanyl-tRNA synthetase mutations underlie fatal infantile Alpers encephalopathy. *Hum Mol Genet*. 2012;21(20):4521-4529. doi:10.1093/hmg/dds294.

282. Bayat V, Thiffault I, Jaiswal M, et al. Mutations in the mitochondrial methionyl-tRNA synthetase cause a neurodegenerative phenotype in flies and a recessive ataxia (ARSAL) in humans. *PLoS Biol*. 2012;10(3):e1001288. doi:10.1371/journal.pbio.1001288.

283. Steenweg ME, Ghezzi D, Haack T, et al. Leukoencephalopathy with thalamus and brainstem involvement and high lactate “LTBL” caused by EARS2 mutations. *Brain*. 2012;135(Pt 5):1387-1394. doi:10.1093/brain/aws070.

284. Edvardson S, Shaag A, Kolesnikova O, et al. Deleterious mutation in the mitochondrial arginyl-transfer RNA synthetase gene is associated with pontocerebellar hypoplasia. *Am J Hum Genet*. 2007;81(4):857-862. doi:10.1086/521227.

285. Scheper GC, van der Klok T, van Andel RJ, et al. Mitochondrial aspartyl-tRNA synthetase deficiency causes leukoencephalopathy with brain stem and spinal

cord involvement and lactate elevation. *Nat Genet*. 2007;39(4):534-539. doi:10.1038/ng2013.

286. Antonicka H, Ostergaard E, Sasarman F, et al. Mutations in C12orf65 in patients with encephalomyopathy and a mitochondrial translation defect. *Am J Hum Genet*. 2010;87(1):115-122. doi:10.1016/j.ajhg.2010.06.004.
287. Smits P, Antonicka H, van Hasselt PM, et al. Mutation in subdomain G' of mitochondrial elongation factor G1 is associated with combined OXPHOS deficiency in fibroblasts but not in muscle. *Eur J Hum Genet*. 2011;19(3):275-279. doi:10.1038/ejhg.2010.208.
288. Coenen MJH, Antonicka H, Ugalde C, et al. Mutant mitochondrial elongation factor G1 and combined oxidative phosphorylation deficiency. *N Engl J Med*. 2004;351(20):2080-2086. doi:10.1056/NEJMoa041878.
289. Smeitink JAM, Elpeleg O, Antonicka H, et al. Distinct clinical phenotypes associated with a mutation in the mitochondrial translation elongation factor EFTs. *Am J Hum Genet*. 2006;79(5):869-877. doi:10.1086/508434.
290. Valente L, Tiranti V, Marsano RM, et al. Infantile encephalopathy and defective mitochondrial DNA translation in patients with mutations of mitochondrial elongation factors EFG1 and EFTu. *Am J Hum Genet*. 2007;80(1):44-58. doi:10.1086/510559.
291. Janer A, Antonicka H, Lalonde E, et al. An RMND1 Mutation causes encephalopathy associated with multiple oxidative phosphorylation complex deficiencies and a mitochondrial translation defect. *Am J Hum Genet*. 2012;91(4):737-743. doi:10.1016/j.ajhg.2012.08.020.
292. Garcia-Diaz B, Barros MH, Sanna-Cherchi S, et al. Infantile encephaloneuromyopathy and defective mitochondrial translation are due to a homozygous RMND1 mutation. *Am J Hum Genet*. 2012;91(4):729-736. doi:10.1016/j.ajhg.2012.08.019.
293. Richards S, Aziz N, Bale S, et al. Standards and guidelines for the interpretation of sequence variants: a joint consensus recommendation of the American College of Medical Genetics and Genomics and the Association for Molecular Pathology. *Genet Med*. 2015;17(5):405-424. doi:10.1038/gim.2015.30.
294. Wong L-JC. Next generation molecular diagnosis of mitochondrial disorders.

Mitochondrion. 2013;13(4):379-387. doi:10.1016/j.mito.2013.02.001.

295. Finsterer J, Bindu PS. Therapeutic strategies for mitochondrial disorders. *Pediatr Neurol*. 2015;52(3):302-313. doi:10.1016/j.pediatrneurol.2014.06.023.
296. Tischner C, Wenz T. Keep the fire burning: Current avenues in the quest of treating mitochondrial disorders. *Mitochondrion*. 2015;24:32-49. doi:10.1016/j.mito.2015.06.002.
297. Viscomi C, Bottani E, Zeviani M. Emerging concepts in the therapy of mitochondrial disease. *Biochim Biophys Acta*. 2015;1847(6-7):544-557. doi:10.1016/j.bbabio.2015.03.001.
298. Pfeffer G, Majamaa K, Turnbull DM, Thorburn D, Chinnery PF. Treatment for mitochondrial disorders. *Cochrane database Syst Rev*. 2012;(4):CD004426. doi:10.1002/14651858.CD004426.pub3.
299. Behbehani R. Clinical approach to optic neuropathies. *Clin Ophthalmol*. 2007;1(3):233-246.
300. Carelli V, Ross-Cisneros FN, Sadun AA. Mitochondrial dysfunction as a cause of optic neuropathies. *Prog Retin Eye Res*. 2004;23(1):53-89. doi:10.1016/j.preteyeres.2003.10.003.
301. MITOMAP: A Human Mitochondrial Genome Database. http://www.mitomap.org 2017.
302. Jonckheere AI, Smeitink JAM, Rodenburg RJT. Mitochondrial ATP synthase: architecture, function and pathology. *J Inherit Metab Dis*. 2012;35(2):211-225. doi:10.1007/s10545-011-9382-9.
303. Houstek J, Pickova A, Vojtiskova A, Mracek T, Pecina P, Jesina P. Mitochondrial diseases and genetic defects of ATP synthase. *Biochim Biophys Acta*. 2006;1757(9-10):1400-1405. doi:10.1016/j.bbabio.2006.04.006.
304. Felhi R, Mkaouar-Rebai E, Sfaihi-Ben Mansour L, et al. Mutational analysis in patients with neuromuscular disorders: Detection of mitochondrial deletion and double mutations in the MT-ATP6 gene. *Biochem Biophys Res Commun*. 2016;473(1):61-66. doi:10.1016/j.bbrc.2016.03.050.
305. Sambrook J, Fritch EF, Maniatis T. Isolation of High Molecular Weight DNA from Mammalian Cells. In: *Molecular Cloning - A Laboratory Manual*. 2nd ed. New York: Cold Spring Harbor Laboratory Press; 1987:9.14-9.22.

doi:10.1101/pdb.prot3225

306. Moore D, Strauss WM, Richards E, et al. Preparation and Analysis of DNA. In: *Current Protocols in Molecular Biology*. Jonh Wiley & Sons; 1997:2.0.1-2.14.8.
307. Zhang W, Cui H, Wong L-JC. Comprehensive one-step molecular analyses of mitochondrial genome by massively parallel sequencing. *Clin Chem*. 2012;58(9):1322-1331. doi:10.1373/clinchem.2011.181438.
308. van Oven M, Kayser M. Updated comprehensive phylogenetic tree of global human mitochondrial DNA variation. *Hum Mutat*. 2009;30(2):E386-94. doi:10.1002/humu.20921.
309. Schagger H. Tricine-SDS-PAGE. *Nat Protoc*. 2006;1(1):16-22. doi:10.1038/nprot.2006.4.
310. Pereira L, Freitas F, Fernandes V, et al. The diversity present in 5140 human mitochondrial genomes. *Am J Hum Genet*. 2009;84(5):628-640. doi:10.1016/j.ajhg.2009.04.013.
311. de Vries DD, van Engelen BG, Gabreels FJ, Ruitenbeek W, van Oost BA. A second missense mutation in the mitochondrial ATPase 6 gene in Leigh's syndrome. *Ann Neurol*. 1993;34(3):410-412. doi:10.1002/ana.410340319.
312. Thyagarajan D, Shanske S, Vazquez-Memije M, De Vivo D, DiMauro S. A novel mitochondrial ATPase 6 point mutation in familial bilateral striatal necrosis. *Ann Neurol*. 1995;38(3):468-472. doi:10.1002/ana.410380321.
313. Moslemi A-R, Darin N, Tulinius M, Oldfors A, Holme E. Two new mutations in the MTATP6 gene associated with Leigh syndrome. *Neuropediatrics*. 2005;36(5):314-318. doi:10.1055/s-2005-872845.
314. Xu T, Pagadala V, Mueller DM. Understanding structure, function, and mutations in the mitochondrial ATP synthase. *Microb cell*. 2015;2(4):105-125. doi:10.15698/mic2015.04.197.
315. Vojtiskova A, Jesina P, Kalous M, et al. Mitochondrial membrane potential and ATP production in primary disorders of ATP synthase. *Toxicol Mech Methods*. 2004;14(1-2):7-11. doi:10.1080/15376520490257347.
316. Wittig I, Schagger H. Structural organization of mitochondrial ATP synthase. *Biochim Biophys Acta*. 2008;1777(7-8):592-598. doi:10.1016/j.bbabio.2008.04.027.

317. Signorini C, Leoncini S, De Felice C, et al. Redox imbalance and morphological changes in skin fibroblasts in typical Rett syndrome. *Oxid Med Cell Longev*. 2014;2014:195935. doi:10.1155/2014/195935.

318. Straub SP, Stiller SB, Wiedemann N, Pfanner N. Dynamic organization of the mitochondrial protein import machinery. *Biol Chem*. June 2016. doi:10.1515/hsz-2016-0145.

319. Criddle DN, Waldron R, Lugea A, Pandol S. Alcohol-Related Mechanisms of Acute Pancreatitis: The Roles of Mitochondrial Dysfunction and Endoplasmic Reticulum Stress. *Pancreapedia Exocrine Pancreas Knowl Base*. 2015. doi:10.3998/panc.2015.28.

320. Yuzefovych L V, Musiyenko SI, Wilson GL, Rachek LI. Mitochondrial DNA damage and dysfunction, and oxidative stress are associated with endoplasmic reticulum stress, protein degradation and apoptosis in high fat diet-induced insulin resistance mice. *PLoS One*. 2013;8(1):e54059-e54059. doi:10.1371/journal.pone.0054059.

321. Filocamo M, Morrone A. Lysosomal storage disorders: molecular basis and laboratory testing. *Hum Genomics*. 2011;5(3):156-169.

322. Sousa SB, Ramos F, Garcia P, et al. Intellectual disability, coarse face, relative macrocephaly, and cerebellar hypotrophy in two sisters. *Am J Med Genet A*. 2014;164A(1):10-14. doi:10.1002/ajmg.a.36235.

323. Thomas AC, Williams H, Seto-Salvia N, et al. Mutations in SNX14 cause a distinctive autosomal-recessive cerebellar ataxia and intellectual disability syndrome. *Am J Hum Genet*. 2014;95(5):611-621. doi:10.1016/j.ajhg.2014.10.007.

324. Akizu N, Cantagrel V, Zaki MS, et al. Biallelic mutations in SNX14 cause a syndromic form of cerebellar atrophy and lysosome-autophagosome dysfunction. *Nat Genet*. 2015;47(5):528-534. doi:10.1038/ng.3256.

325. Plotegher N, Duchen MR. Mitochondrial Dysfunction and Neurodegeneration in Lysosomal Storage Disorders. *Trends Mol Med*. 2017;23(2):116-134. doi:10.1016/j.molmed.2016.12.003.

326. Demers-Lamarche J, Guillebaud G, Tlili M, et al. Loss of Mitochondrial Function Impairs Lysosomes. *J Biol Chem*. 2016;291(19):10263-10276.

doi:10.1074/jbc.M115.695825.

327. Baixauli F, Acin-Perez R, Villarroya-Beltri C, et al. Mitochondrial Respiration Controls Lysosomal Function during Inflammatory T Cell Responses. *Cell Metab*. 2015;22(3):485-498. doi:10.1016/j.cmet.2015.07.020.
328. Sievers F, Wilm A, Dineen D, et al. Fast, scalable generation of high-quality protein multiple sequence alignments using Clustal Omega. *Mol Syst Biol*. 2011;7:539. doi:10.1038/msb.2011.75.
329. Adzhubei IA, Schmidt S, Peshkin L, et al. A method and server for predicting damaging missense mutations. *Nat Methods*. 2010;7(4):248-249. doi:10.1038/nmeth0410-248.
330. Kumar P, Henikoff S, Ng PC. Predicting the effects of coding non-synonymous variants on protein function using the SIFT algorithm. *Nat Protoc*. 2009;4(7):1073-1081. doi:10.1038/nprot.2009.86.
331. Reva B, Antipin Y, Sander C. Predicting the functional impact of protein mutations: application to cancer genomics. *Nucleic Acids Res*. 2011;39(17):e118. doi:10.1093/nar/gkr407.
332. Choi Y, Sims GE, Murphy S, Miller JR, Chan AP. Predicting the functional effect of amino acid substitutions and indels. *PLoS One*. 2012;7(10):e46688. doi:10.1371/journal.pone.0046688.
333. Yachdav G, Kloppmann E, Kajan L, et al. PredictProtein--an open resource for online prediction of protein structural and functional features. *Nucleic Acids Res*. 2014;42(Web Server issue):W337-43. doi:10.1093/nar/gku366.
334. Fisher N, Meunier B. Effects of mutations in mitochondrial cytochrome b in yeast and man. Deficiency, compensation and disease. *Eur J Biochem*. 2001;268(5):1155-1162.
335. MITOMAP: A Human Mitochondrial Genome Database. http://www.mitomap.org 2017. No Title.
336. Katsuragi Y, Ichimura Y, Komatsu M. p62/SQSTM1 functions as a signaling hub and an autophagy adaptor. *FEBS J*. 2015;282(24):4672-4678. doi:10.1111/febs.13540.
337. Moraes CT, DiMauro S, Zeviani M, et al. Mitochondrial DNA deletions in progressive external ophthalmoplegia and Kearns-Sayre syndrome. *N Engl J*

Med. 1989;320(20):1293-1299. doi:10.1056/NEJM198905183202001.

338. Holt IJ, Harding AE, Cooper JM, et al. Mitochondrial myopathies: clinical and biochemical features of 30 patients with major deletions of muscle mitochondrial DNA. *Ann Neurol*. 1989;26(6):699-708. doi:10.1002/ana.410260603.
339. Goto Y, Koga Y, Horai S, Nonaka I. Chronic progressive external ophthalmoplegia: a correlative study of mitochondrial DNA deletions and their phenotypic expression in muscle biopsies. *J Neurol Sci*. 1990;100(1-2):63-69. doi:10.1016/0022-510X(90)90014-E
340. Blakely EL, He L, Taylor RW, et al. Mitochondrial DNA deletion in "identical" twin brothers. *J Med Genet*. 2004;41(2):e19-e19. doi:10.1136/jmg.2003.011296
341. Caballero PEJ, Candela MS, Alvarez CIC, Tejerina AA. Chronic progressive external ophthalmoplegia: a report of 6 cases and a review of the literature. *Neurologist*. 2007;13(1):33-36. doi:10.1097/01.nrl.0000252953.49721.f5.
342. Moraes CT, Ciacci F, Bonilla E, et al. Two novel pathogenic mitochondrial DNA mutations affecting organelle number and protein synthesis. Is the tRNA(Leu(UUR)) gene an etiologic hot spot? *J Clin Invest*. 1993;92(6):2906-2915. doi:10.1172/JCI116913.
343. Seibel P, Lauber J, Klopstock T, Marsac C, Kadenbach B, Reichmann H. Chronic progressive external ophthalmoplegia is associated with a novel mutation in the mitochondrial tRNA(Asn) gene. *Biochem Biophys Res Commun*. 1994;204(2):482-489. doi:10.1006/bbrc.1994.2485.
344. Silvestri G, Servidei S, Rana M, et al. A novel mitochondrial DNA point mutation in the tRNA(Ile) gene is associated with progressive external ophtalmoplegia. *Biochem Biophys Res Commun*. 1996;220(3):623-627. doi:10.1006/bbrc.1996.0453.
345. Chinnery PF, Johnson MA, Taylor RW, Durward WF, Turnbull DM. A novel mitochondrial tRNA isoleucine gene mutation causing chronic progressive external ophthalmoplegia. *Neurology*. 1997;49(4):1166-1168. doi:10.1212/WNL.49.4.1166
346. Taylor RW, Chinnery PF, Bates MJ, et al. A novel mitochondrial DNA point mutation in the tRNA(Ile) gene: studies in a patient presenting with chronic

progressive external ophthalmoplegia and multiple sclerosis. *Biochem Biophys Res Commun*. 1998;243(1):47-51. doi:10.1006/bbrc.1997.8055.

347. Spagnolo M, Tomelleri G, Vattemi G, Filosto M, Rizzuto N, Tonin P. A new mutation in the mitochondrial tRNA(Ala) gene in a patient with ophthalmoplegia and dysphagia. *Neuromuscul Disord*. 2001;11(5):481-484. doi:10.1016/S0960-8966(01)00195-X.
348. Cardaioli E, Da Pozzo P, Malfatti E, et al. Chronic progressive external ophthalmoplegia: a new heteroplasmic tRNA(Leu(CUN)) mutation of mitochondrial DNA. *J Neurol Sci*. 2008;272(1-2):106-109. doi:10.1016/j.jns.2008.05.005.
349. Berardo A, Coku J, Kurt B, DiMauro S, Hirano M. A novel mutation in the tRNAIle gene (MTTI) affecting the variable loop in a patient with chronic progressive external ophthalmoplegia (CPEO). *Neuromuscul Disord*. 2010;20(3):204-206. doi:10.1016/j.nmd.2010.01.006.
350. Pinos T, Marotta M, Gallardo E, et al. A novel mutation in the mitochondrial tRNA(Ala) gene (m.5636T>C) in a patient with progressive external ophthalmoplegia. *Mitochondrion*. 2011;11(1):228-233. doi:10.1016/j.mito.2010.08.008.
351. Schaller A, Desetty R, Hahn D, et al. Impairment of mitochondrial tRNAIle processing by a novel mutation associated with chronic progressive external ophthalmoplegia. *Mitochondrion*. 2011;11(3):488-496. doi:10.1016/j.mito.2011.01.005.
352. Souilem S, Chebel S, Mancuso M, et al. A novel mitochondrial tRNA(Ile) point mutation associated with chronic progressive external ophthalmoplegia and hyperCKemia. *J Neurol Sci*. 2011;300(1-2):187-190. doi:10.1016/j.jns.2010.08.065.
353. Jackson CB, Neuwirth C, Hahn D, et al. Novel mitochondrial tRNA(Ile) m.4282A>G gene mutation leads to chronic progressive external ophthalmoplegia plus phenotype. *Br J Ophthalmol*. 2014;98(10):1453-1459. doi:10.1136/bjophthalmol-2014-305300.
354. Hanisch F, Kornhuber M, Alston CL, Taylor RW, Deschauer M, Zierz S. SANDO syndrome in a cohort of 107 patients with CPEO and mitochondrial DNA

deletions. *J Neurol Neurosurg Psychiatry*. 2015;86(6):630-634. doi:10.1136/jnnp-2013-306748.

355. Van Goethem G, Martin J-J, Van Broeckhoven C. Progressive external ophthalmoplegia characterized by multiple deletions of mitochondrial DNA: unraveling the pathogenesis of human mitochondrial DNA instability and the initiation of a genetic classification. *Neuromolecular Med*. 2003;3(3):129-146. doi:10.1385/NMM:3:3:129.
356. Shoffner JM, Lott MT, Voljavec AS, Soueidan SA, Costigan DA, Wallace DC. Spontaneous Kearns-Sayre/chronic external ophthalmoplegia plus syndrome associated with a mitochondrial DNA deletion: a slip-replication model and metabolic therapy. *Proc Natl Acad Sci U S A*. 1989;86(20):7952-7956.
357. Herrera A, Garcia I, Gaytan N, Jones E, Maldonado A, Gilkerson R. Endangered species: mitochondrial DNA loss as a mechanism of human disease. Front Biosci (Schol Ed). 2015;7:109-124. doi:10.2741/s428
358. Alemi M, Prigione A, Wong A, et al. Mitochondrial DNA deletions inhibit proteasomal activity and stimulate an autophagic transcript. *Free Radic Biol Med*. 2007;42(1):32-43. doi:10.1016/j.freeradbiomed.2006.09.014.
359. Bender A, Krishnan KJ, Morris CM, et al. High levels of mitochondrial DNA deletions in substantia nigra neurons in aging and Parkinson disease. *Nat Genet*. 2006;38(5):515-517. doi:10.1038/ng1769.
360. Hayashi J, Ohta S, Kikuchi A, Takemitsu M, Goto Y, Nonaka I. Introduction of disease-related mitochondrial DNA deletions into HeLa cells lacking mitochondrial DNA results in mitochondrial dysfunction. *Proc Natl Acad Sci U S A*. 1991;88(23):10614-10618.
361. Lezza AM, Boffoli D, Scacco S, Cantatore P, Gadaleta MN. Correlation between mitochondrial DNA 4977-bp deletion and respiratory chain enzyme activities in aging human skeletal muscles. *Biochem Biophys Res Commun*. 1994;205(1):772-779. doi:10.1006/bbrc.1994.2732.
362. Porteous WK, James AM, Sheard PW, et al. Bioenergetics consequences of accumulating the common 4977-bp mitochondrial DNA deletion. *Eur J Biochem*. 1998;257(1):192-201. doi:10.1046/j.1432-1327.1998.2570192.x.
363. Moore D Richards E, Reichardt M, Rogers S, Willson K, Fineey M, Chory J,

Ribaudo RK, Baldwin Jr AS, Brown T, Ellington A, Green R, Richards EJ, Budelier K, Schorr J SWM. Preparation and Analysis of DNA. In: Ausubel FM Kingston RE, Moore DD, Seidman JG, Smith JA, Struhl K BR, ed. *Current Protocols Inn Molecular Biology*. John Wiley & Sons; 1997:2.0.1-2.14.8.

364. He L, Chinnery PF, Durham SE, et al. Detection and quantification of mitochondrial DNA deletions in individual cells by real-time PCR. *Nucleic Acids Res*. 2002;30(14):e68-e68. doi.org/10.1093/nar/gnf067.
365. Yarham JW, McFarland R, Taylor RW, Elson JL. A proposed consensus panel of organisms for determining evolutionary conservation of mt-tRNA point mutations. *Mitochondrion*. 2012;12(5):533-538. doi:10.1016/j.mito.2012.06.009.
366. Putz J, Dupuis B, Sissler M, Florentz C. Mamit-tRNA, a database of mammalian mitochondrial tRNA primary and secondary structures. *RNA*. 2007;13(8):1184-1190. doi:10.1261/rna.588407.
367. White HE, Durston VJ, Seller A, Fratter C, Harvey JF, Cross NCP. Accurate detection and quantitation of heteroplasmic mitochondrial point mutations by pyrosequencing. *Genet Test*. 2005;9(3):190-199. doi:10.1089/gte.2005.9.190.
368. Krishnan KJ, Bender A, Taylor RW, Turnbull DM. A multiplex real-time PCR method to detect and quantify mitochondrial DNA deletions in individual cells. *Anal Biochem*. 2007;370(1):127-129. doi:10.1016/j.ab.2007.06.024.
369. Rygiel KA, Grady JP, Taylor RW, Tuppen HAL, Turnbull DM. Triplex real-time PCR--an improved method to detect a wide spectrum of mitochondrial DNA deletions in single cells. *Sci Rep*. 2015;5:9906. doi:10.1038/srep09906.
370. Cardaioli E, Da Pozzo P, Gallus GN, et al. A novel heteroplasmic tRNA(Ser(UCN)) mtDNA point mutation associated with progressive external ophthalmoplegia and hearing loss. *Neuromuscul Disord*. 2007;17(9-10):681-683. doi:10.1016/j.nmd.2007.05.001.
371. Florentz C, Sohm B, Tryoen-Toth P, Putz J, Sissler M. Human mitochondrial tRNAs in health and disease. *Cell Mol Life Sci*. 2003;60(7):1356-1375. doi:10.1007/s00018-003-2343-1.
372. Wittenhagen LM, Kelley SO. Impact of disease-related mitochondrial mutations on tRNA structure and function. *Trends Biochem Sci*. 2003;28(11):605-611.

doi:10.1016/j.tibs.2003.09.006.

373. Suzuki T, Nagao A, Suzuki T. Human mitochondrial tRNAs: biogenesis, function, structural aspects, and diseases. *Annu Rev Genet*. 2011;45:299-329. doi:10.1146/annurev-genet-110410-132531.

374. Kirchner S, Ignatova Z. Emerging roles of tRNA in adaptive translation, signalling dynamics and disease. *Nat Rev Genet*. 2015;16(2):98-112. doi:10.1038/nrg3861.

375. D'Silva S, Haider SJ, Phizicky EM. A domain of the actin binding protein Abp140 is the yeast methyltransferase responsible for 3-methylcytidine modification in the tRNA anti-codon loop. *RNA*. 2011;17(6):1100-1110. doi:10.1261/rna.2652611.

376. Noma A, Yi S, Katoh T, Takai Y, Suzuki T, Suzuki T. Actin-binding protein ABP140 is a methyltransferase for 3-methylcytidine at position 32 of tRNAs in Saccharomyces cerevisiae. *RNA*. 2011;17(6):1111-1119. doi:10.1261/rna.2653411.

377. Bidooki S, Jackson MJ, Johnson MA, et al. Sporadic mitochondrial myopathy due to a new mutation in the mitochondrial tRNASer(UCN) gene. *Neuromuscul Disord*. 2004;14(7):417-420. doi:10.1016/j.nmd.2004.03.004.

378. Larsen MK, Nissen PH, Berge KE, et al. Molecular autopsy in young sudden cardiac death victims with suspected cardiomyopathy. *Forensic Sci Int*. 2012;219(1-3):33-38. doi:10.1016/j.forsciint.2011.11.020.

379. Oliva A, Brugada R, D'Aloja E, et al. State of the art in forensic investigation of sudden cardiac death. *Am J Forensic Med Pathol*. 2011;32(1):1-16. doi:10.1097/PAF.0b013e3181c2dc96.

380. Probst S, Oechslin E, Schuler P, et al. Sarcomere gene mutations in isolated left ventricular noncompaction cardiomyopathy do not predict clinical phenotype. *Circ Cardiovasc Genet*. 2011;4(4):367-374. doi:10.1161/CIRCGENETICS.110.959270.

381. Charron P, Arad M, Arbustini E, et al. Genetic counselling and testing in cardiomyopathies: a position statement of the European Society of Cardiology Working Group on Myocardial and Pericardial Diseases. *Eur Heart J*. 2010;31(22):2715-2726. doi:10.1093/eurheartj/ehq271.

382. Watkins H, Ashrafian H, Redwood C. Inherited cardiomyopathies. *N Engl J Med*.

2011;364(17):1643-1656. doi:10.1056/NEJMra0902923.

383. Maron BJ, McKenna WJ, Danielson GK, et al. American College of Cardiology/European Society of Cardiology clinical expert consensus document on hypertrophic cardiomyopathy. A report of the American College of Cardiology Foundation Task Force on Clinical Expert Consensus Documents and the European S. *J Am Coll Cardiol*. 2003;42(9):1687-1713. doi:10.1016/S0735-1097(03)00941-0.

384. Seidman JG, Seidman C. The genetic basis for cardiomyopathy: from mutation identification to mechanistic paradigms. *Cell*. 2001;104(4):557-567.

385. Andersen PS, Havndrup O, Bundgaard H, et al. Genetic and phenotypic characterization of mutations in myosin-binding protein C (MYBPC3) in 81 families with familial hypertrophic cardiomyopathy: total or partial haploinsufficiency. *Eur J Hum Genet*. 2004;12(8):673-677. doi:10.1038/sj.ejhg.5201190.

386. Gajendrarao P, Krishnamoorthy N, Selvaraj S, et al. An Investigation of the Molecular Mechanism of Double cMyBP-C Mutation in a Patient with End-Stage Hypertrophic Cardiomyopathy. *J Cardiovasc Transl Res*. 2015;8(4):232-243. doi:10.1007/s12265-015-9624-6.

387. Maron BJ, Maron MS, Semsarian C. Double or compound sarcomere mutations in hypertrophic cardiomyopathy: a potential link to sudden death in the absence of conventional risk factors. *Hear Rhythm*. 2012;9(1):57-63. doi:10.1016/j.hrthm.2011.08.009.

388. Marziliano N, Merlini PA, Vignati G, et al. A case of compound mutations in the MYBPC3 gene associated with biventricular hypertrophy and neonatal death. *Neonatology*. 2012;102(4):254-258. doi:10.1159/000339847.

389. Liu X, Jiang T, Piao C, et al. Screening Mutations of MYBPC3 in 114 Unrelated Patients with Hypertrophic Cardiomyopathy by Targeted Capture and Next-generation Sequencing. *Sci Rep*. 2015;5:11411. doi:10.1038/srep11411.

390. Wessels MW, Herkert JC, Frohn-Mulder IM, et al. Compound heterozygous or homozygous truncating MYBPC3 mutations cause lethal cardiomyopathy with features of noncompaction and septal defects. *Eur J Hum Genet*. 2015;23(7):922-928. doi:10.1038/ejhg.2014.211.

391. Brega A, Narula J, Arbustini E. Functional, structural, and genetic mitochondrial abnormalities in myocardial diseases. *J Nucl Cardiol*. 2001;8(1):89-97. doi:10.1067/mnc.2001.112755.

392. Zaragoza M V, Brandon MC, Diegoli M, Arbustini E, Wallace DC. Mitochondrial cardiomyopathies: how to identify candidate pathogenic mutations by mitochondrial DNA sequencing, MITOMASTER and phylogeny. *Eur J Hum Genet*. 2011;19(2):200-207. doi:10.1038/ejhg.2010.169.

393. Bacalhau M, Pratas J, Simoes M, et al. In silico analysis for predicting pathogenicity of five unclassified mitochondrial DNA mutations associated with mitochondrial cytophaties' phenotypes. *Eur J Med Genet*. December 2016. doi:10.1016/j.ejmg.2016.12.009.

394. Antonio M, Costa C, Venancio M, et al. Left ventricular noncompaction: analysis of a pediatric population. *Rev Port Cardiol*. 2011;30(3):295-311.

395. Chang B, Nishizawa T, Furutani M, et al. Identification of a novel TPM1 mutation in a family with left ventricular noncompaction and sudden death. *Mol Genet Metab*. 2011;102(2):200-206. doi:10.1016/j.ymgme.2010.09.009.

396. Richard P, Charron P, Carrier L, et al. Hypertrophic cardiomyopathy: distribution of disease genes, spectrum of mutations, and implications for a molecular diagnosis strategy. *Circulation*. 2003;107(17):2227-2232. doi:10.1161/01.CIR.0000066323.15244.54.

397. Liu Z, Song Y, Li D, et al. The novel mitochondrial 16S rRNA 2336T>C mutation is associated with hypertrophic cardiomyopathy. *J Med Genet*. 2014;51(3):176-184. doi:10.1136/jmedgenet-2013-101818.

398. Liu Z, Song Y, Gu S, et al. Mitochondrial ND5 12338T>C variant is associated with maternally inherited hypertrophic cardiomyopathy in a Chinese pedigree. *Gene*. 2012;506(2):339-343. doi:10.1016/j.gene.2012.06.071.

399. El-Hattab AW, Scaglia F. Mitochondrial Cardiomyopathies. *Front Cardiovasc Med*. 2016;3:25. doi:10.3389/fcvm.2016.00025.

400. Varani G, McClain WH. The G x U wobble base pair. A fundamental building block of RNA structure crucial to RNA function in diverse biological systems. *EMBO Rep*. 2000;1(1):18-23. doi:10.1093/embo-reports/kvd001.

401. Horvath R, Kemp JP, Tuppen HAL, et al. Molecular basis of infantile reversible

cytochrome c oxidase deficiency myopathy. *Brain*. 2009;132(Pt 11):3165-3174. doi:10.1093/brain/awp221.

402. Uusimaa J, Finnila S, Remes AM, et al. Molecular epidemiology of childhood mitochondrial encephalomyopathies in a Finnish population: sequence analysis of entire mtDNA of 17 children reveals heteroplasmic mutations in tRNAArg, tRNAGlu, and tRNALeu(UUR) genes. *Pediatrics*. 2004;114(2):443-450. doi:10.1542/peds.114.2.443.
403. Brunel-Guitton C, Levtova A, Sasarman F. Mitochondrial Diseases and Cardiomyopathies. *Can J Cardiol*. 2015;31(11):1360-1376. doi:10.1016/j.cjca.2015.08.017.
404. Lynch TL 4th, Sivaguru M, Velayutham M, et al. Oxidative Stress in Dilated Cardiomyopathy Caused by MYBPC3 Mutation. *Oxid Med Cell Longev*. 2015;2015:424751. doi:10.1155/2015/424751.
405. Davidson MM, Walker WF, Hernandez-Rosa E, Nesti C. Evidence for nuclear modifier gene in mitochondrial cardiomyopathy. *J Mol Cell Cardiol*. 2009;46(6):936-942. doi:10.1016/j.yjmcc.2009.02.011.
406. Guillen Sacoto MJ, Chapman KA, Heath D, Seprish MB, Zand DJ. An uncommon clinical presentation of relapsing dilated cardiomyopathy with identification of sequence variations in MYNPC3, KCNH2 and mitochondrial tRNA cysteine. *Mol Genet Metab reports*. 2015;3:47-54. doi:10.1016/j.ymgmr.2015.03.007.
407. Tang S, Wang J, Zhang VW, et al. Transition to next generation analysis of the whole mitochondrial genome: a summary of molecular defects. *Hum Mutat*. 2013;34(6):882-893. doi:10.1002/humu.22307.
408. Niyazov DM, Kahler SG, Frye RE. Primary Mitochondrial Disease and Secondary Mitochondrial Dysfunction: Importance of Distinction for Diagnosis and Treatment. *Mol Syndromol*. 2016;7(3):122-137. doi:10.1159/000446586.
409. Scarpelli M, Todeschini A, Volonghi I, Padovani A, Filosto M. Mitochondrial diseases: advances and issues. *Appl Clin Genet*. 2017;10:21-26. doi:10.2147/TACG.S94267.

Appendix – List of the 513 nuclear genes related to mitochondrial function and structure sequenced by next generation sequencing (Mitome500 panel, Unpublished, Lee-Jun C. Wong).

AARS2	COX7B	MOCS1	NDUFA4	SDHAF2
ABAT	COX7B2	MOCS2	NDUFA4L2	SDHB
ABCB11	COX7C	MOGS	NDUFA5	SDHC
ABCB4	COX8A	MPDU1	NDUFA6	SEPT9
ABCB7	COX8C	MPI	NDUFA7	SHMT2
ABHD5	CPS1	MPV17	NDUFA8	SIRT1
ACACA	CPT1A	MRP63	NDUFA9	SIRT3
ACACB	CPT1B	MRPL1	NDUFAF1	SIRT4
ACAD9	CPT2	MRPL10	NDUFAF2	SIRT5
ACADL (LCAD)	CYC1	MRPL11	NDUFAF4 (C6ORF66)	SLC22A5/OCTN2
ACADM (MCAD)	CYCS	MRPL12	NDUFB1	SLC25A13
ACADS (SCAD)	DAP3	MRPL13	NDUFB10	SLC25A15 (ORNT1)
ACADSB	DARS2	MRPL14	NDUFB11	SLC25A19
ACADVL (VLCAD)	DBT	MRPL15	NDUFB2	SLC25A20/CACT
ACAT1	DGK intron 3	MRPL16	NDUFB4	SLC25A28
ADCK3	DGUOK	MRPL17	NDUFB5	SLC25A3
ADCK3 (COQ8/CABC1)	DLAT	MRPL18	NDUFB6	SLC25A4
ADSL	DLD	MRPL19	NDUFB7	SLC25A5
AGL	DNA2	MRPL2	NDUFB8	SLC26A4
AIFM1	DNAJC19	MRPL20	NDUFB9	SLC35A1
AK2	DNC	MRPL21	NDUFC1	SLC35C1
ALDH9A1	DNLZ	MRPL22	NDUFC2	SLC37A4
ALDOA	DOLK	MRPL23	NDUFS1	SLC37A4/G6PT1
ALDOB	DPAGT1	MRPL24	NDUFS2	SLC6A8
ALDOB Intron 1	DPM1	MRPL27	NDUFS3	SLIRP
ALDOB_Promoter	DPM3	MRPL28	NDUFS4	SMCP
ALG12	EARS2	MRPL3	NDUFS5	SOD2
ALG2	ELOVL4	MRPL30	NDUFS6	SPATA7
ALG3	ENO3	MRPL32	NDUFS7	SPG7
ALG6	ETFA	MRPL33	NDUFS8	SQSTM1
ALG8	ETFB	MRPL34	NDUFV1	SRD5A3
ALG9	ETFDH	MRPL36	NDUFV2	SSBP1
AMPD1	ETHE1	MRPL38	NDUFV3	STAT1
AMT	EYA4	MRPL39	NEUROD1	STAT3
APEX2	FAH	MRPL4	NFE2L2	STAT3
APP	FARS2	MRPL40	NFU1	SUCLA2

APTX	FASTKD2	MRPL41	NME7	SUCLG1
ARG1	FBP1	MRPL43	NOTCH2	SUCLG2
ASL	FH	MRPL44	NRF1	Sulfite oxidase (SUOX)
ASS1	FOXRED1	MRPL45	NT5C	SURF1
ATP12A	FXC1	MRPL46	NT5M	TACO1
ATP5A1	G6PC	MRPL47	NUBPL	TARS2
ATP5B	GAA	MRPL49	OAT	TAZ
ATP5C1	GABPA	MRPL50	OGDH	TCN2
ATP5D	GABPB1	MRPL51	OPA1	TFAM
ATP5E	GALE	MRPL52	OPA3	TFB1M
ATP5F1	GALK1	MRPL53	OTC	TFB2M
ATP5G1	GALT	MRPL54	OXA1L	TFCP2L1
ATP5G2	GAMT	MRPL55	PAH	TIMM10
ATP5G3	GARS	MRPL9	PAM16	TIMM13
ATP5H	GATM	MRPS10	PARK2	TIMM17A
ATP5I	GBE1	MRPS12	PARS2	TIMM17B
ATP5J	GCDH	MRPS14	PC	TIMM22
ATP5J2	GCK	MRPS15	PCCA	TIMM23
ATP5L	GCKR	MRPS16	PCCB	TIMM44
ATP5L2	GCSH	MRPS16	PDHA1	TIMM50
ATP5O	GFM1	MRPS17	PDHB	TIMM8A
ATP6V0A2	GFM2	MRPS18A	PDHX	TIMMDC1
ATP8B1	GK	MRPS18B	PDK1	TK2
ATPAF1 (ATP11)	GLDC	MRPS18C	PDK2	TMEM127
ATPAF2 (ATP12)	GNE	MRPS2	PDK3	TMEM70
ATPIF1	GPD1	MRPS21	PDK4	TMLHE
AUH	GPD2	MRPS22	PDP1	TNFRSF11A
B4GALT1	GTPBP3	MRPS23	PDSS1	TNFRSF11B
BAX	GYS1	MRPS24	PDSS2	TOMM20
BBOX1	GYS2	MRPS25	PET112L	TOMM22
BCKDHA	HADHA (LCHAD)	MRPS26	PFKM	TOMM34
BCS1L	HADHB (TFP)	MRPS27	PGAM2	TOMM40
BOLA3	HARS2	MRPS28	PGC	TOMM40L
BTD	HLCS	MRPS30	PGM1	TOMM5
C10ORF2	HMGCS1	MRPS31	PHKA1	TOMM6
C12ORF65	HMGCS2	MRPS33	PHKA2	TOMM7
C20ORF7	HNF1A	MRPS34	PHKB	TOMM70A
C2orf64	HNF1B	MRPS35	PHKG2	TOP1MT
CARS2	IARS2	MRPS36	PINK1	TRIT1
CBS	IDH3G	MRPS5	PKM2	TRMU

CHCHD4	IMP3	MRPS6	PMM2	TRNT1
CKMT2	ISCU	MRPS7	PMPCB	TSFM
CMYA5	IVD	MRPS9	PNPLA2	TUFM
COG1	JAG1	MRRF	POLG	TUSC3
COG7	KARS	MTERF	POLG2	TYMP
COG8	LACTB	MTERFD3	POLRMT	TYR
COQ2	LARS2	MTFMT	PPARG	UBE3A
COQ9	LDHA	MTHFD1L	PPARGC1A	UNG
COQ9	LIG3	MTIF2	PPARGC1B	UQCR10
COX10	LMBRD1	MTIF3	PPID	UQCR11
COX11	LONP1	MTO1	PTRH2	UQCRB
COX15	LPIN1 (PAP)	MTR	PTRH2	UQCRC1
COX17	LRPPRC	MTRF1	PUS1	UQCRC2
COX18	MARS2	MTRF1L	PYGL	UQCRFS1
COX19	MCCC1	MTRR	PYGM	UQCRH
COX4I1	MCCC2	MTX1	PYGM Intron 5	UQCRQ
COX4I2	MCEE	MUT	QARS	VARS2
COX5A	MECP2	MUTYH	RARS2	VCP
COX5B	MEF2A	NAGS	RBFA	VDAC1
COX6A1	MEN1	NARS2	RET	VDAC2
COX6A2	MFN1	NDUFA1	RFT1	VDAC3
COX6B1	MFN2	NDUFA10	RRM2B	VHL
COX6B2	MGAT2	NDUFA11	SARS2	WARS2
COX6C	MMAA	NDUFA12	SCO1	XDH
COX7A1	MMAB	NDUFA13	SCO2	YARS2
COX7A2	MMACHC	NDUFA2	SDHA	
COX7A2L	MMADHC	NDUFA3	SDHAF1	